UNIVERSIDADE DE LISBOA
FACULDADE DE MEDICINA VETERINÁRIA

Toxoplasma gondii Tubulin Cofactor B plays a key role in host cell invasion and replication

Samuel Nuno Furtado da Conceição Francisco

Orientadora
Doutora Sofia Bizarro Nolasco da Silva Narciso
Orientador
Doutor José Alexandre da Costa Perdigão e Cameira Leitão

Tese especialmente elaborada para obtenção do grau de Doutor em Ciências Veterinárias na Especialidade de Ciências Biológicas e Biomédicas

2020
Lisboa

Intentionally blank page

UNIVERSIDADE DE LISBOA
FACULDADE DE MEDICINA VETERINÁRIA

Toxoplasma gondii Tubulin Cofactor B plays a key role in host cell invasion and replication

Samuel Nuno Furtado da Conceição Francisco

Orientadora
Doutora Sofia Bizarro Nolasco da Silva Narciso
Orientador
Doutor José Alexandre da Costa Perdigão e Cameira Leitão

Tese especialmente elaborada para obtenção do grau de Doutor em Ciências Veterinárias na Especialidade de Ciências Biológicas e Biomédicas

Júri:

Presidente: Professor Doutor Luís Filipe Lopes Costa

Vogais:

- Professor Doutor Andrew Edward Hemphill
- Professor Doutor António José de Freitas Duarte
- Professora Doutora Helena Antunes Soares
- Professora Doutora Sofia Bizarro Nolasco da Silva Narciso

2020
Lisboa

Intentionally blank page

Intentionally blank page

Acknowledgments

I would like to express my deepest gratitude to my supervisor, Dra. Sofia Nolasco. I am pleased for the opportunity to do my Ph.D. under her supervision, for all her support and advice over the last years and for all the knowledge she shared with me during this long walk. I am also thankful for her encouragement and friendship during this work.

I am deeply grateful to my supervisor, Dr. Alexandre Leitão. I am grateful for the opportunity to do my PhD in his laboratory, for all his encouragement, intelligence and friendship over the last years.

I am also thankful to Faculdade de Medicina Veterinária de Lisboa (FMV) and Centro de Investigação Interdisciplinar em Sanidade Animal (CIISA), our home at the university, in the persons of Professor Doutor Luís Tavares, Professor Doutor Luís Costa, Professor Doutor Rui Caldeira and Professor Doutor Carlos Fontes, for all the support since I have initiated my work.

I received generous support from Instituto Gulbenkian de Ciência (IGC). I am thankful for the opportunity to use the facilities and for the projects that supported my work. I would also like to thank the technical support of IGC's Advanced Imaging Facility (AIF-UIC), which is supported by the national Portuguese funding ref# PPBI-POCI-01-0145-FEDER-022122, co-financed by Lisboa Regional Operational Programme (Lisboa 2020), under the Portugal 2020 Partnership Agreement, through the European Regional Development Fund (FEDER) and Fundação para a Ciência e a Tecnologia (FCT; Portugal).

I would also like to express my gratefulness to Dra. Dulce Santos, for the brain's storms, the advisements, the TED talks, for all the help and of course for the friendship.

I am thankful to Professora Doutora Helena Soares, for the long scientific discussions, the advisement, the intelligence, the excitement for science and all the support.

Special thanks to Alexandra Tavares, for the patience, teaching me, for friendship and for all the help.

I would like to offer my special thanks to my lab colleagues. Afonso Bastos, Eduardo Marcelino, Rita Cardoso, Sara Zuquete, João Coelho, Inês Delgado, Helga Waap for their help,

and support whenever it was needed. Also for the friendship and good atmosphere inside and outside the lab. Thank you.

I owe a very important debt to my friends at CIISA, FMV, mainly to Daniel Murta and Margarida Simões. For the long summer days and weekends working in the lab, the friendship, the support and for the smart thoughts. A special thanks for Daniel, due to the common projects, Bolseiros CIISA and all the other projects and ideas. A special word to David Ramilo, Marcos Santos, Rui Seixas, Ferdinando Freitas, Marta Batista, Sofia Henriques e Mariana Batista, colegues at CIISA lab and also Bolseiros CIISA.

I owe my deepest gratitude to Dr. Markus Meissner, Wellcome Trust Centre for Molecular Parasitology, Institute of Infection, Immunity & Inflammation, University of Glasgow. For all the technologies, the *T. gondii* strains, the teachings and for the opportunity for receiving me in his lab in Glasgow. Without their help, we could not accomplish our work. I am also thankful to Meissner group, it was a great place to be and work. A special thanks to Gurman Pall, Johannes Felix Stortz and Matthew Gow.

I owe a very important debt to Leandro Lemgruber, Imaging Technologist at the Wellcome Trust Centre for Molecular Parasitology, Institute of Infection, Immunity & Inflammation, University of Glasgow. For all the teachings and mainly for the Super Resolution Microscopy images.

My heartfelt appreciation goes to Dr. Andrew Hemphill, from the Institute of Parasitology, Vetsuisse Faculty, University of Berne. For all the precious help with the Electron Microscopy images.

I would like to thank Dr. Carlos Novo (IHMT) and to Dr. Eduardo Marcelino, for anti PDI in house antibodies.

Finally, my family that has always supported and provided me in many ways. A special word to my mother, father and sister, for making it easier for me to choose my own path.

This thesis is dedicated to my son, Miguel, who spent his first months of living next to me, while I was writing this thesis. Without his birth, I probably would not have finished it.

Financial Support

This work was supported by Fundação para a Ciência e a Tecnologia (FCT) PhD Fellowship SFRH/BD/79423/2011 and project grants PTDC/CVT/105470/2008, "The katanin role in microtubule cytoskeleton remodeling during host cell invasion by *Toxoplasma gondii*" and EXPL/CVT-EPI/1945/2013, "Mob1 protein: A Critical Factor in *Toxoplasma gondii* Replication". It was also supported by the Funding of R&D Units Strategic Plan - 2013/2015 – OE, UID/CVT/00276/2013, Centre for Interdisciplinary Research in Animal Health (CIISA).

Intentionally blank page

Resumo

O Cofactor B da Tubulina de *Toxoplasma gondii* tem um papel central na invasão da célula hospedeira e na replicação

Os parasitas protozoários pertencentes ao Filo Apicomplexa são agentes patogénicos responsáveis por um vasto leque de doenças. Apesar da grande biodiversidade deste filo, os mecanismos moleculares adjacentes ao processo de invasão das células hospedeiras parecem ser conservados entre as diferentes espécies.

O processo de invasão das células hospedeiras tem gerado grande interesse em vários grupos, incluindo o nosso, visto ser um importante alvo para o delineamento de estratégias médicas profilácticas e terapêuticas. Assim, nos últimos anos o nosso grupo tem vindo a interessar-se pelo estudo e compreensão do envolvimento do citoesqueleto de microtúbulos, tanto do parasita como da célula hospedeira, no processo de invasão.

Os nossos resultados anteriores em *Besnoitia besnoiti* mostraram que este parasita, aquando da interação com a célula hospedeira, sofre alterações dramáticas na sua forma e superfície, acompanhadas pela remodelação de estruturas específicas de microtúbulos (MTs), nomeadamente os MTs subpeliculares. Estas alterações foram evidenciadas através de uma marcação distinta da tubulina na zona posterior do parasita. Para além disso, o citoesqueleto de MTs da célula hospedeira também responde à entrada do parasita, resultados que, posteriormente, foram também obtidos em *Toxoplasma gondii*.

Estudos anteriores em *T. gondii* demonstraram que os MTs subpeliculares são muito estáveis. Esta estabilidade está possivelmente relacionada com modificações pós-traducionais (MPT) da tubulina, uma vez que, ao contrário dos vertebrados, estes organismos possuem uma família multigénica de α- e β-tubulinas composta por um número reduzido de membros. As MPTs referidas parecem modelar a interação dos MTs com as proteínas que lhes estão associadas. Mais ainda, em *T. gondii*, foram descritas proteínas que cobrem os MTs, num padrão complexo e definido, e que são importantes para a estabilidade dos mesmos. Deste modo, as proteínas que interagem com os MTs podem desempenhar um papel crucial na regulação do citoesqueleto do parasita aquando da invasão da célula hospedeira.

Outras proteínas importantes para a regulação da dinâmica do citoesqueleto de MTs são os cofactores da tubulina, os quais participam nas vias de "folding", dimerização e dissociação do dímero de tubulina. Estes cofatores controlam a proteostase da tubulina, através do controlo da "pool" de tubulina solúvel, participando na regulação da dinâmica dos MTs *in vivo*. Consequentemente, estas proteínas são candidatas a desempenhar um papel crucial nas

modificações observadas no citoesqueleto de MTs do parasita aquando da invasão da célula hospedeira.

Neste contexto o nosso objetivo principal foi avaliar e caracterizar o papel do Cofator B da Tubulina (TBCB de "Tubulin-binding cofactor B") em *T. gondii*. Esta é uma proteína relativamente pequena que possui um domínio CAP-Gly na sua extremidade C-terminal e um domínio semelhante à ubiquitina (UBL de "ubiquitin-like") na extremidade N-terminal. Em conjugação com o Cofactor E da tubulina (TBCE de "Tubulin binding cofactor E"), o TBCB dissocia o dímero de tubulina, controlando desta forma a "pool" de tubulina solúvel disponível na célula e consequentemente a dinâmica do citoesqueleto de MTs.

A escolha do parasita protozoário *T. gondii* como modelo biológico deve-se ao facto de o mesmo possuir um genoma totalmente sequenciado e bem anotado, juntamente com o vasto conjunto de ferramentas disponíveis para a sua manipulação genética.

Neste trabalho identificámos o gene do *Tbcb* em *T. gondii*, analisámos os níveis de expressão por RT-PCR durante o processo de invasão da célula hospedeira e de replicação, estudámos a localização intracelular do TgTBCB usando um anticorpo produzido no nosso laboratório e recorrendo a microscopia confocal e de super resolução, examinámos o fenótipo de TBCB em excesso (sobre-expressão por integração ao acaso) e de ausência do TBCB (deleção do gene utilizando o sistema CRISPR/Cas9). Nestes dois últimos casos foram criadas e selecionadas linhas transgénicas de parasitas, as quais foram analisadas em ensaios de crescimento (formação de pacas, invasão, replicação e egresso) bem como por western blot e por microscopia de fluorescência.

Da análise dos níveis da expressão do *Tbcb* de *T. gondii* durante o processo de invasão e de replicação do parasita na célula hospedeira, notámos uma diminuição significativa dos níveis de expressão às 4 horas após a invasão da célula hospedeira, à qual se seguiu uma fase de recuperação desses níveis.

Quanto à localização sub-celular do TgTBCB, observámos que em *T. gondii* esta proteína tem uma localização polarizada, estando localizada essencialmente no polo anterior, junto do conoide, podendo, por vezes, ser também observada uma marcação menos abundante no polo posterior. Constatámos ainda que o TgTBCB co-localiza parcialmente com as proteínas 2 e 3 das micronemas e com a tubulina glutamilada. Foi ainda possível constatar que na região apical o TBCB em *T. gondii* parece co-alinhar com os MTs subpeliculares, MTs que afunilam para estarem ancorados ao anel polar. Desta forma, o TBCB também parece estar junto ou imediatamente abaixo ao anel polar apical.

Observámos que o excesso de TgTBCB causa uma queda acentuada na capacidade de formar placas de lise em tapetes celulares, a qual foi acompanhada de forma proporcional por uma diminuição notória dos níveis de invasão de células pelos parasitas. Curiosamente, não verificámos qualquer alteração na replicação ou no egresso dos mesmos.

Em relação à deleção do gene *Tbcb* do parasita, 72 horas após a indução da CRISPR/Cas9 comprovámos a completa ausência de TgTBCB por western blot. Observámos também que a viabilidade dos parasitas sem TgTBCB não supera uma semana e que após a indução da deleção do gene, os parasitas demonstraram uma enorme redução na capacidade de invasão e também de replicação. Isto é, os poucos parasitas que conseguiam invadir as células hospedeiras apresentavam enormes problemas na replicação. Por western blot, nos extratos proteicos insolúveis, notámos uma diminuição nos níveis de α-tubulina, tubulina acetilada e poliglutamilada. Estes resultados também foram confirmados por imunofluorescência. Constatámos ainda que os parasitas sem TgTBCB apresentavam vários problemas de divisão, entre eles a alteração do eixo de divisão, a perda do controlo da divisão e a formação de células com morfologia arredondada, compatível com a perda de polaridade. Por microscopia eletrónica observámos também a perda de polaridade dos parasitas bem como a presença de núcleos de dimensões muito superiores ao normal ou dois núcleos dentro da célula, sem que a divisão celular tivesse sido concluída.

Concluindo, o TgTBCB é uma proteína com uma localização polar, sendo observada no polo anterior abaixo do conoide e junto ao anel apical polar, acompanhado os MTs subpeliculares na região apical. A sua co-localização parcial com as proteínas das micronemas e com os MTs subpeliculares, bem como os seus parceiros já descritos em células de mamífero (proteínas de ligação aos MTs), juntamente com o fenótipo de invasão, sugerem que esta proteína em *T. gondii* poderá estar envolvida no tráfego vesicular ao longo dos MTs subpeliculares.

A sobre-expressão do TgTBCB demonstrou a importância desta proteína no processo de invasão e a sua deleção provou que é essencial quer para a invasão quer para a replicação do parasita, visto que na ausência de TgTBCB há um comprometimento irreversível do citoesqueleto de MTs do parasita, levando à morte em menos de uma semana. Este fenótipo, aparentemente, está associado à diminuição dos MTs subpeliculares bem como à impossibilidade de formar novos MTs nas células filhas.

Em suma, o TgTBCB é uma proteína essencial em *T. gondii*, podendo constituir um novo potencial alvo para novas estratégias de controlo e tratamento do parasita.

Palavras-Chave: *Toxoplasma gondii*, invasão da célula hospedeira, tubulina, cofatores da tubulina (TBCs), cofator B da tubulina (TBCB)

Abstract

Tubulin cofactors participate in the folding, dimerization, and dissociation pathways of the tubulin dimer, being implicated in the control of tubulin proteostasis and consequently in the control of microtubule (MT) dynamics *in vivo*. We hypothesise that these proteins have a role in the regulation of MT cytoskeleton dynamics during *Toxoplasma gondii* host cell invasion. In this context, we characterized the Tubulin cofactor B (TBCB) in *T. gondii*. TBCB is a CAP-Gly domain-containing protein that together with TBCE, interact with and dissociate the tubulin dimer.

The TBCB sub-cellular localization in *T. gondii* was studied using an in-house anti-TBCB serum. *T. gondii* lines overexpressing TBCB were obtained by random integration as well as TBCB conditional knockout lines by CRISPR/Cas9 system. TBCB transgenic clones were characterized by growing assays (plaque, invasion, replication and egress assays), western blot analysis and fluorescence microscopy (standard, confocal and super-resolution).

TBCB showed a polarized localization, at the anterior region of the parasite, under the conoid and in close association with polar ring and subpellicular MTs. It did not present a clear co-localization with the apical complex secretory vesicles, although the interaction with rhoptries and micronemes cannot be excluded. TBCB overexpression lines showed a significant decrease in the capacity to form plaques, attributable to a proportional reduction in the capacity to invade. No differences were observed in replication and egress assays. The TgTBCB knockout line, showed a complete depletion of the protein and a viability no longer than a week. These lines showed a strong reduction in their capacity to invade the host cell and in their replication rate. In the absence of TBCB, cells have an altered axis of division resulting in abnormal division. Some parasites show the loss of the correct division axis and some parasites have four daughter cells forming inside instead of two.

TBCB is a polarity marker in *T. gondii* and is involved in the invasion and replication processes. Its apical localization, together with TBCB mammalian partners already described (MT associated proteins) and the invasion phenotypes, suggest that TBCB can be involved in the intracellular traffic of secretory vesicles depending on MTs. Importantly, TBCB is an essential protein, constituting a good target for new control strategies.

Keywords: *Toxoplasma gondii*, host cell invasion, tubulin, tubulin-binding cofactors (TBCs), Tubulin-Binding Cofactor B (TBCB)

Intentionally blank page

Index

List of Figures

Intentionally blank page

List of Tables

Intentionally blank page

Abbreviations

APS ---------- Ammonium persulfate

Arl2 ---------- ADP Ribosylation Factor-like Protein 2

ATCC ---------- American Type Culture Collection

BSA ---------- Bovine serum albumin

CAP-Gly---------- Cytoskeleton associated protein glycine-rich domain

Cas9 ---------- CRISPR-associated protein-9 nuclease

CBB ---------- Coomassie Brilliant Blue

CCT ---------- Cytosolic chaperonin-containing TCP1

cDNA ---------- Complementary DNA

CLASP ---------- Cytoplasmic linker protein-associated protein

CLIP ---------- Cytoplasmic linker proteins

CRISPR---------- Clustered Regularly Interspaced Short Palindromic Repeats

crRNAs ---------- CRISPR RNAs

dhfr-ts ---------- Dihydrofolate reductase-thymidylate synthase

DMEM---------- Dulbecco's Modified Eagle's Medium

DMSO ---------- Dimethyl sulfoxide

DSB ---------- Double-strand break

eGFP ---------- Enhanced green fluorescent protein

FBS---------- Fetal Bovine Serum

GAN ---------- Giant axonal neuropathy

gDNA ---------- Genomic DNA

HFF ---------- Human foreskin fibroblasts

HsTBCB---------- Human TBCB

hxgprt ---------- Hypoxanthine-xanthine-guanine phosphoribosyltransferase

IF ---------- Immunofluorescence

IFs ---------- Intermediate filaments

IMC ---------- Inner membrane complex

IPTG ---------- Isopropyl-β-D-thiogalactopyranoside

ISP---------- Inner Membrane Complex Sub-compartment

LRR ---------- Leucine-rich repeats

MCS---------- Multiple cloning site

MICs ---------- Microneme proteins

MJ ---------- Moving junction

MPA ---------- Mycophenolic acid

MAPs ---------- Microtubule associated proteins

MT ---------- Microtubule

MTOC ---------- Microtubule organizing centers

MM---------- Molecular mass

NEB ---------- New England Biolabs

NHEJ---------- Nonhomologous-end-joining

OD---------- Optical density

Pak1 ---------- p21-activated kinase 1

PAM ---------- Protospacer adjacent motifs

PBS---------- Phosphate-buffered saline

PCR ---------- Polymerase chain reaction

PFA ---------- Paraformaldehyde

pI ---------- Isoelectric point

PTMs---------- Post-translational modifications

PV ---------- Parasitophorous vacuole

PVM ---------- Parasitophorous vacuole membrane

REMI ---------- Restriction Enzyme Mediated Insertion

RONs ---------- Rhoptry neck proteins

ROPs ---------- Rhoptry bulgy proteins

RT ---------- Room temperature

SAG ---------- Glycosylphosphatidylinositol-anchored surface antigen

SDS-PAGE-------- Sodium dodecyl sulfate-polyacrylamide gel electrophoresis

sgRNA ---------- Single guide RNA

SPN ---------- Subpellicular network

TAE ---------- Tris-acetate-EDTA

TBCA ---------- Tubulin cofactor A

TBCB ---------- Tubulin cofactor B

TBCC ---------- Tubulin cofactor C

TBCD ---------- Tubulin cofactor D

TBCE ---------- Tubulin cofactor E

TBCs ---------- Tubulin cofactors

TEMED---------- Tetramethylethylenediamine

TgTBCB---------- *Toxoplasma gondii* tubulin binding cofactor B

tracrRNA ---------- Transactivating CRISPR RNA

Triton X-100 ------- 4-(1,1,3,3-Tetramethylbutyl)phenyl-polyethylene glycol

Tween 20 ---------- Polyoxyethylenesorbitan monolaurate

UbL ---------- Ubiquitin-like domain

UFL ---------- Unit length filament

UV---------- Ultra-violet

WB ---------- Western blot

+TIPs---------- MT plus end tracking proteins

Intentionally blank page

Chapter I: Introduction

1. *Toxoplasma gondii*

Toxoplasma gondii is arguably the most successful parasite worldwide. This organism is thought to be capable of infecting all warm-blooded animals including humans and can be found in most regions of the world (Innes, 2010). It is one of the most well-studied parasites due to its medical and veterinary importance (Dubey, 2008).

T. gondii belongs to the Phylum Apicomplexa (Levine, 1970), Class Sporozoasida (Leukart, 1879), Subclass Coccidiasina (Leukart, 1879), Order Eimeriorina (Leger, 1911), and Family Toxoplasmatidae (Biocca, 1956) and it is the single species in the genus *Toxoplasma* (Barta, 1989; Hill & Chirukandoth, 2005). It is a coccidian parasite with felids as the definitive hosts, and warm-blooded animals as intermediate hosts (Frenkel, Dubey, & Miller, 1970).

Members of the phylum Apicomplexa are known for their apical complex, an essential structure for host cell invasion, consisting of a specialized microtubule (MT) structures and secretory organelles (C. A. Hunter & Sibley, 2012).

1.1. History

T. gondii was discovered by accident, in 1908 by scientists working with Leishmania (Dubey, 2009; Innes, 2010). Charles Nicolle and Louis Manceaux, who were working in Tunisia, searching for a reservoir of Leishmania in a native rodent, *Ctenodactylus gundi*, found a new protozoan in tissues. This hamster-like rodent, the gundi, which lives in the foothills and mountains of Southern Tunisia, it was commonly used to study Leishmania at the Pasteur Institute in Tunis (Dubey, 2008; Innes, 2010). In the same year (1908), Alfonso Splendore, also studying Leishmania, discovered the same parasite in a rabbit in Brazil (Dubey, 2008).

Nicolle initially believed the parasite to be a piroplasm rather than Leishmania, but soon realized that he had discovered a new organism and named it *T. gondii* based on the morphology and the host. The name *Toxoplasma* means ‘arc form’ in Greek and was named according to the crescent-shaped morphology of the tachyzoite and bradyzoite stages of the organism observed by the scientists (Dubey, 2008; Innes, 2010). Interestingly, the correct name for the parasite should have been *T. gundii*, but Nicolle and Manceaux had incorrectly identified the host as the rodent *Ctenodactylus gondi gundi* (Dubey, 2008).

Following the next years, several other reports appeared and species of *Toxoplasma* were named with reference to the host species in which they were detected (Dubey, 2008; Innes, 2010). By 1935 Sabin and Olitsky accidentally obtain the first isolation of *T. gondii* early in this year, in the course of experimental work with viruses (Sabin & Olitsky, 1937). Nevertheless, the biological and immunological characteristics of the different *Toxoplasma* isolates obtained from animals and humans showed them to be identical to *T. gondii* (Sabin, 1939). In fact, although *T. gondii* has a worldwide distribution and perhaps the widest host range of any parasite, there is only one species in the genus *Toxoplasma* (Dubey, 2008). In the following years, the research on this parasite increased considerably and important discoveries were made about its biology. The ease with which the parasite can be cultured in the laboratory and the wide range of animal models available have made *T. gondii* a very accessible model organism for scientists (Innes, 2010).

1.2. Epidemiology

T. gondii is one of the world's most common parasites, infecting most genera of warm-blooded animals (virtually all warm-blooded animals, including mammals and birds) (Elmore et al., 2010; Flegr, Prandota, Sovičková, & Israili, 2014; Robert-Gangneux & Dardé, 2012; Wilking, Thamm, Stark, & Aebischer, 2016). It is the most prevalent infection in humans (estimated to be 25–50% of the world population), more than latent tuberculosis which infects about one-third of the human population (Flegr et al., 2014; Robert-Gangneux & Dardé, 2012; World Health Organization, 2016).

The importance of toxoplasmosis in humans remained unknown until the first reports of cases of congenital toxoplasmosis in 1948 (Smitt & Winblad, 1948). Nowadays, toxoplasmosis is considered a very important disease not only for human medicine but also for veterinary medicine. In Humans, severe disease is usually observed in congenitally infected children and in immunosuppressed individuals, including patients with acquired immune deficiency syndrome (HIV/AIDS) (Y. Zhou, Zhang, Cao, Gong, & Zhou, 2016). Moreover, the congenital toxoplasmosis (transmission to the fetus when a pregnant woman acquires *T. gondii* infection for the first time during pregnancy) can result in abortion or lead to severe malformation of the fetus or to visual or neurological injuries in the newborn, such as hydrocephalus, cerebral calcification and/or chorioretinitis (Gargaté et al., 2016). For the veterinary medicine, toxoplasmosis is one of the major causes of neonatal infections and abortion in sheep and goats.

Cats, dogs, and many other pets can die of pneumonia, hepatitis, and encephalitis due to toxoplasmosis (Y. Zhou et al., 2016).

T. gondii has a wide spectrum of prevalence across the globe. Seroprevalence of infection measured by specific anti-Toxoplasma IgG antibodies varies between 1 % and 100 % depending on the geographical area, the environmental and socioeconomic conditions, including eating habits and health-related practices (Flegr et al., 2014; V. Klaren & Kijlstra, 2002). The lowest seroprevalence (~1 %) was found in some countries in the Far East and the highest (>90 %) in some parts of European and South American countries (Flegr et al., 2014). In European countries, the prevalence ranges between 10 % to 60 %, and in some regions, as high as 90 %(Flegr et al., 2014). The global status of *T. gondii* seroprevalence in pregnant women or in reproductive ages ranges from above 60 % in countries such as Brazil, Gabon, Indonesia, Germany and Iran, to <10 % in the UK and Korea (Pappas, Roussos, & Falagas, 2009).

In Portugal, there is a lack of knowledge of the current epidemiological situation in humans, as the unique toxoplasmosis National Serological Survey was performed in 1979/ 1980, the rate of congenital infection is unknown and almost nothing is known about the sequelae of congenital toxoplasmosis (Gargaté et al., 2016; Lopes, Dubey, Darde, & Cardoso, 2014). Recently Maria João Gargaté and colleagues describe the toxoplasmosis seroprevalence trends in the Portuguese general population (with special focus on women of childbearing age) over the past three decades (1979/1980, 2001/2002 and 2013), by age group, region and gender. The *T. gondii* overall seroprevalence decreased from 47% in 1979/1980 to 22% in 2013. Generally, the prevalence of *T. gondii* specific IgG increased significantly with age and it decreased over time, both in the general population and in the childbearing women (18% prevalence in 2013) (Gargaté et al., 2016).

In animals, there are a few studies about the serological and parasitological prevalence of toxoplasmosis. But very little is known of clinical toxoplasmosis in animals in Portugal (Lopes et al., 2014). Serological surveys in cats performed in Portugal include three studies in Lisbon and one, in Trás-os-Montes e Alto Douro (Northeastern Portugal). Serological prevalence varied from 20 to 44 %, the highest being from stray cats from Lisbon (Duarte et al., 2010; Esteves et al., 2014; Lopes, Cardoso, & Rodrigues, 2008; Waap et al., 2012). A study in a wildlife conservation area in southern Portugal reports 83% in wildcats (*Felis silvestris*) and 39% in cats (*Felis catus*) (Waap, Nunes, Vaz, & Leitão, 2016). There is no information concerning congenital transmission (Lopes et al., 2014). The prevalence of *T. gondii* in food animals (Poultry, pork, beef and mutton) was also poorly studied. For cattle, the *T. gondii*

serological prevalence varied from 7.5 % (Lopes et al., 2013) to 29.2 % (Lopes et al., 2014), both studies from the north of Portugal. Among three surveys in pigs, seroprevalence varied from 7.1 to 15.6 % (Esteves et al., 2014; Lopes et al., 2013; Sousa et al., 2006). The seroprevalence in intensively raised chickens is unknown, but in free range chickens (more indicative of soil contamination) was 20.8 % in 225 free range chickens from 18 farms in the north and center of the country (Dubey et al., 2006). For sheep, the seroprevalence varied from 17.1 % (Sousa et al., 2009) to 33.6 % and in goats the seroprevalence was a 18.5 %(Lopes et al., 2013), all studies from the north of Portugal. Finally, in domestic dogs from the northeastern of Portugal, the seroprevalence of *T. gondii* is 38.0 % (Lopes et al., 2011).

1.3. Life Cycle

Although *T. gondii* was discovered in 1908 its entire life cycle was definitively understood only in the late 1960s, with the discovery of the central role of the cat as a definitive host harboring the sexual parasite development phase and spreading oocysts through feces (Dubey & Frenkel, 1972; Frenkel et al., 1970; Hutchison, Dunachie, Siim, & Work, 1969). In the same period of time, it was classified in the coccidian sub-class (Frenkel et al., 1970), phylum Apicomplexa, and the infectivity of the three parasitic stages (tachyzoite, cyst and oocyst) was well characterized (Dubey, 2009; Robert-Gangneux & Dardé, 2012).

T. gondii is a tissue-cyst-forming coccidium with a complex life cycle that alternates between definitive (sexual reproduction) and intermediate (asexual replication) hosts, facultatively heteroxenous. It is unique among this group because it can be transmitted not only between intermediate and definitive hosts (sexual cycle) but also among intermediate hosts via carnivorism (asexual cycle) or even among definitive hosts by oocysts. The parts of the sexual and asexual cycles and transmission dynamics in a given environment vary according to physical characteristics and according to the structures of both intermediate and definitive host populations (Afonso, Thulliez, & Gilot-Fromont, 2006; Dubey, Lindsay, & Speer, 1998; Robert-Gangneux & Dardé, 2012; Tenter, Heckeroth, & Weiss, 2000).

The sexual cycle occurs only in felids. All members of the family *Felidae* are suitable definitive hosts for *T. gondii*, but domestic cats produce the greatest number of oocysts (Webster, Kaushik, Bristow, & McConkey, 2013). In felids *T. gondii*, undergoes a coccidian-like life cycle in the epithelial cells of the small intestine (Figure 1). Briefly, after the ingestion of cysts present in tissues of an intermediate host, the cyst wall is destroyed by gastric enzymes (proteolysis) which leads to the release of the bradyzoites. The bradyzoites penetrate the

enterocytes, where they undergo a self-limiting number of asexual multiplications, characterized by the development of merozoites (merogony) (Figure 1) (Dubey, 1998; Lindsay, Blagburn, & Braud, 1995; Robert-Gangneux & Dardé, 2012). This first step is followed by sexual development, with the formation of male and female gametes (gametogony). After fertilization, oocysts formed within enterocytes are liberated by the disruption of the cell and excreted as unsporulated forms to the intestinal lumen and ultimately to the environment through the feces (Figure 1) (Ferguson, 2002; Lindsay et al., 1995; Montoya & Liesenfeld, 2004; Robert-Gangneux & Dardé, 2012). The process of sporogony occurs in the external environment within 2 to several days, depending on environment conditions. Sporulated oocyst contain two sporocysts, each containing four haploid sporozoites (Figure 1). The sporulated oocyst can infect virtually any warm-blooded animal including cats, although less efficiently (Lindsay et al., 1995; Robert-Gangneux & Dardé, 2012).

In the intermediate hosts, the parasite undergoes only asexual development. When the sporulated oocysts are ingested, the oocyst wall is degraded by the proteolytic enzymes of the digestive track and sporozoites are liberated. They penetrate the intestinal epithelium, where they differentiate into tachyzoites. Tachyzoites rapidly replicate by endodyogeny inside of any kind of cell and disseminate throughout the organism by lymphatic and vascular system. After the acute period of infection, the pressure of the host immune system and likely some intrinsic mechanism of the parasite, lead to the establishment of a chronic stage of the disease, because of the conversion from tachyzoite to bradyzoite, that are much less active and that form cysts in the host (Figure 1). Tissue cysts arise as early as 7 to 10 days post-infection and may remain throughout life in most hosts, predominantly in the brain or musculature. But an active phase of the disease may arise whenever the host immune system is depressed (Hill & Chirukandoth, 2005; Lindsay et al., 1995; Robert-Gangneux & Dardé, 2012).

Alternatively, upon the ingestion of these tissue cysts by an intermediate host through raw or undercooked meat, cysts are ruptured as they pass through the digestive tract, causing the release of bradyzoites. The bradyzoites will penetrate the intestinal epithelium of the new host and begin asexual multiplication within cells. After a few days, bradyzoites differentiate back into the rapidly dividing tachyzoite stage for dissemination throughout the body (Lindsay et al., 1995; Robert-Gangneux & Dardé, 2012).

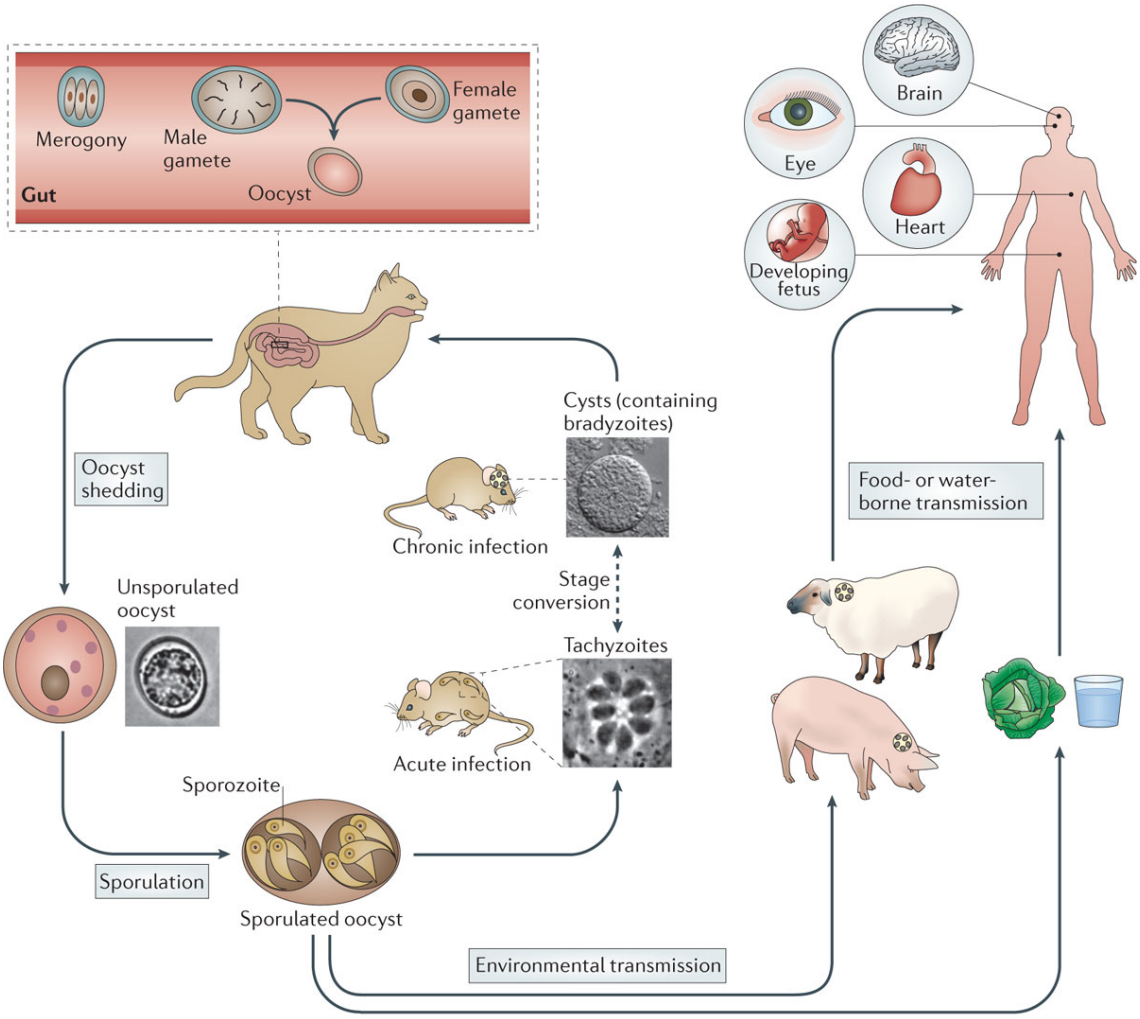

Figure 1. The complex lifecycle of *T. gondii*. Cats are the definitive host in which sexual replication of *T. gondii* takes place. Following replication of merozoites within enterocytes of the cat gut (a process known as merogony), male and female *T. gondii* gametes are formed within the host cell *(Dubey & Frenkel, 1972)*. The fusion of gametes leads to the formation of diploid oocysts that are shed in cat feces and undergo sporogony in the external environment (sporulation). Oocysts can survive in the environment for long periods of time, and sporulated oocysts (which are infectious) can contaminate food and water, providing a route of infection for intermediate hosts. In the intermediate host (rodents, pigs, sheep, humans, etc.), occurs asexual replication. Acute infection is characterized by tachyzoites (rapidly replicating forms) that disseminate throughout the body. Differentiation to slow-growing bradyzoites within tissue cysts leads to long-term chronic infection. Ingestion of tissue cysts via omnivorous or carnivorous feeding can lead to transmission to either other intermediate hosts or to cats, re-initiating the sexual phase of the life cycle. Many animals serve as intermediate hosts, including farm animals. Humans become infected by eating undercooked meat containing tissue cysts or by ingesting sporulated oocysts in contaminated water (From *(C. A. Hunter & Sibley, 2012)* with permission).

1.4. Diversity of *T. gondii* strains

Historically, *T. gondii* isolates have been classified into 3 closely related clonal lineages or strains (referred to as types I, II, III) that dominate North America and Europe (Howe & Sibley, 1995), however recent genetic analysis identifying a fourth lineage in North America (Khan et

al., 2011). The clonal propagation of this lineages is likely favored by the ability of *T. gondii* to be transmitted among intermediate hosts via ingestion of tissue cysts, a trait that distinguishes it from related parasites (C. Su et al., 2003). Although this clonality in *T. gondii* is strongly evident in North America and Europe, much greater genetic diversity, likely reflecting more frequent recombination, is evident in South America (Khan et al., 2011).

Genetically, the clonal lineages are all relatively similar, differing only by approximately 1–2 % at the nucleotide level (Sibley, Khan, Ajioka, & Rosenthal, 2009). Nevertheless, despite their genetic similarity these clonal lineages differ in a wide range of phenotypes, including virulence, persistence, migratory capacity, and how they interface with the immune response, thus, the information of genetic diversity of *T. gondii* is useful for better understanding epidemiological patterns and pathogenicity, as well as exploring of new polymorphic virulence effectors (Ning, Huang, Wang, Xu, & Zhu, 2015). In fact, the virulence in mice of *T. gondii* depends on the parasite strain (Szabo & Finney, 2016). Briefly, type I (e.g. RH, GT1) strains are highly virulent, whereas type II (e.g. ME49) are intermediate virulence and type III (e.g. VEG) are relatively nonvirulent (Sibley & Boothroyd, 1992).

The Type II is the most prevalent *T. gondii* strain in Europe and North America (Lopes et al., 2014). In Portugal there is little information on genetic typing of *T. gondii* isolates circulating. Genotyping 12 isolates obtained from free-ranging chickens, 4 were found to be type III, and 8 were type II (Dubey et al., 2006). Earlier in 2008 Waap and colleagues characterized the genotypes of *T. gondii* in 12 pigeons revealing that 9 strains belonged to type II, 2 were type III and one was type I. They did not find recombinant or atypical genotypes (Waap, Vilares, Rebelo, Gomes, & Ângelo, 2008). In pigs, Sousa and colleagues genotyped 15 isolates showing that 11 were Type II and 4 were Type III (Sousa et al., 2006). Lopes and colleagues characterized the genotypes of *T. gondii* in 20 cattle, 40 sheep, 15 goats and 16 pigs from the North of Portugal and the type II has been confirmed as the most predominant strain between them (Lopes et al., 2015).

1.5. Morphology and Organelles

In contrast to the highly reduced organization of *Plasmodium* and *Theileria*, *Toxoplasma*, exhibits a classic eukaryotic morphology, with readily recognizable organelles (Hager, Striepen, Tilney, & Roos, 1999). The *T. gondii* tachyzoite morphology, which is responsible for the acute phase of the infection caused by this parasite, is often crescent shaped, with approximately 2 X 8 μm. The cell is a permanently polarized, presenting the apical complex at

the pointed anterior end (anterior pole) and the basal complex at the rounded posterior end (posterior pole). Ultrastructurally, it has various organelles and inclusion bodies including a pellicle (outer covering), mitochondria, smooth and rough endoplasmic reticulum, a Golgi apparatus, ribosomes, a micropore, apical rings, polar ring, conoid, rhoptries, micronemes, subpellicular MTs, dense granules, amylopectin granules (which may be absent), a multiple-membrane-bound plastid-like organelle, which has also been called a Golgi adjunct or apicoplast, and a well-defined nucleus. The nucleus is usually situated toward the central area of the cell (Figure 2) (De Souza, Martins-Duarte, Lemgruber, Attias, & Vommaro, 2010; Dubey, 1998; Hill & Chirukandoth, 2005).

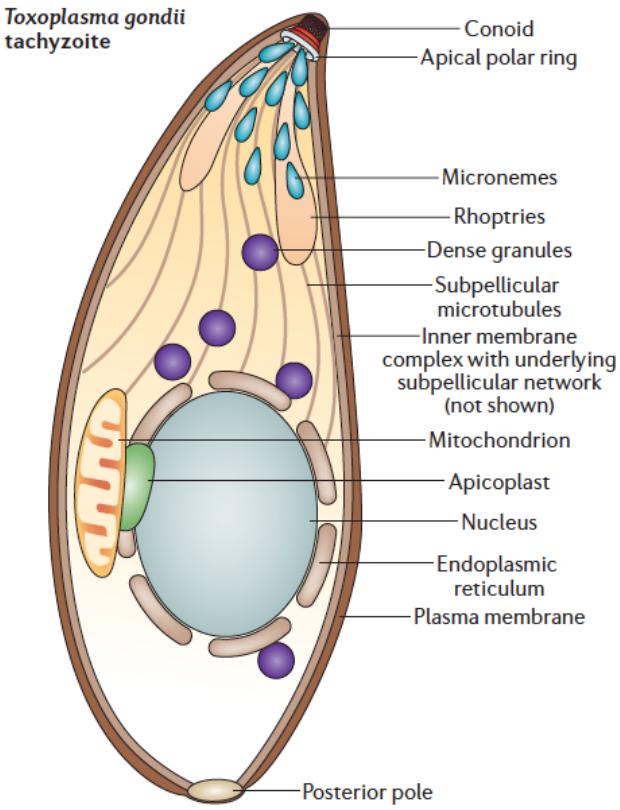

Figure 2. Schematic drawings of a *T. gondii* tachyzoite (From *(J. Baum, Papenfuss, Baum, Speed, & Cowman, 2006)* with permission)

1.5.1. Apical Complex

Apicomplexan parasites share a set of cytoskeletal structures essential for parasite survival and pathogenesis. Nevertheless, the defining feature of this Phylum is a complex assemblage of structural and secretory elements at the apical end of the cell, forming the namesake of the group - the apical complex (Hu et al., 2006; Katris et al., 2014; Morrissette & Sibley, 2002a).

This complex is very important in the host cell invasion processes and it provides both a semi-rigid framework to these apically pointed cells, and a focal point for secretory organelles that release various invasion factors that mediate interaction with the host cell and then the invasion (Gubbels & Duraisingh, 2012; Katris et al., 2014). The elements of the apical complex are highly conserved throughout Apicomplexa and usually include one or more polar rings, rhoptries, micronemes, conoid, and sub-pellicular MTs (Figure 3)(de Souza et al., 2010; Morrissette & Sibley, 2002a). These structures are in close association with the secretory organelles (rhoptries and micronemes).

The conoid is a small cone-shaped structure that it is thought to play a mechanical role in invasion of host cells and is present only in some apicomplexans. The apical polar ring is a hallmark organelle of all members of the Apicomplexa Phylum and it serves as one of the three microtubule-organizing centers (MTOCs). The rhoptries and micronemes are unique secretory organelles that contain products required for motility, adhesion to host cells, invasion of host cells and establishment of the parasitophorous vacuole (PV) (Morrissette & Sibley, 2002a).

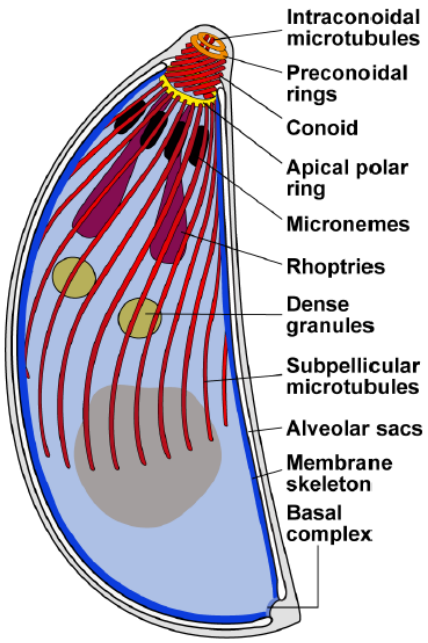

Figure 3. **Schematic drawings of a *T. gondii* representing the structural elements of the apical complex, the cell pellicle, and the secretory organelles** (adapted from *(Katris et al., 2014)* with permission)

1.5.1.1. Conoid

The conoid is a truncated cone shaped structure present at the extreme apical end of the parasite. This is a retractable structure that seems to act like a probe during invasion and egress

although its precise functions are not known (Skariah, Bednarczyk, McIntyre, Taylor, & Mordue, 2012). It has approximately 380 nm in diameter, 280 nm in length and it is a quite remarkable structure (Figure 4 A) (Hu et al., 2006; Hu, Roos, & Murray, 2002b). The conoid itself is exclusively built around a core of tubulin arranged into a unique ribbon-like polymer that is quite different from conventional MTs (Hu, Roos, & Murray, 2002b; Swedlow, Hu, Andrews, Roos, & Murray, 2002). In fact, the conoidal fibers has only nine protofilaments arranged in an open conformation that resembles a comma, a very unusual and unique form of tubulin assembly, completely different from the usual set of 13 protofilaments. Therefore, the specialized arrangement of tubulin in the conoid fibers is probably determined by association with other nontubulin proteins (de Souza & Attias, 2010; Hu et al., 2006). Moreover, the isolation of the *T. gondii* conoid/apical complex led to the identification of approximately 200 proteins that represent 70 % of its cytoskeleton proteins (Hu et al., 2006). Whereas parasites are inside a host cell, the conoid remains enclosed within the shell formed by the subpellicular MTs. However, when the parasites are swimming extracellularly, the conoid intermittently protrudes beyond the apical end of the MTs (Fig 4 B)(Hu, Roos, & Murray, 2002b).

The other apical complex structures closely associated with the conoid are the preconoidal rings, at the distal tip of the conoid, from which the conoid fibers originate; the polar ring, from which the parasite's 22 subpellicular MTs are attached and two short intraconoid MTs, which may be used as tracks for transport of secretory vesicles essential for invasion (Carruthers & Sibley, 1997; Nichols & Chiappino, 1987).

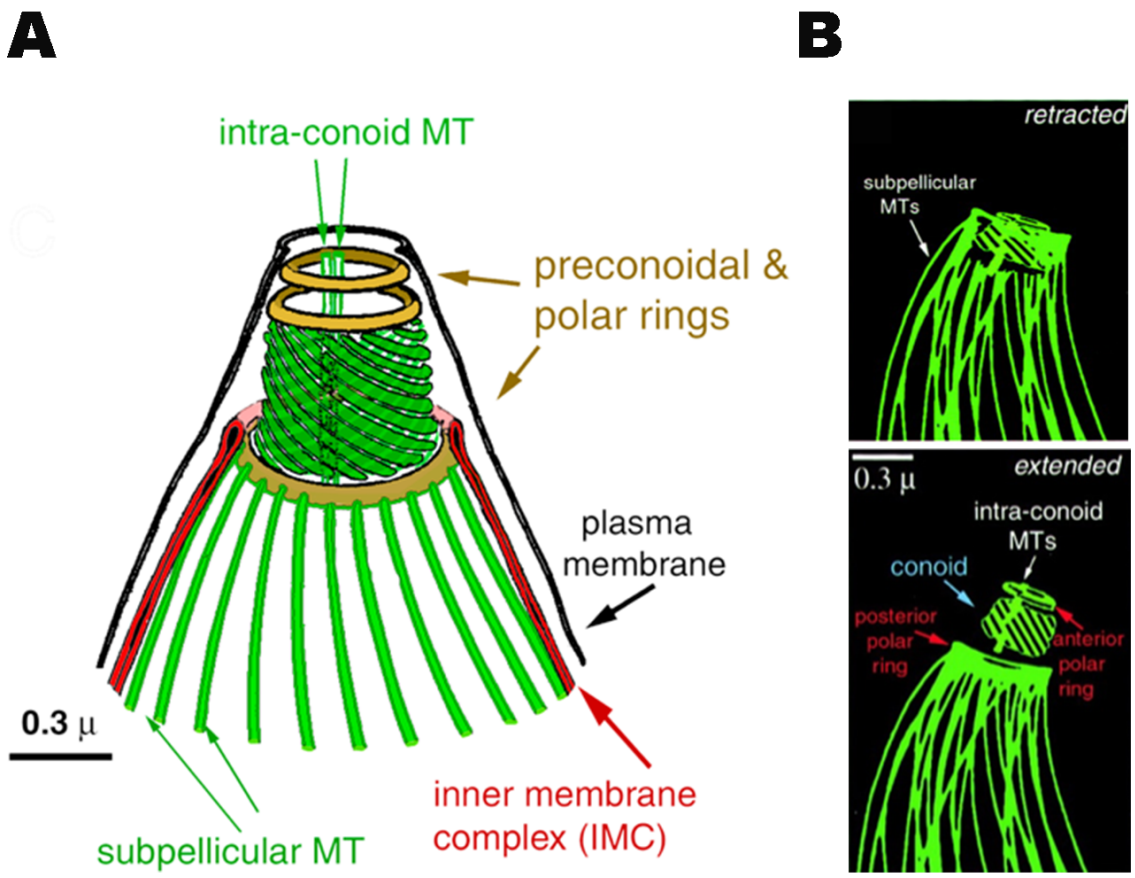

Figure 4. Drawing of *T. gondii* conoid and apical complex. A - Enlarged view of the apical complex cytoskeleton, showing the conoid (green), preconoidal, and polar rings (yelow), and two intra-conoid MTs (green). The conoid is formed of 14 fibers of tubulin (not MTs), 430 nm long, arranged in a left-handed spiral. Cytoskeletal elements, including the subpellicular MTs (green), are closely associated with the cytoplasmic face of the inner membrane complex (IMC). **B** - Cartoon of conoid movement. In extracellular parasites, the conoid alternates between the retracted and extended states (adapted from *(Hu et al., 2006; Hu, Roos, & Murray, 2002b)* with permission).

1.5.1.2. Micronemes

Micronemes are small ellipsoidal organelles located at the apical tip of the parasite (Figure 3). They represent the smallest secretory organelles in Apicomplexans with an internal dimension of 75 nm to 150 nm (Carruthers & Tomley, 2008; Gubbels & Duraisingh, 2012). They are circumscribed by typical membrane unit and have a homogeneous and electron-dense matrix due to the high protein content which are synthetize in endoplasmic reticulum (de Souza et al., 2010). The number of micronemes within one organism varies between species and developmental stages and is correlated with the parasite's motility, migration and invasion. Their contents are secreted in a regulated manner upon external or internal stimuli (Carruthers & Tomley, 2008).

The microneme proteins (MICs) secreted by the microneme play a basic role in the recognition, adhesion, and invasion of parasites into host cells during the invasion process. At the early stage of contact between parasites and host cells, MICs are first secreted from the apex of tachyzoites and facilitate adhesion through the recognition of receptors on the cell membrane of hosts, thus, they play an important role in the early stage of the invasion of host cells by parasites. Currently, there are at least 19 types of known MICs (Y. Wang & Yin, 2015).

1.5.1.3. Rhoptries

The rhoptries are the second key secretory organelle in *T. gondii*. They are larger than micronemes and unlike most secretory and lysosomal granules in mammalian cells, which are of a semi spheroidal shape, the mature rhoptries are pear or club-shaped with a bulbous base and an extended duct (neck), with one end attached to the very apical end of the parasite (Figure 3). In fact, the rhoptry necks are positioned at the extreme apex of the cell, providing a conduit for release of the organellar contents. Nevertheless, nothing is known about the determinants responsible for maintaining this shape (Beck et al., 2013; Dlugonska, 2008; Dubremetz, 2007; Gubbels & Duraisingh, 2012; Lamarque et al., 2012).

T. gondii tachyzoites possess a bundle of 8–12 rhoptries per cell (each of which is approximately 2 to 3 μm in length), occupy 10 to 30% of the total cell volume, and they are the only known acidified organelles in the parasite (Dlugonska, 2008; Dubremetz, 2007). These club-shaped secretory organelles are composed of two sub organellar domains, the bulbous rhoptry bodies and the duct-like rhoptry necks (Gilbert, Ravindran, Turetzky, Boothroyd, & Bradley, 2007). In fact, the rhoptry contents are not a random mixture but are sorted into discrete sub compartments, which are differentially released. Consequently, this segregation of rhoptry proteins into two domains has led to the use of two different denominations for them. ROPs proteins for those located in the bulgy posterior part and RONs proteins for those located in the neck of the organelle (Boothroyd & Dubremetz, 2008; Dubremetz, 2007; Gubbels & Duraisingh, 2012). Interestingly, most RON and ROP proteins are Apicomplexa specific and bear little homologies to higher eukaryotes proteins (Dubremetz, 2007).

These domains appear to carry out very different roles in host cell invasion and establishment of the intracellular niche for survival (Gilbert et al., 2007). The only circumstance in which rhoptries are known to secrete their contents is during the process of invasion into a host cell. The trigger for release is unknown, but it evidently depends on a direct recognition between the apical surface of the parasite and the receptor molecule (or molecules) on the host

cell (Boothroyd & Dubremetz, 2008). Proteins secreted from the rhoptry necks have been shown to be involved in the formation of the moving junction (MJ), a tight-junction structure, through which the parasite passes to invade the host. In contrast, proteins contained within the rhoptry body play a number of roles, such as helping to form the PV and parasitophorous vacuole membrane (PVM), acting as virulence factors, and manipulating host responses by altering host actin disassembly and invasion kinetics (Beck et al., 2013; Boothroyd & Dubremetz, 2008; Delorme-Walker et al., 2012; Gilbert et al., 2007; Gubbels & Duraisingh, 2012; Lei, Wang, Liu, Nan, & Liu, 2014).

1.5.2. Dense granules

Dense granules are electron-dense bodies found in all coccidian parasites. They acquired their name from their apparent density, when observed by transmission electron microscopy. These organelles resemble the secretory vesicles of mammalian cells, have a spherical shape and are distributed throughout the parasite cytosol. Their number varies amongst Apicomplexan parasites, in *T. gondii* there are approximately 20 dense granules, which are microspheres of approximately 200 nm in diameter (Cesbron-Delauw, 1994; de Souza et al., 2010; Gubbels & Duraisingh, 2012; Mercier, Adjogble, Däubener, & Delauw, 2005).

Unlike micronemes and rhoptry, they are not located at the apical end but are instead found throughout the cell, and their content is not secreted in the apical region of the parasite, instead it is typically secreted in the lateral and posterior regions of the parasite (de Souza et al., 2010). Moreover, their content is released immediately and constitutively after invasion and throughout intracellular replication, their proteins have been shown to have functions in the biogenesis and modification of the PV, in the regulatory functions on host cell signaling pathways and also play important roles in host cell manipulation (Braun, Brenier-Pinchart, & Yogavel, 2013; Fox, Sanders, Rommereim, Guevara, & Bzik, 2016; Gubbels & Duraisingh, 2012).

1.5.3. The inner membrane complex (IMC)

Apicomplexans are grouped with dinoflagellates and ciliates in the Alveolata infrakingdom. The unifying morphological characteristic of this group is the presence of alveoli: a highly specialized endomembrane system found beneath the plasma membrane. In

the apicomplexan parasites, this structure is referred to as the inner membrane complex (IMC) (Beck et al., 2010; Gould, Tham, Cowman, McFadden, & Waller, 2008; Keeling et al., 2005).

The IMC is itself composed of a flattened double membrane system termed alveoli (Figure 5), supported on the highly organized cytoplasmic network of intermediate filament-like proteins termed the subpellicular network (SPN) that lines the cytoplasmic side of the IMC membranes and by a final cytoskeletal layer composed of MTs emanating from the apical end of the parasite (Anderson-White et al., 2012; Harding & Meissner, 2014; Mann & Beckers, 2001; Morrissette, Murray, & Roos, 1997). Specialized cytoskeletal structures are present at the extreme anterior and posterior ends of the parasite which are known as the apical and basal complex, respectively (Anderson-White et al., 2012).

In *T. gondii* tachyzoites and bradyzoites, the alveolar sacs of the IMC are arranged as three rows of fused rectangular membrane plates, sutured together like a quilt, and capped by a single large alveolar plate at the apical end of the parasite (Figure 5) (A. L. Chen, Kim, Toh, Vashisht, & Rashoff, 2015a; Harding & Meissner, 2014)

In fact, the IMC can be divided in sub compartments defined by the composition of proteins within the alveoli as can be seen by IMC sub compartment proteins (ISPs). Inner Membrane Complex Sub-compartment 1 (ISP1) can be visualized at the apical cap of the IMC, while ISP2 and ISP4 localizes to the middle part of the IMC and ISP3 can be found at the central and basal part of the IMC membranes (Beck et al., 2010).

The understanding of the structure and components of the IMC has significantly increased with the recognition of various subdomains within the IMC (Figure 5) and its dynamic composition throughout cell division and maturation (Anderson-White et al., 2011; Beck et al., 2010).

In apicomplexan organisms, the IMC has important functions in motility, host cell invasion and intracellular replication. The outer leaflet of the IMC membrane acts as the anchor for the actin-myosin motor that powers parasite gliding and invasion. In addition, the IMC serves as the structural scaffold for the formation of daughter cells within the mother during asexual reproduction and for the organelle genesis and organelle partitioning (Anderson-White et al., 2011; A. L. Chen et al., 2015a; Harding & Meissner, 2014).

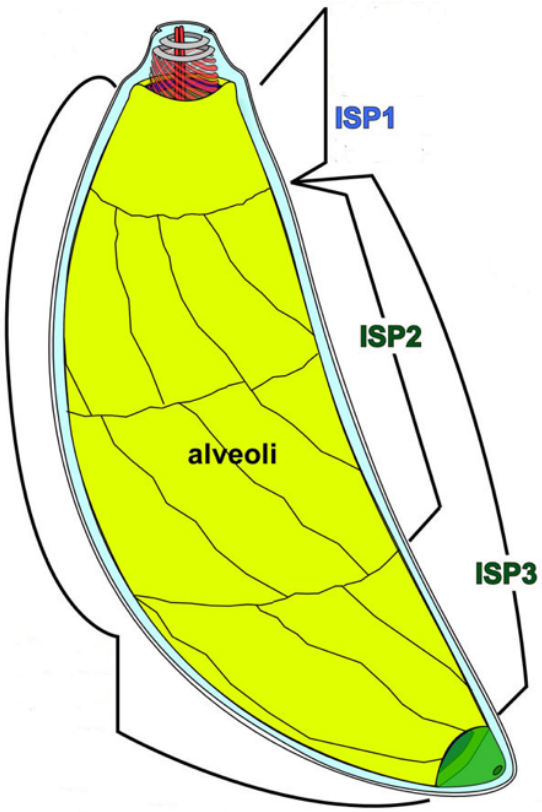

Figure 5. Schematic representation of IMC alveolar vesicles structures in the *T. gondii*. Directly under the plasma membrane lie the alveolar vesicles, shown in yellow. The most unique alveolar vesicle called the apical cap forms a cone around the parasite apex and three bands of rectangular, elongated vesicles fill in the remainder of the IMC below this cap. As marked, different proteins localize to different sections of the alveolar vesicles. (adapted from *(Anderson-White et al., 2012)* with permission).

1.6. Biological model

The phylum Apicomplexa consists of more than 5000 species, most of which are obligate intracellular parasites and include important human and veterinary pathogens, such as *Plasmodium* species, *Eimeria* species, *Toxoplasma, Neospora*, *Babesia*, *Besnoitia*, *Theileria* and *Cryptosporidium*. The defining feature common to all apicomplexans is the presence of the apical complex, from which secretory organelles release their contents during cell invasion (Jiménez-Ruiz, Wong, Pall, & Meissner, 2014; K. Kim & Weiss, 2004).

However, not all apicomplexan parasites are amenable to genetic manipulation due to difficulties in continuous *in vitro* cultivation, transfection or isolation of intracellular developmental stages in sufficient numbers for downstream molecular applications (Jiménez-Ruiz et al., 2014).

Among apicomplexans, *T. gondii* has emerged as the experimentally most tractable organism and is now used by many investigators as a genetic model to understand Apicomplexan biology (K. Kim & Weiss, 2004; Vinayak, Brooks, Naumov, & Suvorova,

2014). The ease with which *T. gondii* can be cultured, along with the ability to genetically manipulate the genome of the parasite and high transfection rates are strong arguments for using this parasite as a model (Sidik et al., 2016; J.-L. Wang et al., 2016). Moreover, methodology for classic and reverse genetics is well established, pathogenic stages are easily propagated and easily quantitated in the laboratory, the mouse animal model is well established and reagents for study of the host response as well as basic biology of the parasite are widely available (K. Kim & Weiss, 2004). Additionally, the development of several reverse genetic tools and several techniques based on the homologous recombination of exogenous DNA, has reinforced the role of *T. gondii* as a major model system for studying other apicomplexan parasites and also for conserved biological processes in less related organisms (Jiménez-Ruiz et al., 2014; Meissner, Breinich, Gilson, & Crabb, 2007). In this context, *T. gondii* has emerged as a major model for the study of apicomplexan biology (K. Kim & Weiss, 2004).

1.7. The lytic cycle of *T. gondii*

T. gondii has a complex life cycle involving different hosts and is dependent on fast responses, as the parasite reacts to changing environmental conditions. *T. gondii* causes disease by lysing the host cells that it infects and it does this by reiterating its lytic cycle, which consists of host cell invasion, replication inside a PV and egress (causing host cell lysis) to find another host cell to invade (Figure 6) (Black & Boothroyd, 2000; Blader, Coleman, Chen, & Gubbels, 2015; Hortua Triana, Márquez-Nogueras, Vella, & Moreno, 2018). Each step during the lytic cycle has to be precise, fast and effective and the parasite possesses specific molecules that become activated at the right moment. A strong body of evidence supports that intracellular calcium oscillations in the parasite precede the activation or stimulation of the specific steps of the lytic cycle. Both extracellular and intracellular Ca^{2+} pools contribute to cytosolic Ca^{2+} increases resulting in downstream signaling pathways that are decoded into critical biological functions of the parasite lytic cycle (Lourido & Moreno, 2015).

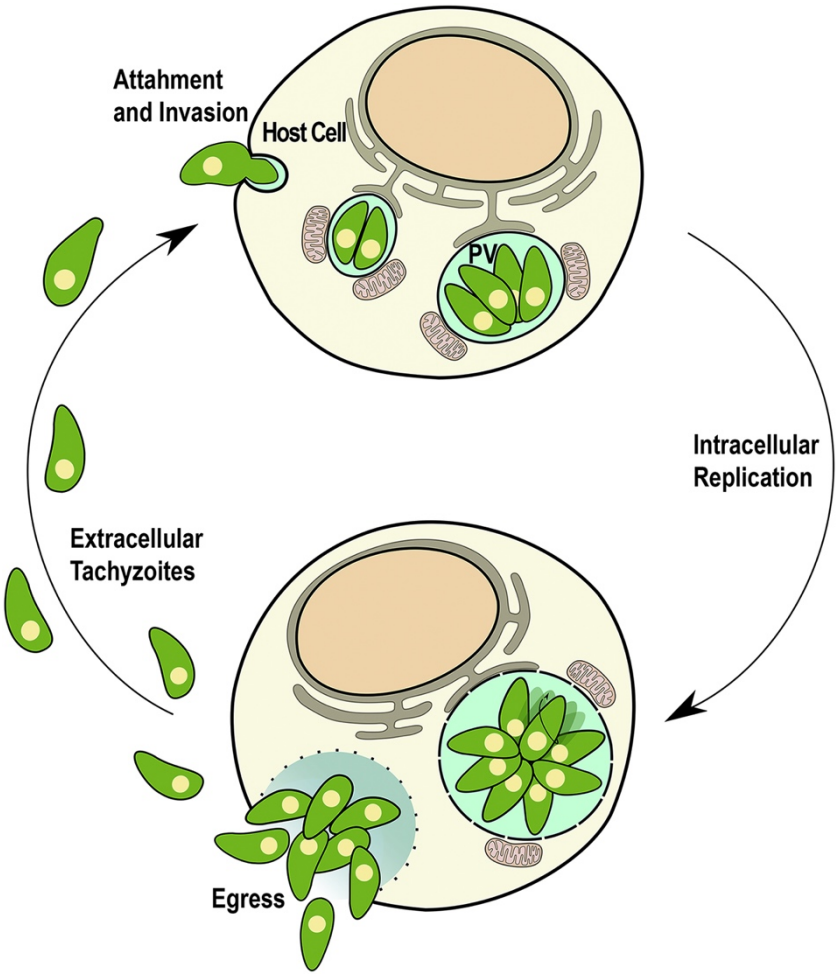

Figure 6. Schematic representation of *T. gondii* lytic cycle. Toxoplasma tachyzoites attach and invade host cells and form a parasitophorous vacuole (PV) where they reside and replicate by endodyogeny. The PV is surrounded by a PVM that allows small molecules to sieve through. After several rounds of replication, they rupture the PVM and the host cell membrane and egress followed by a short extracellular phase and invasion of another host cell (adapted from *(Hortua Triana et al., 2018)* with permission).

1.7.1. Host cell invasion

T. gondii invasion of host cells is an active, complex process composed of multiple steps that are well regulated and orchestrated. After initially attaching to the host cells, the parasite re-orientates itself to form a tight junction before actively penetrating its host (Carruthers & Boothroyd, 2007). In fact, simultaneous to the intimate apical attachment, the parasite re-orientates itself so the extruded conoid is facing the target cell and them forces the entry into a host cell by forming an electron-dense region, visible as a ring of contact between the parasite and host plasma membrane (Tyler, Treeck, & Boothroyd, 2011). Referred to as the moving junction, this is a central structure formed during invasion that starts at the apical pole and moves progressively to the posterior end of the parasite as it enters the cell. It serves as a support to propel the parasite into the PV, but is also thought to be involved in the formation and in

defining the biochemical composition of the PV membrane (Besteiro, Dubremetz, & Lebrun, 2011). After complete entry of the parasite, the moving junction disappears, the newly formed PV separates from the host cell plasma membrane and the parasite replicates and divides within it (Tyler et al., 2011). This whole invasion process is very rapid and completed within 15-30 seconds (Figure 7) (Morisaki, Heuser, & Sibley, 1995).

The surface of *T. gondii* is covered by a family of glycosylphosphatidylinositol-anchored surface antigens (SAGs) and SAG-related sequence proteins (SRS). Six of these proteins are expressed in tachyzoites (SAG1-3 and SRS1-3) and distributed evenly over the surface (Jung, Lee, & Grigg, 2004; Lekutis, Ferguson, Grigg, Camps, & Boothroyd, 2001). Both protein groups are implicated to participate in the initial attachment process through lectin-carbohydrate interactions. The frequency and overall distribution of SAG proteins all over the surface of the parasite positions those proteins ideally for low-affinity lateral interaction with the host cell surface. This circumstance would allow the parasites to glide along the surface of the host cell to scan for optimal invasion sites (Carruthers & Boothroyd, 2007). The invasion process is highly polarised since *T. gondii* solely uses its apical tip to initiate invasion. Due to the fact that SAG proteins are distributed regularly over the surface, another protein group, located at the apical surface and named micronemal proteins (MICs), was attributed with the firm apical attachment. Several MICs possess adhesive domains mediating protein-protein or protein-carbohydrate interactions. After the invasion process has been initiated, micronemes are secreted in a calcium-dependant manner through the apical tip, which strengthens the attachment. This strong apical attachment is also referred to as intimate attachment since the parasite and the host cell are only 6 nm apart (Carruthers & Boothroyd, 2007). Several MIC proteins such as MIC2 and AMA1 were implicated to play a role for intimate attachment (Brossier & David Sibley, 2005; Huynh & Carruthers, 2006; Mital, Meissner, Soldati, & Ward, 2005). At some point, proteins from rhoptries are exocytosed. Among these rhoptry proteins, several (RON2, RON4, RON5, and RON8) are part of a preformed complex that binds the previously secreted AMA1 microneme protein. Together, these proteins form the moving junction complex, which defines the parasite entry site on the host cell plasma membrane. As the invasion process progresses the moving junction migrates from the anterior to the posterior pole of the parasite. That penetration occurs by the parasite propelling itself forward, via actin-myosin-dependent motility, into the host plasma membrane. This causes an invagination of the plasma membrane resulting in the formation of the PV, which is the compartment that the parasite resides in throughout its time in the host cell (Carruthers & Boothroyd, 2007; Sweeney, Morrissette, LaChapelle, & Blader, 2010).

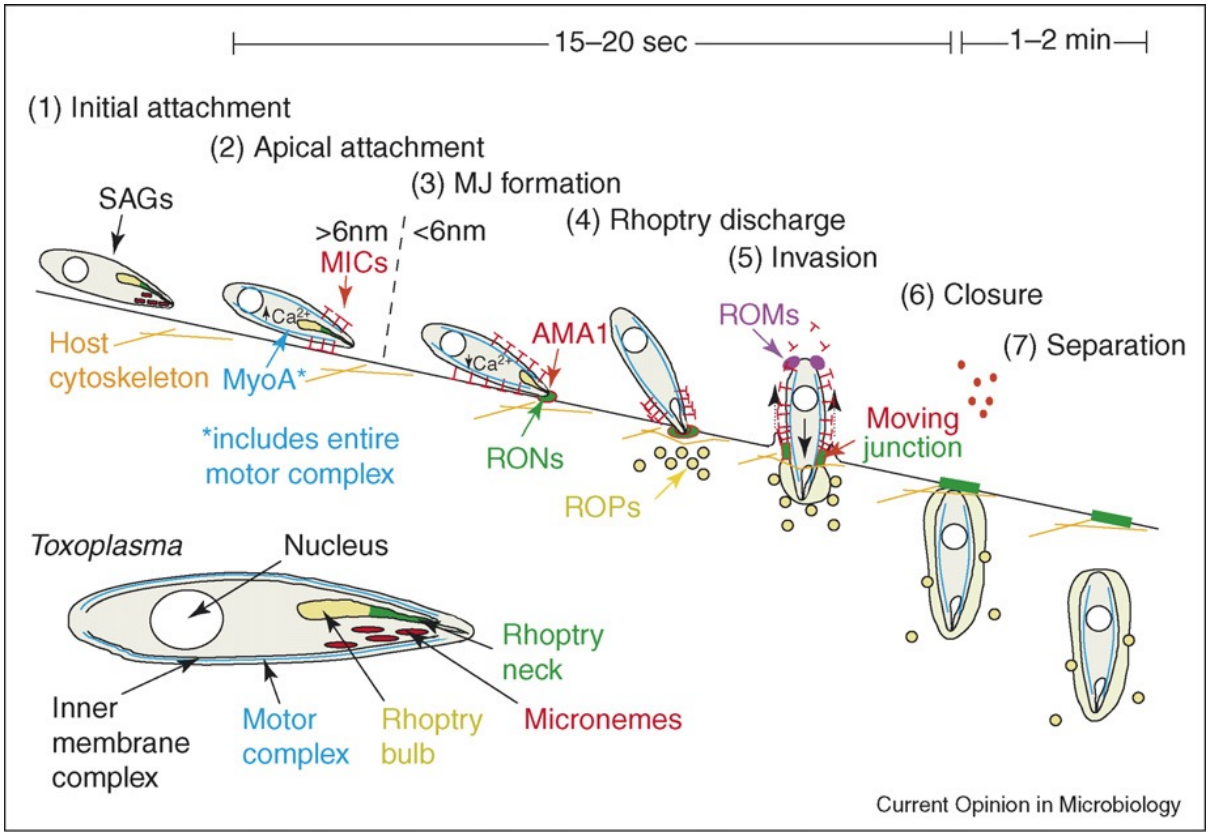

Figure 7. An integrated working model of Toxoplasma invasion. Toxoplasma invasion is depicted in seven steps. Initial attachment might be reversible and involves recognition of surface receptors by SAGs. This initial interaction precedes apical attachment, which involves the calcium-dependent deployment of MICs (red, T-shaped) and their accumulation on the apical surface. Although it is not specifically depicted in the model, conoid extrusion occurs at some point within (2–4). The moving junction (green and red ring) is formed by the release of RON proteins (green), which associate with microneme-derived AMA1 (red circles) during or following discharge. These proteins create an intimate binding interface of <6 nm, in the form of a small ring-like structure. Simultaneously or immediately thereafter, ROPs (gold coloured) are injected into the host cytoplasm at the invasion site. Some ROPs remain associated with small vesicles that fuse with the developing PVM during penetration, whereas other ROPs appear to remain soluble and might target to other sites within the host cell. The parasite actively penetrates by 'pulling' (lateral arrows) transmembrane MICs and/or the AMA1–RON ring posteriorly, thereby invaginating the host plasma membrane to create the PV. A rhomboid protease(s) (ROM; purple) appears to be responsible for shedding of the MICs from the posterior end. During invasion (5), the invaginating PV somehow traverses the host cytoskeleton (orange), perhaps involving some sort of anchoring to the cytoskeletal molecules (see text). Whereas the parasite accomplishes steps 2–5 in 15–20 sec, the final steps, closure and separation, are rate limiting and require 1–2 min to complete. Closure involves fission of the PVM and host plasma membrane and this step might be facilitated by the residual moving junction complex or other parasite and host proteins (adapted from *(Carruthers & Boothroyd, 2007)* with permission).

1.7.2. Cellular Division

Apicomplexan parasites replicate by the formation of daughter parasites within a mother cell. Three distinct replication mechanisms have been described on that parasites based on the

extent and timing of nuclear division before cytokinesis: these mechanisms are known as endodyogeny (Figure 8A), schizogony (Figure 8B) and endopolygeny (Figure 8D) (Francia & Striepen, 2014). *T. gondii* tachyzoites divide by endodyogeny, also known as internal daughter budding (Hu, Mann, Striepen, Beckers, et al., 2002a; Morrissette & Sibley, 2002b). During this mechanism, a single round of DNA replication and nuclear mitosis is followed by the assembly of two daughter cells and cytokinesis. In *T. gondii* endodyogeny there is the formation of two daughter cells within the mother parasite. These daughter cells are delimited by an inner membrane complex and associated subpellicular MTs, and each contains a complete set of apical organelles (conoid, rhoptries and micronemes), nucleus, mitochondrion, Golgi apparatus and apicoplast. Once daughter cells are mature, the maternal apical complex is disassembled and the daughter parasites emerge from the maternal plasma membrane (Morrissette & Sibley, 2002b).

The earliest events of cell division in *T. gondii* started with the enlargement and duplication of the Golgi apparatus duplicated late in G1 phase (Pelletier et al., 2002). Second, the centrioles migrate around the nucleus prior their division early in S1-phase, ensuring the polarity of the daughter parasites (Hartmann et al., 2006; Nishi, Hu, Murray, & Roos, 2008). Following this, DNA is replicated and the centrioles migrate back to the apical pole of the parasite. Synchronously with the nucleus, the apicoplast divides (Striepen et al., 2000). Late in S1 phase, the earliest components of the cytoskeleton are build and the internal daughter budding begins (Agop-Nersesian et al., 2010; Hu, 2008; Radke et al., 2001; L. G. Tilney & Tilney, 1996; White et al., 2004). The development of the conoid marks the formation of the cytoskeleton of the daughter cell (Hu et al., 2006). Concurrently, spindle poles and intranuclear MTs are formed. Afterwards, the assembly of the Inner Membrane Complex (IMC) of the daughter parasites is initialised (Mann & Beckers, 2001) and followed by distribution of organelles to the forming daughter buds. These organelles are the nucleus, apicoplast and endoplasmic reticulum (Hager et al., 1999; Hu, Mann, Striepen, Beckers, et al., 2002a; Striepen et al., 2000). Similar to the apicoplast, the mitochondrion is not autonomously replicated. During early replication the mitochondrion forms branches but its integration into the growing daughter parasites occurs late during replication (Nishi et al., 2008). The last step of cytokinesis involves separation of all organelles between the two daughter parasites and completion of IMC formation. Following, the apical organelles of the mother cell are degraded, and the plasma membrane of the mother cell is adopted by the daughter parasites. A residual body is left, which contains material such as maternal micronemes, rhoptries and parts of the mitochondrion (Nishi et al., 2008). The synthesis of the micronemes and rhoptries occurs *de novo* in the forming daughter parasites (Nishi et al., 2008). The generation time of *T. gondii* tachyzoites depends on the culture

conditions and varies between six and seven hours (Gubbels, White, & Szatanek, 2008; Radke et al., 2001).

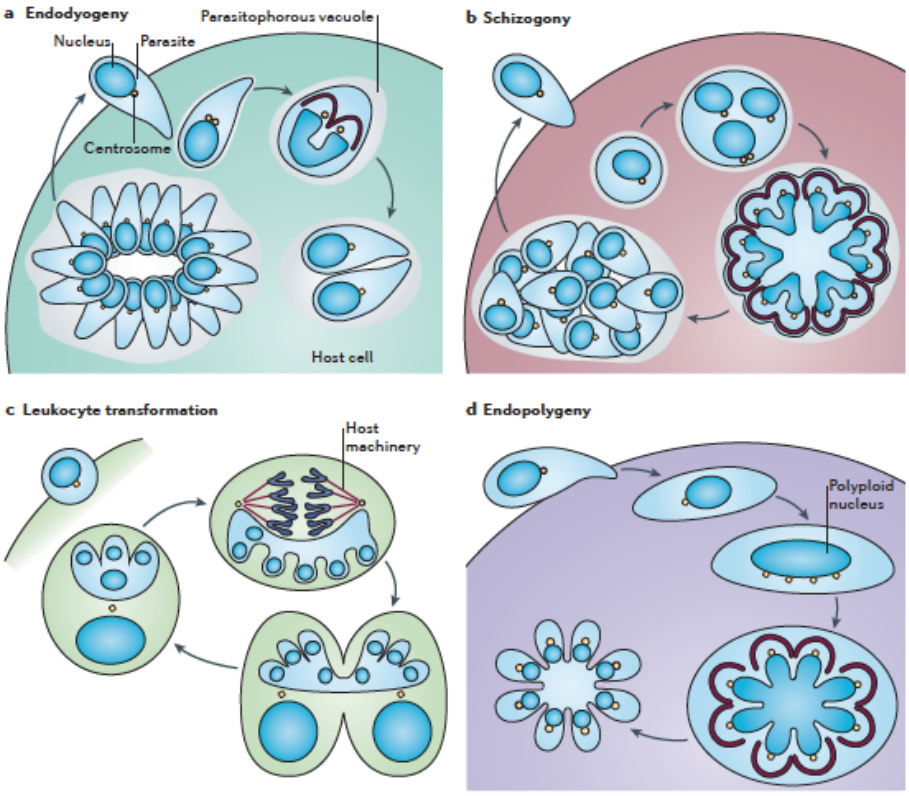

Figure 8. Replication cycles of different Apicomplexan species. **A - Endodyogeny**. Each DNA replication cycleis followed by mitosis and budding. **B - Schizogony**. Initially, nuclei multiply by asynchronous rounds of mitosis. The last round is synchronous for all nuclei and coincides with budding at the parasite surface. **C** - *Theileria spp.* sporozoites infect leukocytes after the bite of an infected tick. The parasite transforms the leukocytes and divides by exploiting the mitotic and cytokinetic machinery of the host. **D - Endopolygeny**. DNA replicates without nuclear division, using multiple synchronous mitotic spindles. The final mitotic cycle coincides with budding and the emergence of a new generation of merozoites. Some Apicomplexan parasites, such as *Toxoplasma spp.* and *Plasmodium spp.*, replicate in a parasitophorous vacuole, whereas *Theileria spp*. and *Sarcocystis spp.* are free in the host cell cytoplasm (adapted from *(Francia & Striepen, 2014)* with permission).

1.7.3. Egress

After tachyzoites multiplication, once the host cell cytoplasm space has been filled with a large PV, and the host cell nutrients become limiting, it is possible that the parasites sense extrinsic signals, including host K^+, to promote egress and invade neighbouring cells to ensure their survival. Egress occurs very quickly, relies on calcium signalling and gliding motility, and it is necessary that the PVM and the host cell plasma membrane to be lysed (Frénal & Soldati-Favre, 2009; Roiko & Carruthers, 2009). Additionally, the intracellular Ca^{2+} level increases through

release from intracellular compartments (Lovett & Sibley, 2003). This leads to activation of the parasites motility machinery and secretion of egress effector proteins including the pore forming proteins such as perforin-like protein (TgPLP1) (Kafsack et al., 2009) or protein proteases like subtilisin1 (TgSUB1) (X. W. Zhou et al., 2005). Disruption of the PVM is followed (Roiko & Carruthers, 2009) by the release of free parasites into the cytoplasm. Parasite and host proteins such as the calcium-dependent protease Calpain1 and TgPLP-1 act to disrupt host cytoskeleton and host plasma membrane (HPM) (Chandramohanadas et al., 2009; Kafsack et al., 2009; Kafsack & Carruthers, 2010). Interestingly, and although to a lesser extent, egress from the host cell can also occur through a non-active mechanism, in which rupture of the host cell membrane would be a consequence of mechanical forces applied on the host cell membrane as the volume of the PV increases upon parasite division (Lavine & Arrizabalaga, 2008). Once the HPM is destroyed, parasites use their motility system to escape the lysed host cell.

2. Cellular Cytoskeleton

The cytoskeleton underlies many aspects of cell physiology, including mitosis, cell division, volume control, cell stiffness, cell polarity and extracellular matrix patterning. (Bezanilla, Gladfelter, Kovar, & Lee, 2015). In eukaryotes cell cytoskeleton is composed of three different types of fibers: actin filaments, MTs and intermediate filaments (IFs) (Figure 9) (Mostowy & Cossart, 2012).

The actin filaments determine the shape of the cell's surface and are involved in cell locomotion. The major component of the actin cytoskeleton is actin, an ATP-binding protein that exists in two forms in the cell: monomers (globular-actin or G-actin) and filaments (filamentous-actin or F-actin). Actin filaments are assembled by the reversible endwise polymerization of monomers, and polymerization stimulates ATP hydrolysis and release of inorganic phosphate (Pi). In microfilaments, long polymerized chains of actin are intertwined in a helix, generating filaments with a diameter of ~7 nm. Actin filaments are polar, with a plus end, where monomers preferentially assemble (see the figure 9), and a minus end, where monomers preferentially disassemble (Mostowy & Cossart, 2012; Welch & Mullins, 2002).

IFs provide mechanical strength to the cell with many subcellular organelles and macromolecules attached to the network. They are individual proteins assembled to form a tetrameric subunit composed of two antiparallel half-staggered coiled-coil dimers. Next, eight tetrameric subunits associate laterally to form a unit length filament (ULF). Individual ULFs join end-to-end to form short filaments, and these grow into longer filaments by longitudinally annealing to other ULFs and existing filaments (see the figure 9). IFs have a diameter of ~11

nm, and they are non-polar because of the antiparallel orientation of tetramers (Mostowy & Cossart, 2012).

MTs, integrating the MT cytoskeleton, are structures that display enormous plasticity that allows them to intervene in many crucial cellular functions such as cell division, motility, intracellular transport, and various cell signaling pathways. MTs are cylindrical structures that are built from 13 parallel protofilaments made of α-tubulin and β-tubulin heterodimers. Each tubulin monomer of ~50 kDa binds one GTP molecule, and the α-tubulin GTP is locked in the interface between the α-tubulin and β-tubulin; only the β-tubulin GTP undergoes hydrolysis. The tubulin dimers assemble in a head-to-tail manner, producing MT polymers with a diameter of ~25 nm. Similarly to actin, MTs are polar, with one end (the plus end) growing faster than the other end (the minus end). MTs can assemble and disassemble at the plus end (see the figure 9), through a process known as dynamic instability; disassembly is known as catastrophe and rapid growth is known as rescue (Desai & Mitchison, 1997; Mostowy & Cossart, 2012).

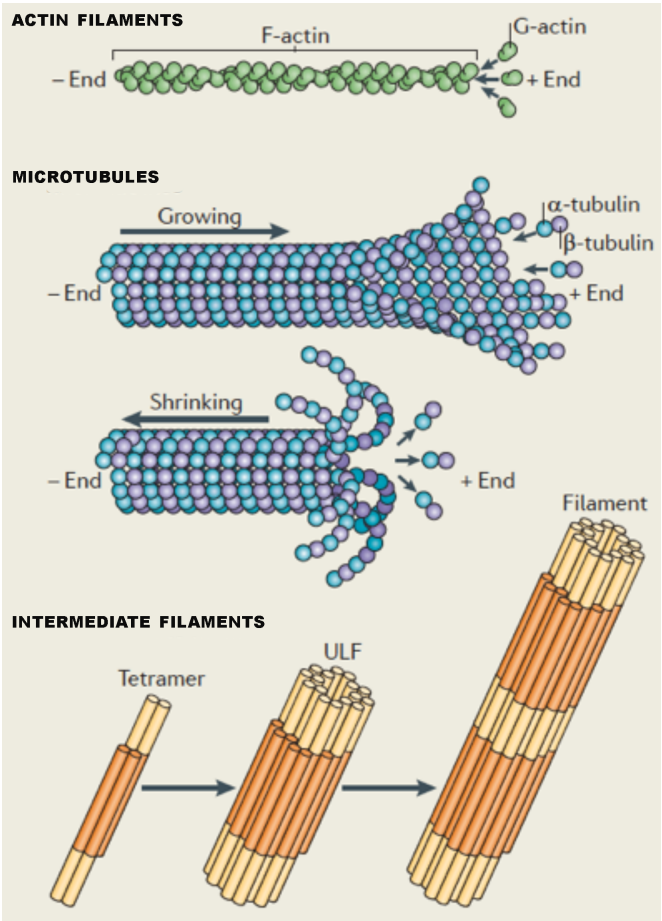

Figure 9. The cytoskeletal components, actin filaments, MTs, and intermediate filaments. Actin filaments are assembled by the reversible polymerization of actin monomers. **MTs** are cylindrical structures that are built from 13 parallel protofilaments made of α-tubulin and β-tubulin heterodimers. **Intermediate filaments** are individual proteins assembled to form a tetrameric subunit composed of two antiparallel half-staggered coiled-coil dimers (adapted from *(Mostowy & Cossart, 2012)* with permission).

2.1. Microtubule Cytoskeleton

MTs are non-covalent cytoskeletal polymers found in all eukaryotic cells, playing a major role in cell migration, intracellular trafficking (serving as tracks for transport of vesicles, organelles, other cytoskeletal elements, protein assemblies and mRNA), control of cell shape, spindle assembly and chromosome motion during mitosis. They are tubular structures constituted of heterodimers of α-tubulin and β-tubulin, nucleated in organized structures, MTOCs, through interaction with γ-tubulin; with a minus-end capped and anchored at the MTOC, and a plus-end generally localized at the periphery of the cell, forming polarized structures (Amos & Schlieper, 2005; Fletcher & Mullins, 2010; R. Li & Gundersen, 2008).

2.1.1. Microtubule structure

MTs are the most rigid of the cytoskeletal filaments and have the most complex structure. Their outer diameter is ~25 nm, whereas length can vary from tens of nanometers to tens or even hundreds of micrometers, frequently spanning the whole cell (Schaap, Carrasco, de Pablo, MacKintosh, & Schmidt, 2006).

They are polymers consisting of α-tubulin and β-tubulin heterodimers, which have the molecular mass of ∼100 kDa and are 8 nm long. The MTs assemble by addition of the αβ-tubulin heterodimers at either end or disassemble by loss of them. The tubulin dimers stick to each other in a head-to-tail manner, forming a protofilament. *In vivo* MTs are composed of 10–15 protofilaments (usually 13 in mammalian cells) that associate laterally to form a 24 nm wide hollow cylinder (Figure 10). In the MT wall, longitudinal contacts are established between tubulins arranged head to tail along the protofilament axis, whereas adjacent protofilaments interact laterally. The number of protofilaments of MTs polymerized *in vitro* has been found to vary between 11 and 17, depending on buffer conditions. The head-to-tail association of the αβ heterodimers makes MTs polar structures, and they have different polymerization rates at the two ends. In each protofilament, the αβ heterodimers are oriented with their β-tubulin monomer pointing towards the faster-growing end (plus end) and their α-tubulin monomer exposed at the slower-growing end (minus end). In the animal cell, the MT minus ends are embedded into MT organizing center (MTOC) called centrosome and the plus ends are exposed to the cytosol (Desai & Mitchison, 1997; Pierson, Burton, & Himes, 1978; Schaap et al., 2006).

A third tubulin isoform, γ-tubulin, functions as a template for the correct assembly of MTs. On addition of a new dimer at the plus end, the catalytic domain of α-tubulin contacts the nucleotide exchangeable site (E site) of the previous β-subunit and becomes ready for hydrolysis; the plus end generally has a minimum GTP cap of one tubulin layer that stabilizes the MT structure. When this GTP cap is stochastically lost, the protofilaments splay apart and the MT rapidly depolymerizes. During or soon after polymerization, the tubulin subunits hydrolyse their bound GTP and become non-exchangeable. Thus, the MT lattice is predominantly composed of GDP–tubulin, with depolymerization being characterized by the rapid loss of GDP–tubulin subunits and oligomers from the MT plus end. At the minus end, contact is made between the E site of the new dimer and the catalytic region of the last subunit at the end; therefore, no GTP cap should be present (Conde & Cáceres, 2009).

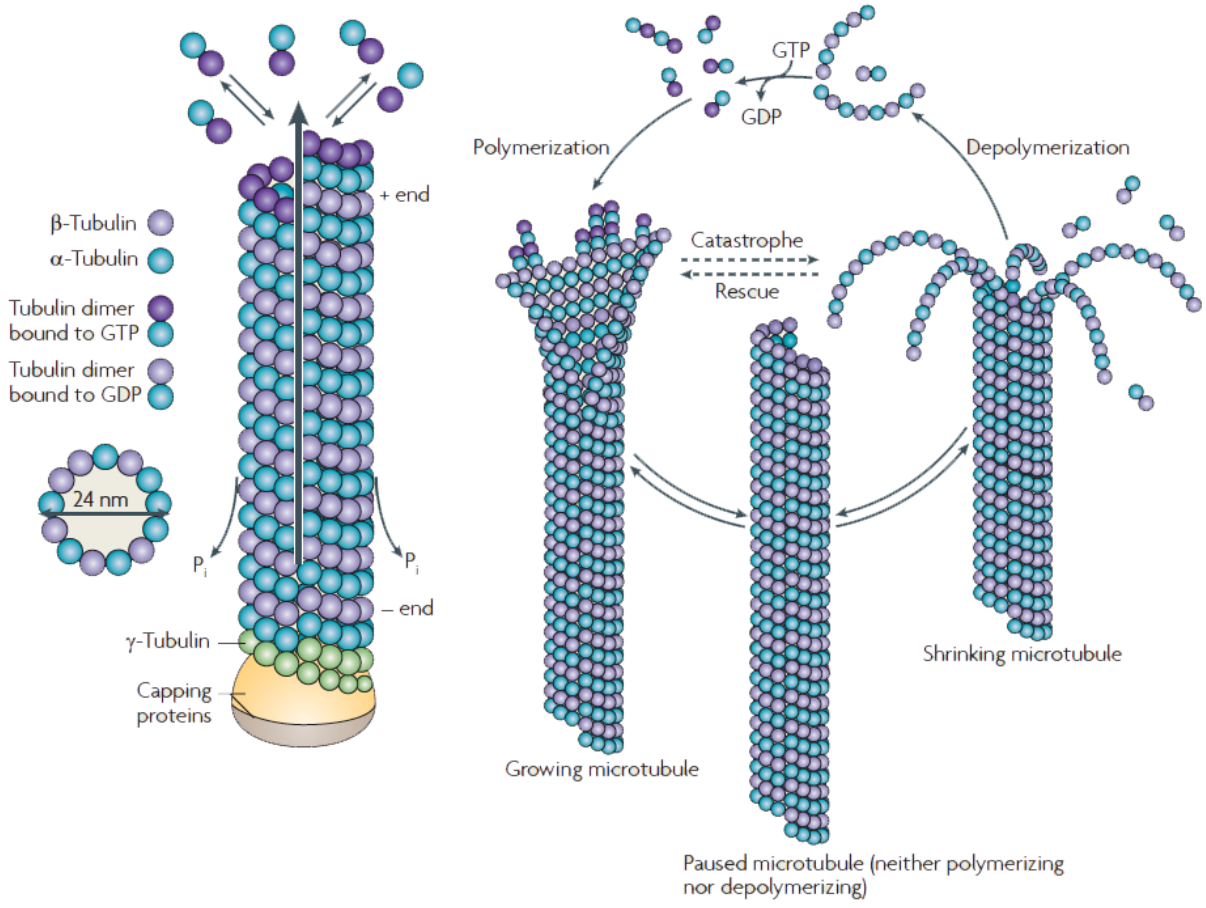

Figure 10. MT structure. Mts are polarized structures composed of α- and β-tubulin heterodimer subunits assembled into linear protofilaments. A single MT is comprised of 10–15 protofilaments (usually 13 in mammalian cells) that associate laterally to form a 24 nm wide hollow cylinder. The head-to-tail association of the αβ heterodimers makes MTs polar structures, and they have different polymerization rates at the two ends. In each protofilament, the αβ heterodimers are oriented with their β-tubulin monomer pointing towards the faster-growing end (plus end) and their α-tubulin monomer exposed at the slower-growing end (minus end). The lateral interaction between subunits of adjacent protofilaments has been described as a B-type

lattice with a seam (long arrow). A third tubulin isoform, γ-tubulin, functions as a template for the correct assembly of MTs (adapted from *(Conde & Cáceres, 2009)* with permission).

2.1.2. Tubulin heterodimer structure

The protomer unit of the MT system, the αβ-tubulin heterodimer, is a stable ~110 kDa protein complex, composed of two subunits with ~40% polypeptide sequence identity and a high degree of conservation between species (Nogales, Wolf, & Downing, 1998a). In fact, α- and β-tubulin are so similar in structure that the two kinds of monomer subunits cannot be distinguished except at very high resolution (Amos & Schlieper, 2005). The roughly spherical subunits are assembled in tandem with the front of α-tubulin facing the back of β-tubulin, resulting in a polar peanut-like arrangement (Figure 11) (Nogales, Wolf, & Downing, 1998a). Each tubulin has a nucleotide-binding site (GTP-binding): an inactive non-exchangeable site (N-site, intradimer) on α-tubulin, which is suggested to stabilize αβ-tubulin dimers during their biogenesis, and an active exchangeable site (E-site) on β-tubulin, which is stimulated to hydrolyse GTP upon αβ-tubulin incorporation into MT lattices at the plus ends (Georgiev, 2003). The overall heterodimer structure revealed that α- and β-tubulins adopt rather globular conformations and form a dimer in which the two proteins exhibit a curvature of ~12˚relative to each other. The degree of curvature is very similar between tubulin in which GTP or GDP is bound to β-tubulin (Nawrotek, Knossow, & Gigant, 2011).

Both αβ-tubulin show a compact structure formed by a core of two interacting β sheets surrounded by twelve α helixes and with three functional domains. The N-terminal domain responsible for the interaction with the GTP nucleotide; the intermediate domain, where antimitotic agents such as taxol are bound; and the C-terminal domain, involved in the interaction with MT-binding proteins and motor proteins (Nogales, Wolf, & Downing, 1998a).

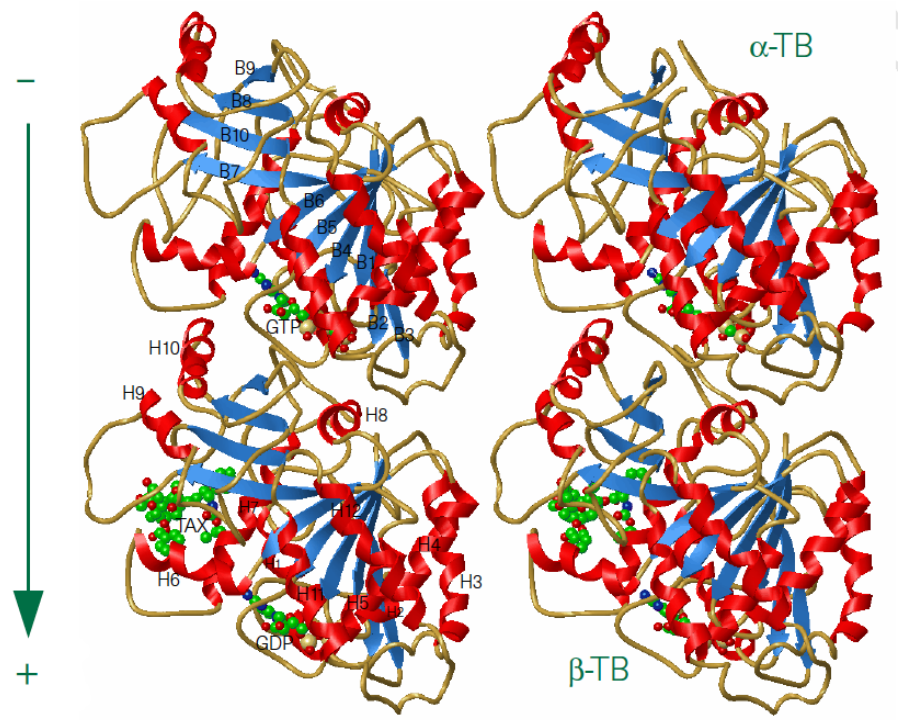

Figure 11. Ribbon diagram of the tubulin dimer showing a stereo front view from the putative outside of the MT. α-tubulin with bound GTP (top), and β-tubulin containing GDP and taxotere (bottom). Labels for strands (in the α-subunit) and helices (in the β-subunit) are included. The arrow indicates the direction of the protofilament and MT axis. (adapted from *(Nogales, Wolf, & Downing, 1998a)* with permission).

2.1.3. Microtubule dynamics

MTs have a complex behaviour with some MTs being in a growing phase, others being stationary and some being in a state of disassembly. This characteristic dynamic behaviour, named dynamic instability, was detected by Mitchison and Kirschner in 1984 (Mitchison & Kirschner, 1984). Membrane-bound organelles and trafficking routes use this dynamic instability network to organize and connect intracellular compartments: the nucleus, the ER, the Golgi apparatus and the endosomes/lysosomes. Dynamic instability is also very important to establish and maintain cell polarity during cell migration: inhibition of MT dynamics with nocodazole reduces cell migration into a wound in monolayer cultures (Liao, Nagasaki, & Gundersen, 1995).

The stochastic switch between growth to shortening (catastrophe) and shortening to growth (rescue) (Figure 11), and its mechanic basis has been explained by the "GTP-cap model". The model proposes that GTP-tubulin is mainly present at the growing end of the MTs and is thought to stabilize the structure and to maintain the association between protofilaments (Heald & Nogales, 2002). Over time, GTP at the E-site become hydrolysed to GDP due to the GTPase activity of β-tubulin. As result, the MT body contains mainly GDP-tubulin, which is unstable

as GDP-tubulin dissociates more readily than GTP-tubulin and as it induced a strain in the curvature of individual protofilaments. This explains why MTs quickly disassemble since their GDP-tubulin becomes exposed. Furthermore, it also defines why the MT end undergoes catastrophe when GTP hydrolyses faster than the addition of GTP tubulin heterodimers (Heald & Nogales, 2002; Mitchison & Kirschner, 1984).

Moreover, the GTP-tubulin was found also in older parts of the polymer, along the MT (GTP-tubulin remnants). In this case, when depolymerization occurs, they behave as a GTP cap to promote rescue events. Besides this intrinsic regulation (the presence of the GTP-cap and GTP islands), the regulation of MT dynamics depends also of an extrinsic regulation through MT associated proteins (MAPs) that bind to MTs, and through MT post-translational modifications (PTMs) (Dimitrov et al., 2008).

Being so, the end of a MT that terminates with β-tubulin is more dynamic than the other end, which has an *α*-tubulin monomer as its final subunit. In cells, MTs usually grow out from MTOC from which the more dynamic end, known as the plus end, is able to grow and shrink, whereas the minus end may not be able to change. If both ends are free, as *in vitro*, assembly and disassembly can occur from either end, although at different rates. MTs can continue to grow as long as the free tubulin concentration is above a critical level. The critical concentration at a minus end is somewhat higher than at a plus end and thus minus ends tend to stop growing first (Amos & Schlieper, 2005).

In addition to the dynamic instability, the MTs also have another dynamic behaviour, both *in vitro* and *in vivo*, the treadmilling. This behaviour is characterized by the flow of subunits from the plus end to the minus of the free MTs without a significant change in the length of the MTs; resulting from the different critical concentrations of the tubulin subunits at both polymer ends (Margolis & Wilson, 1998).

In summary, the intracellular MT dynamics (dynamic instability and treadmilling) critically relies on a tightly controlled pool of soluble αβ-tubulin dimers in the cytoplasm (Tian et al., 2010a).

2.1.4. Microtubule nucleation

MT nucleation is the process in which several tubulin molecules interact to form a MT seed. The de novo formation of MT polymers occurs at specific structures called MTOCs. MTOCs prevent the random formation of MTs throughout the cell by restricting nucleation to specific locations. The MT minus ends are embedded within the MTOC, while the plus ends

extend into either the cytoplasm or the nucleus. The structure of the MTOCs varies considerably between species and cell types. Despite the variation in MTOC morphology, all MTOCs rely on γ-tubulin, a homologue of α-tubulin and β-tubulin, for nucleating MTs. γ-tubulin was first discovered in *Aspergillus nidulans* genetic screens as a suppressor of a β-tubulin mutation, and it was subsequently found localized at all MTOCs. Purification of γ-tubulin from animal and yeast cells showed it to be part of larger complexes, which can directly nucleate MT growth *in vitro*. γ-tubulin is essential for normal MT organization in every organism in which it has been studied, and it is nearly ubiquitous throughout the eukaryotes. Moreover, it is also involved in nucleation from non-MTOC sites within cells, such as nucleation that occurs through the chromosome-mediated nucleation pathway, and in plants, which lack centrosome-like structures, suggesting that it is critical for the initiation of all new MTs *in vivo*. It exists in a large complex that did not include α-tubulin or β-tubulin and that as at least six other proteins: γ-tubulin complex protein 2 (GCP2), GCP3, GCP4, GCP5, GCP6 and NEDD1. This complex had approximately 2.2 MDa and a striking ring shape in electron micrographs, leading to the name γTuRC.

The γTuRC functions as a minus end capping factor for MT nucleation. Nevertheless, the complex is also present in the cytosol but must be recruited to the MTOC to become active. This is despite the fact that it can nucleate MTs *in vitro* (Figure 12). These would then serve as adaptors for tubulin binding to form the 13 protofilaments of a MT. This way, the γ-tubulin complex not only nucleates MTs but also stabilizes their minus ends by capping them (Job, Valiron, & Oakley, 2003; Kollman, Merdes, Mourey, & Agard, 2011; Roostalu & Surrey, 2017; Teixidó-Travesa, Roig, & Lüders, 2012) (Kollman et al., 2011).

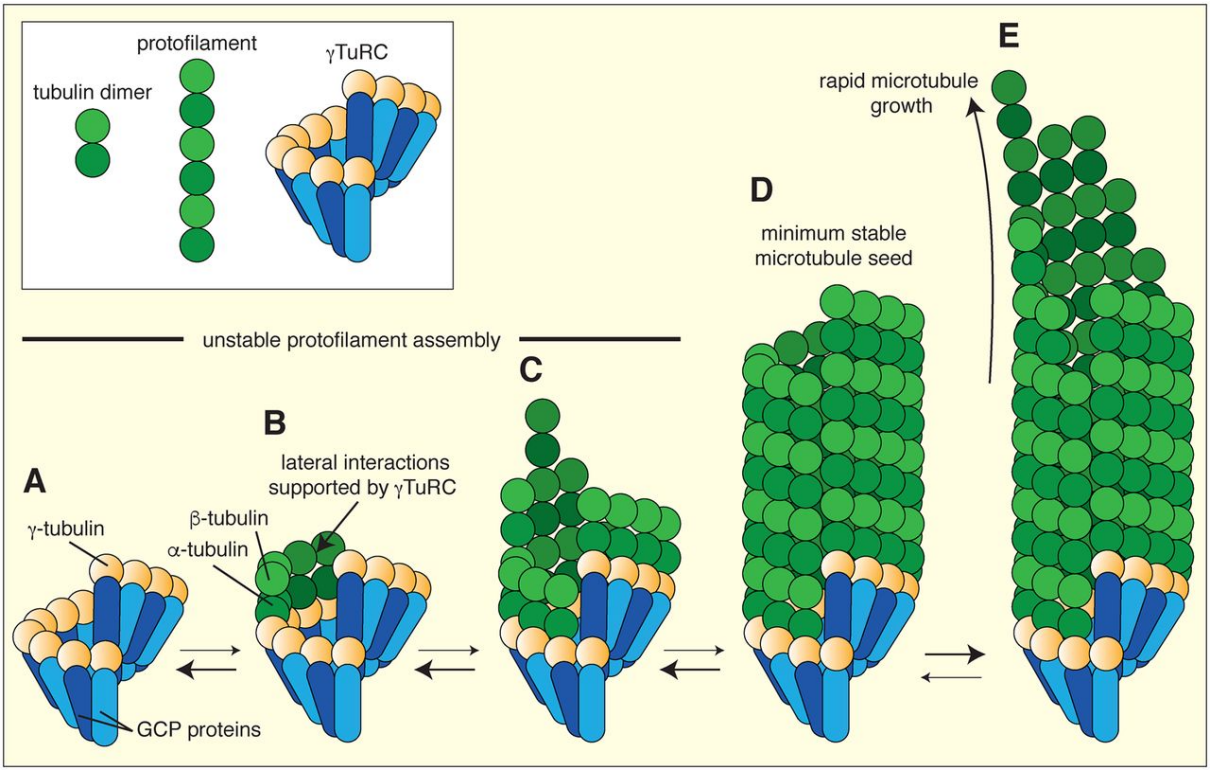

Figure 12. Templated MT nucleation. A - γ-tubulin molecules (yellow) within the γ-TuRC are positioned in a single-turn helix via their binding to GCP proteins (blue). **B** - γ-tubulin molecules bind to incoming α/β-tubulin dimers from the cytosol and this is thought to promote the lateral interaction between the α/β-tubulin dimers as they grow into protofilaments (a protofilament is a single end-to-end chain of tubulin dimers). **C** - MTs assembly progresses slowly through an unstable stage where disassembly is more likely than continued assembly (as indicated by the thickness of the two-way arrows). **D** - Assembly is thought to reach a stable stage, where a MT seed containing sufficient tubulin dimers has formed (although the size of this stable seed remains unclear). **E** - Once the stable seed has formed, MT polymerisation is favored and can progress rapidly (From *(Tovey & Conduit, 2018)* with permission).

2.1.4.1. Centrosome

As their name implies, centrosomes have long been thought to have a central role in many aspects of cell organization. More than a hundred years ago, it was recognized that centrosomes form the two poles of the bipolar mitotic spindle, which separates chromosomes to daughter cells during animal cell division. If embryos from certain species were induced to assemble too many centrosomes, multipolar spindles could form, leading to the mis-segregation of chromosomes and usually embryo death. However, some embryos survived for long enough to develop into abnormal ‘monsters’, prompting Boveri to famously speculate that the disturbance to homeostasis resulting from such chromosome imbalance might predispose cells to malignant transformation (Azimzadeh & Bornens, 2007; Bornens, 2012; Doxsey, 2001; Conduit, Wainman, & Raff, 2015).

We now know that centrosomes contain a pair of centrioles at their core, each having a ninefold symmetric structure (Figure 13). In animal cells, the centrioles exhibit a complex behaviour during the cell cycle, often forming a cilium in quiescent cells and a centrosome in proliferating cells. Cilia have many important functions in cells, and their dysfunction has been linked to many human pathologies. Centrosomes are formed when centrioles assemble and organize a matrix of pericentriolar material around themselves. The pericentriolar material contains hundreds of proteins, including important cell cycle regulators and signalling molecules, and many proteins that help to organize and nucleate microtubules, explaining why centrosomes function as the dominant MTOCs in many cell types. Through the microtubules that they organize and the proteins that they recruit, centrosomes seem to play an important part in many cell processes (Azimzadeh & Bornens, 2007; Bornens, 2012; Doxsey, 2001; Conduit, Wainman, & Raff, 2015).

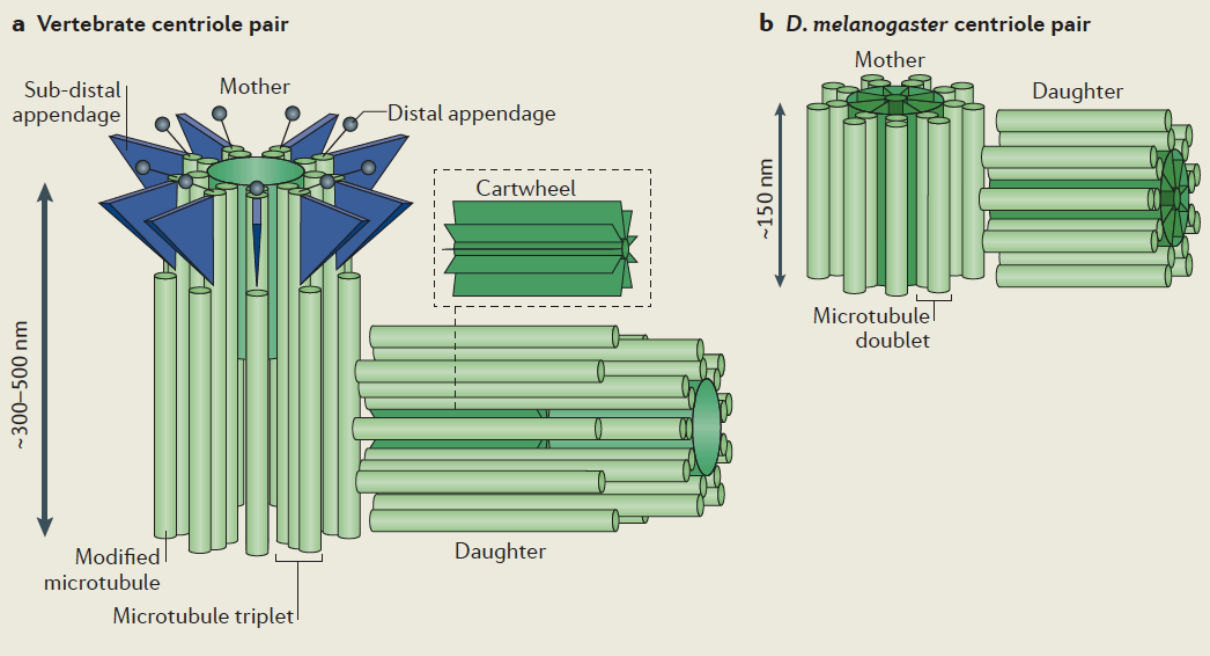

Figure 13. A schematic illustration of centriole structure. In most vertebrate cells (see the figure, part a), new centrioles (called 'daughter centrioles') are assembled around a central cartwheel structure (shown in dark green), which sets the ninefold symmetrical arrangement of the microtubules (light green). The older centriole of the pair (the 'mother') usually loses its central cartwheel and is often decorated with distal (grey) and sub-distal (blue) appendages. In vertebrate centrioles, the microtubules are usually arranged as triplets, which often become doublets towards the distal end. The new daughter centriole is formed at right angles to the mother during the S phase of the cell cycle, and the centrioles remain in this tightly apposed 'engaged' configuration until the late stages of mitosis, when they disengage, allowing the daughter centriole to mature into a mother that is now competent to form its own daughter and to organize its own pericentriolar material. In some species, such as worms and flies, centrioles are simpler in structure. A typical Drosophila melanogaster centriole pair is illustrated here (see the figure, part b): the centrioles are usually shorter than vertebrate centrioles and are usually composed of microtubule doublets rather than triplets; the mother centriole lacks appendages; and the cartwheel is present in both mother and daughter centrioles. (From *(Conduit, Wainman, & Raff, 2015)* with permission).

2.2. Microtubule associated proteins (MAPs)

The stability and dynamic behaviour of the cytoskeleton are regulated by structural MT associated proteins (MAPs). The MAPs that regulate assembly of the MTs can be categorized functionally as stabilizers, destabilizers (including severing proteins), capping proteins, and bundlers/cross-linkers. Other MT binding proteins include motors that use MTs as tracks for intracellular transport and cytoplasmic linker proteins (CLIPs), which anchor organelles to MTs to promote cell organization. Some MAPs are cytoskeletal integrators (i.e., proteins that connect to other components of the cytoskeleton). In addition, some proteins involved in signal transduction, translation, and metabolism also bind MTs or other components of the cytoskeleton. (Goodson & Jonasson, 2018).

2.2.1. Stabilizers

Stabilizers are proteins that promote polymerization and/or slow depolymerization. Although these two activities are similar, they are not identical: A protein could potentially stabilize MTs by inducing a pause (inhibiting shortening but also inhibiting growth) without promoting polymerization. In practice, it can be difficult to distinguish between these two activities. Examples of these proteins are the MAP1, MAP2, tau and MAP4 (Amos & Schlieper, 2005; Desai & Mitchison, 1997; Goodson & Jonasson, 2018).

2.2.2. Destabilizers

The destabilizers are proteins that shift a pool of dynamic MTs toward free subunits by one or more mechanisms. They are divided in: sequestering proteins which depolymerize MTs indirectly by binding free tubulin subunits and preventing them from polymerizing (as the stathmin); Tip destabilizers, that act by directly attacking the sensitive MTs tip (as the kinesins); and MTs severing proteins which use the energy of ATP to cut MTs into pieces (as the Katanin, spastin, fidgetin) (Cassimeris, 2002; Sharp & Ross, 2012).

2.2.3. Microtubule plus end trafficking proteins

They are proteins that adhere to the MTs plus end; having the potential to regulate the MTs dynamic. They can stop both dimer association or dissociation, control the growing orientation and also the MTs interaction with the components of the cellular cortex. There are several MT plus end tracking proteins (+TIPs), among them are the CLIPs, which promote MT growth and regulate dynein-dynactin localization, and cytoplasmic linker protein-associated proteins (CLASPs), which stabilize specific subsets of MTs on reception of signalling cues. CLIPs and CLASPs interact and cooperate to direct the MT network, thereby regulating cellular asymmetry (Galjart, 2005).

Another group of +TIPs are the End binding as the End binding 1 (EB1), a canonical +TIP, specific not to plus ends but to growing ends, as it will track growing minus ends if presented with the opportunity, at least *in vitro*. That protein modulates the MTs dynamics and interactions with intracellular organelles. The EB1 regulates the dynamics and structure of MTs assembly, stimulating spontaneous nucleation and growth of MTs, and promoting both catastrophes (transitions from growth to shrinkage) and rescues (reverse events) (Goodson & Jonasson, 2018; Vitre et al., 2008).

The EB1 family of MT-associated proteins is conserved in eukaryotes. Members of the EB1 family have a conserved domain structure, with a single N-terminal calponin homology domain (CH domain), followed by a less conserved, unstructured region, a short coiled-coil region and the EB1-like domain. CH domains are found in many cytoskeletal and signalling proteins. Proteins with more than one CH domain were shown to be able to bind actin. However, the CH domain of EB1 binds to MTs *in vitro*; probably through electrostatic interactions. Also, full-length EB1 was shown to bind directly to polymerized tubulin. The C-terminus of EB1, with the coiled-coil and EB1-like domain regions, forms a four-helix bundle, and requires dimerization of the protein for its proper structure. This structure is responsible for the binding of several interacting proteins, for example adenomatous polyposis coli or p150glued, a component of the dynactin complex (Berrueta et al., 1998; Bu & Su, 2003; Juwana et al., 1999).

2.2.4. Microtubule motors proteins

The MT motor proteins are a class of molecular motors that can move along the MTs, that power a wide variety of motile processes within eukaryotic cells, including the beating of cilia

and flagella and intracellular trafficking along MTs. Among them are the kinesin, dynein and their accessories such as dynactin complex (Goodson & Jonasson, 2018).

2.3. Tubulin superfamily

Tubulin heterogeneity is the result of two mechanisms. Primary, tubulins are encoded by multigene families in most organisms, including the angiosperms, and the differences between the tubulin isotypes are sufficient to account for some if not all of the electrophoretic heterogeneity. Second, both α-tubulin and β-tubulin may be modified by one or more posttranslational mechanisms that can produce charge heterogeneity; producing different tubulin isoforms.

2.3.1. Tubulin Isotypes

In a large number of organisms, including animals, plants, fungi and protist, both α-tubulin and β-tubulin are encoded by multigenic families. So, the expression of the diverse isotypes lead to the increase of it diversity (Ludueña, 1993).

The tubulin isotypes are quite similar, in terms of its amino acid sequence, in fact the main differences between them are found in the C-terminal region of the proteins. This region is rich in acidic amino acid residues being a primary target of the post-translational modifications and also responsible for the interaction with several MAPs (Ludueña, 1993).

Since the different isotypes of α-tubulin and β-tubulin can copolymerize, the cells might determine the dynamic properties and functions of its MTs network in part by altering the relative amounts of the different tubulin isotypes (Panda, Miller, Banerjee, Ludueña, & Wilson, 1994). Additionally, there are evidence that different isotypes may undergo distinctive post-translational modifications and that the different isotypes also have a differential ligand binding properties with MAPS (Ludueña, 1993).

2.3.2. Tubulin post-translational modifications

Tubulin post-translational modifications (PTMs) are directly linked to the regulation of MT dynamics. They participate in this regulation by recruiting MAPs or by affecting the behaviour of motor proteins, being mostly linked to MT stability (de Forges, Bouissou, & Perez, 2012). In fact, recent work has shown that PTMs of the tubulin building blocks mark

subpopulations of MTs and selectively affect downstream MT-based functions. In this way, the tubulin modifications generate a "code" that can be read by MT-associated proteins in a manner analogous to how the histone code directs diverse chromatin functions (Verhey & Gaertig, 2007).

MTs can acquire a variety of evolutionarily conserved PTMs including poly-glutamylation, polyglycylation, detyrosination (and related D2 modification), acetylation, phosphorylation and palmitoylation. In most cases, the modification enzymes act preferentially on tubulin subunits already incorporated into MTs. Most PTMs are enriched on MTs that are "stable" as defined by their slow subunit turnover and resistance to drugs that depolymerize MTs such as nocodazole. Nevertheless, at least some PTMs do not affect polymer dynamics by changing the intrinsic properties of MTs. Rather, an emerging hypothesis is that tubulin modifications specify a code that dictates biological outcomes through changes in higher-order MT structure and/or by recruiting and interacting with effector proteins (Verhey & Gaertig, 2007).

2.3.2.2. Acetylation

While most known tubulin PTMs occur on the outer surface of polymerized MTs, acetylation has been identified on lysine 40 (K40) of α-tubulin, a residue exposed at the inner MT surface, i.e. in the MT lumen (L'Hernault & Rosenbaum, 1985; LeDizet & Piperno, 1987). So, the enzyme catalysing K40 acetylation needs to penetrate the narrow MT lumen to find its substrate (Janke & Montagnac, 2017).

Acetylated MTs have been considered to be stable, long-lived MTs. However, until recently there was little information about whether the longevity, of these MTs, is the cause or the consequence of the acetylation. Current advances suggest that this PTM helps the MT lattice to cope with mechanical stress, thus facilitating MT self-repair. These observations now shed new light on the structural integrity of MTs, as well as on the mechanisms and biological functions of tubulin acetylation (Janke & Montagnac, 2017).

2.3.2.2. Polyglutamylation

Tubulin polyglutamylation can act as a direct regulator of MT functions, for example it regulates MT-dynein interactions and long glutamate side chains on tubulin provide a signal for MT severing by spastin (Kubo, Yanagisawa, Yagi, Hirono, & Kamiya, 2010; Lacroix et al.,

2010; Suryavanshi et al., 2010). Tubulin polyglutamylation is a completely reversible PTM. In mammalian cells, the length controlling of the polyglutamate side chains on tubulin is critical for neural survival. Polyglutamylase enzymes have recently been identified as belonging to the tubulin tyrosine ligase-like (TTLL) protein family. Deglutamylase enzymes are members of cytosolic carboxipeptidases (CCP) family. The maintenance of the correct levels of tubulin polyglutamylation, by the coordinated action of polyglutamylases and deglutamylating enzymes, is crucial for the cell (Kimura et al., 2010; Rogowski et al., 2010; van Dijk et al., 2007).

2.4. Tubulin folding pathway

The maturation of tubulin heterodimers is a complex multistep process involving the interaction of tubulins with molecular chaperones and tubulin cofactors (Figure 13) (Gonçalves, Tavares, Carvalhal, & Soares, 2010).

In the begin of the tubulin folding pathway, the cytosolic chaperonin-containing TCP1 (CCT) captures the tubulin folding intermediates, with significant native-like domain structures, either directly from ribosomes or from the hetero-hexameric chaperone prefoldin. It is now well established that the CCT complex mediates the folding, driven by ATP binding and hydrolysis, of a wide range of newly synthesized proteins and that tubulins (α, β and γ) and actin are its quantitatively major substrates (Gonçalves et al., 2010; Lewis, Tian, biology, 1997, 1997; Vainberg et al., 1998).

After interacting with CCT, tubulins follow two different folding pathways: α-tubulin is captured by the tubulin cofactor B (TBCB) and β-tubulin by the tubulin cofactor A (TBCA). Then, tubulin cofactors E (TBCE) and D (TBCD) capture α-tubulin and β-tubulin, respectively. The two pathways converge and α-tubulin, β-tubulin, TBCE and TBCD form a supercomplex. Tubulin cofactor C (TBCC) interacts with this complex and promotes GTP hydrolysis by β-tubulin and the consequent release of α/β- tubulin-GDP heterodimers. Upon exchange of GDP by GTP these heterodimers become competent to polymerize into MTs (Fontalba, Paciucci, Avila, & Zabala, 1993; Gonçalves et al., 2010).

In summary, the biogenesis and degradation of the αβ-tubulin heterodimer are non-spontaneous processes that rely on five highly conserved tubulin cofactors (TBCs) proteins: TBCA, TBCB, TBCC, TBCD, and TBCE (Lewis et al., 1997; Lundin, Leroux, & Stirling, 2010).

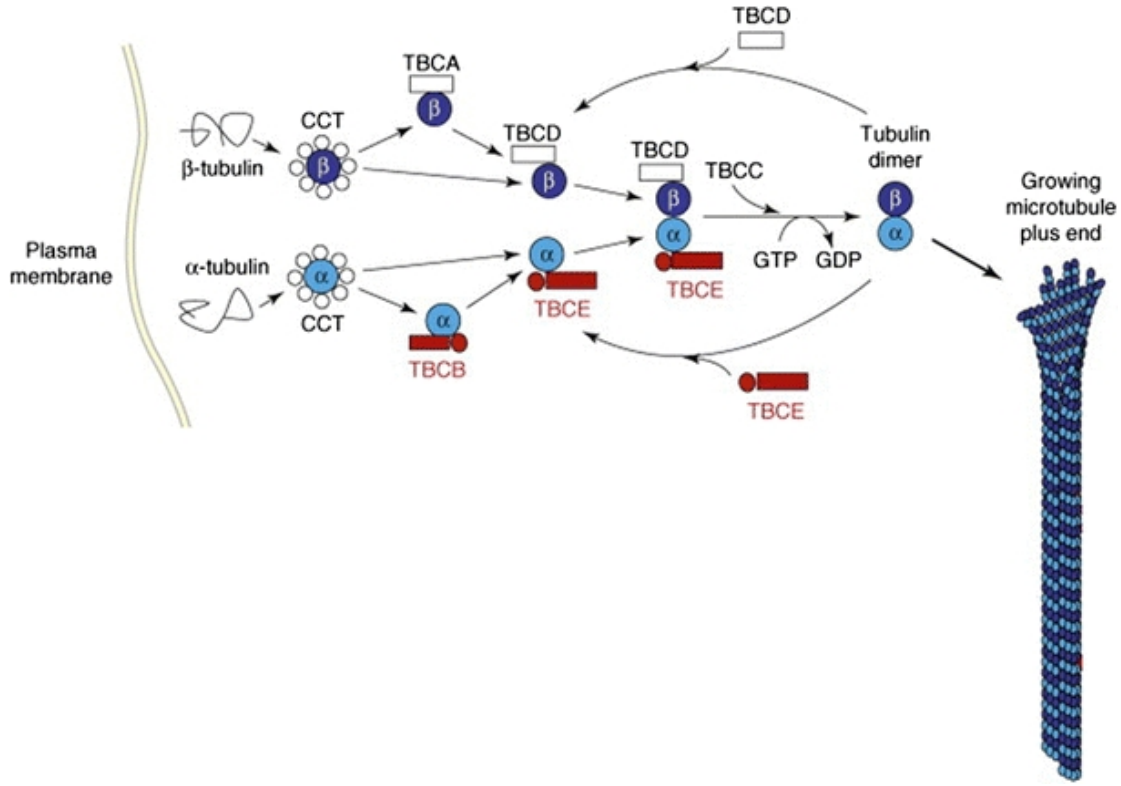

Figure 14. Schematic illustration of the tubulin folding pathway. **CCT** - denotes cytosolic chaperonin, a ring-like protein complex involved in folding of tubulin subunits. Tubulin cofactors B and E (TBCB and TBCE) are involved in the folding and dimerization pathway of α-tubulin monomers (light blue circle), while cofactors A and D (TBCA and TBCD) fulfil this function for β-tubulin monomers (dark blue circle). Note that TBCE (in addition to TBCD) can also dissociate tubulin dimers into α- and β-tubulin monomers (shown by backward directed arrows), leading to a reduction of the tubulin dimers pool available for MTs polymerization (adapted from *(Szolajska & Chroboczek, 2011)* with permission).

2.4.1 Tubulin folding cofactors

Tubulin cofactors, originally discovered as proteins required for proper tubulin folding and heterodimer formation (Tian et al., 1997), have also been shown to participate in tubulin dissociation (Bhamidipati, Lewis, & Cowan, 2000; H. Martín, Rodríguez-Pachón, Ruiz, Nombela, & Molina, 2000a; Tian, Bhamidipati, Cowan, & Lewis, 1999), transitory tubulin storage (Keller & Lauring, 2005), and tubulin degradation processes (Bartolini et al., 2005; Kortazar et al., 2007), all of which suggest that these proteins, in addition to their original role as tubulin folding machines, might be the clue to understanding the MT dynamic.

In mammals, five proteins have been identified in the folding and association of α- and β-tubulin polypeptides (Lewis et al., 1997): TBCA, TBCB, TBCC, TBCD, and TBCE. These cofactors have been implicated in tubulin dimer formation, as well as in MT dynamics, through the *in vivo* and *in vitro* regulation of tubulin heterodimer assembly and disassembly (Gao, Vainberg, Chow, & Cowan, 1993; Tian et al., 1997).

2.4.1.1. Tubulin cofactor A (TBCA)

The mammalian TBCA protein was initially identified as a protein that integrate the tubulin folding pathway *in vitro* (Gao et al., 1993). It was shown that TBCA binds to β-tubulin intermediates derived from CCT, and that, in a next step β-tubulin is transferred to TBCD (Melki, Rommelaere, Leguy, Vandekerckhove, & Ampe, 1996)(Melki et al., 1996; Tian et al., 1996). TBCA seems to function as a β-tubulin chaperone, capturing and storing β-tubulin monomers after dissociation reactions, serving as a reservoir of still functional β-tubulin polypeptides and thereby as a buffer protecting the cell from an unbalanced α/β-tubulin ratio (Fanarraga et al., 1999; Kortazar et al., 2006; Melki et al., 1996). In *in vitro* folding assays, the TBCA isn't essential to the α/β-tubulin heterodimer assemble (Tian et al., 1996), but its addition to the reaction, led to a significantly increase of the β-tubulin, tubulin heterodimer and β-tubulin bound to TBCA (Fanarraga et al., 1999).

Although TBCA is not essential *in vitro* to the folding of the α/β-tubulin heterodimer, the TBCA knockdown in human cell lines (HeLa and MCF-7), by RNAi gene silencing, has a lethal effect, with cells presenting a slightly disturbed MT cytoskeleton. This may reflect the decrease of β-tubulin steady-state levels detected in this cell lines upon transfection, that are accompanied also by a decrease of the steady-state levels of α-tubulin. Although it is still not clear how TBCA knockdown affects the MT cytoskeleton, it is probably a consequence of a decrease in the pool of α/β-tubulin heterodimers competent to polymerize (Nolasco, Bellido, Gonçalves, Zabala, & Soares, 2005). The overexpression experiments of TBCA and Rbl2p (*Saccharomyces cerevisiae* TBCA orthologue) have failed to demonstrate a clear phenotype. In contrast, overproduction of Alp31 (*Schizosaccharomyces pombe* TBCA orthologue) is toxic to the cell, resulting in the disappearance of intact MT structures associated with cell polarity defects, but no effects were founded at the cellular tubulin levels (Lopez-Fanarraga, Avila, Guasch, Coll, & Zabala, 2001). Meanwhile, the knockout of the TBCA gene is not lethal to budding yeast and in fission yeast under normal growth conditions(Radcliffe & Toda, 2000).

2.4.1.2. Tubulin cofactor B (TBCB)

The TBCB is a conserved α-tubulin interacting protein involved in the ‘‘postchaperonin’’ tubulin folding pathway, that also collaborate in the regulation of MT dynamics (Kortazar et al., 2007; Lewis et al., 1997; Lopez-Fanarraga et al., 2001). The protein was initially purified

from a crude extract of bovine testis tissue and migrated with an apparent mass of 130 kDa upon gel filtration, and consisted of a single polypeptide of 38 kDa upon analysis by sodium dodecyl sulfate-polyacrylamide gel electrophoresis (SDS-PAGE) and 27,561 kDa by mass spectrometry (Tian et al., 1997). Although it is not essential to the α/β-tubulin heterodimers assembly, the TBCB greatly enhances the efficiency of α-tubulin folding *in vitro* (Tian et al., 1997). In humans, TBCB has been implicated in cancer (Vadlamudi et al., 2005), neurodevelopment malformations (Tian et al., 2010a), schizophrenia (Martins-de-Souza et al., 2009) and neurodegenerative processes (W. Wang et al., 2005).

This protein is composed of two functional structural domains connected by a coiled-coil segment, composed of leucine-rich repeats (LRR) (Figure 15). At the N-terminus, TBCB contains a ubiquitin-like (UbL) domain. This domain is spherical, behaves as a monomer of about 14 kDa and is a ubiquitous protein interaction domain present in many unrelated proteins. The C-terminal domain is a cytoskeleton associated protein glycine-rich (CAP-Gly) characteristic of +TIP proteins that are implicated in essential cellular processes such as chromosome segregation, establishment and maintenance of cell polarity, intracellular organelle and vesicle transport, cell migration, intracellular signalling and oncogenesis (S. Li et al., 2002; Weisbrich et al., 2007). This domain is also globular, three antiparallel β-sheets and one α-helix, as represented by the *Caenorhabditis elegans* F53f4.3 protein CAP-Gly domain (Carranza et al., 2013; S. Li et al., 2002). The unique α-helix is preceded by a disordered stretch of 17 residues, and the last six or seven amino acid residues protrude from the globular domain. CAP-Gly domains serve as recognition domains for EEY/F-COO^- peptides (Carranza et al., 2013; Weisbrich et al., 2007). Furthermore, the structural prediction for the last nine amino acid residues of human TBCB is that of a disordered peptide (EEDYGLDEI) protruding from the globular domain which apparently are similar to the EEY/F-COO^- element characteristic of EB proteins, CLIP-170, α-tubulin and are also able to interact with its own CAP-Gly domain groove, controlling its autoinhibition (Carranza et al., 2013). Finally, the TBCB CAP-Gly domain has a conserved motif (DEI/M-COO^-), which is required for TBCE–TBCB heterodimer formation and thus for tubulin dimer dissociation (Carranza et al., 2013).

TBCB is a soluble cytoplasmic protein in interphase cells and localizes at the centrosome and at the basal body of the primary cilium. As mitosis progresses towards metaphase, TBCB is often localized to spindle MTs. In anaphase most of this cofactor has progressively disappeared from the centrosome and is concentrated on the midbody MTs. By the end of telophase, TBCB is apparently absent from the centrosome, concentrating at the midbody. These localizations show that TBCB can bind to MTs. However, this binding is indirect,

occurring through the interaction of TBCB with a MT binding protein like EB1. Since EB1 is known to stabilize the plus ends of MTs, its interaction with TBCB explains how TBCB is able to promote a MT catastrophe when overexpressed, by sequestering EB1 from MT plus ends (Carranza et al., 2013).

Interestingly, the TBCB interacts with the protein p21-activated kinase 1 (Pak1), a serine/threonine kinases, enriched in MTOCs, that play an important role in mitosis and MT dynamic (Vadlamudi et al., 2005). Pak1 directly phosphorylates the TBCB *in vitro* and *in vivo* on serines 65 and 128 and colocalizes with TBCB on newly polymerized MTs and on centrosomes. By other side, the TBCB interacts with the GTPase-binding domain of Pak1 and activates Pak1 *in vitro* and *in vivo*. Therefore, the Pak1 phosphorylation is necessary for normal TBCB function, since it plays an essential role in MT regrowth after depolymerization (Vadlamudi et al., 2005). Curiously, the TBCB was overexpressed and phosphorylated in breast tumours, indicating that may be there is a coordinately deregulated of Pak1 and TBCB in human cancers (Vadlamudi et al., 2005).

Moreover, the TBCB is efficiently nitrated, mainly on tyrosine 64 and 98, and that nitration attenuates the synthesis of new MTs. Furthermore, the nitration also antagonizes signalling-dependent phosphorylation of TBCB, whereas optimal nitration requires the presence of functional Pak1 phosphorylation sites, thus providing a feedback mechanism to regulate phosphorylation-dependent MT regrowth. Thus, the phosphorylation and nitration of TBCB may play a role in maintaining a constant balance between growth and regrowth of MTs (Rayala et al., 2007).

TBCB was additionally identified as an interacting factor of gigaxonin. This protein is mutated in human giant axonal neuropathy (GAN), an autosomal recessive neurodegenerative disorder, characterized by the presence of generalized cytoskeletal abnormalities, including few MTs and accumulated IFs. Gigaxonin binds to TBCB and controls its degradation via the Ubiquitin-Proteasome Pathway, a critical function to the maintenance of the MT network. Interestingly, the TBCB overexpressing could recapitulate the MT pathology in GAN cells, moreover in COS7 cells the TBCB overexpressing lead to the MT network disappearing, what can be restored by the gigaxonin coexpression. These results suggest that gigaxonin can play an essential role in cytoskeletal organization and dynamics (W. Wang et al., 2005) and TBCB is an important protein in the development of the nervous system (Lopez-Fanarraga et al., 2001; 2007). Curiously, TBCB is predominantly expressed during neurogenesis, its knockdown enhances axonal growth and, in contrast, excess of TBCB, a feature of GAN, leads to MT depolymerization, growth cone retraction and axonal damage followed by neuronal

degeneration. These results suggest that TBCB regulates the axonal growth, probably by the regulation of the MT dynamics, acting in combination with the TBCE, to regulate the pool of tubulin dimers available for polymerization (Lopez-Fanarraga et al., 2007). This author also suggests that TBCB might participate in the biology of cilia, for instance, contributing to the growth or renewal of the MT in these structures, based on an abundance of TBCB in the basal bodies of cilia in the respiratory tract (Lopez-Fanarraga et al., 2007).

Recently, TBCB was found to associate with the CCT, probably recognizing α-tubulin still bound to CCT (Carranza et al., 2013). The proposed mechanism predicts that α-tubulin is released from CCT and bound to TBCB ensuring that the α-tubulin monomer would never aggregate. Later, the monomeric tubulin subunit would be transferred to TBCE for dimer assembly and incorporation into growing MTs or would be transferred to the degradative pathway involving the proteasome, if not properly folded (Voloshin et al., 2010).

Later, it was described that TBCB interacts with the PIWIL2, aka HILI, a member of PIWI subfamily containing PIWI and PAZ domains, that played crucial roles in self-renew of stem and germ cells, RNA silencing and translational regulation in different organisms during evolution and is ectopically expressed in different cancer cells. HILI regulates MT dynamics through two pathways. First, HILI interacts with TBCB and promotes the interaction between HSP90 and TBCB, inhibiting its interaction with gigaxonin, and suppressing the gigaxonin mediated ubiquitination and degradation of TBCB. Second, HILI inhibits TBCB phosphorylation induced by PAK1. The up-regulation of TBCB expression and down-regulation of TBCB phosphorylation level induced by HILI overexpression suppress MT polymerization. Thus, HILI can promote tumour cells proliferation, migration and invasion via TBCB (Figure 16) (Tan et al., 2017).

In *S. cerevisiae* the TBCB homologues, Alf1p, is able to associate with both nuclear and cytoplasmic MTs *in vivo*, this localization being dependent on the CLIP170 domain. While overexpression of Alf1p has no effect in wild-type strains, a null mutation of yeast TBCB is lethal, only in combination with an α-tubulin mutation (Tian et al., 1997). In *S. Pombe* the TBCB homologues is the Alp11, a gene essential for cell viability and its overproduction results in cell lethality, plus the disappearance of cell MT (Radcliffe, Hirata, Vardy, & Toda, 1999).

In Drosophila, the studies confirm that TBCB is required for tubulin dimerization and for tubulin heterodimer dissociation, affecting the levels of both α- and β-tubulins and dramatically destabilizing the MT network in different fly tissues. Surprisingly, TBCB is dispensable for the early MT-dependent steps of oogenesis in Drosophila, including cell division, not being required for mitosis in several tissues. In contrast, the absence of TBCB during later stages of

oogenesis causes major defects in cell polarity. This establishes a developmental function for TBCB in Drosophila: essential for viability, for MT network integrity and for cell polarity; but not for cell proliferation (Baffet et al., 2012).

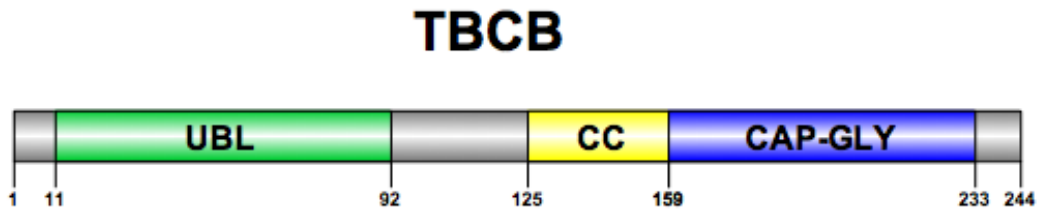

Figure 15. Schematic representation of the human TBCB functional structural domains. **UbL** - ubiquitin-like domain at the N-terminus. CC - coiled-coil domain composed of leucine-rich repeats (LRR). **CAP-GLY** - cytoskeleton associated protein glycine-rich domain at the C-terminus (Adapted from *(Carranza et al., 2013)* with permission).

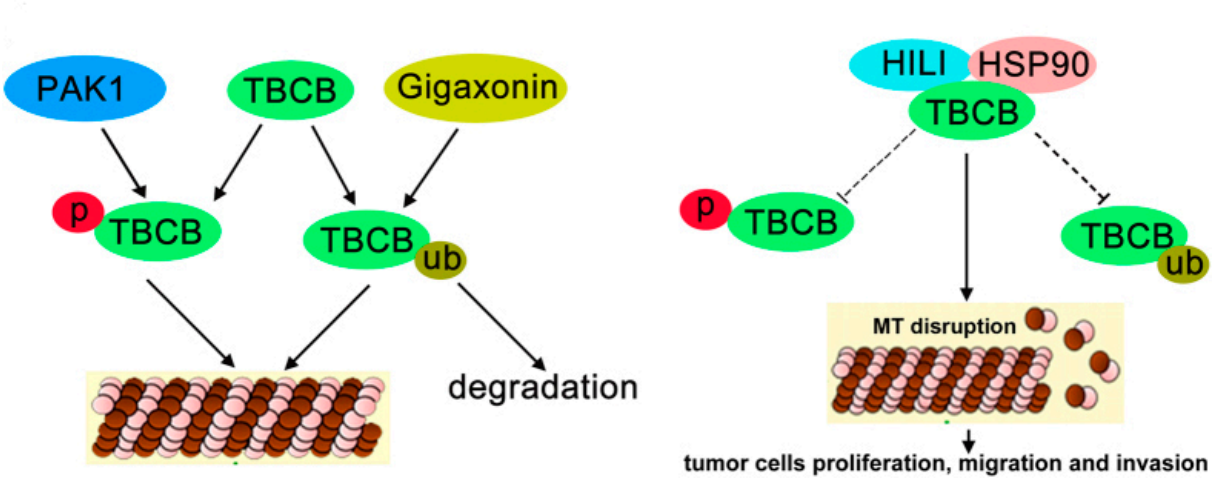

Figure 16. Model of how HILI regulates MT dynamics via TBCB (From *(Tan et al., 2017)* with permission).

2.4.1.3. Tubulin cofactor C (TBCC)

The Human TBCC is a post-chaperonin involved in the folding and assembly of α- and β-tubulin monomers leading to the release of productive tubulin heterodimers ready to polymerize into MTs. In this process it collaborates with other cofactors (TBC's A, B, D, and E) and forms a supercomplex with TBCD, β-tubulin, TBCE and α-tubulin (Garcia-Mayoral et al., 2011). The TBCC is capable of inducing the TBCD/β-tubulin/TBCE/α-tubulin complex to release the native α-/β-heterodimer, since complexes formed between α-tubulin, β-tubulin, TBCD, and TBCE are not sufficient to release tubulin heterodimers (Zabala & Cowan, 1992). This way, the hydrolysis of GTP by tubulin, stimulated by TBCC and TBCD, is part of the heterodimer assembly reaction: hydrolysis of GTP by β-tubulin acts as a switch for the release from the

supercomplex of native, newly made tubulin heterodimers. In fact, TBCC and TBCD in combination have been shown to be GTPase activators (GAP) for native tubulin; with TBCE enhancing this tubulin-GAP activity (Tian et al., 1999).

The tubulin chaperone protein TBCC has a profound influence on tubulin pools and MT dynamics: cells with reduced TBCC content displayed increased MT dynamics; cells with increased TBCC content contain less polymerizable tubulin and display reduced MT dynamics (Hage-Sleiman, Herveau, Matera, Laurier, & Dumontet, 2010; 2011). TBCC is a protein found at the centrosome and is implicated in bipolar spindle formation (Garcia-Mayoral et al., 2011). Cells depleted of TBCC proliferate faster and show an altered cell cycle distribution, with a higher percentage in the S-phase of the cell cycle. This demonstrates that TBCC is a crucial protein in the control of the eukaryotic cell cycle, and supports the hypothesis that this tubulin binding cofactor could be implicated in genomic instability and cancer (silencing of TBCC is associated with enhanced tumour growth *in vivo*) (Hage-Sleiman et al., 2011).

2.4.1.4. Tubulin cofactor D (TBCD)

TBCD was originally discovered via its purification as a 120 kDa protein from bovine testis tissue that was responsible for forming a characteristic co-complex with β-tubulin in *in vitro* folding assays done with CCT in the presence of ATP and GTP (Tian et al., 1996; 1997). This protein preferentially binds *in vivo* and *in vitro* to GTP-bound β-tubulin released from TBCA, being part of the formed supercomplex TBCE/α-tubulin/TBCD/β-tubulin (Bhamidipati et al., 2000; Tian et al., 1999). Additionally, the TBCD is also associated to the α-/β-tubulin heterodimer dissociation, since its overexpression in mammalian cells let to the MT network depolymerization, to the heterodimer dissociation and to the β-tubulin sequestering (Bhamidipati et al., 2000; L. Martín, Fanarraga, Aloria, & Zabala, 2000b). As result of the TBCD overexpression was also found a decrease in the β-tubulin levels due to its degradation in the proteasome (H. Martín et al., 2000a). However, the efficiency with which TBCD effects tubulin disruption *in vivo* depends on its origin: bovine (but not human) TBCD efficiently destroys tubulin and MTs upon overexpression in cultured cells (Cunningham & Kahn, 2008; Fanarraga, Bellido, Jaén, Villegas, & Zabala, 2010). Actually, both proteins led to MTs depolymerization, but the bovine protein is more efficient than the human TBCD. In fact, the human TBCD need more time to completely depolymerize the MT network (Fanarraga et al., 2010). That inability of human TBCD to disrupt MT integrity upon overexpression *in vivo* can be overcome by siRNA-mediated suppression of expression of the TBCD regulator ADP

Ribosylation Factor-like Protein 2 (Arl2) as the MTs of HeLa cells are protected from human TBCD-mediated disruption via interaction of this protein with Arl2 (Tian, Thomas, & Cowan, 2010b). The evidence that the TBCD does not interact with the MTs shows that the MT depolymerization is due to a TBCD action on the native heterodimers and not directly on the MTs (Fanarraga et al., 2010; H. Martín et al., 2000a), what is also supported by the evidences of its high affinity towards the GTP β-tubulin than the GDP form (H. Martín et al., 2000a; Tian et al., 1999).

TBCD also contributes to tubulin GAP (GTPase Activating Protein) activity, in which TBCD, TBCC and TBCE induce GTPase activity via hydrolysis of E-site GTP in the native tubulin heterodimer at a concentration far below that required for polymerization into MTs (Tian et al., 1999). That GAP activity of TBCD, TBCE and TBCC is downregulate by the Arl2, which inhibits the binding of TBCD to native tubulin *in vitro* and *in vivo*. The GDP-bound Arl2 interacts with cofactor TBCD, thereby averting tubulin and MT destruction (Bhamidipati et al., 2000). In addition to its participation in *de novo* tubulin heterodimer assembly and tubulin GAP activity, recent evidence implicates TBCD in recruitment of the γ-tubulin ring complex at centrosomes and organization of the mitotic spindle (Cunningham & Kahn, 2008; Fanarraga et al., 2010). The accumulation of TBCD in procentrioles is gradually lost during the maturation process, coinciding with MT glutamylation. This might indicate that TBCD participates in the supply of tubulin to procentrioles, while binding and protecting the developing centriolar blades until MT assembly is complete (Fanarraga et al., 2010). The gene encoding TBCD is essential for life in eukaryotes, as shown by genetic experiments in the model organisms *S. pombe* and *Arabidopsis thaliana* (Hirata, Masuda, Eddison, & Toda, 1998; Radcliffe et al., 1999; Steinborn et al., 2002).

The depletion of TBCD results in mitotic spindle defects (Cunningham & Kahn, 2008) and incomplete MT retraction at the midbody during cytokinesis (Fanarraga et al., 2010). On the other hand, overexpression of TBCD leads to the loss of anchoring of the γTuRC and of nucleation of MT growth at centrosomes (Cunningham & Kahn, 2008) and G1 arrest (Fanarraga et al., 2010). Neither overexpression, nor knockdown, nor expression of mutants of TBCD, leads to any detectable changes in the levels of α-, β-, or γ-tubulins, indicating that the phenotypes observed are not due to changes in tubulin protein levels. These activities each appear to be distinct from the previously described role for TBCD in tubulin heterodimer assembly/disassembly (Cunningham & Kahn, 2008).

2.4.1.5. Tubulin cofactor E (TBCE)

The TBCE was originally discovered via its purification from bovine testis tissue. This protein was responsible for forming a characteristic co-complex with α-tubulin in *in vitro* folding assays done with CCT in the presence of ATP and GTP (Tian et al., 1996; 1997). Subsequently, was reported that this polypeptide, has about 60 kDa in denaturing gels, binds to α-tubulin after it has been released from the CCT and then associates with the C300 complexes, resulting in a larger complex that migrates more slowly in nondenaturing gel electrophoresis (Tian et al., 1996).

In mammalian the TBCE has two terminal domains, same as in TBCB, but in a reversed order. The CAP-Gly domain is on the N-terminus (in TBCB it was on the C-terminus), and the ubiquitin domain is in the C-terminal part (region 453–526). Additionally, the protein has also ten leucine rich repeats (LRRs) which are usually involved in protein-protein interactions, in its central region (Grynberg, Jaroszewski, & Godzik, 2003). It is mostly a cytoplasmic protein, like all TBCs (in accordance with their tubulin-chaperoning function), but it also accumulates at the Golgi apparatus of motor neurons, where it is essential for axonal tubulin routing (Schaefer et al., 2007). As was previously said the TBCE is a protein that associates with α-tubulin after it is released from TBCB, being necessary for the α/β-tubulin heterodimer assembly. It has also been described that it increases the ability of TBCC and TBCD to promote the GTPase activity of α-tubulin (Tian et al., 1999).

Moreover, the TBCE, as the TBCD, also participate in MT dynamics, dissociating the tubulin heterodimer by the sequestering of the α-tubulin (Kortazar et al., 2006; 2007; Tian et al., 1997). Interestingly, its overexpression disrupts the cellular MT network, due to the dissociation of the α/β-tubulin heterodimer and the capture the β–tubulin released from the heterodimer (Bhamidipati et al., 2000; Kortazar et al., 2007; Tian, Huang, Parvari, Diaz, & Cowan, 2006). Since the TBCE/ α-tubulin complex is intrinsically unstable (Lewis et al., 1997), the overexpression of TBCE leads to the loss of α-tubulin and the accumulation of a small amount of β-tubulin complexed with endogenous cofactors (Bhamidipati et al., 2000). Interestingly, TBCE interacts with TBCB, originating the TBCE–TBCB complex, which displays a more efficient stoichiometric tubulin dissociation activity than TBCE alone. Upon dissociation, TBCB, TBCE, and α-tubulin form a stable ternary complex. The disassembly of this ternary complex results in either TBCB/α-tubulin, free TBCE, TBCE/α-tubulin and free

TBCB. Free β-tubulin subunits might be recyclable in the presence of TBCA or TBCD (Kortazar et al., 2007).

Homologues of TBCE have been identified in several eukaryotic species, such as *S. cerevisiae* (Pac2p (Hoyt, Macke, Roberts, & Geiser, 1997)), *S. pombe* (Alp21 (Radcliffe et al., 1999)) and *A. thaliana* (PFI (Steinborn et al., 2002)). Pac2p, which has 26% identity to human TBCE, is required for normal MT stability and, when overexpressed in *S. cerevisiae*, is detected in a complex with α-tubulin (Hoyt et al., 1997). Alp21 is an essential protein in *S. pombe* involved in the generation of normal MTs (Radcliffe et al., 1999). Although the exact mechanism involved in the binding of TBCE to α-tubulin is still unknown, several TBCE homologs contain a N-terminal CAP–Gly domain, an UbL domain and LRR (frequently involved in protein–protein interactions) (Grynberg et al., 2003).

Consistent with TBCE predicted multifunctional role in the biogenesis and regulation of the tubulin heterodimer, are the following findings: mutations in the *A. thaliana* TBCE gene (PFI) result in microtubular defects (Steinborn et al., 2002); an amino acid deletion in murine TBCE results in a progressive motor neuropathy in mice that causes premature death in homozygotes (Martín et al., 2002); human mutations of the TBCE gene lead to both Kenny–Caffey and Sanjad–Sakati syndromes - microtubular defects consistent with alterations in the tubulin folding and dimerization pathways (Parvari et al., 2002). There is a recruitment of this cofactor into round structures that surround a γ-tubulin central spot, which are called «centriolar rosettes» (Fanarraga et al., 2010a; Fanarraga et al., 2010b), and is detectable at the base of the mammalian spermatozoa flagellum, where highly sophisticated MTs are also assembled and maintained (Fanarraga et al., 2010b).

3. Cytoskeleton in *T. gondii*

Apicomplexan protozoa share a number of cytoskeletal elements (MTs, actin, myosin, and intermediate filament-like proteins) with other “typical” eukaryotic systems used to study the cytoskeleton. Nonetheless, studies of the cytoskeletons of apicomplexans have revealed startling differences from model organisms that are worth mentioning at the outset. The singlet subpellicular MTs of Apicomplexans are one example of that, since they are unusually stable and withstand the high pressure, cold, and detergents typically used to isolate them, conditions incompatible with the maintenance of most MTs. In contrast, the microfilaments of Apicomplexans are thought to be exceedingly transient. Microfilaments are observed only after

treatment with jasplakinolide (a drug that drives actin polymerization), and the bulk of actin (>98%) is sequestered in globular form (Morrissette & Sibley, 2002a).

3.1. Microtubule cytoskeleton in *T. gondii*

The *T. gondii* cytoskeleton is composed of several tubulin-based structures: the conoid (a truncated cone–shaped structure) made up of 14 novel tubulin polymers in spiral, a pair of intraconoid MTs, subpellicular (cortical) MTs that extend in spiral down two-thirds the length of the parasite and centrioles, as well as a spindle in replicating parasites (Hu, Roos, & Murray, 2002b; Morrissette et al., 1997; Morrissette & Sibley, 2002a; Nichols & Chiappino, 1987; Swedlow et al., 2002).

Subpellicular MTs are essential for host cell invasion, since they are important for shape and apical polarity of the parasite, for secretion and play an important role in segregation of organelles to daughter buds. Conversely, spindle MTs are necessary for chromosome segregation and nuclear scission (Morrissette & Sibley, 2002a; Russell & Burns, 1984).

In *T. gondii*, and in close related apicomplexan organisms, subpellicular MTs are rooted at one end in the apical polar ring, which is supposed to serve as a MTOC. In *Eimeria* parasites, the "hook decoration" (Heidemann & McIntosh, 1980) suggested that the apical polar ring might be attached to the minus end of the MTs (Russell & Burns, 1984), as in mammalian cells MTOCs. Consistently with this observation, subpellicular MT growth only occurs at the distal end to the apical polar ring (Hu, Roos, & Murray, 2002b). However, it is still unknown how the apical polar ring determines the exact MT number, the precise spacing among them, the precise orientation and also the polarity of these MTs.

Subpellicular MTs run through the cytosolic face of the pellicle, and ending in the region below the nucleus (Morrissette & Sibley, 2002a; Nichols & Chiappino, 1987), these spirally arranged MTs closely follow the serpentine body shape of the parasites, conferring an elongated shape and apical polarity, and also contributing to motility by providing tracks that direct the actin-myosin-based activity. The subpellicular MTs are closely associated with the cytosolic face of the IMC, demonstrating a periodicity which suggests that they directly associate with unidentified proteins of the IMC lattice (Morrissette et al., 1997; Tran, Li, Chyan, Chung, & Morrissette, 2012), probably MAPs. To support this association, and since MAPs are stabilizing agents, is the fact that subpellicular MTs are highly resistant to conditions that lead to MTs depolymerization, like MT-depolymerizing compounds, detergent extraction, and low-temperature conditions (Jun Liu et al., 2016; Morrissette et al., 1997; Nichols & Chiappino,

1987). This extraordinary stability is conferred by coating proteins that heavily decorate these MTs (Hu, Roos, & Murray, 2002b; Jun Liu et al., 2016; 2013; Morrissette et al., 1997; Tran et al., 2012). The first characterized MT-coating proteins characterized in *T. gondii* were SPM1 and SPM2 (Tran et al., 2012). *T. gondii* SPM1 is localized along the entire length of the subpellicular MTs but does not localize to the conoid, the intraconoid MTs, or the spindle. SPM2 has a more restricted localization pattern than SPM1, being associated with the middle third of the subpellicular MTs. Neither of these proteins seems essential for tachyzoite viability, but loss of SPM1 decreases overall parasite fitness and eliminates the stability of subpellicular MTs to detergent extraction (Tran et al., 2012). In fact, the importance of SPM1 might be related with the recent discovery of a new MAP: TrxL1 (Thioredoxin-Like protein 1), as TrxL1 does not seem to bind to MTs directly, instead it associates with a protein complex containing SPM1. Besides SPM1, several other proteins are found in the TrxL1-containing complex, including TrxL2, a close homolog of TrxL1 (Jun Liu et al., 2013). TrxL1 is localized to both the intraconoid and the subpellicular MT, being dependent on SPM1 in the latter (Jun Liu et al., 2013; 2016). Recently, two more proteins were identified, TLAP2 and TLAP3, as protect the stability of the subpellicular MTs in a region-dependent manner ("An ensemble of specifically targeted proteins stabilizes cortical microtubules in the human parasite," 2016).

Another form of subpellicular MTs stabilization in the Apicomplexan *T. gondii* is through post-translational modifications (PTM) of tubulin, which is also a mechanism to generate tubulin diversity since the tubulin gene family is quite small (only two α-and three β-tubulin genes). PTM are more abundant in less dynamic MTs, suggesting that they may contribute to MT stability and modulate their interaction with MAPs. In *T. gondii* the PTMs identified on α-tubulin include acetylation of Lys40, removal of the last C-terminal amino acid residue Tyr453 (detyrosinated tubulin), and the truncation of the last five amino acid residues. Polyglutamylation is detected on both α- and β-tubulins. Finally, methylation is detected on both tubulins and may be a modification characteristic of the phylum Apicomplexa (Morrissette, 2015; Xiao et al., 2010).

During mitosis, parasites employ spindle MTs. Spindle MTs are nucleated from electron dense, amorphous plaques associated with nuclear invaginations and embedded in the nuclear membrane, adjacent to cytoplasmic centrioles/centrosome. This spindle-organizing structure can be referred to as the centrocone, the centriolar plaque, the spindle pole body or spindle pole plaques (Morrissette & Sibley, 2002a).

Besides being associated with the spindle pole plaques, responsible for nucleating the assembly of intra-nuclear spindle MTs, the centrosome has also been described as playing a

role in the division of membrane-bounded organelles, including the apicoplast (Hartmann et al., 2006; Striepen et al., 2000); and implicated in the biogenesis of the Golgi apparatus (Hartmann et al., 2006; Stedman, Sussmann, & Joiner, 2003). Another function for the presence of the centrosome in *T. gondii* might be that the centrioles are maintained throughout the asexual life cycle in order to serve as a template for the construction of basal bodies that nucleate flagellar axonemes in the male gametes (Morrissette & Sibley, 2002a).

3.2. Assembly of *T. gondii* cytoskeleton

The assembly of the cytoskeleton is a well-orchestrated process that can be divided into four different periods: Initiation of budding, early budding, mid budding and late budding (Anderson-White et al., 2012).

Initiation of budding begins after centrosome duplication where the DNA content is 1.2N. The centrosome plays an important role for the coordination of the mitotic and the cytokinetic cycle (Gubbels et al., 2008). The centrosomes themselves are very dynamic and co-localise early during the initiation phase with IMC15 and the small GTPase Rab11B. These observations make IMC15 and Rab11B the earliest markers for daughter cell budding (Anderson-White et al., 2012). The termination of the bud initiation step can be monitored by the accumulation of MORN1 on the daughter buds (Gubbels et al., 2008). Additionally, the subpellicular MTs and the conoid are formed during this phase. Those early structures of the IMC and MTs serve as a scaffold for the next steps of daughter cell budding (Agop-Nersesian et al., 2010; Hu et al., 2006).

The early budding stage is identified as beginning by the appearance of the IMC subcompartment proteins ISP1-3 (Beck et al., 2010). During this phase, at a DNA content of 1.8N, additional elements are identified within the daughter cells. These include IMC proteins, IMC1 and IMC3, and components of the MyoA motor complex, the gliding associated proteins GAP40 and GAP50 (Frénal et al., 2010; Gaskins et al., 2004).

After these early components are assembled the middle budding phase begins. It is typified by the elongation of the daughter parasite cytoskeleton towards the basal end. The basal end of the growing daughter cells is marked by MORN1 protein. It is suspected that first the apical end of the parasite is formed then the cytoskeleton scaffold grows in direction of the basal end. This is because ISP1 remains apical while the cytoskeleton grows in the direction of the midpoint of budding (Beck et al., 2010). At this stage the IMC proteins, IMC5, 8, 9 and 13, are relocated from the periphery of the growing daughter parasites to the basal ends where MORN1 can be visualised (Anderson-White et al., 2011).

Maturation of the daughter cell occurs during the late budding phase while the cytoskeleton of the mother parasites is disassembled. A marker of this period is RNG1 that localizes to the apical polar ring and can be detected just before the mother cell's cytoskeleton breaks down (Tran et al., 2010). The plasma membrane of the mother cell is integrated into the pellicle of the newly formed daughter cells in a Rab11A dependant manner. The MyoA motor complex is then incorporated between the plasma membrane and the IMC of the nascent daughter parasites (Agop-Nersesian et al., 2009).

3.3. Microtubule cytoskeleton dynamic during the *T. gondii* host cell invasion

In 2006 our group studied the *Besnoitia besnoiti* host cell invasion process and MT cytoskeleton behaviour during its initial steps. In this work, we observed that upon interaction with the host cell, *B. besnoiti* undergoes dramatic modifications of shape and surface, which correlates with rearrangements of the parasite MT cytoskeleton. In the host cell, the MT cytoskeleton shows a re-arrangement around the invading parasite suggesting a filamentous interaction with the parasite cytoskeleton during invasion (Reis et al., 2006). Therefore, we proposed that host cell invasion by *B. besnoiti* requires a crosstalk between both MT cytoskeletons. Walker and colleagues and Sweeney and colleagues proposed a similar model for *T. gondii*. Walker and colleagues suggested an intimate interaction between *T. gondii* and host MTs resulting in the suppression of cell division and/or cause a mitotic defect, thus providing a larger space for parasite duplication (Walker et al., 2008). Sweeney and colleagues on their work reported that *T. gondii* host cell invasion is temporally regulated by the host MT cytoskeleton, by other words, the host MT cytoskeleton is a structure used by Toxoplasma to rapidly infect its host cell (Sweeney et al., 2010).

Considering all these data, we have been interested in the identification of crucial players involved in MT arrays rearrangements and dynamics that can be essential for invasion. In *T. gondii*, MT dynamics is probably regulated by tubulin PTM, by MAPs and also by TBCs that control tubulin pool by folding/dissociating tubulin heterodimers and by recycling/degradation of tubulin.

4. Objectives

The main goal of this work was to contribute for a better understanding of the MTs cytoskeleton role and function during host cell invasion in *T. gondii* as an apicomplexan model. Proteins involved in the MT cytoskeleton remodelling and dynamics are excellent targets for this study, since they are strong candidates to take part in the apicomplexan process of host cell invasion.

Tubulin proteostasis is regulated by a group of molecular chaperones termed tubulin-binding cofactors (TBCs). TBCs participate in the folding, dimerization and dissociation pathways of the tubulin dimer; being implicated in MT dynamics *in vivo*. Our major working hypothesis is that TBCs play a crucial role in MT arrays rearrangement and dynamics, and thus be essential for infection. In this context, our aim was to characterize the *T. gondii* Tubulin Cofactor B (TBCB) in the MT dynamics regulation during host cell invasion. More specifically, we aim to:

- Determine the *T. gondii* TBCB predicted gene and protein
- Studied the *T. gondii* TBCB predicted gene and protein
- Characterize *T. gondii* TBCB sub-cellular localization
- Analyse the *T. gondii* TBCB function by overexpression
- Analyse the *T. gondii* TBCB function by knockout

Intentionally blank page

Chapter II: Material and Methods

1. Molecular cloning

1.1. Cells and culture conditions

1.1.1. Bacterial strains

In this work we used two different *Escherichia coli* strains for general cloning and sub-cloning applications (DH5α and JM109) and one *E. coli* strain for protein expression (BL21):

- DH5α – It is a well-known versatile strain used for general cloning and sub-cloning applications. Genotype: *fhuA2 lac(del)U169 phoA glnV44 Φ80' lacZ(del)M15 gyrA96 recA1 relA1 endA1 thi-1 hsdR17*;

- JM109 – It is a K strain that is recA$^-$ and endA$^-$ to minimize recombination and improve the quality of plasmid DNA. Genotype: *end*A1, *rec*A1, *gyr*A96, *thi, hsd*R17 (r_k^-, m_k^+), *rel*A1, *sup*E44, Δ(*lac-pro*AB), [F′ *tra*D36, *pro*AB, *laq*I^{q}ZΔM15];

- BL21 – It is a widely used non-T7 expression *E. coli* strain and is suitable for transformation and protein expression. This strain does not express the T7 RNA Polymerase. Genotype: F$^-$ *ompT gal dcm lon hsdS$_B$*($r_B^-m_B^-$) [*malB*$^+$]$_{K\text{-}12}$(λ^S).

1.1.2. Growth media and culture conditions

E. coli cells were cultured at 37º C in liquid medium, with vigorous shaking (~180 rpm), or in solid medium.

The liquid culture medium used was Luria Broth (LB, Nzytech) and the solid medium used was LB agar (Nzytech). For plasmid selection, according to the plasmid resistance, these media were supplemented with ampicillin (100 µg/ml, Sigma) or Kanamycin (50 µg/ml, Sigma). These cells can be stored in solid medium for a few days, but their preservation for long periods was done in liquid medium containing 15% (v/v) of glycerol at -80 °C.

1.2. Preparation of chemically competent cells

E. coli subculture was prepared by the inoculation of 50 ml of LB medium, without antibiotic(s), followed by overnight incubation at 37 °C, with shaking. Next day, the saturated

culture was used to inoculate a new culture with 300 ml of fresh medium at an optical density (OD) 600 of 0,075 (~1:100 dilution). Then, cells were grown at 37 °C in a shaking incubator until the OD600 is 0.3. At that time, all the material and reagents were precooled on ice and all the procedures, except the centrifugation, were taken in a cold room. The bacterial culture was immediately transferred into a centrifuge tube and centrifuged at 7500 g for 2 minutes at 4 °C. The supernatant was discarded, and the cells were gently resuspended in 150 ml of ice-cold 0.1M $MgCl_2$. Then, the bacterial cells were again centrifuged (in the same tube) at 7500 g for 2 minutes at 4 °C. The supernatant was discarded, and the cells were gently resuspended in 150 ml of ice-cold 0.1M $CaCl_2$. The bacterial cells were incubated on ice for 20 minutes and then were centrifuged at 7500 g for 2 minutes at 4 °C. The supernatant was discarded, and the cells were gently resuspended in 6 ml of 0.1M $CaCl_2$/15% Glicerol (v/v). Finally, 100 µl of chemically competent cells were aliquoted into 1.5 ml microtubes and snap-frozen on dry ice. After that, cells were stored at -80 °C.

1.3. Transformation of chemically competent cells by heat shock

One aliquot (100 µl) of chemically competent cells was thawed on ice. Then, 40 ng of a ligation reaction or 10-15 ng of a plasmid DNA were added to the bacteria suspension and incubated on ice for 20 minutes. After that, the cells were subjected to heat shock by placing the bottom of the tube into a 42 °C water bath for 90 seconds and putting the tubes back on ice for 2 minutes. Then, 600 µl of sterile LB medium was added and the cells were incubated for 30-60 minutes at 37 °C, in a shaking incubator (~180 rpm), to express the gene that confers resistance to the antibiotic. Finally, the cells were plated on LB agar supplemented with the specify antibiotic.

1.4. Extraction of plasmid DNA from *E. coli*

The plasmid purification from *E. coli* was done using the commercial kits available, accordingly to the manufacturer's instructions (QIAGEN). The protocols are based on a modified alkaline lysis procedure, followed by binding of plasmid DNA to a resin under appropriate low-salt and pH conditions. RNA, proteins, dyes, and low-molecular–weight impurities are removed by a medium-salt wash. Plasmid DNA is eluted in a high-salt buffer and then concentrated and desalted by isopropanol precipitation.

Bacteria cultures in 10 ml, 100 ml or 500 ml of LB medium, containing the specific antibiotic for the plasmid selection, were grown overnight, at 37 °C with constant shaking at 180 rpm, and plasmid DNA was isolated using QIAprep Spin Miniprep Kit, Plasmid Plus Midi Kit or Plasmid Plus Maxi Kit, according to the culture volume.

1.5. Cloning vectors

All the vectors (plasmids) used in this work are summarized in the table 1.

Table 1. Vectors used in this work.

Vectors used in *E. coli*		
Vector Name	**Resistance**	**Source**
pET3a	Ampicillin	Novagen
pGEM®-T Easy	Ampicillin	Promega
Vectors used in Mammalian Cells		
Vector Name	**Resistances (bacteria/mammalian cells)**	**Source**
pIC113	Kanamycin/Neomycin	I. M. Cheeseman Lab
pIC111	Ampicillin /Neomycin	I. M. Cheeseman Lab
Vector used in *T. gondii*		
Vector Name	**Resistances (bacteria/*T. gondii*)**	**Source**
TUB8-myc-GFP-Ty-HXGPRT	Ampicillin/HXGPRT	Markus Meissner Lab
TUB8-myc-GFP-Ty- HXGPRT	Ampicillin/HXGPRT	Markus Meissner Lab
TUB8-ddFKBP-myc-GFP-Ty-HXGPRT	Ampicillin/HXGPRT	Markus Meissner Lab
TUB8-LoxP-myc-GOI-Ty-LoxP-YFP-HXGPRT	Ampicillin/HXGPRT	Markus Meissner Lab
pU6-sgRNA-DHFR	Ampicillin/DHFR-TY	Markus Meissner Lab

hxgprt - hypoxanthine-xanthine-guanine phosphoribosyltransferase. *dhfr-ts* - dihydrofolate reductase-thymidylate synthase.

1.6. Restriction endonucleases

The restriction enzymes used in this work were purchased from New England Biolabs (NEB) and used with adequate NEB buffer and bovine serum albumin (BSA) when required, according to manufacturer's instructions.

1.7. Plasmid dephosphorylation at the 5'end

After plasmid hydrolysis, with restriction enzymes, the 5'end was dephosphorylated to prevent plasmid self-ligation. This was done using the Antarctic Phosphatase (NEB), following manufacturer's instructions. This enzyme removes the phosphate from the DNA 5' end. The ligation between plasmid and a DNA fragment is still possible due the 5' phosphate from the insert.

1.8. Annealing oligonucleotides

This protocol was used to add a new multiple cloning site (MCS) to the vector TUB8-LoxP-myc-GOI-Ty-LoxP-YFP-HXGPRT. This alteration was performed with the oligonucleotides presented in the table 2, increasing the number of cloning sites available in the vector. This vector gained the following restriction sites: *Eco*RI/Myc-Tag/*Afl*II/*Ase*I/*Bst*Z17I/*Pac*I.

Briefly, the lyophilized primers were resuspended in molecular grade water to a final concentration of 900 pmol/µl. Then 1µl of each primer (900 pmol) was added to 48µl of annealing buffer (100 mM potassium acetate, 30 mM Hepes KOH pH 7.4, 2 mM magnesium acetate). The final concentration of each primer is 18 pmol/µl. First the primers were incubated for 4 minutes at 95º C, following an incubation for 10 minutes at 70º C, then the solution was left at room temperature (RT) for at least for 4 h and subsequently it was transferred to 4º C. Before ligation, if the plasmid was previously dephosphorylated, the annealed oligonucleotides were phosphorylated. The ligation reaction was done with 40 ng of the hydrolyzed vector and 8 pmol of the annealed oligonucleotides.

Table 2. Oligonucleotides sequences used to improve the MCS of the vector TUB8-LoxP-myc-GOI-Ty-LoxP-YFP-HXGPRT.

TUB8-LoxP-myc-GOI-Ty-LoxP-YFP-HXGPRT – MCS Modification	
Oligonucleotide Name	**Oligonucleotide Sequence**
F_polylinker_KO	5'AATTCCGACAAAATGCAGGAGCAGAAGCTCATCTCCGAGGAGGACCTGGCCATGGC CCTTAAGATTAATGTATACTTAAT3'
R_polylinker_KO	5'TAAGTATACATTAATCTTAAGGGCCATGGCCAGGTCCTCCTCGGAGATGAGCTTCTG CTCCTGCATTTTGTCGG3'

1.9. DNA ligation

The ligation of DNA fragments into plasmids was done using the T4 DNA ligase from Thermo Fisher Scientific, according to the manufacturer's instructions. The vector:insert molar ratios used were between 1:2 and 1:8. In all ligations were used 40 ng of plasmid DNA. The ligations were always incubated overnight at 4 °C.

For ligations of PCR products, into a cloning vector via TA (Thymine, Adenine), we used the pGEM-T Easy Vector System (Promega) according to the manufacturer's instructions.

1.10. DNA sequencing

DNA sequencing was performed by the Genomics Unit of Instituto Gulbenkian da Ciência and by Eurofins GATC Biotech.

2. Extraction of nucleic acids and amplification by polymerase chain reaction (PCR)

2.1. Extraction of genomic DNA (gDNA) from extracellular *Toxoplasma gondii* tachyzoites

The gDNA, used as a DNA template to amplify genomic sequences by PCR, was isolated and purified from *T. gondii* tachyzoites. Freshly egressed parasites were separated from host cell debris by centrifugation at 30 g, for 10 min at 4 °C, and the obtained pellet was washed twice with phosphate-buffered saline (PBS). Then, the gDNA isolation was performed using the DNeasy Blood & Tissue Kit from QIAGEN, according to the manufacturer's manual for cultured cells. The gDNA was eluted in 100 µl of molecular grade water. The gDNA was stored at -20 °C.

2.2. Extraction of total RNA

The complementary DNA (cDNA), used as a template to amplify coding regions for cloning, was produced from total RNA that was extracted from *T. gondii* tachyzoites. Freshly egressed parasites were separated from host cell debris by centrifugation at 30 g, for 10 min at 4 °C. The obtained pellet was washed twice with PBS. Then, the total RNA isolation was performed using the RNeasy Mini Kit from QIAGEN, according to the manufacturer's manual. The RNA was eluted in 50 µl of RNase free water.

For the analysis of *T. gondii* tubulin binding cofactor B (TgTBCB) transcription levels during invasion, total RNA was extracted at different time points after the invasion of Human Foreskin Fibroblasts (HFF) cells (confluent T25 flask) with 2.5 x 10^5 *T. gondii* parasites. RNA extracted from extracellular parasites was used as a control. Total RNA was extracted using the E.Z.N.A.® Total RNA Kit I (Omega Bio-Tek), according to the manufacturer's instructions.

The RNA was stored at -20 °C.

2.2.1. cDNA synthesis

The cDNA synthesis was done with 1 μg of total RNA, using the SuperScript™ III Reverse Transcriptase (Invitrogen) and oligo (dT)/random primers (Invitrogen), following the manufacturer's protocol. Before the cDNA synthesis, to remove the gDNA contamination, the RNA was incubated with the DNase I Amplification Grade (Invitrogen), according to the manufacturer's instructions.

The cDNA was stored at -20 °C.

2.3. Polymerase Chain Reaction (PCR)

PCR allows the *in vitro* specific amplification of DNA sequences, using two oligonucleotides (primers) that are complementary to the 3' ends of each of the sense and anti-sense strand of the target DNA.

2.3.1. DNA Polymerases

The DreamTaq™ Green DNA Polymerase (Thermo Fisher Scientific) and the KAPA2G Fast PCR (KapaBiosystems) were used for regular PCRs while Phusion High-Fidelity DNA Polymerase (Thermo Scientific) and KAPA HiFi HotStart PCR (KapaBiosystems) were used when the correct DNA sequence of the PCR products was of vital importance (e.g. cloning and sequencing). These last two polymerases were used due their improved performance and proof-reading activity.

All these enzymes were used according to the manufacturer's protocol.

2.4. Colony PCR

After a molecular cloning experiment, colony PCR is a method used to screen for plasmids containing the desired insert, directly from bacterial colonies, without the need of plasmid purification. In this PCR, a single bacteria colony, that have grown up on selective media following a transformation step, was picked to PCR tube and streaked to a replica plate. The PCR tubes and the replica plate were previously labelled with numbers corresponding to the bacteria colonies picked.

A PCR Master Mix with the DreamTaq™ Green DNA Polymerase (Thermo Fisher Scientific) or the KAPA2G Fast PCR (KapaBiosystems), with specific oligonucleotides to the insert, was prepared and added to the PCR tubes.

The replica plate was kept overnight at 37 °C and then stored at 4º C.

The PCR products were analysed by DNA electrophoresis (see Material and Methods, C-1). Bacteria cultures, from the positive colonies, were inoculated using the replica plate and were grown overnight for plasmid purification (see Material and Methods, A-4).

2.5. Analysis of TgTBCB Expression, by Real Time PCR

Real-time PCR was performed for 40 cycles on an ABI Prism 7700 Sequence using SYBR Green detection system (Applied Biosystems). The transcripts from *gapdh* and α-*tubulin* genes were used as endogenous controls in relative quantification using the standard curve method. Primers were designed using the Roche Design Centre (for primer sequences see table 3). All samples were done in duplicate and the data showed are from three independent experiments.

Table 3. Oligonucleotides sequences used in the Analysis of TgTBCB Expression, by Real Time PCR.

Primers for Real Time PCR	
Oligonucleotide Name	**Oligonucleotide Sequence**
Tbcb Forward	5' CGATGAAACATACGACAAACG 3'
Tbcb Reverse	5' TCTTCTTCGATCTTCTCTTCCTTC 3'
a-Tubulin Forward	5' CGCCTGCTGGGAGCTCTT 3'
a-*Tubulin* Reverse	5' GAAGGTGTTGAAGGCGTCG 3'
Gapdh1 Forward	5' CGTGGAGGTTTTGGCGATC 3'
Gapdh1 Reverse	5' GACTTCGCCGGGGTAGTG 3'

3. Nucleic acid analysis and quantification

3.1. Agarose gel electrophoresis

Agarose gel electrophoresis is a technique used to separate DNA fragments according to their size and conformation.

The DNA analysis was done using agarose gels at a concentration of 1% to 2% (w/v) in 1X Tris-acetate-EDTA (TAE) buffer (40 mM Tris, 1 mM EDTA, pH 8.3), supplemented with the DNA-binding dye GreenSafe Premium (Nzytech). 6X DNA loading dye were added to the DNA samples and the electrophoresis was performed in TAE at a constant voltage of 80V. The GeneRuler 1 kb DNA Ladder (Thermo Fisher Scientific) was run with the samples to estimate

the size of the DNA fragments. After electrophoresis, the DNA was visualized on an ultra-violet (UV) transilluminator.

3.2. Extraction and purification of DNA fragments from agarose gel

DNA fragments were extracted from agarose gel slices using the QIAquick Gel Extraction Kit (QIAGEN), according to the manufacturer's instructions. The purified DNA was eluted in 30 µl of molecular grade water, to increase the DNA concentration.

3.3. Determination of nucleic acid concentrations and purity

NanoDrop 2000c spectrometer (Thermo Scientific) was used to quantify and assess the purity of the DNA and RNA.

3.4. DNA precipitation

DNA precipitation can be performed to concentrate DNA and/or purify nucleic acids from salts or buffers. For extraction of DNA fragments from agarosel gels we performed ethanol precipitation. To each DNA solution was added 1/10 volume of 3 M sodium acetate pH 5.2 and 2.5 volumes of cold ethanol (-20 °C). The mixture was incubated 1 hour at -80 °C or overnight at -20 ºC. Then, the mixture was centrifuged at 17,000 g, for 30 minutes at 4 °C. The supernatant was removed and the DNA pellet, was washed twice with 70% ethanol to remove residual salts. After each wash, the mix was centrifuged at 17,000 g, for 15 min at 4 °C. The supernatant was removed, and the pellet was air dried. DNA for transfections was air dried under sterile conditions.

4. Bioinformatics

The programs used for plasmid mapping/editing were the pDRAW32, ApE and SnapGene Viewer. The chromatograms, from sequencing analysis, were analyzed by the 4Peaks software. Sequence alignment was done by CLC sequence Viewer.

The sequences restriction maps were done by NEBcutter V2.0 online tool (http://nc2.neb.com/NEBcutter2/).

The DNA and protein sequences comparison were done using BLAST (Basic Local Alignment Search Tool) tool of databases like NCBI (http://www.ncbi.nlm.nih.gov/) and ToxoDB (http://ToxoDB.org).

The calculation of the theoretical isoelectric point (pI) and molecular weight (Mw) of proteins was done using Compute pI/Mw tool from ExPASy (https://web.expasy.org/compute_pi/).

Multiple Alignment of the protein sequences were done using ClustalW tool from ExPASy (https://embnet.vital-it.ch/software/ClustalW.html).

The Search for Conserved Domains within a protein was done using the Conserved Domains search from NCBI (https://www.ncbi.nlm.nih.gov/Structure/cdd/wrpsb.cgi).

The sequences access number, used in this work, are listed in the table 4.

Table 4. Sequences access number.

Sequences and Access Numbers	
Sequence Name	**Sequence Access Number**
CAP-Gly domain-containing protein *Toxoplasma gondii*	TGME49_305060 / TGGT1_305060
Tubulin Cofactor B *Homo sapiens*	NP_001272.2 (isoform 1)/NP_001287900.1 (isoform 2)
CAP-Gly domain containing protein *Hammondia hammondi*	HHA_305060
Putative tubulin-specific chaperone *Neospora caninum*	NCLIV_001310
CAP-Gly domain containing protein *Cystoisospora suis*	CSUI_000538
Tubulin-specific chaperone, putative *Babesia bovis*	BBOV_IV005610
CAP-Gly domain containing protein *Theileria equi*	BEWA_030750
Tubulin-specific chaperone, putative *Plasmodium vivax*	PVP01_0705400
Tubulin-specific chaperone, putative *Plasmodium ovale curtisi*	PocGH01_07014400
Tubulin-specific chaperone, putative *Plasmodium falciparum*	PF3D7_0906910

5. Anti TgTBCB specific antibody production

To produce TgTBCB protein in amount sufficient to immunize animals, TgTBCB cDNA was cloned into the bacteria expression vector pET3a under the operon *Lac* promoter. The primers used to amplify the TgTBCB cDNA are in the table 5. *E. coli* BL21 bacteria cells were then transformed and grown to an optical density of 0.4 to 0.5. At this point, the production of the protein was induced by the addition of 1 mM IPTG (isopropyl-β-D-thiogalactopyranoside, NZYtech). To determine the best time of induction, after the addiction of IPTG, we did an analysis of different time points. The analysis of the total protein extracts from these time points

were done by 15% SDS-PAGE, (see Material and Methods 6.4), that was after stained with Coomassie. After these tests, we scaled up the culture production to obtain enough yield of the protein to purify and immunize two rabbits. Therefore, using the same protocol, we induced *E. coli* BL21 bacteria cells transformed with the pET3a-TgTBCB for 2 h. At this time, we prepared total protein extracts and analyzed them by 15% SDS-PAGE, followed by copper staining. Then, the TgTBCB band was extracted from the gel and the protein was electroeluted from the gel slice (Tessmer & Dernick, 1989). At Zabala lab (IFIMAV-Universidad de Cantabria, Santander, Spain), the purified protein was used to immunize 2 rabbits. The rabbits were inoculated three times, at three-week intervals, with approximately 500 µg of TgTBCB protein per inoculation.

Table 5. Primer sequences used to amplify the TgTBCB cDNA by PCR (restriction sites are underlined)

Primers used for the TgTBCB cDNA amplification	
Primer Name	**Primer Sequence**
F_Nde_TgTBCB	$^{5'}$GGTGGTCATATGTCGGGCTTGTCTATCAA$^{3'}$
R_Bam_TgTBCB	$^{5'}$GGTGGTGGATCCTTAGATTTCGTCCAGCAAATC$^{3'}$

6. Cell biology

6.1. Organisms

6.1.1. Mammalian cell lines and cell culture

Human foreskin fibroblasts (HFF) cells were purchased from American Type Culture Collection (ATCC) (Catalog No. SCRC-1041). HFF cells can be cryopreserved in culture medium with 20 % Fetal Bovine Serum (FBS) heat inactivated (Invitrogen) and 10 % dimethyl sulfoxide (DMSO) in liquid nitrogen for many years. After thawing, HFF cells should not be sub-cultured for more than 30 passages. After 30 passages, new cryovials with frozen HFF cells should be thawed. HFF confluent monolayers were used to culture and maintain *T. gondii* tachyzoites.

This cell lines are adherent cells and were maintained in subconfluent monolayers through passages with Trypsin-EDTA (0.05 %) phenol red (Invitrogen) treatment, to detach them from the flask surface. They were grown in Dulbecco's Modified Eagle's Medium (DMEM), high glucose, GlutaMAX™ (Invitrogen), supplemented with 10 % FBS heat inactivated (Invitrogen), without any antibiotics, in a 5 % CO_2 humidified atmosphere at 37º C.

6.1.2. *Toxoplasma gondii* Strains and Culture

In this work was used 3 different *T, gondii* strains:

a) RHΔHX, *hxgprt*-deficient *T. gondii* strain RH (Donald, Carter, Ullman, & Roos, 1996);

b) RH:DiCreΔku80ΔHX 'cleanup' strain, has a DiCre cassette randomly integrated into the parasite genome and the Ku80 has been deleted. The DiCre is highly expressed and gives a good efficiency of LoxP recombination upon the addition of rapamycin (Andenmatten et al., 2012);

c) RH:SplitCas9 has SplitCas9 cassette randomly integrated into the parasite genome. The SplitCas9 is highly expressed and gives a good efficiency of Cas9 activity upon the addition of rapamycin.

All strains were provided by Markus Meissner (Wellcome Centre for Molecular Parasitology, University of Glasgow, Glasgow, Scotland, UK. And Department of Veterinary Sciences, Ludwig-Maximilians-Universität, Munich, Germany) nevertheless, the RH:DiCreΔku80ΔHX 'cleanup' strain was provided with the permission of Vern B. Carruthers (Department of Microbiology & Immunology, University of Michigan Medical School, USA)

T. gondii is an obligate intracellular parasite, for this reason *T. gondii* tachyzoites were maintained in HFF cells cultured in DMEM, high glucose, GlutaMAX™ media (Invitrogen) supplemented with 10% FBS heat inactivated (Invitrogen), at 37 °C and 5 % CO_2 in humid environment.

Before cell lysis, *T. gondii* undergo several rounds of replication inside the host cell. Once they are extracellular, they need to be transferred to new cells.

If needed, intracellular parasites can be artificially released from the host cells. For this, the host cell layer is detached from the tissue culture dish/flask with a cell scraper. Then, the host cells are syringed twice, using a needle with 23 gauge, to destroy the host cells and release the parasites.

The ratio parasite / host cell was adjusted according to the needs. For example, to obtain freshly lysed parasites in 2 days, we inoculated 1 X 10^7 tachyzoites in a T25 confluent with

HFF cells. To obtain the same, but in 4 days, we inoculated 1 X 10^5 tachyzoites. We scaled up the inoculum, maintaining the proportion, according to the dish/flask cells area.

6.1.2.1. *T. gondii* cryopreservation

T. gondii is an intercellular parasite and dies rapidly in the extracellular environment (~24 h). Thus, it is preferable to freeze parasites when they are still within host cells.

For long-term storage, intracellular parasites were frozen within HFF host cells. HFF cells were infected with 5-10 X 10^6 parasites/confluent HFF T25 flask. The day after, most cells contained large parasites vacuoles. Then, the host cells were treated with 0.1 ml Trypsin-EDTA (0.05%) phenol red (Invitrogen) to detach them from the flask surface. Detached host cells, carrying the parasites inside, were gently resuspended in 1 ml freezing media (20% Fetal Bovine Serum heat inactivated (Invitrogen), 10% DMSO and 70% DMEM, high glucose, GlutaMAX™ media (Invitrogen) and transferred into a 2 ml cryotube. The cryotubes were placed overnight at -80º C in an appropriate container (Mr. Frosty, Nalgene) to freeze slowly (1º C/minute). Next day, the cryotubes were transferred to liquid nitrogen containers.

6.1.3. Transfection of *T. gondii* by electroporation

The transfection of *T. gondii* with DNA was done by electroporation.

The Nucleofector™ 2b Device (Lonza), was used with the Amaxa® Basic Parasite Nucleofector® Kit 2 (Lonza) and the program U-033. We followed the manufacturer's protocol with some alterations. Briefly, the DNA was precipitated and dissolved in 100 µl electroporation buffer (Nucleofector). Subsequently, the freshly lysed parasites were centrifuged at 800 g for 10 min at 4 °C and then the pellet was washed twice with PBS. Finally, the sediment was resuspended in 100 µl of electroporation buffer (Nucleofector) containing the DNA. After the electroporation, the parasites were added to a T25 and to a 24 well plate with cover glasses, both with confluent HFF cells. The T25 is to maintain the parasite culture and the 24 well plate is to check the electroporation efficiency by immunofluorescence (IF).

6.1.3.1. Transient transfection of *T. gondii*

In the transient transfection, the DNA plasmids were introduced into *T. gondii* tachyzoites and remained extra-chromosomal, so they were lost over subsequent cell divisions. Parasites

were transfected with the DNA plasmids not linearized and without any selection. Normally were used 30 μg of DNA. We used this kind of transfection to test some electroporation conditions and to test its efficiency.

6.1.3.2. Stable transfection of *T. gondii*

Stable transfections involve the integration of the Plasmid DNA (or part of the plasmid) into the parasite's genome and it can be done by random integration or homologous recombination. In the random integration, the DNA insertion occurs undirected, randomly distributed over the genome and the number of copies per genome is variable (Donald & Roos, 1994). In contrast to transient transfections and to the homologous recombination, in the random integration 10 U of the single cutting restriction enzyme used to linearizing the Plasmid DNA were added to the transfection mix. In doing so, the genomic DNA is cut undirected and the DNA repair mechanisms are activated. This process is called Restriction Enzyme Mediated Insertion (REMI) and increases the insertion of DNA in *T. gondii* genome (Black, Seeber, Soldati, Kim, & Boothroyd, 1995).

In the homologous recombination, the DNA is inserted at the specific genomic region using homology arms, and the single cutting restriction enzyme used to linearize the Plasmid DNA cannot be added to the transfection mix since it would enhance the random integration.

For a successful stable transfection, it is necessary to select the positive parasites using a respective selection marker. The time of its addition to the transfected parasites depends on the selection marker used but normally it can be done immediately after transfection or 24h later.

The vectors used in this work had the *dhfr-ts* (dihydrofolate reductase-thymidylate synthase) gene for pyrimethamine resistance (Donald & Roos, 1993) or the *hxgprt* (hypoxanthine-xanthine-guanine phosphoribosyltransferase) gene for mycophenolic acid (MPA) resistance (Donald et al., 1996). The selection was done with the following concentrations: 1 μM of pyrimethamine or with 40 μg/ml of xanthine plus 25 μg/ml of MPA, respectively. A 5 days treatment should result in a pool with stable transfected parasites.

6.1.3.2.1. *T. gondii* cloning by limiting dilution

After selection, the isolation of a clonal stable line of parasites can be done by limiting dilution. For this, serial dilutions of the stable transfected parasite pool were inoculated in a 96 well plate containing confluent HFF cell cultures. Therefore, some wells received only one

parasite. After one week the parasites invaded the host cells, replicated within, lysed them and invaded the next cells and so on, forming a small lysis plaque. After this time, wells with only one lysis plaque indicated a parasite clone, because only one parasite was originally present in this well. The parasites within this well were isolated and transferred to a 24 well plate with new HFF cells. Subsequently, a second steep of cloning by limiting dilution was performed.

6.2. Phenotypic analysis of *T. gondii*

6.2.1. Plaque assay

The lytic growth (host cell invasion, intracellular replication, host cell egress and gliding motility) of *T. gondii* tachyzoites results in plaques, within host cell monolayers, due the lysis of the infected cells. Plaque assays are the first approach to investigate invasion, replication and egress over time. The size and the number of these plaques reflect the infectivity of the respective parasite strain. For a plaque assay, 6 well plate with HFF monolayers were inoculated with 1000 parasites and incubated for 5-7 days under normal growth conditions. Afterwards, the cells were washed once with PBS, fixed with ice-cold methanol for 20 minutes and stained with Giemsa (diluted in water in the proportion of 1 /10) for 45 minutes. Finally, the plaques were analysed and counted using a light microscope. Their size can also be analysed and quantified using an image process program. At least three independent assays were done in different days.

Transgenic strains with significant differences in the plaque assay, compared to the control strain, were further characterized by invasion, replication and egress assays.

6.2.1.1. Invasion assay

The invasion assay is used to analyse the ability of extracellular *T. gondii* tachyzoites to invade host cells. Confluent cultures of HFF cells, growing on glass coverslips in 24 well plates, were inoculated with 5 x 10^5 freshly egressed parasites. The parasites were allowed to invade host cells under normal growth conditions for 1 hour. Then, the extracellular parasites were removed by washing the coverslips three times with PBS and new fresh media was added to each well. The parasites were incubated for more 16 h (overnight), under normal growth conditions. In the next day, the coverslips were fixed, permeabilized and processed for IF

analysis, labelling the intracellular parasites. For each coverslip, the number of parasitophorous vacuoles was counted within 6 randomly selected fields under an amplification of 400X.

At least three independents assays were done, in different days, and 3 different coverslips were counted for each condition/strain. The invasion was calculated as a percentage value of control parasites normalised to 100 %.

6.2.1.1.1. Invasion assay in the presence of TgTBCB specific polyclonal serum

The invasion assay in the presence of TgTBCB specific polyclonal serum was used to analyse the ability of extracellular *T. gondii* tachyzoites to invade host cells in the presence of that specific polyclonal serum. The protocol used was the standard protocol for the invasion assay (as described above), with some modifications. Confluent cultures of HFF cells, growing on glass coverslips in 24 well plate, were inoculated with 5 x 10^5 freshly egressed parasites in the presence of TgTBCB specific polyclonal serum in the following dilutions: 1:50; 1:100 and 1:200. The same assay was done in the presence of a rabbit polyclonal serum as a control, using equal dilutions.

6.2.1.2. Replication assay

The replication assay was used to analyse the *T. gondii* tachyzoites ability to undergo normal intracellular replication within infected host cells. Confluent cultures of HFF cells, growing on glass coverslips in 24 well plate, were inoculated with 2 x 10^4 freshly egressed parasites for 24 h under normal growth conditions. Then, coverslips were fixed, permeabilized and processed for IF analysis to stain the intracellular parasites. The number of parasites/vacuole was determined in 200 vacuoles. For that, from each coverslip, at least 12 images from random fields were taken under an amplification of 400X.

Were done a minimum of three independents assays, in different days, and 3 different coverslips were counted for each condition/strain.

6.2.1.3. Egress assay

The egress assays were performed, to analyse the ability of intracellular parasites to egress the infected host cell. Parasites can be tested for natural egress or for calcium ionophore A23187 artificially induced egress. Confluent HFF cells growing on coverslips in 24 well plates were

inoculated with 16 x 10^4 freshly egressed parasites and intracellular growth was allowed for 36 h. After this time, cells were washed with PBS to remove all serum, since it inhibits the calcium ionophore. Then, warmed media (37 °C) without serum and supplemented with calcium ionophore was added to the cells. The parasites were incubated for 1 min at standard condition and then fixed with ice-cold methanol for 10 minutes. An IF assay was performed to stain the parasites. For each coverslip, the number of vacuoles with non-egressed parasites were counted within 6 aleatory fields under an amplification of 400X.

At least three independents assays were done, in different days, and 3 different coverslips were counted for each condition/strain.

6.2.2. Microneme secretion assays

The microneme secretion assays were used to test if TBCB is secreted by these organelles. It was used the protocol previously described by Carruthers and Sibley (Carruthers & Sibley, 1999) with modifications described by Hall et al. (Hall et al., 2011) and minor modifications introduced by us. The microneme secretion was induced with calcium ionophore A23187 in the presence of 40 mM of NH_4Cl or, alternatively 1% ethanol. Briefly, to obtain freshly egressed tachyzoites, host cells were syringe passed through a 23-gauge needle twice, filtered through a 8 µm pore-sized membrane, pelleted by centrifugation (800 g for 10 minutes at RT) washed with PBS twice and resuspended in PBS. Then the parasites were counted and, for each condition, 4 × 10^8 tachyzoites were used. The secretion assays were typically performed in "LoBind microcentrifuge tubes" (Eppendorf), with 100 µl of PBS per tube. The parasite suspension with the secretion inducer were incubated at 37 °C for 30 seconds in a water bath. After, the parasites were gently mixed and the treatment was continued for more 30 min at 37 °C. Secretion was arrested by placing the tubes on ice for 5 minutes and the supernatants were collected after removing parasites by centrifugation (1200 g, 5 min, 4 °C). 95 µl of supernatant were transferred to a new LoBind microcentrifuge tube and recentrifuged (1,200 × g, 5 min, 4 °C). 90 µl of this supernatant were transferred to a new LoBind microcentrifuge tube. Reducing SDS/PAGE sample buffer was added and 60 µl of this mixture were analysed by SDS/PAGE.

6.3. Generation of *T. gondii* TBCB transgenic parasite lines

6.3.1. *T. gondii* TBCB overexpression

The TgTBCB cDNA was amplified and cloned in two different types of overexpression plasmids, under three different constructions (Figure 17):

i) Overexpression plasmid with TgTBCB in fusion with c-Myc and eGFP ("enhanced green fluorescent protein", fluorescent tag);
ii) Overexpression plasmid with TgTBCB in fusion with c-Myc;
iii) Overexpression plasmid with TgTBCB in fusion with a destabilization domain (ddFKBP), c-Myc and eGFP. The ddFKBP domain allow the modulation of the fusion protein levels in a Shdl1 dependent manner.

The primers and the plasmids used in that cloning process are listed in the table 6 and 1 (see in Material and Methods 1.5.), respectively. The plasmids, that were provided by Dr. Markus Meissner, contain the tubulin strong promoter TUB8 and the selection marker HXGPRT.

6.3.1.1. Plasmid construction, TBCB overexpression in fusion with c-Myc and GFP

The TgTBCB cDNA was cloned in fusion with c-Myc and eGFP at its N-terminal end in the TUB8-Myc-GFP-Ty-HXGPRT plasmid, producing the construction: 5' TUB8-Myc-eGFP-TgTBCB-HXGPRT 3′.

6.3.1.2. Plasmid construction, TBCB overexpression in fusion with c-Myc

We cloned the TgTBCB cDNA in fusion with the c-Myc, at its N-terminal end in the TUB8-Myc-GFP-Ty-HXGPRT plasmid, producing the construction: 5' TUB8-Myc-TgTBCB-HXGPRT 3′.

6.3.1.3. Plasmid construction, TBCB overexpression in fusion with ddFKBP, c-Myc and eGFP

The TgTBCB cDNA was cloned in fusion with the ddFKBP domain, c-Myc and eGFP, at TBCB N-terminal end in the TUB8-ddFKBP-Myc-GFP-Ty-HXGPRT plasmid, producing the construction: 5' TUB8-ddFKBP-Myc-eGFP-TgTBCB-HXGPRT 3′. During the cloning process, the GFP from the original plasmid was swapped by the eGFP.

The destabilization domain ddFKBP is an engineered mutant of the human FKBP12 protein that is rapidly and constitutively degraded and this instability is conferred to other proteins fused to this domain. But, when it is added a synthetic ligand, termed morpholine-containing ligand Shield-1 (Shield-1 - FKBP ligand that binds FKBP with F36V mutation with 1000 selectivity over wt-FKBP) that binds to the destabilizing domains protecting them from degradation, fused proteins can perform their cellular functions (Figure 18) (Banaszynski, Chen, Maynard-Smith, Ooi, & Wandless, 2006; Herm-Götz et al., 2007; Lampson & Kapoor, 2006).

The overexpressed ddFKBP-c-Myc-GFP-TBCB is degraded by the proteasome. However, in the presence of the shield-1, the produced ddFKBP-c-Myc-GFP-TBCB protein is protected against degradation and accumulates inside the parasites.

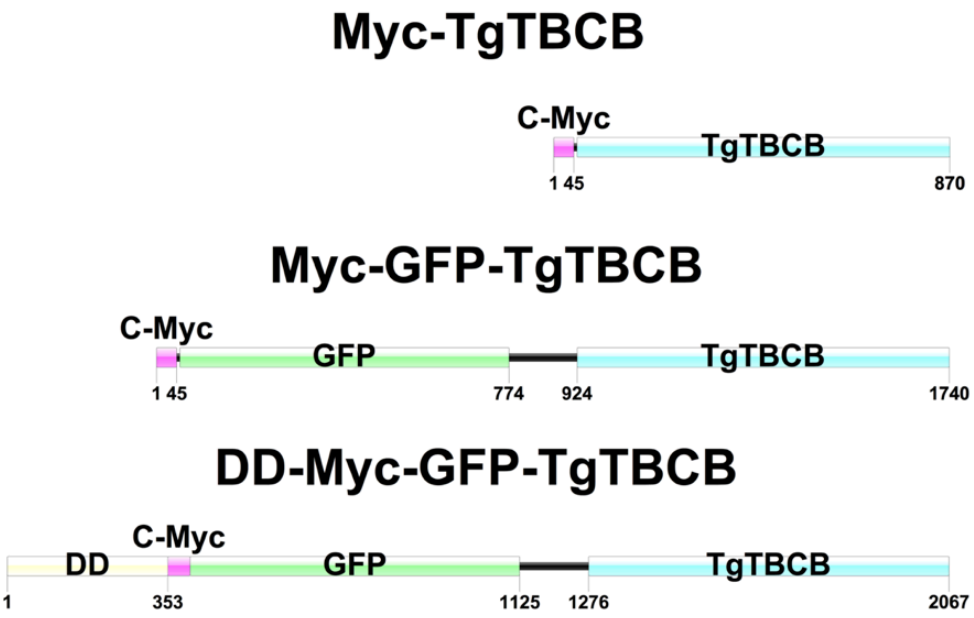

Figure 17. Schematic representation of the three different fused proteins for the TgTBCB overexpressions.

Table 6. Nucleotide sequences of the primers used in the TBCB cDNA amplifications by PCR for overexpression in *T. gondii*

TgTBCB with c-Myc-eGFP	
Primer Name	**Primer Sequence**
F MycGFPNTBCBTgNsi	5' CCA ATGCAT GTG AGC AAG GGC GAG GAG 3'
R MycGFPNTBCBTgPac	5' CCC TTAATTAA TTA GAT TTC GTC CAG CAA ATC A 3'
TgTBCB with C-Myc	
Primer Name	**Primer Sequence**
F MycNTBCBTgNsi	5' CCA ATGCAT TCG GGC TTG TCT ATC AAC G 3'
R MycGFPNTBCBTgPac	5' CCC TTAATTAA TTA GAT TTC GTC CAG CAA ATC A 3'
TgTBCB with ddFKBP-c-Myc-eGFP	
Primer Name	**Primer Sequence**
F MycGFPNTBCBTgNsi	5' CCA ATGCAT GTG AGC AAG GGC GAG GAG 3'
R MycGFPNTBCBTgPac	5' CCC TTAATTAA TTA GAT TTC GTC CAG CAA ATC A 3'

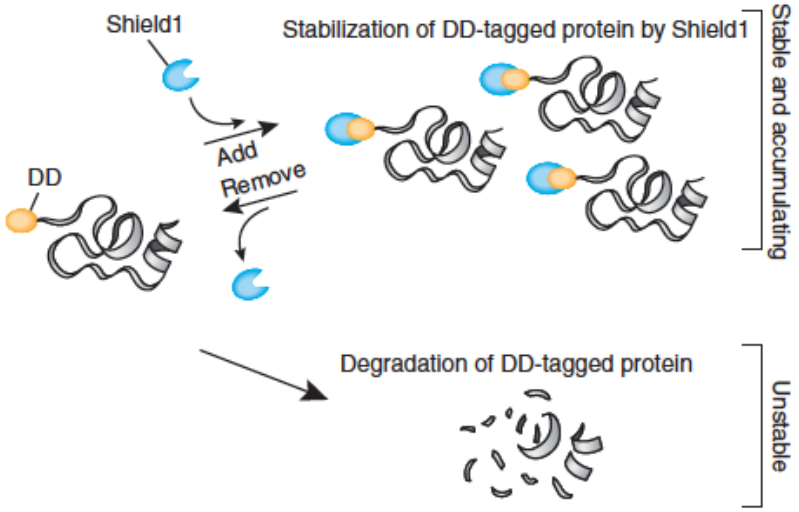

Figure 18. Schematic representation of the ddFKBP destabilization domain function. The ddFKBP domain allows the control of protein overexpression by using a shield-1 molecule that binds to the domain, preventing protein target for degradation. In the absence of shield-1 the target is labelled and degraded by the proteasome. In the presence of shield-1, the target protein is protected against degradation and accumulates inside the organinsm (adapted from *(Haugwitz, Nourzaie, Gandlur, & Sagawa, 2008)* with permission).

6.3.2. *T. gondii* TBCB conditional knockout

To evaluate the role of TBCB in *T. gondii*, especially during host invasion and parasite replication, we produced a TgTBCB conditional knockout strain by two different methodologies:

i) *T. gondii* DiCre system;

ii) *T. gondii* CRISPR/Cas9.

All *T. gondii* specific plasmids were provided by Dr Markus Meissner.

6.3.2.1. *T. gondii* TBCB conditional knockout by DiCre system

Our first approach to produce a conditional KO strain used the *T. gondii* DiCre system (Andenmatten et al., 2012), a method based on site-specific recombination using dimerizable Cre recombinase. For this were used a specific *T. gondii* strain (RH:DiCreΔku80ΔHX 'cleanup' strain has DiCre cassette randomly integrated into the parasite genome and subsequently Ku80 has been deleted) that expresses two inactive fragments, each of them fused to one of the rapamycin-binding proteins FRB and FKBP (Figure 19). The addition of rapamycin brings FRB and FKBP together, reconstituting the functional enzyme and causing the loxP-flanked gene of interest to be excised. The Ku80 depletion avoids random integration, increasing the homologous recombination efficiency.

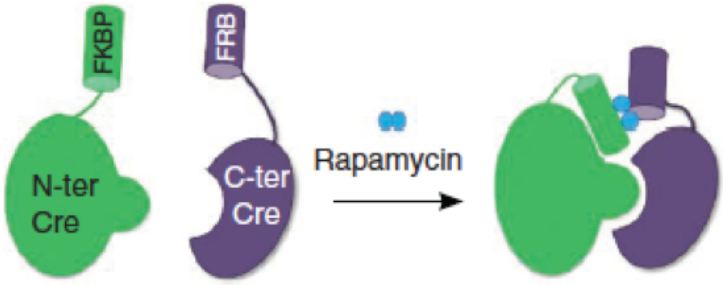

Figure 19. Conditional Cre recombinase system in *T. gondii*. In the DiCre system, N-terminal (N-ter) Cre (Cre recombinase amino acids 1–59) is fused to FKBP12 and C terminal (C-ter) Cre (Cre recombinase amino acids 60–343) is fused to FRB. Rapamycin dimerizes the subunits to reconstitute Cre recombinase activity (adapted from *(Andenmatten et al., 2012)* with permission).

It was used a gene-swap strategy in which TgTBCB gene was replaced at genome locus by a c-Myc-TgTBCB cDNA flanked by loxP sites. Then, after the addition of rapamycin, c-MycTgTBCB cDNA was excised by Cre recombinase and an YFP cDNA was left under the control of a constitutive promoter, resulting in YFP-expressing parasites. The exchange between wild-type TgTBCB gene and Myc-TgTBCB loxP flanked plus YFP and selection cassette was done by homologous recombination (using homology arms, see figure 20).

c-Myc-TgTBCB cDNA, ~2000 bp of the TgTBCB 5'UTR and ~2000 bp 3′UTR were cloned into TUB8-LoxP-myc-GOI-Ty-LoxP-YFP-HXGPRT plasmid, generating the construction: 5' UTR-TUB8-LoxP-c-Myc-TgTBCB-LoxP-YFP-HXGPRT-3′UTR (Figure 20). The cloned sequences were amplified by PCR and the specific primers are listed at table 7.

Table 7. Nucleotide sequences of the primers used to amplify the cloned sequences by PCR to produce the TBCB conditional knockout in *T. gondii* by DiCre system.

1st - TgTBCB with c-Myc Tag	
Primer Name	**Primer Sequence**
F MYCTBCBTg _KO	5'CG GAATTC *GAC AAA* ATG CAG GAG CAG AAG CTC3'
R cDNATBCBTg_ KO	5'CC TTAATTAA TTA GAT TTC GTC CAG CAA ATC3'
2nd - TgTBCB 5' UTR	
Primer Name	**Primer Sequence**
F 5'UTRTBCBTg_ KO	5'GA GGTACC CAT CCG CCT GTT TCT GTC G3'
R 5'UTRTBCBTg_ KO	5'C GGGCCC GTT GCT TCG ATT GAG AAT GAA3'
3rd - TgTBCB 3' UTR	
Primer Name	**Primer Sequence**
F 3'UTRTBCBTg_ KO	5'C GAGCTC AGC TTT CGG ATG GAA AGA AGC3'
R 3'UTRTBCBTg_ KO	5'CC GCTCTTCTTAA GCG AAA CAA GGC GAT TAT CTT3'

Italics - *T. gondii* kozak consensos sequence of translational initiation sites (Seeber, 1997).

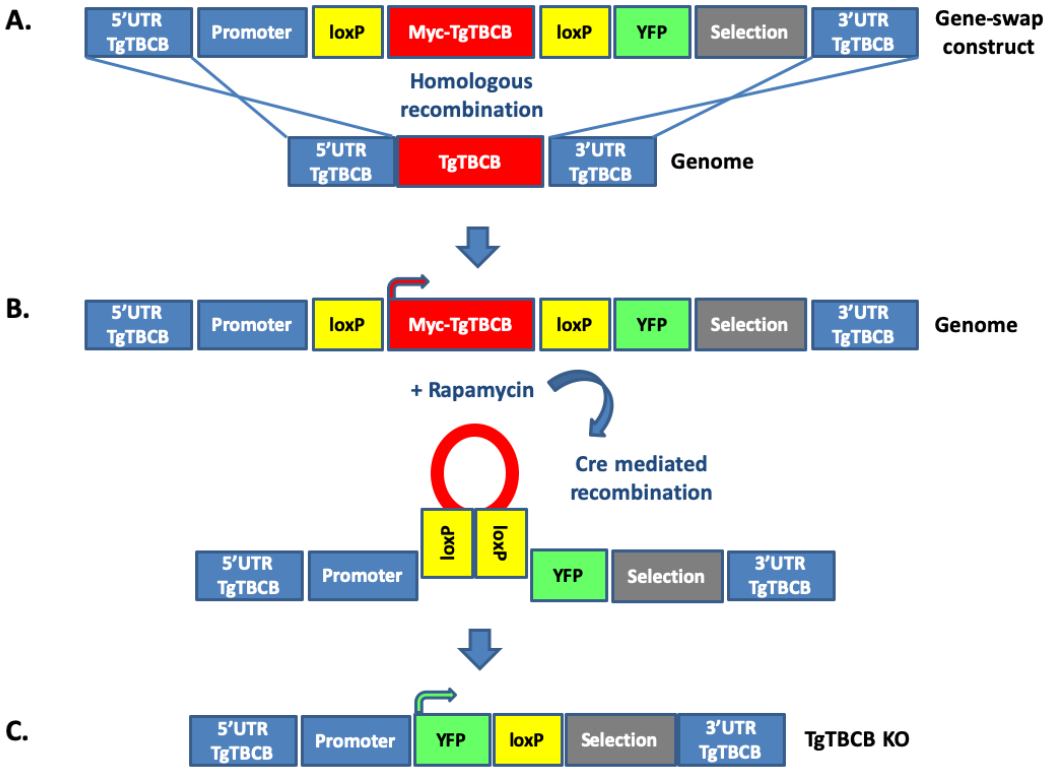

Figure 20. Schematic representation of the construct of TBCpB conditional KO. A. Gene-swap strategy, gene-swap construct inserted into the genome by homologous recombination; B. Cre mediated recombination by rapamycin addition; C. TBCB KO with YFP expression.

After selection, a PCR strategy allowed us to test whether the mutant parasites (resistant to the selection marker) have undergone random integration or homologous recombination. Primers used are listed at table 8.

In this strategy the PCR will produce products with different sizes: TgTBCB wild type locus (553 bp) and recombinant TgTBCB (1092 bp, see figure 21). Expected results:

- Homologous recombination: one PCR product of 1092 bp

- Random integration: two PCR products, 553 bp from the TgTBCB intact endogenous locus and 1092 bp from the plasmid random integration

Table 8. Nucleotide sequences of the primers used in PCR strategy to check the homologous recombination after transfection.

TgTBCB KO Test	
Primer Name	**Primer Sequence**
F_TBCB KO Teste	$^{5'}$TGCCGAGATACGTAGTTGC$^{3'}$
R_TBCB KO Teste	$^{5'}$GTCACCGTTGATAGACAAGC$^{3'}$

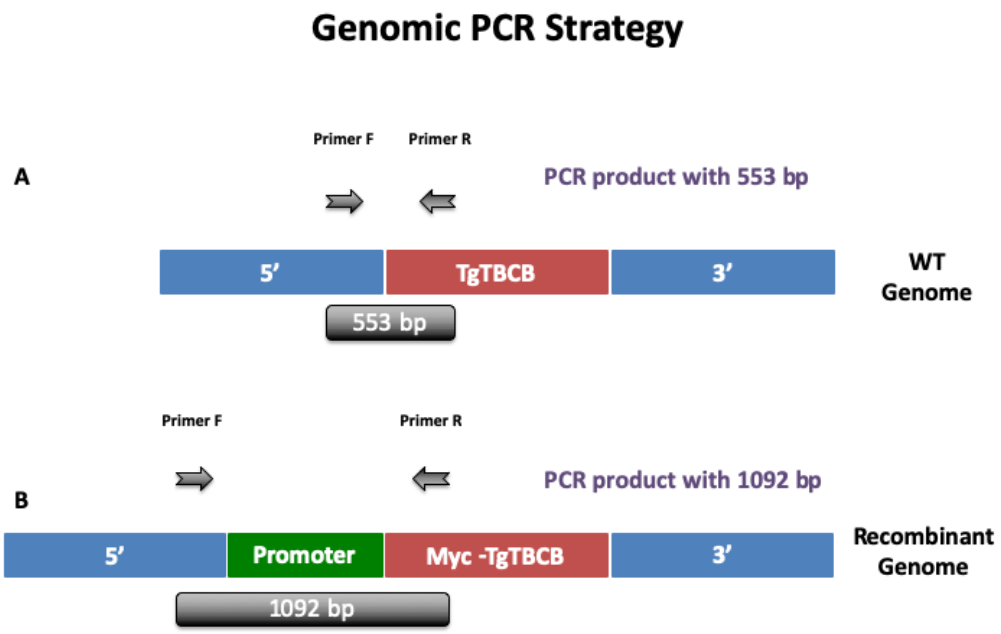

Figure 21. Illustration of genomic PCR strategy to check the efficient of the transfection by homologous recombination. Primer F and Primer R were design to hybridize with 5' region of TgTBCB gene and with the initial coding region of TgTBCB gene, respectively. **A** – PCR product expected length for WT genome amplification (553 bp). **B** – PCR product expected length for Recombinant genome amplification (1092 bp). In case of "random integration" we expect two PCR products (one from the construct and other from the wild-type locus).

6.3.2.2. *T. gondii* TBCB conditional knockout by CRISPR/Cas9 system

The second approach to produce a TgTBCB conditional KO in *T. gondii* was the CRISPR/Cas9 system. Succinctly, the CRISPR/Cas9 systems is an adaptable immune mechanism used by many bacteria to protect themselves from foreign nucleic acids, such as viruses or plasmids. Type II CRISPR systems incorporate sequences from invading DNA between CRISPR repeat sequences encoded as arrays within the bacterial host genome. Transcripts from the CRISPR repeat arrays are processed into CRISPR RNAs (crRNAs), each harbouring a variable sequence transcribed from the invading DNA, known as the

"protospacer" sequence, and part of the CRISPR repeat. Each crRNA hybridizes with a second RNA, known as the transactivating CRISPR RNA (tracrRNA), and these two RNAs, complex with the Cas9 nuclease. The protospacer-encoded portion of the crRNA directs Cas9 to cleave complementary target-DNA sequences (Figure 22), if they are adjacent to short sequences known as protospacer adjacent motifs (PAM) (Figure 23) (Sander & Joung, 2014).

The system that we used in *T. gondii* is based on the Type II CRISPR from *S. pyogenes* and has been adapted for inducing sequence-specific double-stranded break. Briefly, a SplitCas9 nuclease has been introduced in the parasite, in order to create a *T. gondii* SplitCas9 strain. This specific Cas9 is expressed in two inactive fragments, each of them fused to one of the rapamycin-binding proteins FRB and FKBP (similar to DiCre system described above). The addition of rapamycin brings FRB and FKBP together, reconstituting the functional enzyme. The use of this mechanism can control the exact moment when the system is triggered (Figure 24) (Zetsche, Volz, & Zhang, 2015).

The second component is a single guide RNA (sgRNA), consisting of a fusion of a crRNA and a fixed tracrRNA, which is introduced in the parasite by electroporation. Briefly, twenty nucleotides at the 5′ end of the sgRNA (corresponding to the protospacer portion of the crRNA) direct Cas9 to a specific target DNA site using standard RNA-DNA complementarity base-pairing rules. These target sites must lie immediately 5′ of a PAM sequence that matches the canonical form 5′-NGG. Thus, with this system, Cas9 nuclease activity can be directed to any DNA sequence of the form N20-NGG simply by altering the first 20 nt of the sgRNA to correspond to the target DNA sequence (Figure 22 and 23) (Sander & Joung, 2014).

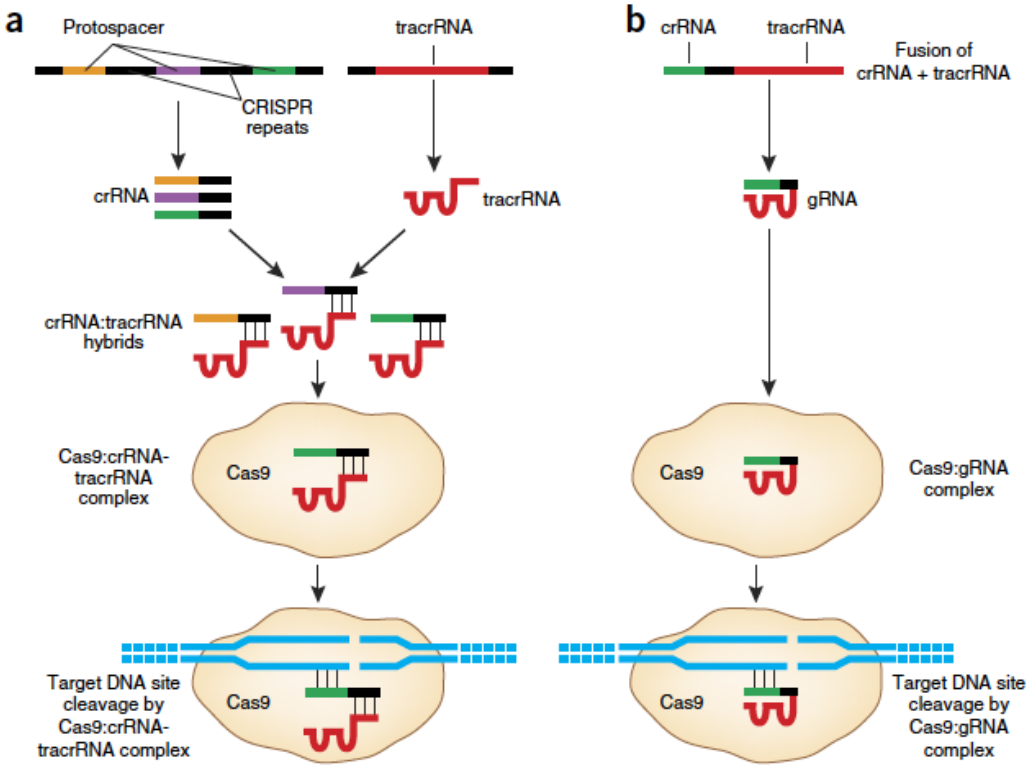

Figure 22. Naturally occurring and engineered CRISPR/Cas9 systems. A - Naturally occurring CRISPR systems incorporate foreign DNA sequences into CRISPR arrays, which then produce crRNAs bearing "protospacer" regions that are complementary to the foreign DNA site. crRNAs hybridize to tracrRNAs (also encoded by the CRISPR system) and this pair of RNAs can associate with the Cas9 nuclease. crRNA-tracrRNA: Cas9 complexes recognize and cleave foreign DNAs bearing the protospacer sequences. **B** - The most widely used engineered CRISPR/Cas9 system utilizes a fusion between a crRNA and part of the tracrRNA sequence. This sgRNA complexes with Cas9 to mediate cleavage of target DNA sites that are complementary to the 5′ 20 nt of the sgRNA and that lie next to a PAM sequence (adapted from *(Sander & Joung, 2014)* with permission).

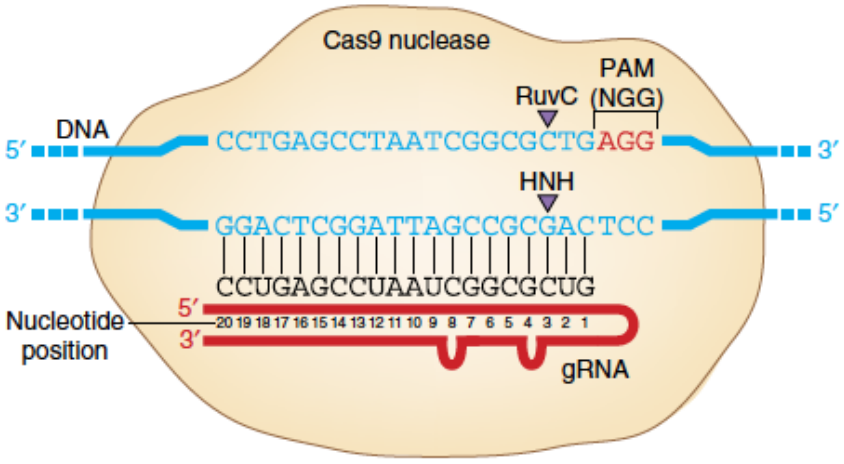

Figure 23. Cas9 nuclease creates double-strand breaks at DNA target sites with complementarity to the 5′ end of a sgRNA. Cas9 contains RuvC and HNH nuclease domains (arrowheads) (adapted from *(Sander & Joung, 2014)* with permission).

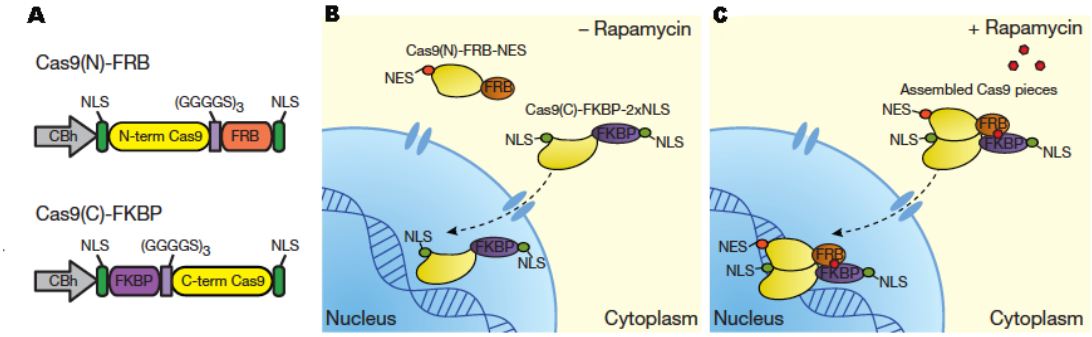

Figure 24. Inducible split-Cas9 fragments. A - Diagram of inducible split-Cas9 fusions. N- and C-terminal pieces of human codon–optimized Streptococcus pyogenes Cas9 are fused to FRB and FKBP dimerization domains, respectively. B and C - Strategy for the split-Cas9 system. In the absence of rapamycin (B), the Cas9(N)-FRBNES piece is sequestered in the cytoplasm owing to the addition of a NES. The Cas9(C)-FKBP piece contains two NLSs and is actively imported into the nucleus. In the presence of rapamycin (C), Cas9(N)-FRB-NES binds to Cas9(C)-FKBP. NLSs of the resulting reassembled Cas9 mediate nuclear importation and subsequent binding to the targeted locus. (adapted from *(Zetsche et al., 2015)* with permission).

To produce the *T. gondii* TBCB conditional knockout with CRISPR/Cas9 system we choose three different sgRNAs, using the Eukaryotic Pathogen CRISPR sgRNA Design Tool and respecting all the CRISPR/Cas9 sgRNA peculiar specificities. The simulation was done with the *T. gondii* GT1 ToxoDB-26 release since the *T. gondii* RH ToxoDB-26 was a limited annotation at the time, and the *T. gondii* GT1 genome is the closest to the *T. gondii* RH genome. All of the sgRNAs were directed to the first TgTBCB exon and one of them was complementary with the antisense non-coding strand of TgTBCB (Table 9). The three sgRNAs were then cloned by directed mutagenesis in the vector pU6-sgRNA-DHFR using specific primers for each sgRNA (Table 9) and the Q5 Site-Directed Mutagenesis Kit (New England Biolabs, Inc), according to the manufacture protocol. The constructions were then randomly integrated in the genome of the SplitCas9 *T. gondii* strain by electroporation, allowing us to induce the TgTBCB KO at any time.

Table 9. sgRNAs and primer sequences used in the construction and analysis of the TgTBCB conditional knockout in *T. gondii* by CRISPR/Cas9 system

TgTBCB sgRNAs	
sgRNA Number/ID	**sgRNA Sequence**
1 / TGGT1_305060_160	5'GACAAGCTGTACAGACACAC3'
2 / TGGT1_305060_121_revcom ♀	5'G* TCTCCATCCATCTGCGTCCA3' (revcom)
3 / TGGT1_305060_82	5'G* ATCACACACAATTTGCACCC3'
TGGT1_305060_160	
Primer Name	**Primer Sequence**
TBCBgRNA_Exon_1_F	5'ACAGACACACGTTTTAGAGCTAGAAATAGC3'
TBCBgRNA_Exon_1_R	5'ACAGCTTGTCaACTTGACATCCCCATTTAC3'
TGGT1_305060_121_revcom	
Primer Name	**Primer Sequence**
TBCBgRNA_Exon_2_F	5'TCTGCGTCCAGTTTTAGAGCTAGAAATAGC3'
TBCBgRNA_Exon_2_R	5'TGGATGGAGACaACTTGACATCCCCATTTAC3'
TGGT1_305060_82	
Primer Name	**Primer Sequence**
TBCBgRNA_Exon_3_F	5'ATTTGCACCCGTTTTAGAGCTAGAAATAGC3'
TBCBgRNA_Exon_3_R	5'TGTGTGTGATCaACTTGACATCCCCATTTAC3'
Primers used in the clonal lines amplification	
Primer Name	**Primer Sequence**
gRNAs_TBCB_pFext	5' ATGATACGGTGTGTCGCTGA 3'
gRNAs_TBCB_pRext	5'G* TCAGCGACACACCGTATCAT 3'
Primers used for Sequencing	
Primer Name	**Primer Sequence**
gRNAs_TBCB_pFint	5' GGCCGGTAATTTTCGACTTC 3'
gRNAs_TBCB_pRint	5' CTCCCTGCGATTTTCCATCT 3'

♀ revcom- complementary with the antisense non-coding strand of TgTBCB

*was added a G to the start of the sgRNA sequence since it does not start with G

6.4. Biochemistry

6.4.1. Preparation of parasite protein extracts for sodium dodecyl sulphate polyacrylamide gel electrophoresis (SDS-PAGE)

Two different protocols were used to prepare protein extracts from parasites for SDS-PAGE. One protocol was used to obtain total protein extracts and the other to obtain, separately, soluble and insoluble protein extracts.

For each sample, total protein extracts were obtained from 5 x 10^6 freshly lysed parasites (counted in a Neubauer chamber). Parasites were spindown in 1.5 ml tubes at 2500 g, for 10 min at RT. The pellet was washed with PBS. The obtained pellet was lysed with 8 µL of RIPA buffer (150 mM NaCl; 1 % Triton X-100; 0.5 % DOC; 0.1 % SDS; 50 mM Tris pH 8.0 and 1 mM EDTA) with Protease and Phosphatase Inhibitor Cocktail, EDTA-free 1X (Halt, Thermo Scientific), and the protein extracts were incubated on ice for 5 minutes. After, the solution was

centrifuged at 16000 g, for 1 hour at 4 ºC and the supernatant was transferred to a new tube. Finally, loading buffer 2X (table 10) was added to the protein extracts and the samples were boiled during 5 minutes at 95 ºC. The total amount of each sample was loaded to one well.

The soluble and insoluble protein extracts were prepared from freshly lysed parasites from one T25 flask. Parasites were centrifuged at 1300 g, for 10 min at 4 °C. The pellet was washed twice with PBS. The parasite pellet was lysed with 300 µl of lysis buffer (H Solution – see table 10; 0.1% Triton X-100 and Protease and Phosphatase Inhibitor Cocktail, EDTA-free) and then centrifuged at 16000 g, for 20 minutes at 4º C. The soluble protein extract (supernatant) was transferred to a new tube. The pellet was first resuspended in 150 µl of urea 8M and then 150 µl of loading buffer 2X (table 10) were added. The samples were boiled during 5 minutes at 95 ºC. The quantification of soluble protein was done by the Bradford Protein Assay and the same amount of protein was loaded to each well.

Table 10. Solutions used for the preparation of soluble and insoluble protein extracts from *T. gondii*.

Reagents for parasite cell lysates	
Solution Name	**Solution Composition**
Loading buffer 2X	83 mM Tris, pH 6.8; 13.3 % glycerol (w/v); 2.7 % SDS; 0.5 % bromophenol blue and 6.7 % β-mercaptoethanol
Loading buffer 5X	250 mM Tris, pH 6.8; 30 % glycerol (w/v); 0.4 % SDS; 0.5 % bromophenol blue and 16 % β-mercaptoethanol
H Solution	50 mM Hepes pH 7.6, 2 mM EDTA, 100 mM NaCl and 250 mM Sucrose

6.4.2. Determination of protein concentration by Bradford Protein Assay

The Bradford Protein assay was invented by Bradford in 1976 (biochemistry1976, 1976) and uses the dye Coomassie Brilliant Blue G-250 to measure the concentration of total protein in a sample. The principle of this assay is that the binding of protein molecules to Coomassie dye under acidic conditions results in a colour change from brown to blue. This method actually measures the presence of the basic amino acid residues, arginine, lysine and histidine, which contributes to the formation of the protein-dye complex. Unlike other assays, reducing agents and metal chelators at low concentration do not cause interference. However, the presence of SDS even at low concentrations can interfere with protein-dye binding.

The Bradford reagent (Bio-Rad Protein Assay) was used according to the manufacturer instruction for the microassay procedure intended for protein concentrations between 1.2 and 10 µg/ml. Brifley, in 1.5 ml microtube, it was added: 800 µl H_2O, 200 µl of Bradford reagent and 1µl of the protein soluble extract. The solutions were mixed by the inversion of the tubes

and incubated at RT for 15 minutes. Finally, the absorbance was measure at 595 nm and the sample concentration was calculated using a protein standard curve.

The protein standard curve was set using five standard solutions containing known concentrations of BSA between 1.2 to 10 µg/ml and following the procedure described above.

6.4.3. SDS-PAGE

Separation of proteins was achieved by SDS-PAGE, first described by Laemmli (Laemmli, 1970). Using the SDS-PAGE proteins can be separated according to their molecular weight. SDS is a detergent that binds to the protein at a constant molar ratio, denaturing and conferring a negative charge to the protein. Polyacrylamide gels are built by co-polymerization of acrylamid and bis-acrylamide. This reaction is initiated by a free radical-generating system. The polymerisation is catalysed by ammonium persulfate (APS) and tetramethylethylenediamine (TEMED). According to the system from Laemmli the gel consists of a large pore sized stacking gel (and a small pore sized resolving gel. Upon applying an electrical field, the proteins wander in direction of the anode, while first being concentrated in the stacking gel and secondly being separated according to their molecular weight in the resolving gel. The protein ladder helps to estimate the size of the proteins. SDS-PAGE was carried out with the Mini-Protean Tetra Vertical Electrophoresis Cell (BioRad) according to manufacturer's instructions and the protein ladder was the Precision Plus Protein™ Dual Color Standards (BioRad). The solutions of the stacking and the resolving gels are detailed in the table 11. The samples were loaded into the gel using a Hamilton Syringe and for each gel 10 µl of protein ladder were loaded. The gel migrates in running buffer (25 mM Tris base, 192 mM glycine, 0.1% SDS) at 25 mA/gel. After electrophoresis, gels were transferred to nitrocellulose membranes to perform immunoblotting.

Table 11. SDS-PAGE gels.

SDS-PAGE	
Solution Name	**Solution Composition**
5 % Stacking gel – stock solutions	**5 % Stacking gel - Final concentrations**
Acrylamide-40 %	5 % Acrylamide
1 M Tris HCl pH 6.8	0.125 M Tris HCl pH 6.8
20 % SDS	0.1 % SDS
10 % APS	0.1 % APS
TEMED	0.1 % TEMED
10 % Resolving gel – stock solutions	**10 % Resolving gel - Final concentrations**
Acrylamide-40 %	10 % Acrylamide
1.5 M Tris HCl pH 8.8	0.372 M Tris HCl pH 8.8
20 % SDS	0.1 % SDS
10 % APS	0.05 % APS
TEMED	0.05 % TEMED
15 % Resolving gel – stock solutions	**15 % Resolving gel - Final concentrations**
Acrylamide-40 %	15 % Acrylamide
1.5 M Tris HCl pH 8.8	0.372 M Tris HCl pH 8.8
20 % SDS	0.1 % SDS
10 % APS	0.05 % APS
TEMED	0.05 % TEMED

6.4.4. Staining of proteins in SDS-PAGE with Coomassie Brilliant Blue (CBB)

Coomassie blue dyes R and G types are commonly used for the visualization of proteins separated by SDS-PAGE, because of their low cost, ease of use and good compatibility with mass spectrometric protein identification. However, despite these advantages, CBB is regarded as less sensitive than fluorescence or silver staining and, therefore, is rarely used for the detection of proteins in analytical gel-based proteomic approaches.

Coomassie blue R-250 dye is used to visualize proteins via a regressive staining approach in which gels are saturated with dye and then destained with an aqueous solution containing methanol and acetic acid. The proteins are visible after destaining because they have a higher affinity for the dye molecules than does the gel matrix.

The gels were stained with 0.25 % CBB R250 (m/v), 10 % glacial acetic acid (v/v), 50% methanol (v/v) in water for 30 minutes. Then, the gel was destained by soaking, for at least 2 h, in the strong destaining solution (10 % glacial acetic acid (v/v), 50 % methanol (v/v) in water), changing the solution at least two times during this period. After, the gel was destained with a soft destaining solution (7 % glacial acetic acid (v/v), 10 % methanol (v/v) in water), until the background is clear.

6.4.5. Transfer of proteins from SDS-PAGE to nitrocellulose membrane

After the SDS-PAGE, the proteins were transferred onto a nitrocellulose membrane, Amersham Protran 0.45 NC nitrocellulose Western blotting membrane (GE Healthcare). For that it was used a Wet/Tank blotting system from Bio-Rad (Mini Trans-Blot Cell) according to manufacturer's instructions. The membrane was equilibrated for 15 minutes in distilledwater. The gel, the membrane and the 3MM filter papers were equilibrated in transfer buffer (25 mM Tris base, 192 mM Glycine, 10 % methanol in water) for 10 minutes. Next, the sandwich for blotting was assembled (One Foam pads, 3MM filter papers, blotting membrane, gel, 3MM filter papers, One Foam pads) and the blot was run at 350 mA for 60 minutes or at 30 V overnight. The gel should be the side of the cathode (-) and the nitrocellulose membrane should be to the side of the anode (+).

6.4.6. Ponceau-S-staining

To detect proteins on the nitrocellulose membranes we used the Ponceau-S staining. Ponceau S is a negative stain that binds reversible to the positively charged amino groups of the proteins. For the staining, the nitrocellulose membrane was incubated with Ponceau S solution (Sigma-Aldrich) a few minutes and subsequently washed with water until red stained protein bands were visible.

6.4.7. Immunoblotting

Blotted membranes were washed with PBS to remove the Ponceau-S staining and then were blocked in 5 % (w/v) Molico skimmed milk powder (Nestlé) in PBS, 0.2 % Tween20 (v/v) at 4 °C for overnight. Primary antibodies were diluted to the appropriate concentration (table 12) in the blocking solution. After blocking, the membrane was incubated with the primary antibodies for 1 hour at RT in the orbital shaker. Then the membrane was rinsed once in PBS and washed three times for 10 minutes with PBS, 0.2 % Tween20 (v/v) in an orbital shaker. Horseradish peroxidase (HRP) labelled secondary antibodies were diluted to the appropriate concentration (table 12) in blocking solution and the membrane was incubated with the secondary antibodies for 1 hour at RT in the orbital shaker. Afterwards, the membranes were washed three times for 10 minutes in PBS, 0.2 % Tween20 (v/v) in an orbital shaker. HRP conjugated secondary antibodies were detected with the Amersham ECL Prime Blocking Reagent

(GE Healthcare) or with WesternBright Quantum HRP substrate (Advansta), according to manufacturer's instructions. The visualization was done by manually exposing the membranes to Amersham Hyperfilm ECL (GE Healthcare) X-ray films and developing with D-19 Developer and Fixer Carestream Kodak Processing chemicals (Kodak) or using the ChemiDoc™ XRS+ System (Bio-Rad).

6.5. Microscopy

6.5.1. Immunofluorescence (IF) microscopy

For IF assays, confluent HFF cell monolayers on glass coverslips in 24 well plates were infected with *T. gondii* tachyzoites strains to be analysed. Cells were fixed either with 4 % paraformaldehyde (w/v) (PFA) in PBS for 20 minutes at RT or with methanol for 10 minutes at -20 °C, depending on the primary antibodies that are used and, the structures to be analysed. After the fixation, cells were washed two times with PBS during 5 minutes in an orbital shaker. Cells fixed by PFA were permeabilized and blocked with a solution containing 2 % BSA and 0.2 % Triton X-100 in PBS for 30 minutes at RT. Cells fixed by methanol were blocked with 2 % BSA in PBS for 30 minutes at RT. The primary antibodies (table 12) were diluted in blocking solution and incubated for 1h at RT. The coverslips were washed two times with PBS, 0.1 % Tween-20, and one time with PBS, during 5 minutes at RT and on an orbital shaker. The secondary antibodies (table 12) were diluted in blocking solution and incubated for 1h at RT. Then, the coverslips were washed two times with PBS, 0.1% Tween-20, and one time with PBS, during 5 minutes at RT and on an orbital shaker. Finally, the coverslips were mounted with DAPI Fluoromount-G Mounting Medium (SouthernBiotech) on glass slides and the excess of mounting medium was removed with 3MM filter papers.

Table 12. Primary and secondary antibodies used in our work

Primary Antibodies				
Antibody	**Specie**	**IF Dilution**	**WB Dilution**	**Source**
Anti-c-Myc antibody	Rabbit	1:200	1:2000	Sigma
Anti-GFP	Mouse	-	1:1000	Roche
Monoclonal Anti-α-Tubulin antibody (DM1A)	Mouse	1:200	1:2000	Sigma
Monoclonal Anti-γ-Tubulin antibody	Mouse	1:200	1:2000	Sigma
Monoclonal Anti-Acetylated Tubulin antibody	Mouse	1:200	1:2000	Sigma
Polyglutamylation Modification, mAb (GT335)	Mouse	1:200	1:4000	Adipogen
TgTBCB specific polyclonal serum	Rabbit	1:100 1:200	1:1000 1:2000	In house
ISP1 7E8	Mouse	1:500	-	Peter J. Bradley
Rop2-4 T34A7	Mouse	1:500	-	Jean-François Dubremetz
MIC2 6D10	Mouse	1:500	-	Vern Carruthers
MIC3 T82C10	Mouse	1:300	-	Maryse Lebrun
Anti-PDI	Rabbit	-	1:500	In house
Anti-human Centrin	Rabbit	1:200	-	Iain Cheeseman
Secondary Antibodies				
Antibody	**Specie**	**Dilution IFA**	**Dilution WB**	**Source**
Alexa Fluor® 594 Goat Anti-Mouse IgG (H+L)	Goat	1:500	-	Invitrogen
Alexa Fluor® 594 Donkey Anti-Rabbit IgG (H+L)	Donkey	1:500	-	Invitrogen
Alexa Fluor® 488 Goat Anti-Mouse IgG (H+L)	Goat	1:500	-	Invitrogen
Alexa Fluor® 488 Goat Anti-Mouse IgG1 (γ1)	Goat	1:500	-	Invitrogen
Alexa Fluor® 488 Donkey Anti-Rabbit IgG (H+L)	Donkey	1:500	-	Invitrogen
Alexa Fluor® 594 Chicken Anti-Rabbit IgG (H+L)	Chicken	1:500	-	Invitrogen
Anti-Rabbit IgG (H+L) Secondary Antibody, HRP conjugate	Goat	-	1:1000 to 1:2000	Invitrogen
Anti-Mouse HRP	Goat	-	1:4000	Jackson ImmunoResearch

6.5.2. Microscopy equipment and settings

Microscopes used on our work:

- Leica DMRA2 DMR HC microscope, equipped with a Leica DFC340FX camera, using all objectives, including the 100x Oil immersion objective;
- Leica DMRA2 upright microscope, equipped with a CoolSNAP HQ CCD camera, using the 100x Oil immersion objective, controlled with the MetaMorph V7.5.1 software.
- Olympus AppliedPrecision DeltaVision Core system, mounted on an Olympus inverted microscope, equipped with a Cascade II 2024 EM-CCD camera, using the 100x Oil immersion objective. Images were deconvolved with the Huygens deconvolution software.
- Olympus Deltavision Core microscope (Image Solutions - Applied Precision, GE) attached to a CoolSNAP HQ2 CCD camera. For image acquisition, z-stacks were

collected using a UPLSAPO 100x oil (1.40NA) objective. Deconvolution was performed using SoftWoRx Suite 2.0 (Applied Precision, GE);

- Yokogawa CSU-X Spinning Disk confocal, mounted on a Leica DMi8 microscope, with a 63x 1.3NA Glycerine immersion objective. For image acquisition, z-stacks were collected using a Andor iXon Ultra EMCCD 1024x1024 camera. The system was controlled with Metamorph software.
- Elyra S1 microscope with Superresolution Structured Illumination (SR-SIM) (Zeiss) was used for super resolution microscopy.

6.5.3. Imaging

All images were further processed with Fiji software, a distribution of ImageJ with many plugins useful for scientific image analysis in fields such as life sciences.

6.6. Statistic

The statist analyses were done with IBM SPSS Statistic software Version 21, from IBM and with the Prism 7 Version 7.0e from GraphPad Software, Ins.

Intentionally blank page

1. Identification of *Toxoplasma gondii* TBCB gene

The search for the TBCB gene in the *T. gondii* genome started with a simple quest in ToxoDB for "Tubulin Cofactor". Since we did not find any candidate gene with that quest, we had to use a second approach, by means of the Blast engine from ToxoDB. For this we used the amino acid sequence of Human TBCB isoform 1 (*Homo sapiens* TBCB – HsTBCB, NP_001272.2) to blast against all the sequences available in the data base. Genes with an E-value above the borderline (E-11) were excluded and we looked for the *T. gondii* genes with the best Score and E-value. The results are showed in the table 13.

Using the Blast tool to compare amino acid sequences, we were able to find one putative gene for *T. gondii* TBCB (TgTBCB). The gene found is transversal to all *T. gondii* strains and have the same Score and E-value in all of them. It was also interesting that the gene with highest Score and E-value, 90.5, belongs to *Neospora caninum*. Moreover, when we used the HsTBCB isoform 2 (NP_001287900.1) instead the isoform 1 the blast results were similar to those in the table 13.

Table 13. Blast results from ToxoDB using the amino acid sequence of the HsTBCB isoform 1 (NP_001272.2).

Gene ID	Source_id	Organism	Score	E-Value
NCLIV_001310	NCLIV_001310-t26_1	*Nneospora caninum* Liverpool	90.5	3.00E-20
CSUI_000538	CSUI_000538-t36_1	*Cystoisospora suis* strain Wien I	77	1.00E-15
HHA_305060	HHA_305060-t26_1	*Hammondia hammondi* strain H.H.34	76.3	2.00E-15
TGARI_305060	TGARI_305060-t30_1	*Toxoplasma gondii* ARI	74.7	8.00E-15
TGDOM2_305060	TGDOM2_305060-t30_1	*Toxoplasma gondii* GAB2-2007-GAL-DOM2	74.7	8.00E-15
TGFOU_305060	TGFOU_305060-t30_1	*Toxoplasma gondii* FOU	74.7	8.00E-15
TGGT1_305060	TGGT1_305060-t26_1	*Toxoplasma gondii* GT1	74.7	8.00E-15
TGMAS_305060	TGMAS_305060-t30_1	*Toxoplasma gondii* MAS	74.7	8.00E-15
TGME49_305060	TGME49_305060-t26_1	*Toxoplasma gondii* ME49	74.7	8.00E-15
TGP89_305060	TGP89_305060-t30_1	*Toxoplasma gondii* p89	74.7	8.00E-15
TGPRC2_305060	TGPRC2_305060-t30_1	*Toxoplasma gondii* TgCatPRC2	74.7	8.00E-15
TGRUB_305060	TGRUB_305060-t30_1	*Toxoplasma gondii* RUB	74.7	8.00E-15
TGVAND_305060	TGVAND_305060-t30_1	*Toxoplasma gondii* VAND	74.7	8.00E-15
TGVEG_305060	TGVEG_305060-t26_1	*Toxoplasma gondii* VEG	74.7	8.00E-15
EfaB_MINUS_32574.g2464	EfaB_MINUS_32574.g2464.t1	*Eimeria falciformis* Bayer Haberkorn 1970	73.6	8.00E-14
EAH_00008110	EAH_00008110-t26_1	*Eimeria acervulina* Houghton	68.2	8.00E-13

1.1. *T. gondii* TBCB putative gene

The gene identified as TBCB in *T. gondii* was the 305060 (Table 14). Since in our work we were using the ME49 *T. gondii* strain, all our subsequent studies were done with the TGME49_305060 gene. This gene encodes a CAP-Gly domain-containing protein, sharing an identity of 38 % (Gajria et al., 2008) with the HsTBCB isoform 1 (Figure 25), coding a protein with 273 amino acids, with an expected molecular mass (MM) of approximately 30 kDa and an isoelectric point (pI) of 5.14.

Table 14. Functional domains of the HsTBCB and TgTBCB proteins.

TBCB Human and *T. gondii* functional domains				
Gene IF	**Functional Domain**	**Start**	**End**	**Source/E-Value**
HsTBCB - NP_001272.2	Ubiquitin-like domain	10	92	(Carranza et al., 2013)
	Coiled-Coil domain	125	158	
	CAP-Gly domain	159	233	
TgTBCB - TGME49_305060	Ubiquitin-like domain	25	107	4.62E-11
	CAP-Gly domain	181	257	1.22E-15

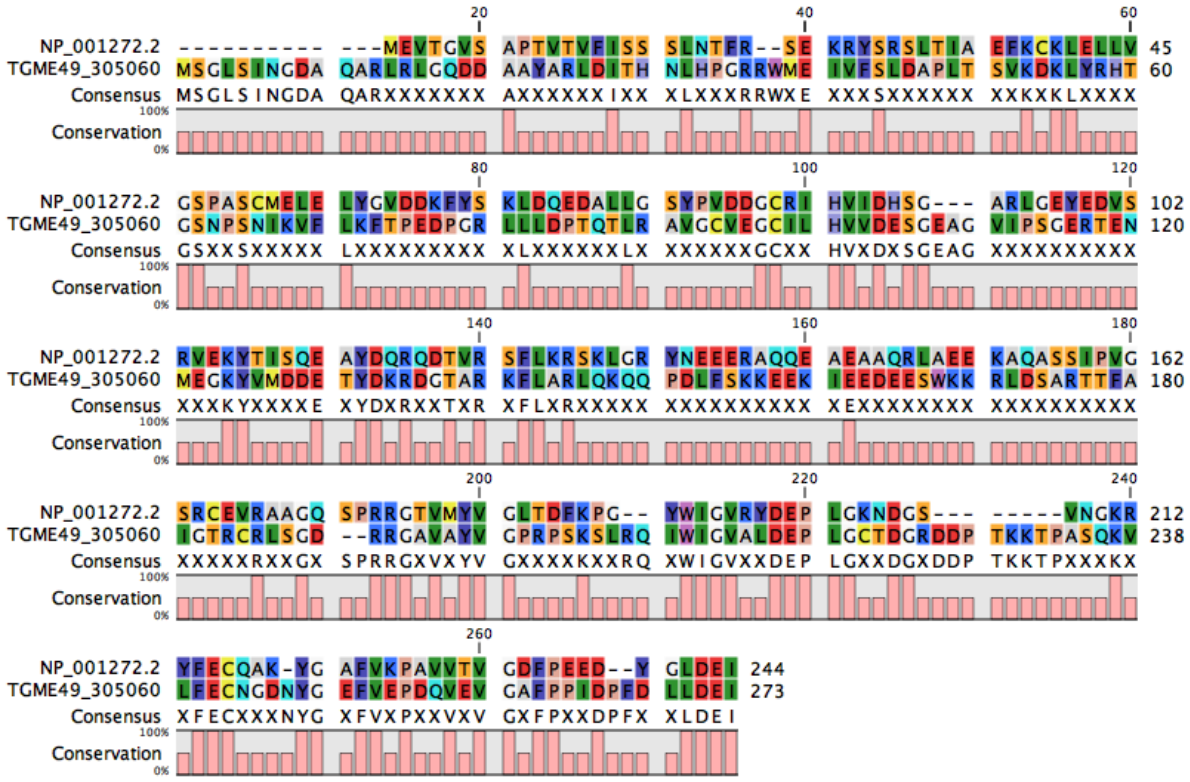

Figure 25. Amino acids sequences alignment, using CLC sequence viewer, of *T. gondii* TBCB (TgTBCB) (TGME49_305060) and *Homo sapiens* TBCB (NP_001272.2). According to ClustalW program, these proteins share an amino acid sequence identity of 38 %.

The TgTBCB predicted protein sequence possesses the characteristic domains of this TBCs, the CAP-Gly and the UbL domain. Interestingly, the HsTBCB and the TgTBCB share

the same specific domains, in the same positions, but the TgTBCB protein is slightly bigger (Figure 26 and Table 14).

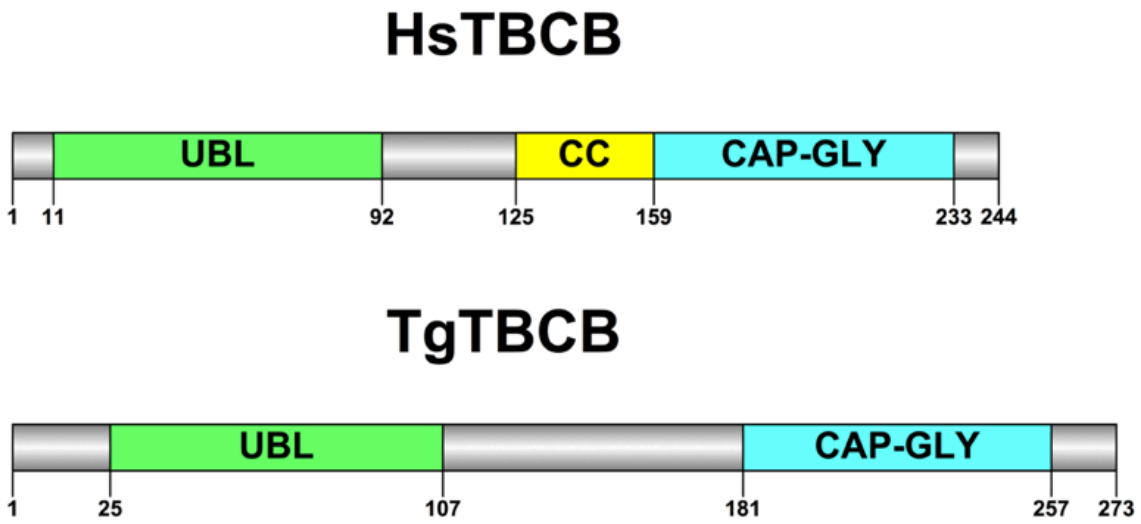

Figure 26. Schematic representation of the functional domains of the HsTBCB and TgTBCB proteins (DOG, Domain Graph, version 1.0). UbL - ubiquitin-like domain in the region N-terminal of both genes; CC - coiled-coil domain present only in the HsTBCB; CAP-Gly domain present in the C-terminal Region of both genes.

The 3D predicted structure of TgTBCB was done using the Protein Homology/analogY Recognition Engine from the Structural Bioinformatics Group, Imperial College, London (Figure 27).

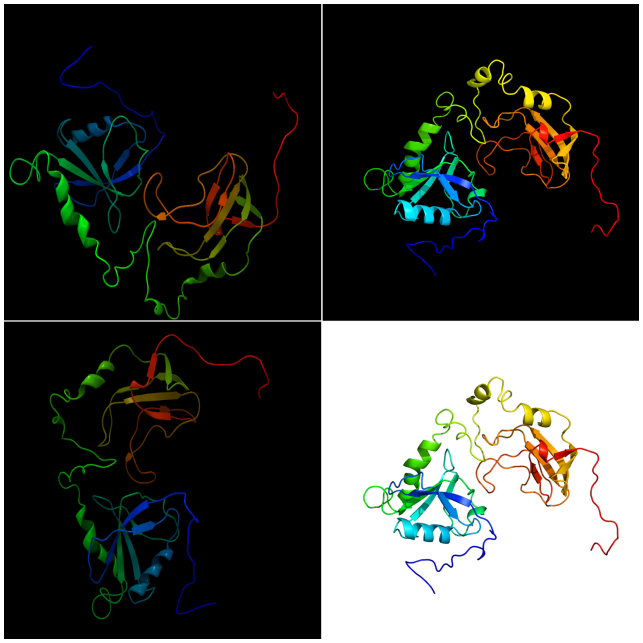

Figure 27. Predicted 3D structure of the *T. gondii* TBCB protein. Image coloured by rainbow from N to C terminus. N-Terminal region (UbL) in red and orange, middle region in blue and C-terminal region (Cap-Gly) in green *(Kelley, Mezulis, Yates, Wass, & Sternberg, 2015)*.

1.2. Comparative analysis of TBCB sequences in Apicomplexa

To create a quick analysis of TBCB sequences in Apicomplexa, we blasted the HsTBCB isoform 1 (NP_001272.2) against all the Apicomplexa available at the Eukaryotic Pathogen Genomics Database Resource (EupathDB) (table 15). The obtained result show that all the found genes code for putative or hypothetical TBCB related proteins. However, from the 50 genes found only 14 were annotated as CAP-Gly domain-containing protein. Among apicomplexan organisms, *Babesia bovis* and *Neospora caninum* present the highest scores for TBCB genes.

Some of these genes were chosen to create a sequence alignment with the HsTBCB isoform 1 (Figure 28). The result suggests that the apicomplexan parasites share some conserved amino acid sequences, some of them in the Cap-Gly region, but they do not keep the integrity of the highly conserved GK(N/H)DG sequence. Only the first and last two amino acids of this sequence are conserved among Apicomplexa.

Table 15. Blast results from the EupathDB using the protein sequence of the HsTBCB isoform 1 (NP_001272.2).

Gene ID	Source_id	Organism	Score	E-Value
BBOV_IV005610	BBOV_IV005610-t26_1	*Babesia bovis* T2Bo	92.8	9.00E-21
NCLIV_001310	NCLIV_001310-t26_1	*Neospora caninum* Liverpool	90.5	6.00E-20
PCOAH_00018560	PCOAH_00018560-t30_1	*Plasmodium coatneyi* Hackeri	85.1	4.00E-18
PRELSG_0704300	PRELSG_0704300.1	*Plasmodium relictum* SGS1-like	85.1	3.00E-18
BBBOND_0209120	BBBOND_0209120-t26_1	*Babesia bigemina* strain BOND	84	1.00E-17
YYE_01887	YYE_01887-t30_1	*Plasmodium vinckei vinckei* strain vinckei	83.6	1.00E-17
BOVATA_011480	BOVATA_011480-t37_1	*Beroe ovata* strain Miyake	82.8	2.00E-17
BEWA_030750	BEWA_030750-t26_1	*Theileria equi* strain WA	82	5.00E-17
PBANKA_0808420	PBANKA_0808420.1	*Plasmodium berghei* ANKA	82	4.00E-17
PRCDC_0905010	PRCDC_0905010.1	*Plasmodium reichenowi* CDC	82	4.00E-17
PRG01_0914400	PRG01_0914400-t36_1	*Plasmodium reichenowi* G01	82	4.00E-17
PPRFG01_0905900	PPRFG01_0905900.1	*Plasmodium praefalciparum* strain G01	81.6	5.00E-17
PF3D7_0906910	PF3D7_0906910.1	*Plasmodium falciparum* 3D7	81.3	9.00E-17
PFIT_0907110	PFIT_0907110.1	*Plasmodium falciparum* IT	81.3	9.00E-17
PBLACG01_0906300	PBLACG01_0906300-t36_1	*Plasmodium blacklocki* G01	80.9	9.00E-17
YYG_01053	YYG_01053-t30_1	*Plasmodium vinckei petteri* strain CR	80.9	2.00E-16
PGAL8A_00419600	PGAL8A_00419600.1	*Plasmodium gallinaceum* 8A	80.5	1.00E-16
PBILCG01_0910600	PBILCG01_0910600-t36_1	*Plasmodium billcollinsi* G01	80.1	2.00E-16
PCHAS_0808720	PCHAS_0808720.1	*Plasmodium chabaudi chabaudi*	79.3	3.00E-16
AK88_00884	AK88_00884-t30_1	*Plasmodium fragile* strain nilgiri	79	4.00E-16
PGABG01_0904500	PGABG01_0904500-t36_1	*Plasmodium gaboni* strain G01	79	4.00E-16
PKNH_0704700	PKNH_0704700.1	*Plasmodium knowlesi* strain H	79	4.00E-16
PKNOH_S06406200	PKNOH_S06406200-t35_1	*Plasmodium knowlesi* strain Malayan Strain Pk1 A	79	4.00E-16
PGSY75_0906910	PGSY75_0906910-t31_1	*Plasmodium gaboni* strain SY75	77.4	1.00E-15
CSUI_000538	CSUI_000538-t36_1	*Cystoisospora suis* strain Wien I	77	3.00E-15
PVP01_0705400	PVP01_0705400.1	*Plasmodium vivax* P01	77	2.00E-15
PADL01_0906100	PADL01_0906100-t36_1	*Plasmodium adleri* G01	76.6	3.00E-15
HHA_305060	HHA_305060-t26_1	*Hammondia hammondi* strain H.H.34	76.3	4.00E-15
PCYB_071470	PCYB_071470-t26_1	*Plasmodium cynomolgi* strain B	75.1	1.00E-14
PVX_098786	PVX_098786.1	*Plasmodium vivax* Sal-1	75.1	9.00E-15
PcyM_0704800	PcyM_0704800-t36_1	*Plasmodium cynomolgi* strain M	75.1	1.00E-14
TGARI_305060	TGARI_305060-t30_1	*Toxoplasma gondii* ARI	74.7	2.00E-14
TGDOM2_305060	TGDOM2_305060-t30_1	*Toxoplasma gondii* GAB2-2007-GAL-DOM2	74.7	2.00E-14
TGFOU_305060	TGFOU_305060-t30_1	*Toxoplasma gondii* FOU	74.7	2.00E-14
TGGT1_305060	TGGT1_305060-t26_1	*Toxoplasma gondii* GT1	74.7	2.00E-14
TGMAS_305060	TGMAS_305060-t30_1	*Toxoplasma gondii* MAS	74.7	2.00E-14
TGME49_305060	TGME49_305060-t26_1	*Toxoplasma. gondii* ME49	74.7	2.00E-14
TGP89_305060	TGP89_305060-t30_1	*Toxoplasma gondii* p89	74.7	2.00E-14
TGPRC2_305060	TGPRC2_305060-t30_1	*Toxoplasma gondii* TgCatPRC2	74.7	2.00E-14
TGRUB_305060	TGRUB_305060-t30_1	*Toxoplasma. gondii* RUB	74.7	2.00E-14
TGVAND_305060	TGVAND_305060-t30_1	*Toxoplasma gondii* VAND	74.7	2.00E-14
TGVEG_305060	TGVEG_305060-t26_1	*Toxoplasma. gondii* VEG	74.7	2.00E-14
EfaB_MINUS_32574.g2464	EfaB_MINUS_32574.g2464.t1	*Eimeria falciformis* Bayer Haberkorn 1970	73.6	2.00E-13
PocGH01_07014400	PocGH01_07014400.1	*Plasmodium ovale curtisi* GH01	73.2	5.00E-14
PY05144	PY05144-t26_1	*Plasmodium yoelii yoelii* 17XNL	72	1.00E-13
PY17X_0811700	PY17X_0811700.1	*Plasmodium yoelii yoelii* 17X	72	1.00E-13
PYYM_0811410	PYYM_0811410.1	*Plasmodium yoelii yoelii* YM	72	1.00E-13
C922_01505	C922_01505-t30_1	*Plasmodium inui* San Antonio 1	69.3	1.00E-12
EAH_00008110	EAH_00008110-t26_1	*Eimeria acervulina* Houghton	68.2	2.00E-12
PmUG01_07018500	PmUG01_07018500.1	*Plasmodium malariae* UG01	66.6	2.00E-11

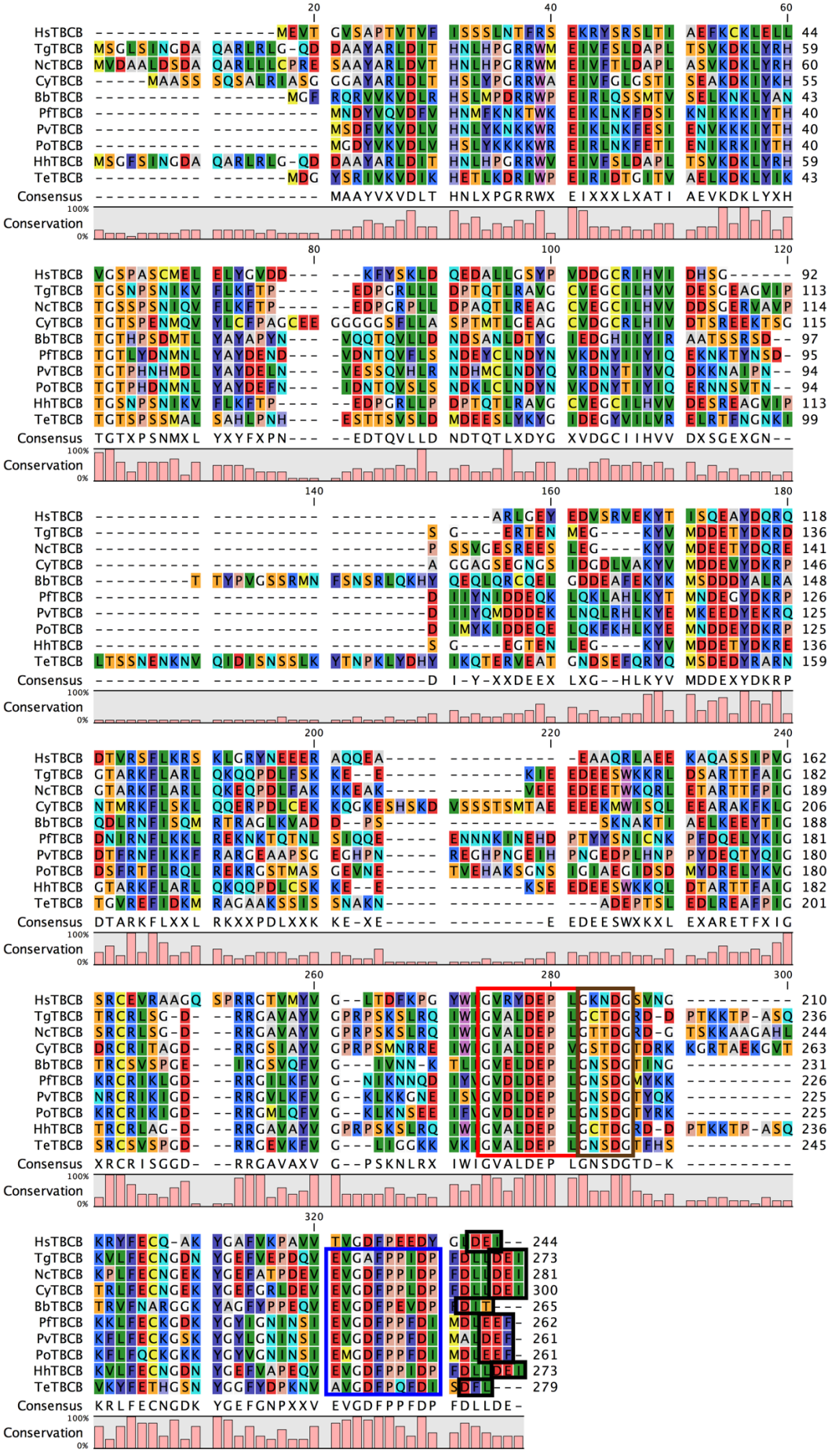

Figure 28. Amino acid sequence alignment of Homo sapiens (NP_001272.2) – HsTBCB – With: TgTBCB – *T. gondii* TBCB (TGME49_305060); NcTBCB - *Neospora caninum* (NCLIV_001310); CyTBCB - *Cystoisospora suis* (CSUI_000538);

BbTBCB - *Babesia bovis* (BBOV_IV005610); PfTBCB - *Plasmodium falciparum* (PF3D7_0906910); PvTBCB - *Plasmodium vivax* (PVP01_0705400); PoTBCB - *Plasmodium ovale curtisi* (PocGH01_07014400); HhTBCB - *Hammondia hammondi* (HHA_305060) and TeTBCB - *Theileria equi* (BEWA_030750). Highly conserved GK(N/H)DG sequence **– brown square**. GVALDEPL conserved amino acid sequence in Apicomplexa – **red square**. EVGDFPPIDP conserved amino acid sequence in Apicomplexa **– blue square**. DEI/M motif – **black square** (alignment performed by CLC sequence viewer).

2. Expression analysis of *T. gondii Tbcb* during the host cell invasion by Real time PCR

As a first approach to investigate the role of *Tbcb* gene in *T. gondii* we studied the expression profile of the gene during different phases of host cell invasion by quantitative real time PCR using specific primers for this gene.

For this analysis, total RNA was extracted from freshly egressed tachyzoites (control, 0h) and from tachyzoites inside their host cells at 0.5, 1, 4 and 8 h after cell invasion (Figure 29).

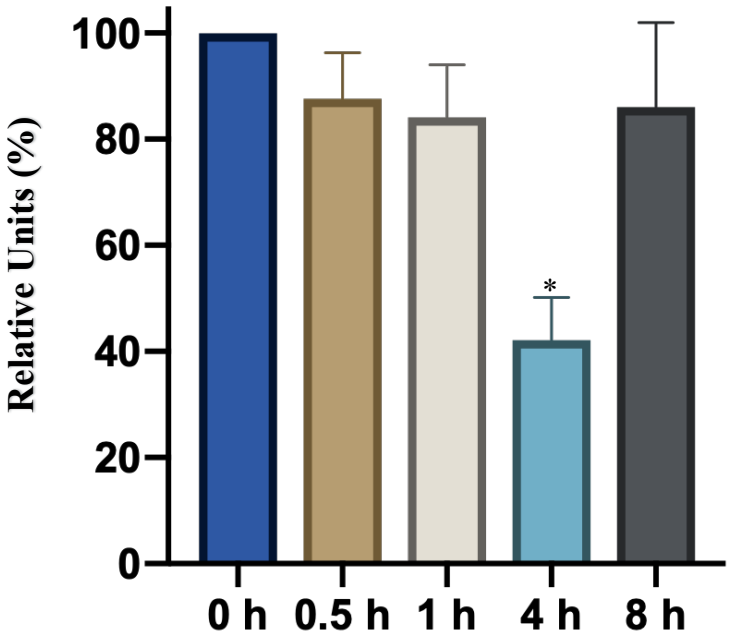

Figure 29. Quantitative Real-Time PCR analysis of TgTbcb expression in *T. gondii* after host cell invasion. Total RNA was extracted from freshly released tachyzoites (control) and from tachyzoites inside host cells at 0.5, 1, 4 and 8h after cell invasion. The gene glyceraldehyde-3-phosphate dehydrogenase 1 (Gapdh1) was used as internal control. The data obtained for each time point was normalized to the TgTbcb levels as a percentage of maximal value (100 %) for the free and freshly released tachyzoites (0 h). The graphic bars are the mean ± SEM (error bars) of three independent assays. Statistical significance was calculated using the student t-test (* $p < 0.005$)

TgTbcb RNA levels from three independent experiments were evaluated and the data obtained for each time point was normalized to *TgTbcb* levels in the free and freshly released tachyzoites (0 h). In these experiments, we used the *glyceraldehyde-3-phosphate*

dehydrogenase 1 (*Gapdh1*) transcript levels as internal control. So, to access the real *T. gondii Tbcb* expression we normalized the obtained Tg*Tbcb* values to the *TgGapdh* values.

The only significant difference observed in comparison to the free parasites (corresponding to 100 %, relative units) was the decrease in *TgTbcb* RNA levels 4 h after the invasion (to ~ 42%) (Figure 29).

3. Production of TgTBCB specific polyclonal serum

As previously described, to start the production of the anti-TgTBCB specific polyclonal serum, we had to clone the TgTBCB cDNA in a bacteria expression vector (pET3a) and make a preliminary induction test to determine the best induction time. Two different expression time points were tested and the best one was chosen to start the TgTBCB protein production. The figure 30A shows the results of this test, documenting that the highest protein production was obtained 2 h after induction.

Recombinant TgTBCB was in the insoluble fraction and it was purified by SDS-PAGE, followed by copper staining and electroelution of the induced protein. The purified protein was analyzed in a 15 % SDS-PAGE, and then the gel was Coomassie stained to check for contaminant proteins. Only a protein band slightly above 37 kDa was visible in the SDS-PAGE (Figure 30B) suggesting that no contaminant proteins with different sizes were present.

Finally, in collaboration with Juan Carlos Zabala (Departamento de Biología Molecular, Facultad de Medicina, Universidad de Cantabria, Santander, Spain), the purified protein was used to immunize tow rabbits. The obtained polyclonal serum was tested against *T. gondii* protein extracts by western blot (WB) (Figure 30C). The obtained polyclonal serum recognized a protein with approximately 37 kDa (Figure 30C), presenting exactly the same size of the recombinant TgTBCB produced in bacteria protein extracts.

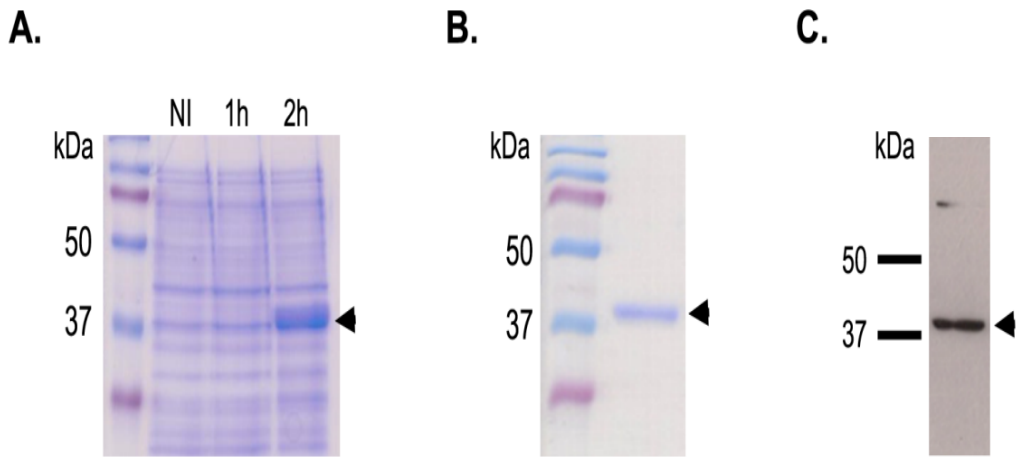

Figure 30. *T. gondii* TBCB protein antibody production. A - TgTBCB produced in *Escherichia coli* BL21. Total protein extracts were prepared from bacteria after 1 h and 2 h of TgTBCB protein induction. Total protein extracts without induction were also prepared as a control (NI - no induction). The arrow head indicates the TgTBCB protein. The protein extracts were analyzed by 15 % (w/v) SDS-PAGE. The gel was stained with Coomassie Brilliant Blue; **B -** After purification, TgTBCB was analyzed by 15 % (w/v) SDS-PAGE. The gel was stained with Coomassie Brilliant Blue; **C -** WB analysis of TgTBCB. Protein extracts from *T. gondii* were analyzed by 15 % (w/v) SDS–PAGE followed by WB with our specific polyclonal antibody directed to TgTBCB.

4. TgTBCB sub-cellular localization

After the successful production of TgTBCB specific polyclonal serum, we used it to study the TgTBCB sub-cellular localization by immunolocalization.

In *T. gondii*, tubulin glutamylation occurs close to the conoid and progressively decreases towards the distal end of the subpellicular MTs (Plessmann, Reiter-Owona, & Lechtreck, 2004). As a first approach to address the TgTBCB we performed an immunolocalization assay with antibodies anti-TgTBCB and anti-glutamylated tubulin (MT cytoskeleton apical marker). The results obtained with intracellular tachyzoites showed that TgTBCB is localized at the anterior region of the parasite, close to the apical complex and immediately below the conoid region, presenting a polarised distribution (Figure 31).

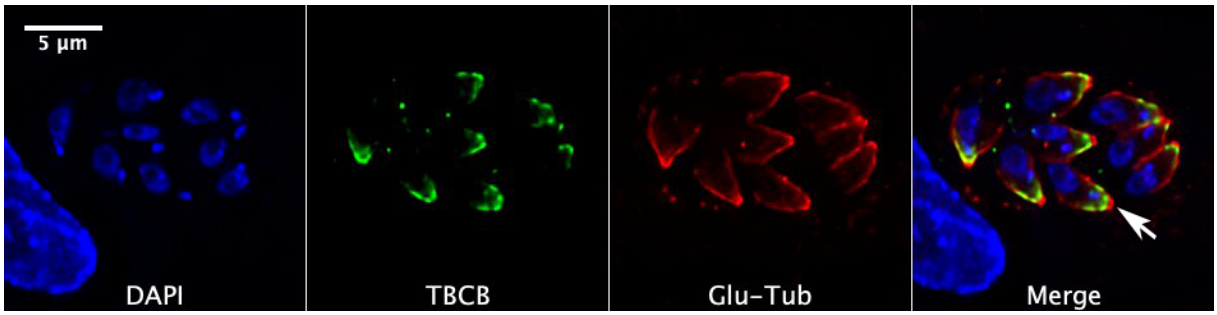

Figure 31. TgTBCB presents an apical localization in intracellular tachyzoites. HFF cells were invaded with *T. gondii* for 24 h, then cells were immunostained with antibodies against TgTBCB (green) and polyglutamylated tubulin (GT335, red). DNA was stained with DAPI (blue). TgTBCB is localized at the anterior region of the parasite, close to the apical complex and immediately below the conoid. Arrow indicates the conoid. Images were acquired using the Olympus AppliedPrecision DeltaVision Core system. Scale bar, 5 µm.

In extracellular tachyzoites, TgTBCB seems to have the same localization as in the intracellular parasites (Figures 32 and 33).

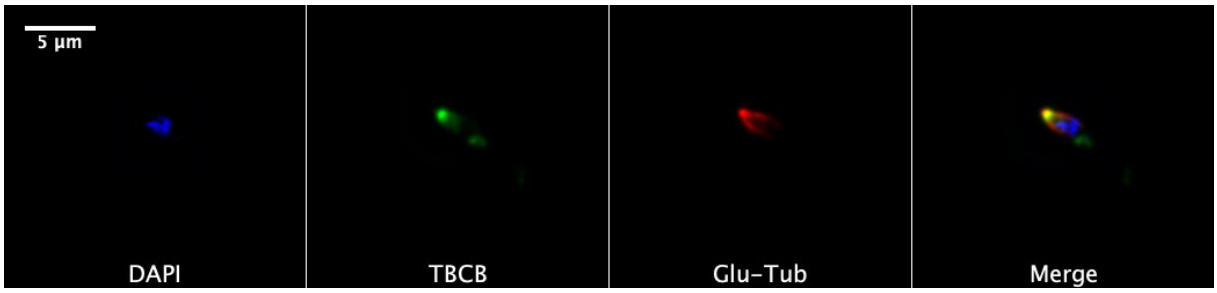

Figure 32. **TgTBCB presents an apical localization in extracellular tachyzoites**. Parasites were immunostained with antibodies against TgTBCB (green) and polyglutamylated tubulin (GT335, red). DNA was stained with DAPI (blue). TgTBCB is localized at the anterior region of the parasite, close to the apical complex. Images were acquired using the Olympus AppliedPrecision DeltaVision Core system. Scale bar, 5 µm.

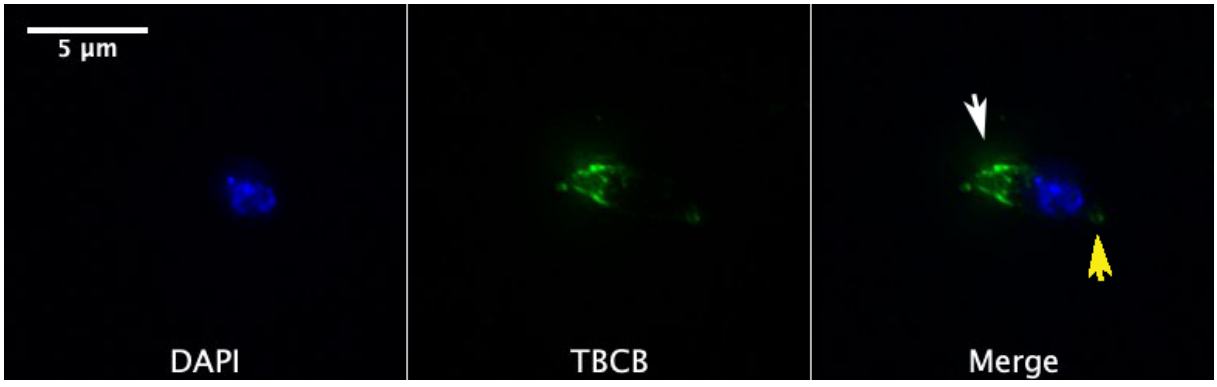

Figure 33. TgTBCB seems to localize at the apical region of the subpellicular MTs in extracellular tachyzoites. Parasites were immunostained with antibodies against TgTBCB (green). DNA was stained with DAPI. The white arrow indicates the apical region and the yellow arrow indicates the posterior region. Images were acquired using the Olympus Deltavision Core microscope. Scale bar, 5 µm.

Afterwards, several assays were performed to better characterize the TgTBCB apical localization. These assays were mostly done at Dr. Markus Meissner Lab by conventional and super resolution microscopy (ELYRA). Some assays were performed in our lab and analyzed at the Unit of Imaging and Cytometry of the Instituto Gulbenkian de Ciência (IGC).

Using the super resolution microscopy, we were able to see in more detail the TgTBCB sub-cellular localization. It is definitely located at the apical region, starting near the conoid and extended till one third of the parasite. Some staining dots at the posterior region were also observed (Figure 34), as suggested in previous IFs (Figures 32 and 33).

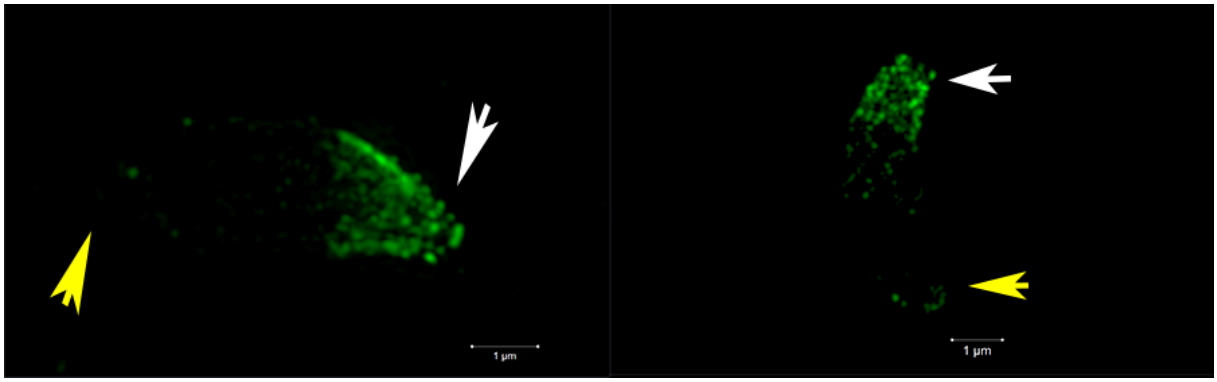

Figure 34. TgTBCB sub-cellular localization in extracellular tachyzoites. Cells were immunostained with antibodies against TgTBCB (green). The white arrow indicates the apical region and the yellow arrow head indicates the posterior region. Images were acquired by ELYRA. Scale bar, 1 µm.

The inner membrane complex sub-compartment protein 1 (ISP1) is known as a apical cap marker (Beck et al., 2010) so, to better characterize the TgTBCB apical localization, we performed a co-staining using anti-TgTBCB and anti-ISP1 antibodies. The anti-ISP1 antibody stains the apical cap, the apical region that is delimited by TgCentrin2 peripheral annuli (~1.5 µm from apical end) (Beck et al., 2010).

Our results showed that, in both extracellular and intracellular tachyzoites, TgTBCB is at apical cap and progressively decreases towards the distal end (Figure 35). Super resolution microscopy of extracellular tachyzoites, showed a TgTBCB staining that resembles the subpellicular MTs suggesting a possible colocalization (Figure 36).

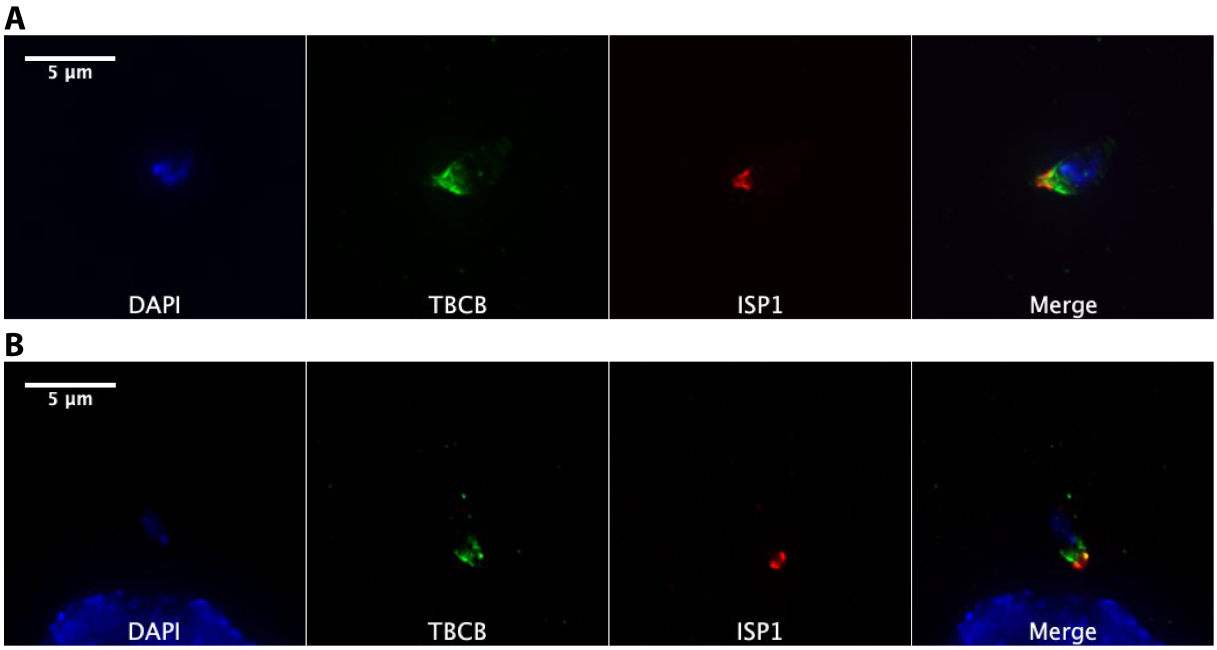

Figure 35. TgTBCB is at apical cap and progressively decreases towards the distal end. A - Extracellular tachyzoites. **B** - Intracellular tachyzoites, HFF cells invaded with *T. gondii* for 24 h. Parasites were immunostained with antibodies against TgTBCB (green) and ISP1 (red). DNA was stained with DAPI (blue). The images were acquired using the Olympus Deltavision Core microscope. Scale bar, 5 µm.

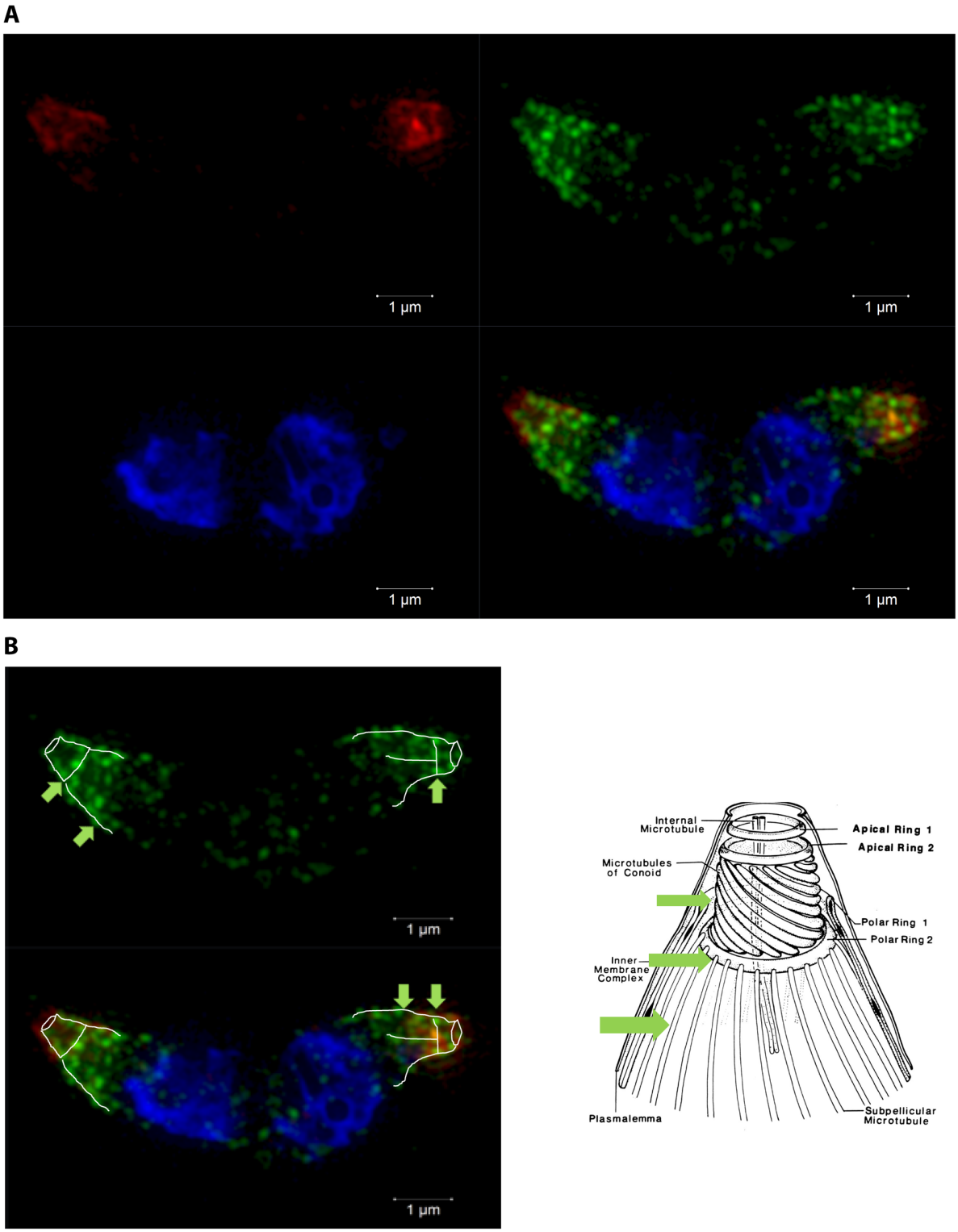

Figure 36. In extracellular tachyzoites, super resolution microscopy shows that TgTBCB seems to be in close association with subpellicular MTs. **A** - Cells were immunostained with antibodies against TgTBCB (green) and ISP1 (red). DNA was stained with DAPI (blue). **B** - Merge image with the scheme of subpellicular MTs, suggested by TgTBCB staining. Images were acquired by ELYRA. Scale bar, 1 µm (adapted from *(Dubey et al., 1998)* with permission).

The super resolution results from TgTBCB localization prompted us to investigate deeper the relationship between this protein and the apical MT cytoskeleton structures. For this, in an attempt to visualize the subpellicular MTs at the region close to the conoid, we performed

immunolocalization assays with antibodies against acetylated α-tubulin and glutamylated tubulin. The acetylated α-tubulin, as a rule, labels the subpellicular MTs and the glutamylated tubulin progressively decreases from the conoid towards the distal end of the subpellicular MTs (Plessmann et al., 2004).

Contrary to what we were expecting, it was not possible to observe the subpellicular MTs with the acetylated α-tubulin staining neither in extracellular nor in intracellular tachyzoites (Figure 37).

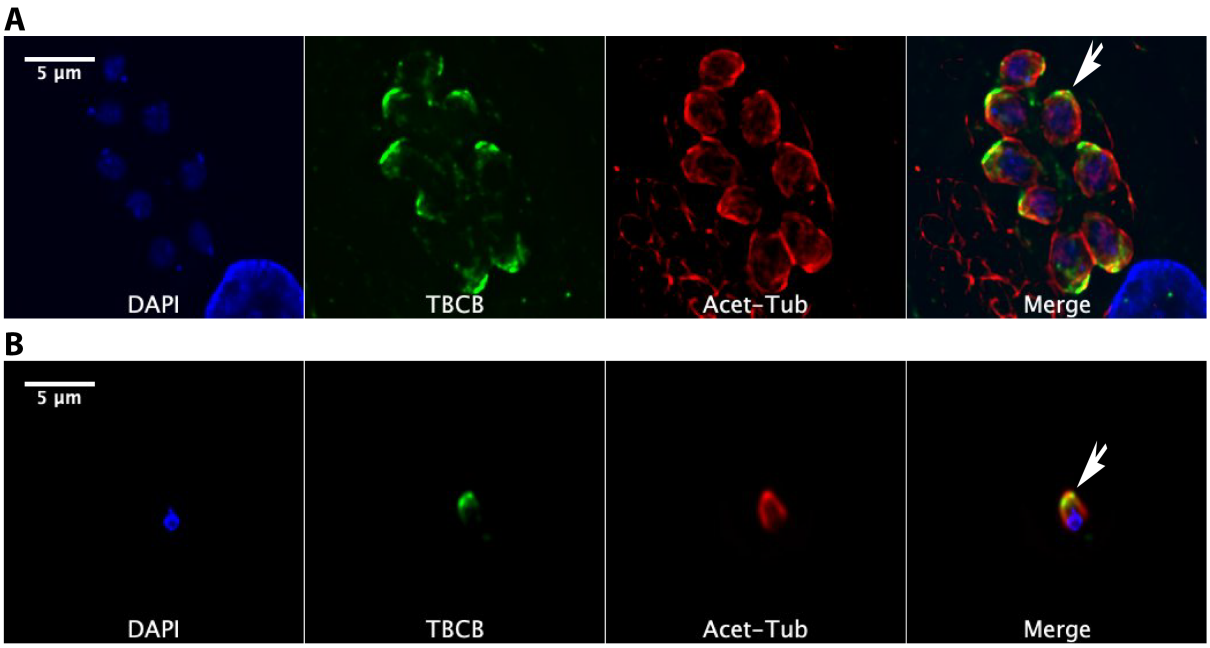

Figure 37. TgTBCB is at apical cap around a tubulin structure. **A** - Intracellular tachyzoites, HFF cells 24h post-invasion. **B** - Extracellular tachyzoites. The arrow points to TgTBCB around tubulin. Cells were immunostained with antibodies against TgTBCB (green) and acetylated α-tubulin (red). DNA was stained with DAPI (blue). Images were acquired using the Olympus AppliedPrecision DeltaVision Core system. Scale bar, 5 µm.

After the acetylated α-tubulin staining we performed the glutamylated tubulin staining. This assay was more informative because glutamylated tubulin presents a staining pattern similar to TgTBCB.

Unfortunately, using DeltaVision it was not possible to observe the individualized MTs with the glutamylated tubulin staining (Figure 38). However, TgTBCB seems to be enriched at the region immediately below the polar ring. This result is much clearer in the intracellular tachyzoites (Figure 38A) than in the extracellular tachyzoites (Figure 38B).

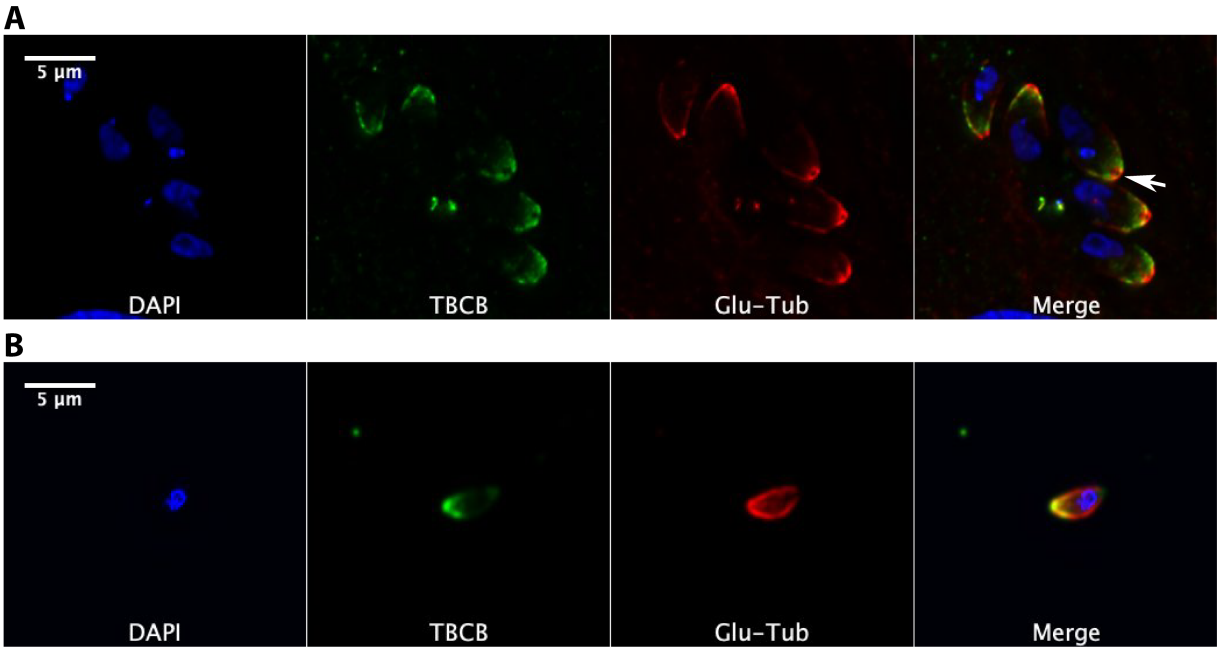

Figure 38. TgTBCB staining is enriched at the region immediately below of the polar ring. **A** - Intracellular tachyzoites, HFF cells 24 h post-infection, arrow indicates the TgTBCB ring-like shape. **B** - Extracellular tachyzoites. Parasites were immunostained with antibodies against TgTBCB (green) and polyglutamylated tubulin (GT335, red). DNA was stained with DAPI (blue). Images were acquired with Olympus AppliedPrecision DeltaVision Core system. Scale bar, 5 µm.

Using super resolution microscopy, TgTBCB staining presents a partial co-localization with the glutamylated tubulin, being in a ring-like shape (Figure 39). At the apical region, TgTBCB can be in close association with the subpellicular MTs and, since they are attached to the apical polar ring, TgTBCB can be "around/below" this structure originating the ring-like shape.

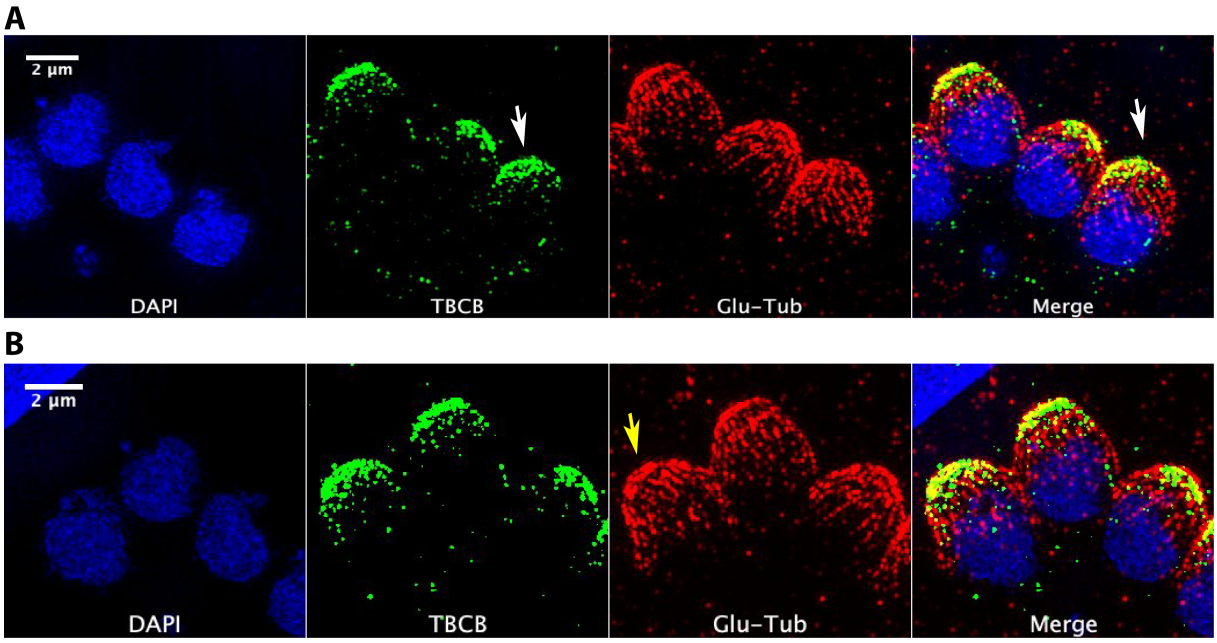

Figure 39. **Super resolution microscopy showed, in intracellular tachyzoites, that TgTBCB is in a ring-like shape at the apical region. A** - White arrow indicates the TgTBCB ring-like structure. B - Yellow arrow suggest a polar ring stainedwith glutamylated tubulin. HFF cells 24h post-invasion were immunostained with antibodies against TgTBCB (green) and polyglutamylated tubulin (red). DNA was stained with DAPI (blue). Images were acquired using Deltavision OMX system. Scale bar, 5 µm in "A" and 2 µm in "B".

In an attempt to better characterize the TgTBCB staining, we produced parasites expressing mEmeraldFP-α1-tubulin (TUBA1, green) under the control of a *T. gondii* tubulin promoter (Leung et al., 2017).

We successfully obtained this transgenic line but, for unknown reasons, the mEmeraldFP-α1-tubulin quickly faded during image acquisition at Olympus AppliedPrecision DeltaVision Core system. Therefore, we were only able to acquire images using the Leica Spinning Disk.

The mEmeraldFP-α1-tubulin staining confirmed the TgTBCB staining, previously observed with glutamylated tubulin, where it appears to be in a ring-like shape around the tubulin at the apical end (Figure 40). Interestingly, in replicating parasites, TgTBCB is present in the mother cell close to the anterior pole and is also present in the early forming daughter cells (Figure 41). Also, the TgTBCB is not present in the mitotic spindle (Figure 42).

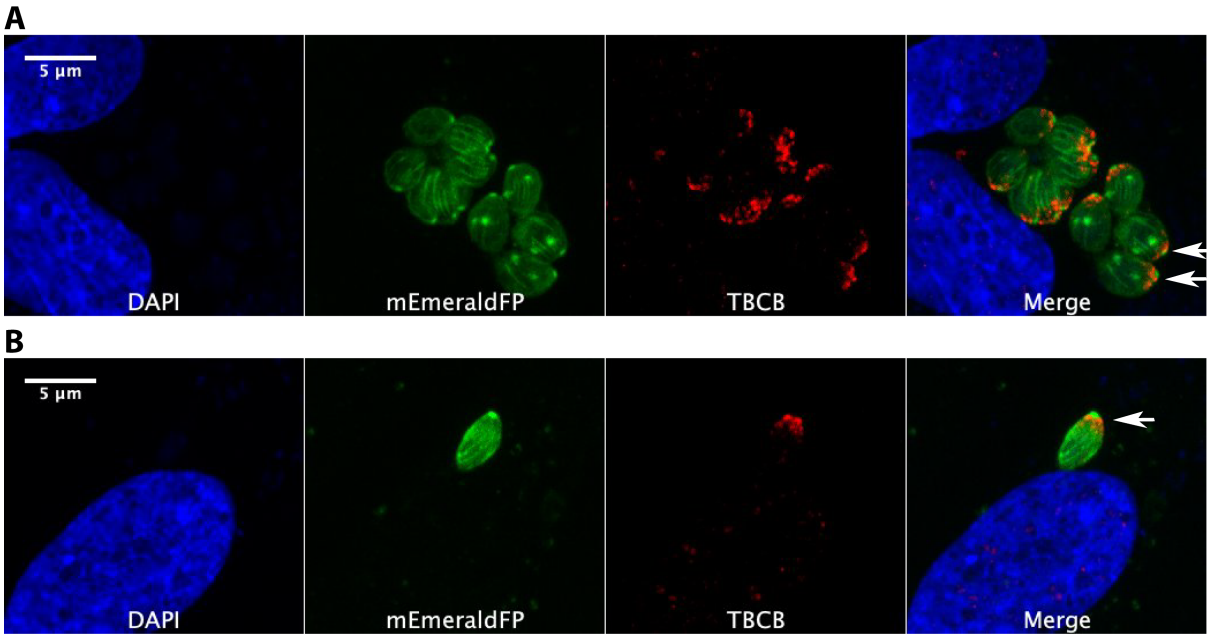

Figure 40. mEmeraldFP-α1-tubulin staining supports that TgTBCB is present in a ring-like shape around the tubulin at the apical end. A and B – White arrows indicate TgTBCB in a ring like shape. Intracellular tachyzoites, from HFF cells 24h post-invasion. Cells were immunostained with antibodies against TgTBCB (red). mEmeraldFP-α1-tubulin is green. DNA was stained with DAPI (blue). Images were acquired using a Leica Spinning Disk. Scale bar, 5 µm

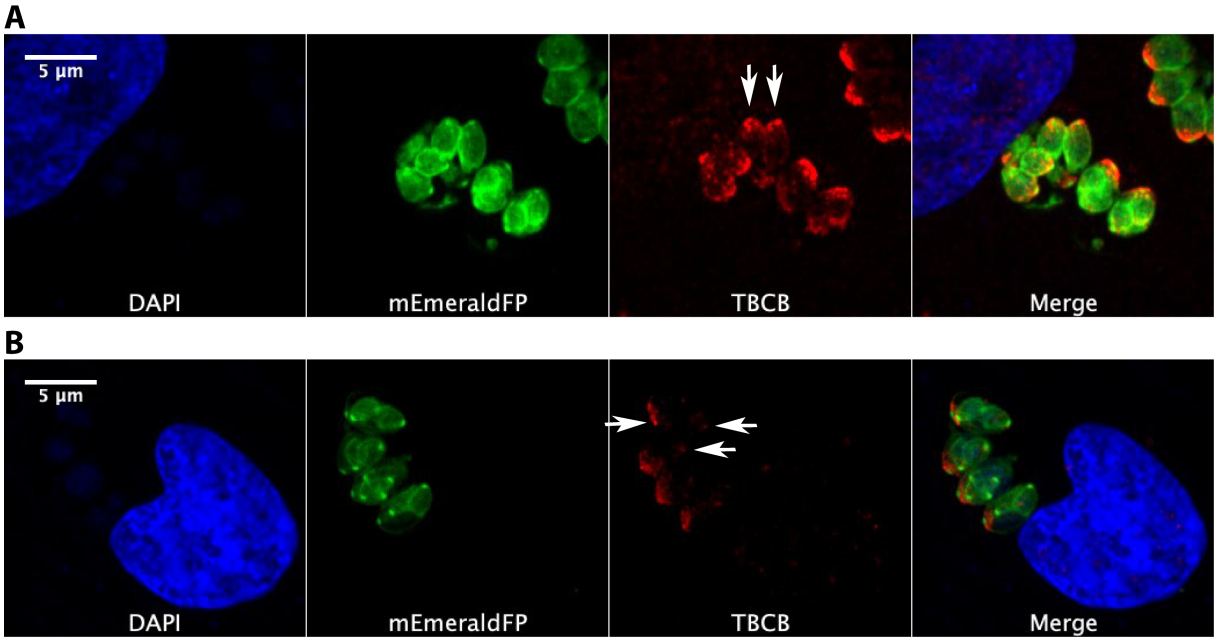

Figure 41. mEmeraldFP-α1-tubulin staining supports that TgTBCB is present in late daughter cells (White arrows). Intracellular tachyzoites, from HFF cells 24h post-invasion. Cells were immunostained with antibodies against TgTBCB (red). mEmeraldFP-α1-tubulin is green. DNA was stained with DAPI (blue). Images were acquired using a Leica Spinning Disk. Scale bar, 5 µm.

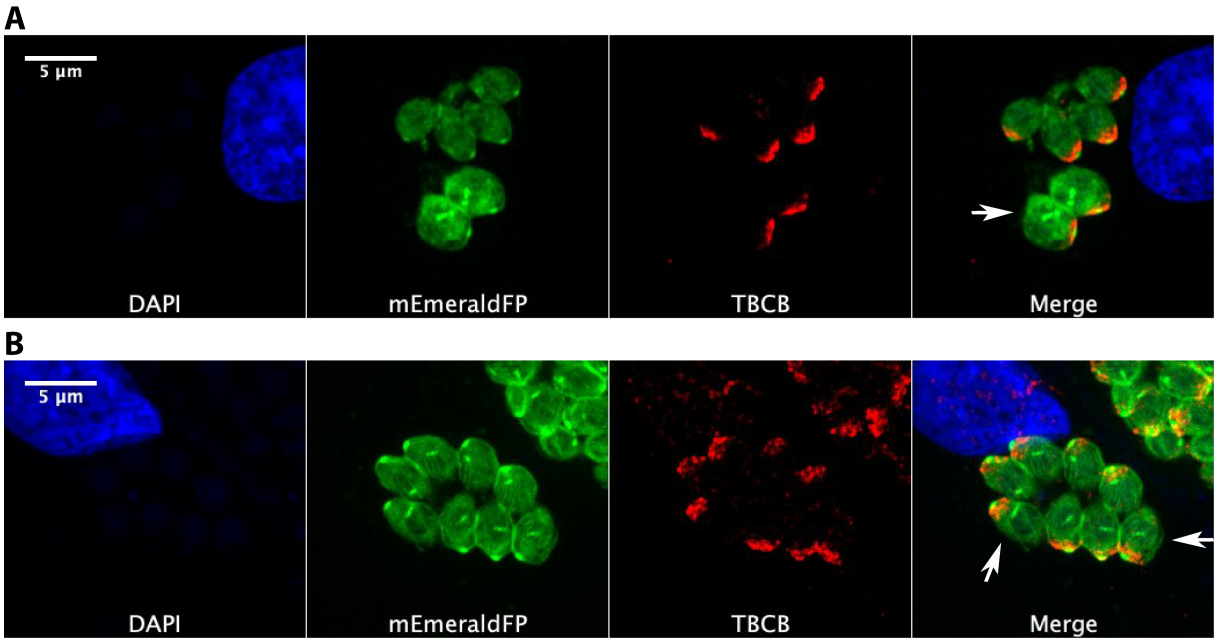

Figure 42. mEmeraldFP-α1-tubulin staining supports that TgTBCB is not present in the mitotic spindle. White arrows indicate TgTBCB is absent of the mitotic spindle. Intracellular tachyzoites, from HFF cells 24h post-invasion. Cells were immunostained with antibodies against TgTBCB (red). mEmeraldFP-α1-tubulin is green. DNA was stained with DAPI (blue). Images were acquired using a Leica Spinning Disk. Scale bar, 5 µm

The apical complex also contains a high density of secretory organelles, particularly rhoptries and micronemes and, due its localization, we admitted that TgTBCB could be in close association with these organelles. To address this hypothesis, we performed immunolocalizations with a monoclonal antibody against rhoptry proteins 2, 3 and 4 and with with the antibodies against microneme proteins 2 and 3 (Figures 43 to 47).

Although we cannot exclude the interaction with other secretory proteins, our results demonstrate that there is no co-localization of TgTBCB with rhoptry proteins 2 - 4 (Figure 43) and there are only a few dots of co-localization with the microneme proteins 2 and 3 (Figures 44 to 47). Interestingly, these observations were obtained mainly in intracellular and not in extracellular parasites.

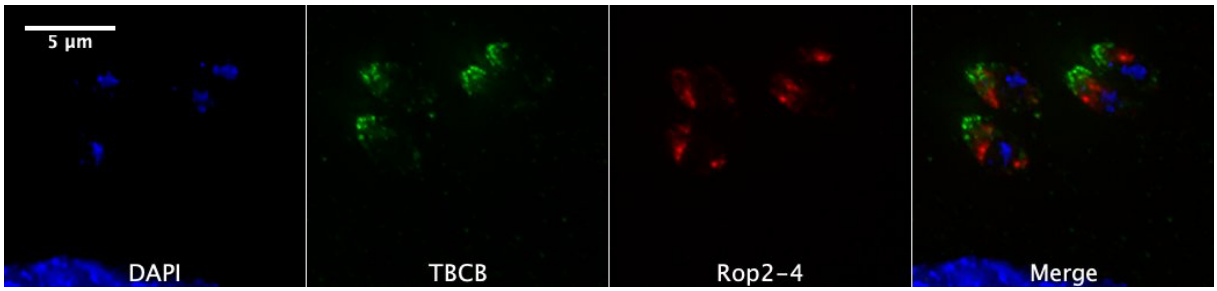

Figure 43. TgTBCB did not colocalize with rhoptries proteins 2 – 4 in intracellular tachyzoites. HFF cells were invaded with *T. gondii* for 24 h, then cells were immunostained with antibodies against TgTBCB (green) and rhoptries proteins 2 - 4 (red). DNA was stained with DAPI (blue). Images were acquired using the Olympus Deltavision Core microscope. Scale bar, 5 µm.

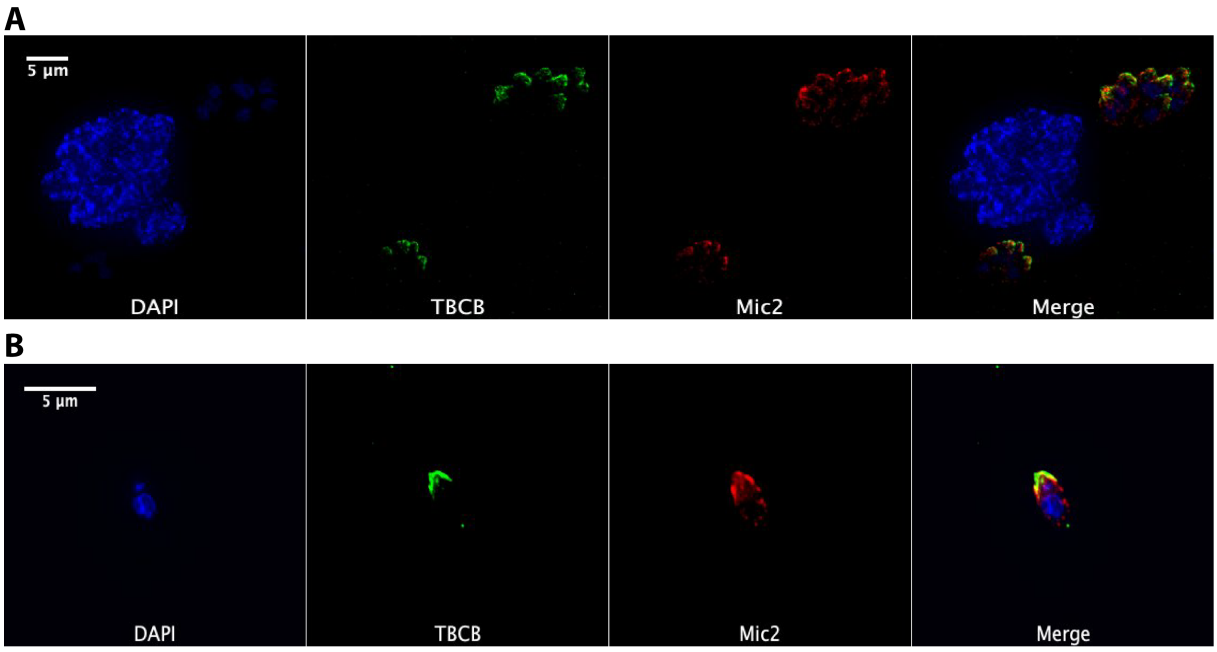

Figure 44. TgTBCB had some dots of co-localization with microneme protein 2. A - Intracellular tachyzoites, HFF cells were invaded with *T. gondii* for 24 h. **B -** Extracellular tachyzoites. Cells were immunostained with antibodies against TgTBCB (green) and microneme protein 2 (red). DNA was stained with DAPI (blue). Images were acquired using the Olympus Deltavision Core microscope. Scale bar, 5 µm.

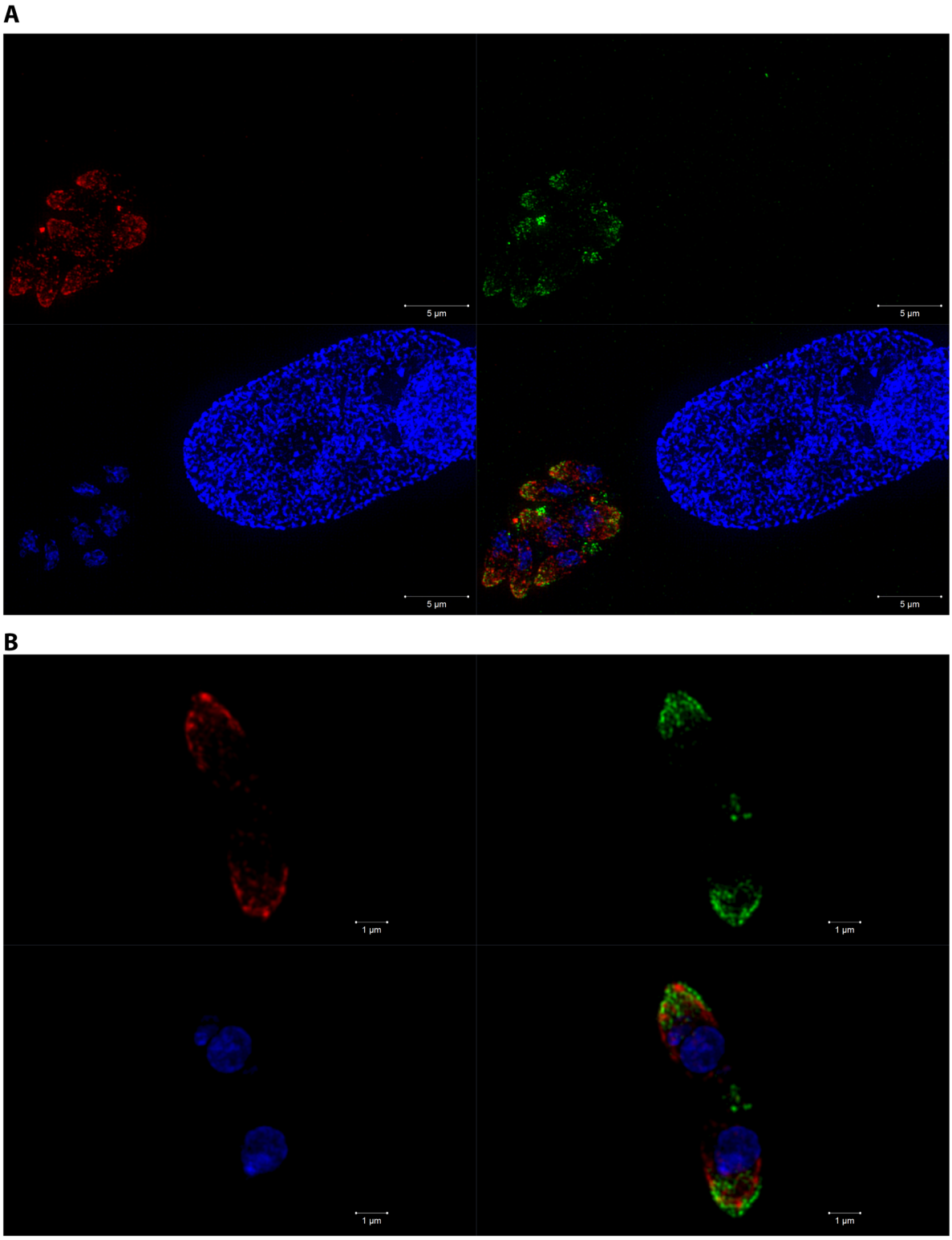

Figure 45. Confirmation, by super resolution microscopy, that TgTBCB had some dots of co-localization with microneme protein 2, manly in intracellular parasites. A - Intracellular tachyzoites, HFF cells were invaded with *T. gondii* for 24 h. **B** - Extracellular tachyzoites. Cells were immunostained with antibodies against TgTBCB (green) and microneme protein 2 (red). DNA was stained with DAPI (blue). Images were acquired using the ELYRA microscope. Scale bars, in "A" 5 µm and in "B" 1 µm.

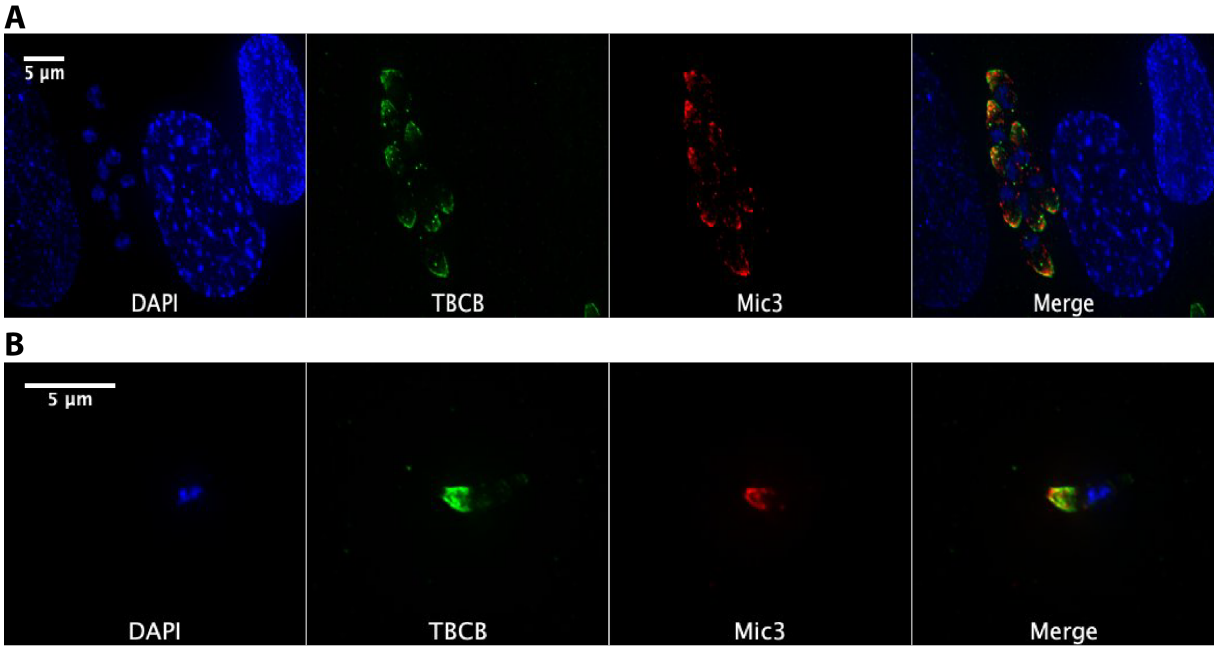

Figure 46. TgTBCB had some dots of co-localization with microneme protein 3. A - Intracellular tachyzoites, HFF cells were invaded with *T. gondii* for 24 h. **B** - Extracellular tachyzoites. Cells were immunostained with antibodies against TgTBCB (green) and microneme protein 3 (red). DNA was stained with DAPI (blue). Images were acquired using the Olympus Deltavision Core microscope. Scale bar, 5 µm.

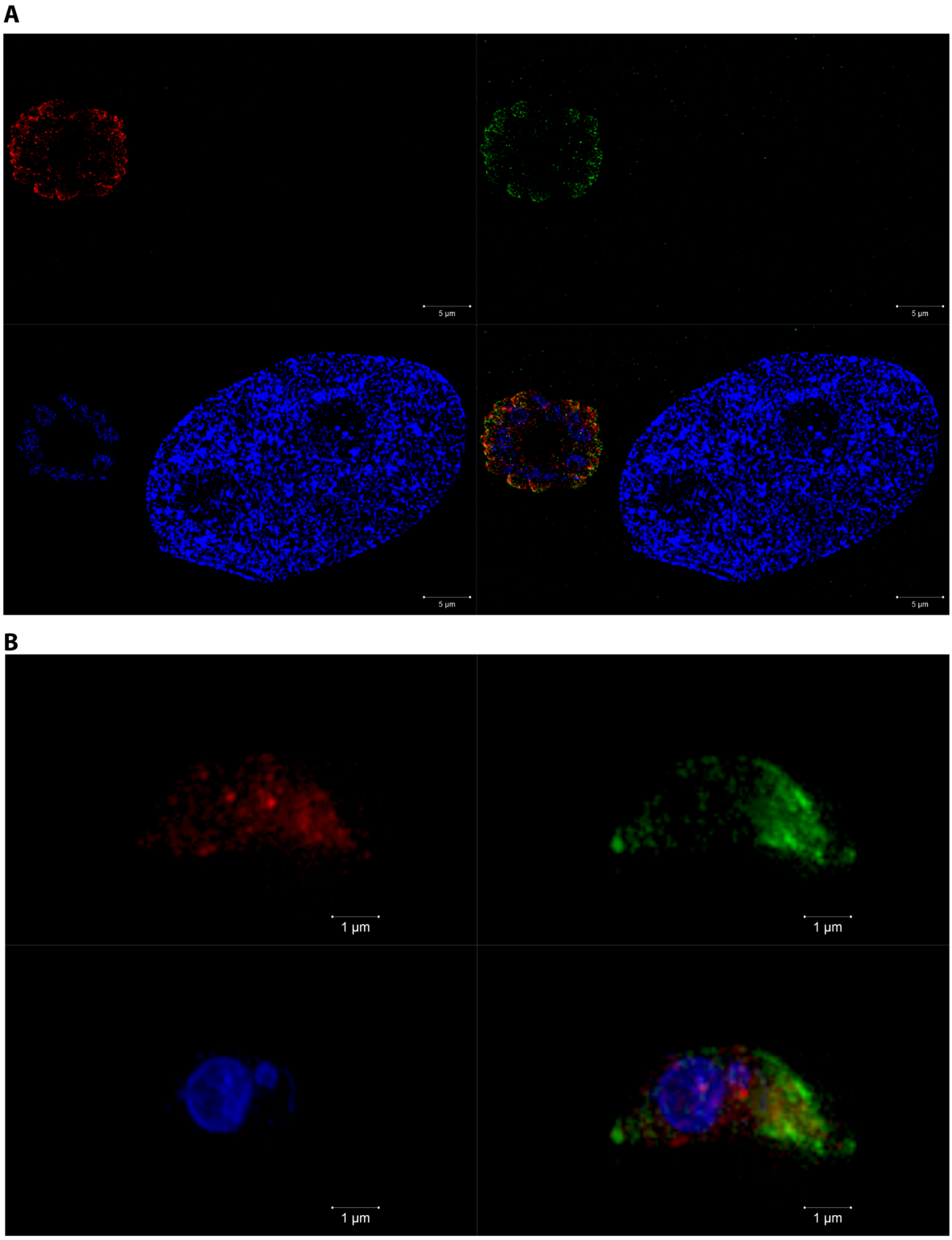

Figure 47. Confirmation, by super resolution microscopy, that TgTBCB had some dots of co-localization with the microneme protein 3, mainly in intracellular parasites. A - Intracellular tachyzoites, HFF cells were invaded with *T. gondii* for 24 h. **B** - Extracellular tachyzoites. Cells were immunostained with antibodies against TgTBCB (green) and microneme protein 3 (red). DNA was stained with DAPI (blue). Images were acquired using the ELYRA microscope. Scale bars, in "A" 5 µm and in "B" 1 µm.

5. TgTBCB secretion analysis

TgTBCB shows a polarized localization mainly at the anterior region of the cell, under the conoid, suggesting an association with the subpellicular MTs close to the apical polar ring and/or with the secretory organelles. Considering its localization, TgTBCB can be secreted and/or be involved in the secretion process. Although we did not detect a clear colocalization with rhoptry proteins 2 - 4 neither with microneme proteins 2 and 3, we cannot exclude this hypothesis. Therefore, to study the possibility of TgTBCB being secreted, we performed two different secretion assays in which we induced secretion by incubation with either calcium ionophore A23187 or ethanol. After the secretion induction, the supernatants, containing the secreted proteins, were collected and analyzed by WB.

As a positive control in these assays, we used the protein disulfide isomerase (PDI), an essential enzyme in protein folding that is secreted in *T. gondii* (Meek, Back, Klaren, Speijer, & Peek, 2002). To detect the protein, we used a mouse serum obtained in our lab, raised against *Besnoitia besnoiti* PDI, that cross-reacts with *T. gondii* PDI (Marcelino et al., 2011).

As expected, PDI is present in all supernatants, but its amount clearly increases after incubation of the parasites with ethanol (the white band means very high signal, the band bleached out) or, although less pronounced, with calcium ionophore A23187, supporting a more successful secretion induction in the presence of ethanol than calcium ionophore A23187. The amount of TgTBCB in the supernatants shows the same variation, supporting the hypothesis that it is present in secretory compartment (Figure 48). However, due to very low concentrations of secreted TBCB in the supernatants, these preliminary results need to be confirmed.

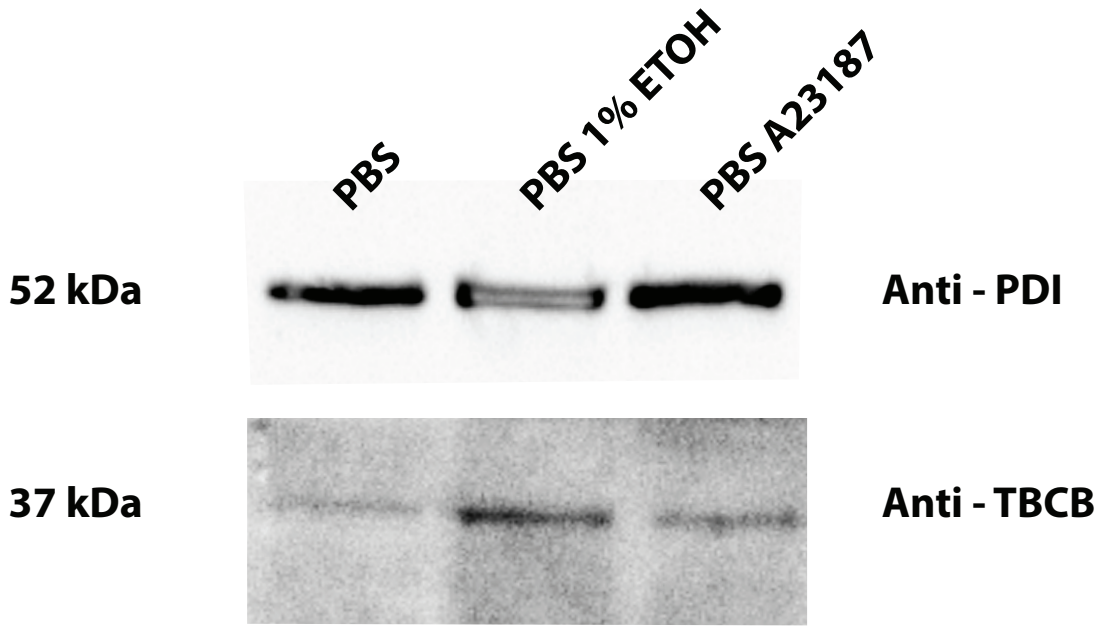

Figure 48. TgTBCB seems to be a secreted protein. Two secretion assays were performed by incubation with ethanol or with calcium ionophore A23187. In both assays, TgTBCB amount is increased after secretion induction. Anti-PDI was used as a positive secretion control.

6. Invasion assay in the presence of TgTBCB specific polyclonal serum

Given the hypothesis that TgTBCB is secreted, we decided to test whether we could demonstrate a role for this protein in the invasion process. For this, we performed invasion assays in the presence of the anti-TgTBCB specific polyclonal serum.

These assays did not show any significant difference in the invasion rate, in the presence or absence of anti-TgTBCB antibody (Figure 49), indicating that, even if it is secreted, its extra-cellular role is not related with the invasion process.

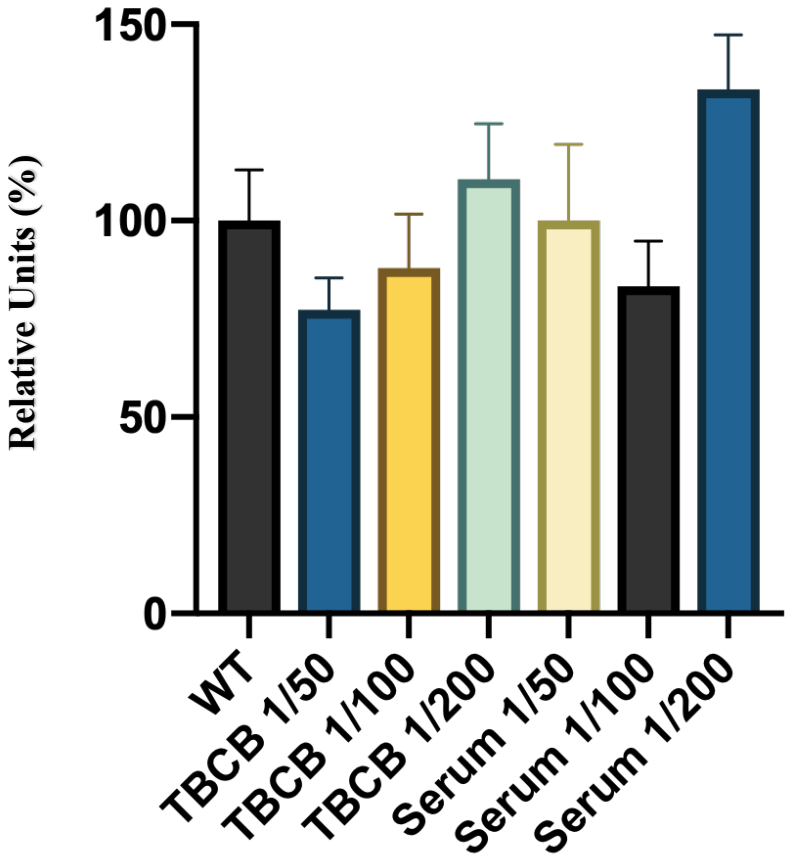

Figure 49. Extracellular TgTBCB is not a key protein in the invasion process. Invasion assays of extracellular *T. gondii* tachyzoites in the presence of TgTBCB specific polyclonal serum. The number of parasites that invaded the host cells was counted in 6 fields using a 40× objective and calculated as a percentage value of the control parasites (without TgTBCB specific polyclonal serum) normalized to 100 %. As control, a non-immunized rabbit serum was used at similar dilutions. The graphic bars are the mean±SEM (error bars) of three independent assays. Statistical significance was calculated using a student t-test.

7. Overexpression of *T. gondii* TBCB

We started the functional analysis of TgTBCB by studying the parasite phenotype resulting from overexpression of the protein. For this, the TgTBCB cDNA was cloned in three different plasmid constructs that were used for parasite transfection: 1) TgTBCB in fusion with a small tag, the c-myc tag; 2) TgTBCB in fusion with c-myc tag plus eGFP and 3) TgTBCB in fusion with c-myc tag, eGFP and a destabilization domain (ddFKBP). In this last construct we can modulate the overexpression levels of the fusion protein in a Shield-1 dependent manner.

7.1. Expression analysis of the TgTBCB recombinant proteins by WB

Following the random integration, the stable transgenic parasite lines obtained for each construction were analyzed by WB, using specific antibodies against the tag proteins or

alternatively against the TgTBCB, in order to confirm the expression of the recombinant proteins and their expected molecular size (molecular mass, MM) (Table 16).

The results showed that the anti-TgTBCB and anti-Myc are able to recognize the expected recombinant proteins in all transgenic lines: Myc-TBCB, DD-Myc-GFP-TBCB and Myc-GFP-TBCB. Although the expected MM for Myc-TgTBCB is ~32 kDa, we detected a protein with ~37 kDa which is consistent with our previous results when we produced the TgTBCB in bacteria (see figure 50). In addition, as expected, the anti-GFP only recognizes the recombinant proteins with GFP. Using this antibody no proteins were detected in the *T. gondii* expressing Myc-TBCB. We also observed truncated versions of the recombinant proteins (DD-Myc-GFP and Myc-GFP) (Figure 50).

Table 16. Expected size of the recombinant TgTBCB proteins

Expected MM for the Overexpression Constructions	
Fusion Proteins	**Expected MM**
Myc-TBCB	32.36 kDa
Myc-eGFP-TBCB	64.65 kDa
DD-Myc-eGFP-TBCB	76.71 kDa
Truncated Fusion Proteins	**Expected MM**
eGFP	32.59 kDa
Myc-eGFP	34.31 kDa
DD-Myc-eGFP	46.36 kDa

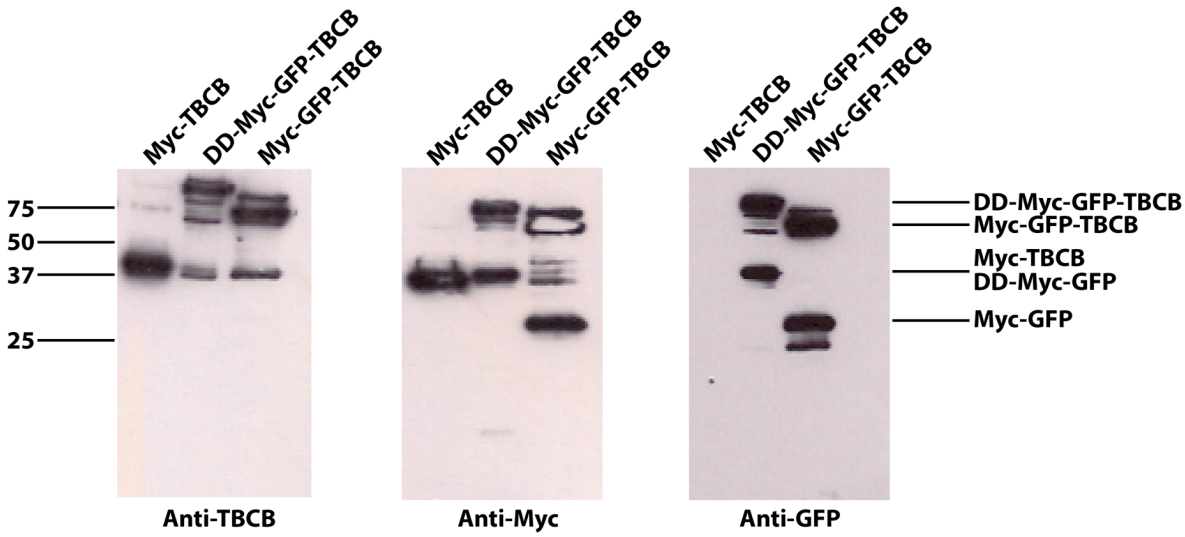

Figure 50. The recombinant TgTBCB proteins are expressed with the expected size. Soluble protein extracts from 3 different clones overexpressing TgTBCB (Myc-TBCB, ~32.3kDa; DD-Myc-GFP-TBCB, ~80.7kDa; Myc-GFP-TBCB, ~64.7kDa) were analysed by 15 % SDS-PAGE followed by WB with anti-TBCB, anti-Myc and anti-GFP antibodies.

7.2. Expression analysis of the DD-Myc-eGFP-TBCB recombinant protein in a Shield-1 dependent manner, by immunofluorescence

The transgenic stable parasite line overexpressing the DD-Myc-eGFP-TBCB recombinant protein was also analyzed by immunofluorescence (Figure 51). The results confirmed the expression of the TgTBCB recombinant protein in a Shield-1 dose dependent manner; the amount of protein increases as the amount of Shield-1 decreases (Figure 52). Under overexpression, TgTBCB lost its apical localization being spread throughout the cell cytoplasm.

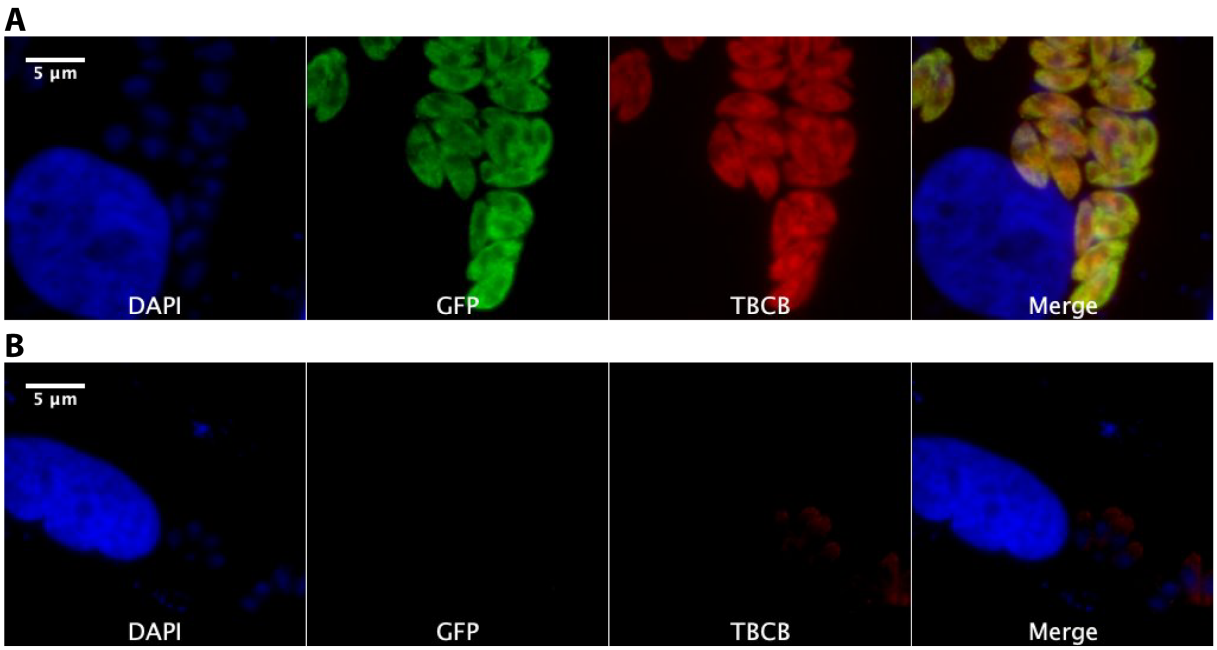

Figure 51. Analysis of DD-Myc-eGFP-TBCB expression. HFF cells were invaded with *T. gondii* for 24 h, then the cells were immunostained with antibodies against TgTBCB (red). DNA was stained with DAPI (blue). **A** – Parasites were incubated with Shield-1. **B** - Parasites were incubated without Shield-1. Images were acquired using the Leica DMRA2 DMR HC microscope. Scale bar 5µm.

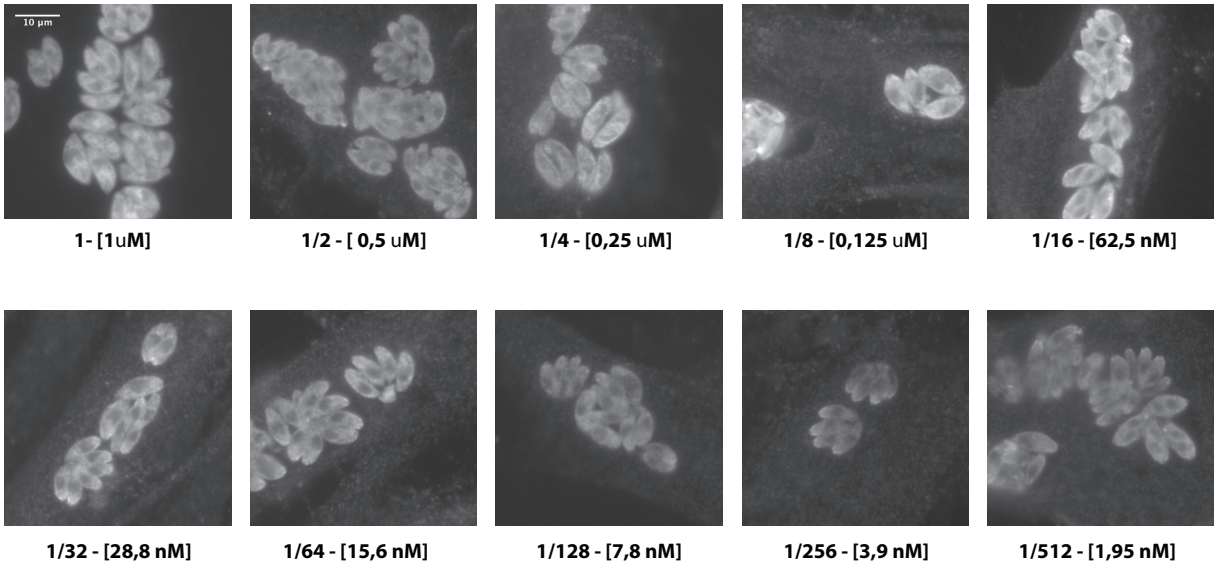

Figure 52. Analysis of DD-Myc-eGFP-TBCB expression under serial dilutions of the Shield-1. HFF cells, with culture medium containing a serial dilution of the Shield-1, were invaded with *T. gondii* for 24 h. Then, the cells were fixed and the GFP signal was detected. The GPF images were obtained with the same conditions, same exposition time, in the same channel and without any kind of imaging treatment. Images were acquired using the Leica DMRA2 DMR HC microscope. Scale bar 10 µm.

7.3. Phenotypic characterization of *T. gondii* TBCB overexpression clones

After confirming that the overexpressing clones were expressing the expected TgTBCB recombinant proteins, we started the phenotypic characterization.

As a first approach we performed plaque assays (growing assays) to test the capacity of the transgenic parasites to form plaques in monolayers of HFF cells. The plaque assay was performed in confluent monolayers in six-well plates that were inoculated with the same number of tachyzoites, overexpression transgenics (TgTBCB clones) or wild-type (control). After one week of incubation, at normal growth conditions, cells were fixed and stained with Giemsa stain and the total number of plaques originated was counted. Curiously, all the overexpressing clones presented a reduction in their ability to form plaques in comparison to the control: Myc-TBCB presents a decrease of 25 %, the DD-Myc-GFP-TBCB of 34 % and Myc-GFP-TBCB of 40 % (Figure 53).

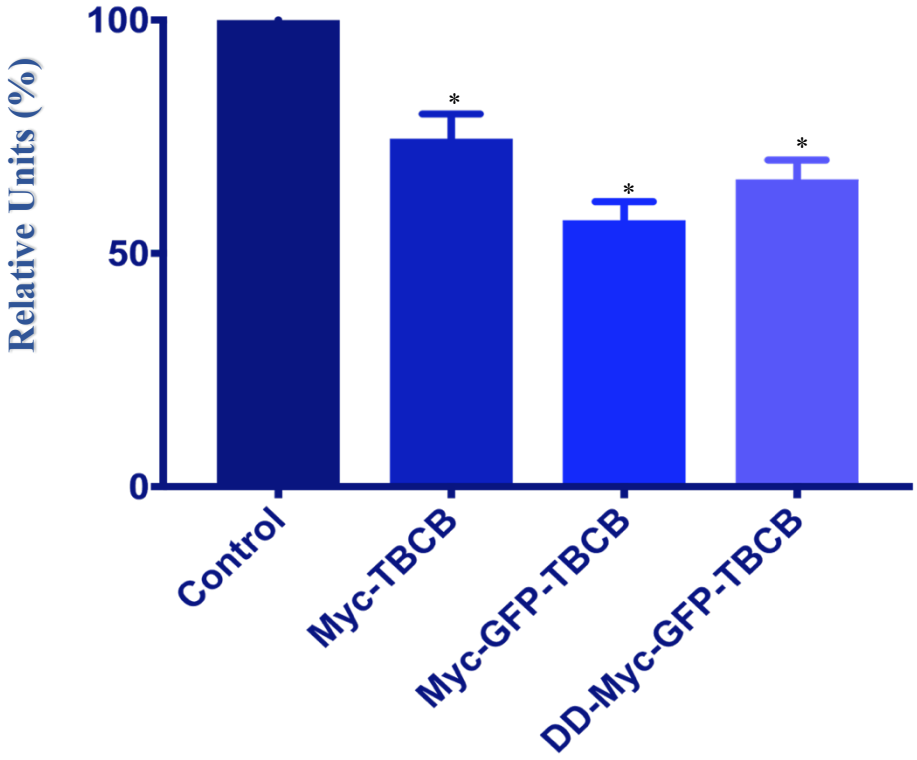

Figure 53. TgTBCB overexpression decreases the ability to form plaques. Plaque assays of TgTBCB overexpression clones showed a decrease in the number of plaques when compared to the control (wild-type tachyzoites). The number of plaques was counted and calculated as a percentage value of control parasites (wild-type) normalized to 100 %. *p<0.01. The p values were determined in comparison to the control strain. The graphic bars are the normalized values ± SEM (error bars) of three independent assays. Statistical significance was calculated using a student t-test.

The decreased capacity in plaque formation showed by the TgTBCB overexpressing clones can be due to problems in invasion and/or replication and/or egress. To discriminate among the different possibilities we performed invasion, replication and egress assays. Since we found that the three clones presented similar results in the plaque assays, we decided to pursue this characterization using only the Myc-TBCB and DD-Myc-GFP-TBCB clones.

In the invasion assay, confluent monolayers of HFF cells were invaded for 1 h with the same number of transgenic and wild type tachyzoites. Then, extracellular parasites were removed, and the cells were incubated for further 18 h before fixation. After that, cells were processed for immunofluorescence and the number of parasitophorous vacuoles, corresponding to successful invasion, was scored.

Interestingly, in comparison to wild type parasites, DD-Myc-GFP-TBCB clone shows a decrease of 41 % and the Myc-TBCB of 45 % in the ability to invade host cells (Figure 54). This decrease in invasion capacity is probably related with TgTBCB overexpression and explains the decrease in the capacity of plaque formation.

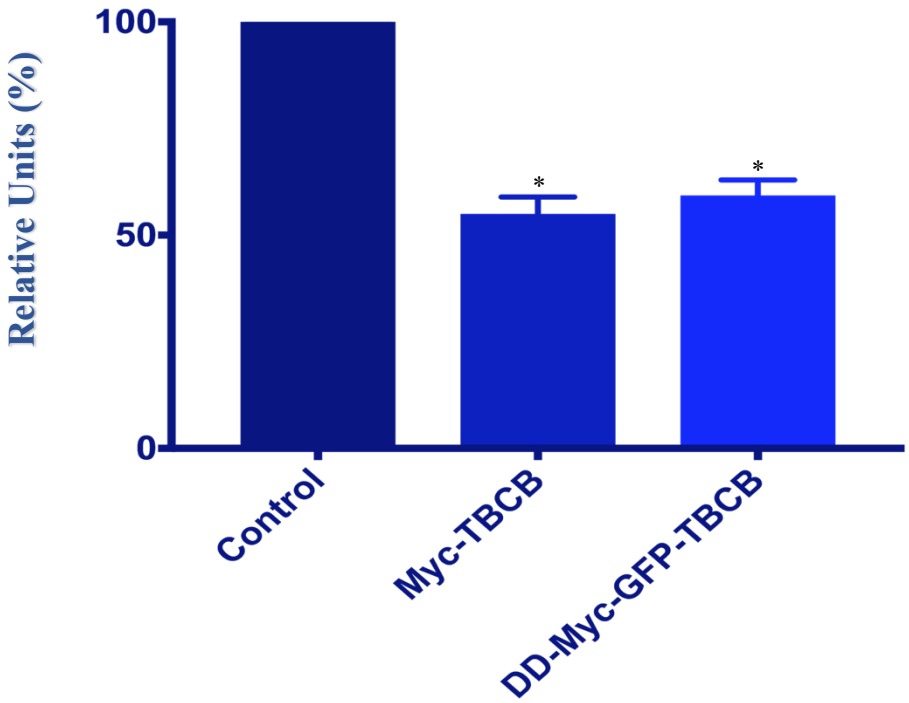

Figure 54. TgTBCB overexpression decreases the ability to invade host cells. In the invasion assays, the number of invaded parasites was counted in 6 fields using a 40× objective and calculated as a percentage value of control parasites (wild-type) normalized to 100%. *p<0.001. The p values were determined in comparison to the control. The graphic bars are the normalized values ± SEM (error bars) of three independent assays. Statistical significance was calculated using a student t-test.

The replication assays were performed to analyze the ability of *T. gondii* tachyzoites overexpressing TgTBCB to undergo normal replication within the infected host cells. The assays were performed similarly to the invasion assays, except that extracellular tachyzoites were not washed out and were let to invade for 24 h before fixation. Then, cells were processed for immunofluorescence and the number of parasites per parasitophorous vacuole was scored. In this assay, no significant differences were observed between the TgTBCB overexpressing clones and the wild-type strain (Figure 55).

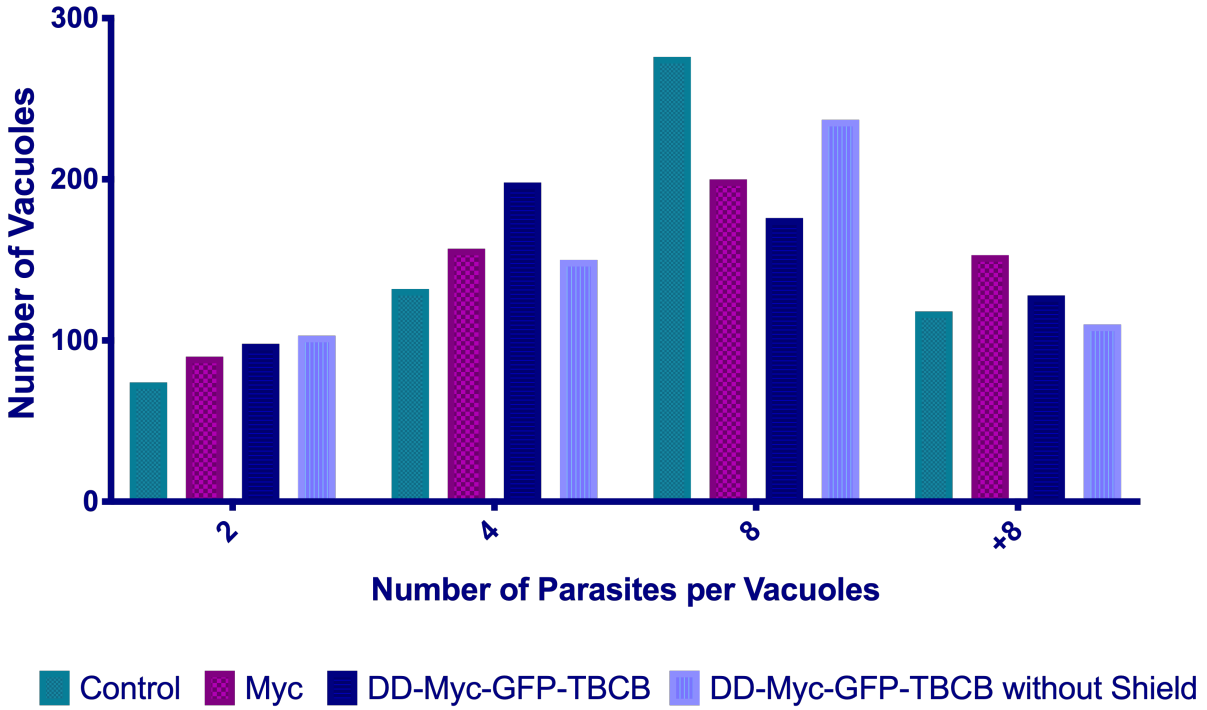

Figure 55. TgTBCB overexpression does not affect the replication rate in *T. gondii*. In replication assays, control (wild-type), Myc-TBCB and DD-Myc-GFP-TBCB presented similar distribution of the parasite number/vacuole. Total number of vacuoles counted = 600. 200 vacuoles were counted in each independent experiment. The graphic bars indicate the frequency of each condition.

Finally, the egress assays were performed to analyze the ability of *T. gondii* overexpressing TgTBCB to *exit* the *host* cell in order to *infect* new *hosts*. Confluent monolayers of HFF cells were invaded with the same amount of transgenic or wild type tachyzoites. Cells were incubated for more 36 h and, after that, the egress was induced by incubation with calcium ionophore. The cells were then fixed, processed for immunofluorescence and the number of vacuoles with non-egressed parasites was counted. We performed this assay only with the Myc-TBCB overexpression clone. Although we detected a slight increase of intact vacuoles in the overexpression clone, our results did not present significant differences between the control and the overexpression (Figure 56).

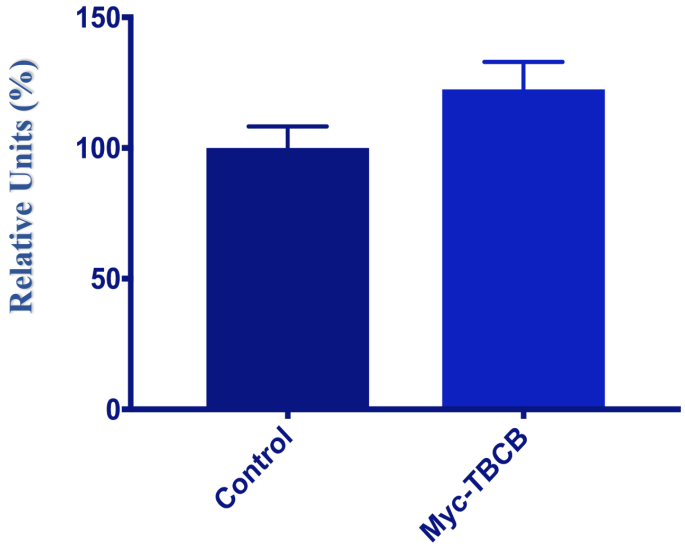

Figure 56. TgTBCB overexpression does not affect the egress in *T. gondii*. Egress assays, control (wild-type) and Myc-TBCB presented similar number of intact vacuoles (non-egress vacuoles). The number of non-egress vacuoles was counted in 6 fields using a 40× objective and calculated as a percentage value of control parasites (wild-type) normalized to 100%. The graphic bars are the normalized values ± SEM (error bars) of three independent assays.

8. *T. gondii* TBCB loss of function studies by knockout

The study of the TBCB loss of function phenotype was expected to contribute to clarify its role in *T. gondii*. However, the establishment of these technologies in our lab was a great challenge and allowed us to optimize important tools for future work.

8.1. *T. gondii* TBCB conditional knockout (KO) using DiCre system

The *T. gondii* DiCre system (Andenmatten et al., 2012), is based on site-specific recombination using dimerizable Cre recombinase. The system uses a *T. gondii* strain (*ku80::diCre*: *ku80* strain hxgprt−) that expresses two inactive fragments of the Cre recombinase, each of them fused to one of the rapamycin-binding proteins FRB and FKBP. The addition of rapamycin brings FRB and FKBP together, reconstituting the functional enzyme and causing the loxP-flanked gene of interest to be excised. The deletion of *ku80* gene in this strain should avoid random integration, increasing the homology recombination efficiency.

The first step was the use of a gene-swap strategy in which TgTBCB gene was replaced at genome locus by a Myc-TgTBCB cDNA flanked by loxP sites. Then, after the addition of rapamycin, MycTgTBCB cDNA was excised by Cre recombinase and an YFP cDNA was left under the control of the promoter, resulting in YFP-expressing parasites (KO parasites are

green). The exchange between wild-type TgTBCB gene and Myc-TgTBCB loxP flanked plus YFP and selection cassette was done by homologous recombination.

Our first priority was to establish the best transfection scenarios to favor the homologous recombination instead of random integration. Being so, during approximately two years' various transfection settings have been tested to isolate a TgTBCB KO clonal line positive for homologous recombination at the TgTBCB genomic locus. In fact, several attempts were made using two different electroporators: the Nucleofector™ 2b Device Amaxa® with the Basic Parasite Nucleofector® Kit, Lonza and Gene Pulser® II Electroporation System, Biorad with a home-made Citomix. We used the manufacture protocol but some alterations were also done in the DNA amount used. In the Nucleofector™ 2b Device Amaxa were used 10, 5 and 2.5 µg of DNA and for the Gene Pulser were used 60, 30 and 15 µg of DNA.

After selection, isolated clones were tested by a genomic PCR strategy in which products with different sizes are generated from TgTBCB wild type locus (553 bp) or from TgTBCB recombinant locus (1092 bp). Therefore, positive homologous recombination will produce a PCR product of 1092 bp and random integration will produce two PCR products, one from the TgTBCB endogenous locus (553 pb) and the other from the plasmid (1092 pb) randomly integrated in the genome.

When tested by the genomic PCR strategy, our first transfection attempts were all negative for homologous recombination. The tested clonal lines presented two PCR products (553 pb and 1092 pb), consistent with a plasmid random integration. Meantime, the positive control (plasmid construct) presented only the product for TgTBCB recombinant locus (1092 bp), the negative control (wild type strain) presented only the product for TgTBCB wild type locus (553 bp) and the non-template control did not amplify any product (Figure 57). The transfection conditions used were enhancing the random integration instead of homologous recombination, which was not at all expected for a strain deleted for *ku80*.

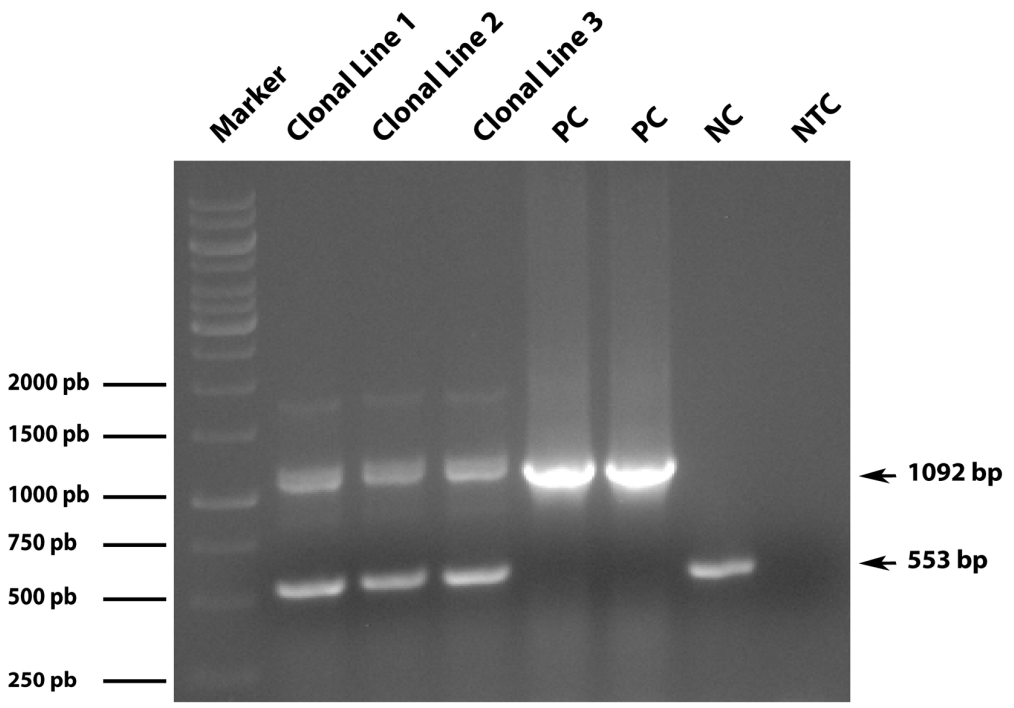

Figure 57. TgTBCB KO clonal lines (1 to 3) were negative for homologous recombination. Electrophoretic analysis (1 % agarose gel) of the genomic PCR products to check the gene-swap of the TgTBCB KO construct at the TgTBCB endogenous locus. Tested clonal lines presented two PCR products (553 pb and 1092 pb), consistent with a random integration. Marker - GeneRuler 1 kb DNA Ladder. PC – Positive control, plasmid construction. NC – Negative control, wild-type strain. NTC – Non-template control.

In these initial tests we found two clonal lines (4 and 8) positive for homologous recombination by genomic PCR, presenting only one PCR product of 1092 pb (Figure 58). However, when tested by IF, these clones were phenotypically negative, since the overexpressing of the Myc-TgTBCB construction was not visible (Figure 59).

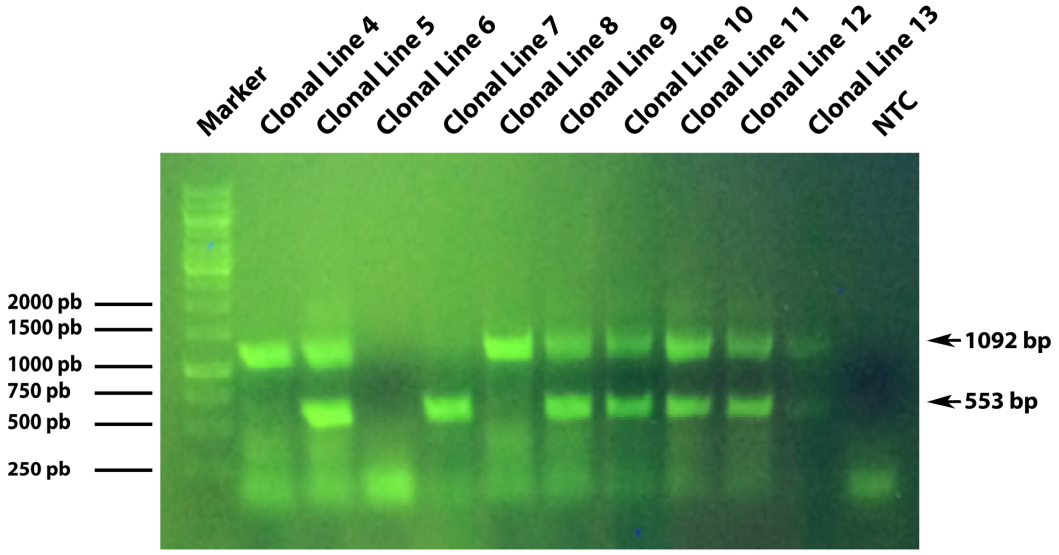

Figure 58. Clonal lines 4 and 8 are positive for homologous recombination. Electrophoretic analysis (1 % agarose gel) of the genomic PCR products to check the gene-swap of the TgTBCB KO construct at the TgTBCB endogenous locus. Clonal

lines 4 and 8 presented only one PCR product (1092 pb), consistent with the homologous recombination. Marker - GeneRuler 1 kb DNA Ladder. Clonal lines 1 to 10. NTC – Non-template control.

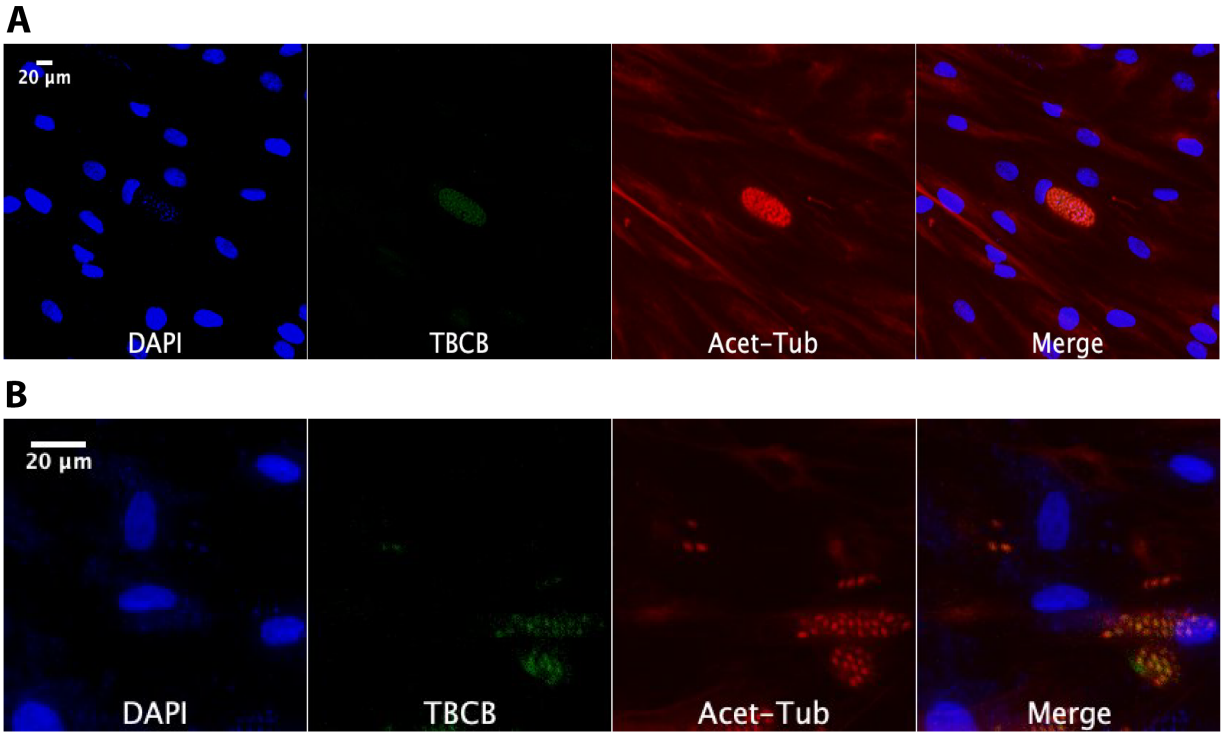

Figure 59. Clonal lines positive for homologous recombination by PCR did not overexpress the Myc-TBCB as expected. HFF cells were invaded with *T. gondii* for 24 h, then cells were immunostained with antibodies against TgTBCB (green) and acetylated tubulin (red). DNA was stained with DAPI (blue). Images were acquired using the Leica DMRA2 DMR HC microscope. **A** - Negative control (*T. gondii* wild type strain). **B** - Representative image of clonal lines 4 and 8, positive by PCR for homologous recombination. Phenotypic negative, no overexpression of Myc-TgTBCB was observed. Scale bar 20 µm.

Afterward, we kept trying with both electroporators using the conditions described, but all the clones positive by IF (Figure 60) were negative by genomic PCR analysis (Figure 61), presenting our construction randomly integrated in the parasite genome. Curiously, clonal lines 21 and 25 survived to the drug selection but, by PCR, are compatible with a wild-type strain.

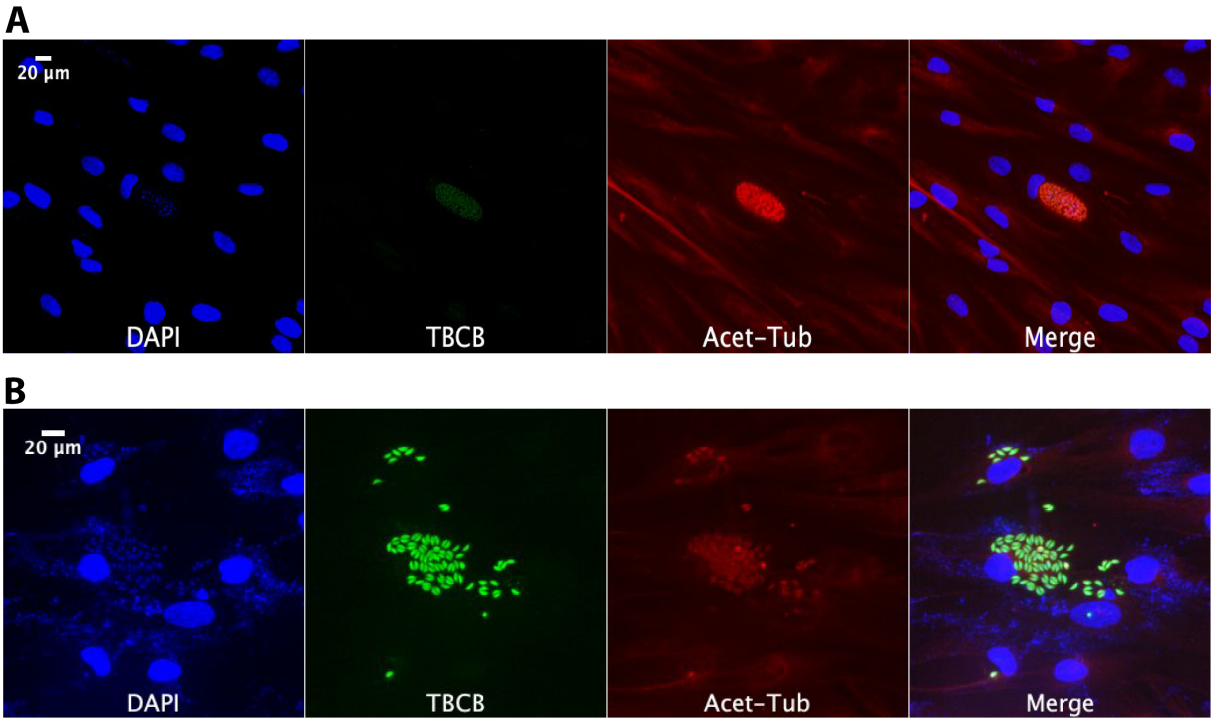

Figure 60. Clonal lines overexpressing the Myc-TBCB are negative for homologous recombination by genomic PCR. HFF cells were invaded with *T. gondii* for 24 h, then cells were immunostained with antibodies against TgTBCB (green) and acetylated tubulin (red). DNA was stained with DAPI (blue). Images were acquired using the Leica DMRA2 DMR HC microscope. **A** - Negative control (*T. gondii* wild type strain). **B** - Representative image of a negative PCR clonal line of TgTBCB KO (phenotypic positive, overexpressing the Myc-TgTBCB). Scale bar 20 µm.

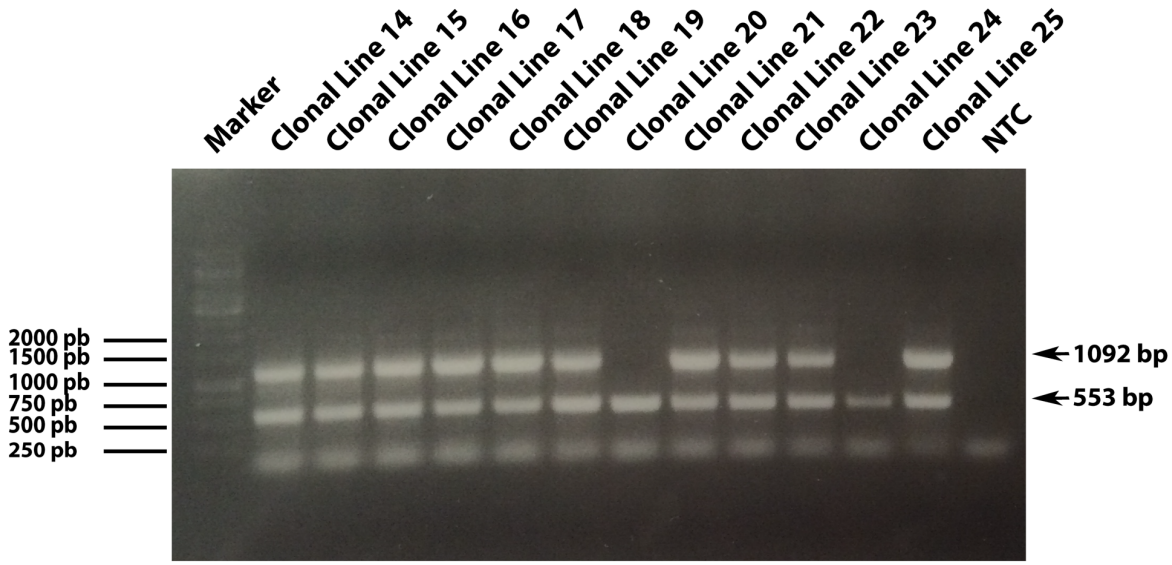

Figure 61. **TgTBCB KO clonal lines negative for homologous recombination.** Electrophoretic analysis (1% agarose gel) of the genomic PCR products to check the gene-swap of the TgTBCB KO construct at the TgTBCB endogenous locus. The majority of clonal lines tested presented two PCR products (553 pb and 1092 pb), consistent with a random integration. Clonal lines 20 and 24 presented a PCR product compatible with a wild-type strain. Marker - GeneRuler 1 kb DNA Ladder. NTC – Non-template control.

Our failure, concerning the homologous recombination, led us to use a different approach in the transfections. This time we planned to use only the Nucleofector™ 2b Device, Lonza with two different DNA concentrations and also some changes in the linearization of the plasmid construction and in the use of the restriction enzyme in the transfection mixture. Being so were stablished three different conditions:

1. 10 µg of the linearized plasmid, with the restriction enzyme in the transfection mixture;
2. 10 µg of the non-linearized plasmid, without the restriction enzyme in the transfection mixture;
3. 1 µg of the linearized plasmid, with the restriction enzyme in the transfection mixture;
4. 1 µg of the and non-linearized plasmid without the restriction enzyme in the transfection.

Were performed 4 transfections, one for each condition. The isolated clones were tested by the genomic PCR strategy, to confirm the correct insertion of the KO construct in the *T. gondii* TgTBCB endogenous locus (homologous recombination) (Figure 62) and then, the PCR positive clonal lines were checked by immunofluorescence to confirm the overexpression of the Myc-TgTBCB (Figure 63).

By genomic PCR, we found three clonal lines (28-30) positive for homologous recombination (only one PCR product with 1092 bp). However, only one of them (the clonal line 30) was phenotypically positive (Figure 63), overexpressing the Myc-TgTBCB, as observed by immunofluorescence. For this latter clone, we confirmed the above results and extracted total RNA to synthetize cDNA and confirm the expression of the Myc-TgTBCB (Figure 64). After all confirmations, we started the KO induction tests. For this, rapamycin was added to the cultures and, after an overnight incubation, the cells were processed for immunofluorescence, to verify the excision of the Myc-TgTBCB and the subsequent overexpression of YFP.

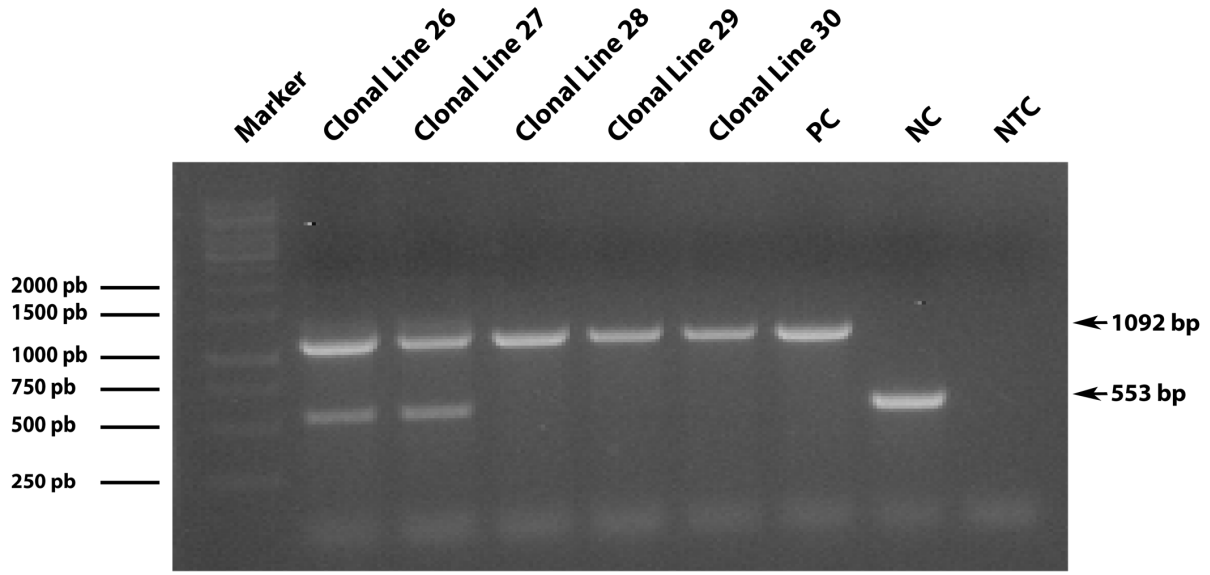

Figure 62. **Clonal lines 28-30 are positive for homologous recombination.** Electrophoretic analysis (1 % agarose gel) of the genomic PCR products to check the gene-swap of the TgTBCB KO construct at the TgTBCB endogenous locus. Clonal lines 28-30 presented only one PCR product (1092 pb), consistent with the homologous recombination. Marker - GeneRuler 1 kb DNA Ladder. PC – Positive control, plasmid construction. NC – Negative control, wild-type strain. NTC – Non-template control.

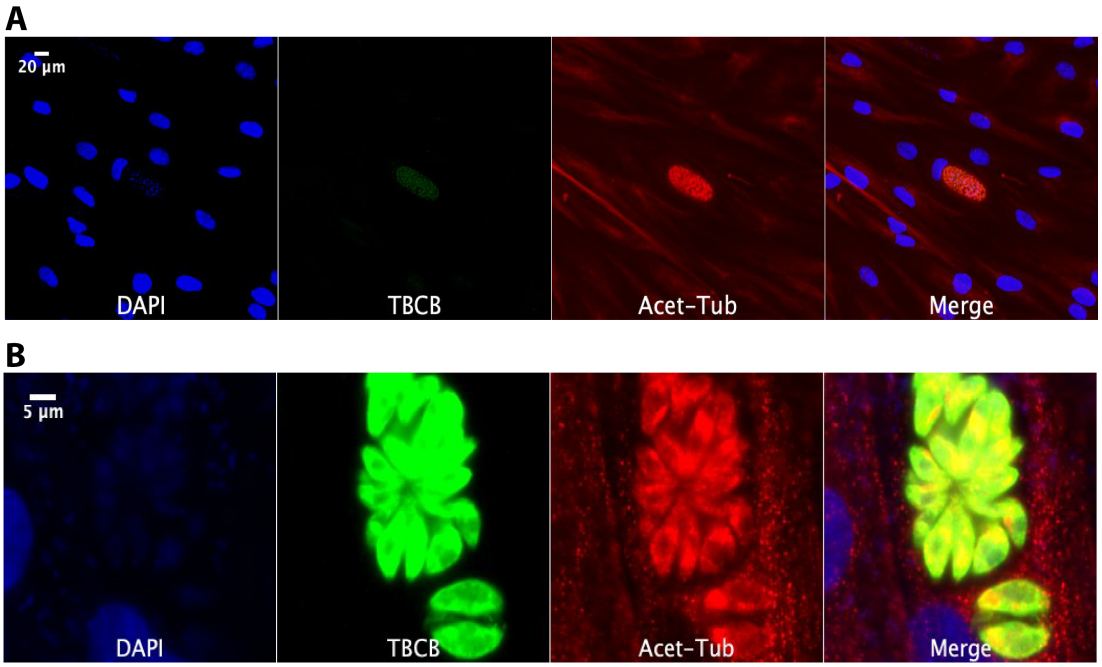

Figure 63. Clonal line 30 overexpressing the Myc-TBCB. HFF cells were invaded with *T. gondii* for 24 h, then cells were immunostained with antibodies against TgTBCB (green) and acetylated tubulin (red). DNA was stained with DAPI (blue). Images were acquired using the Leica DMRA2 DMR HC microscope. A - Negative control (*T. gondii* wild type strain). B – Clonal line of TgTBCB KO overexpressing the Myc-TgTBCB. Scale bar 20 µm (A) and 5 µm (B).

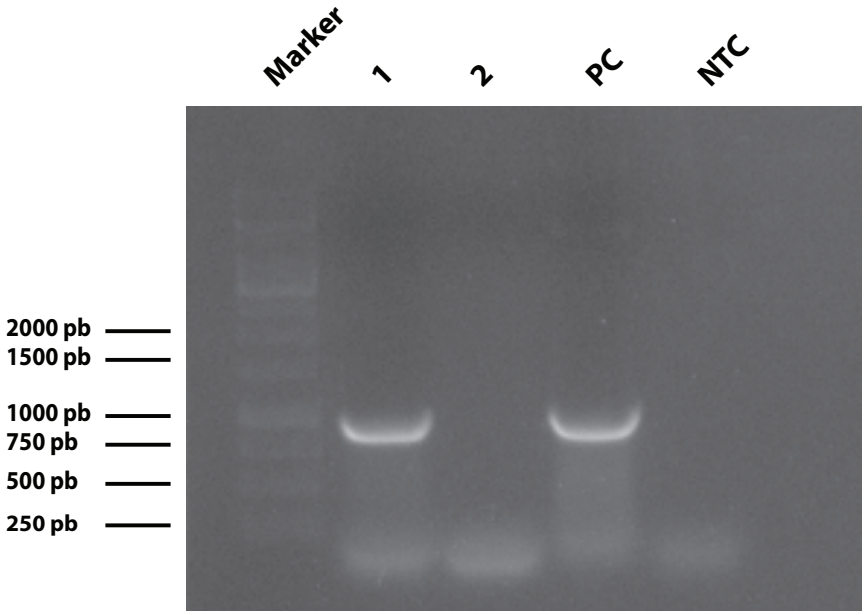

Figure 64. Confirmation of Myc-TgTBCB expression by reverse transcribed PCR. Total RNA was extracted from Myc-TBCB positive clone, RNA was treated with DNase, cDNA was synthetized, and PCR was performed with specific primers to amplify the Myc-TgTBCB. Electrophoretic analysis (1 % agarose gel) of the PCR products confirms the Myc-TgTBCB expression. M - GeneRuler 1 kb DNA Ladder. 1 – PCR from the cDNA. 2 – PCR from the total RNA after DNase treatment (DNA genomic contamination control). PC – PCR from the plasmid construct (positive control). NTC – Non-template control.

The attempts to induce the KO included different induction times, specifically 1, 2, 4, 8, 16, 24, 48, 72 and 96 h, and rapamycin from two different brands. In all cases the results were negative (one example is presented in figure 65)

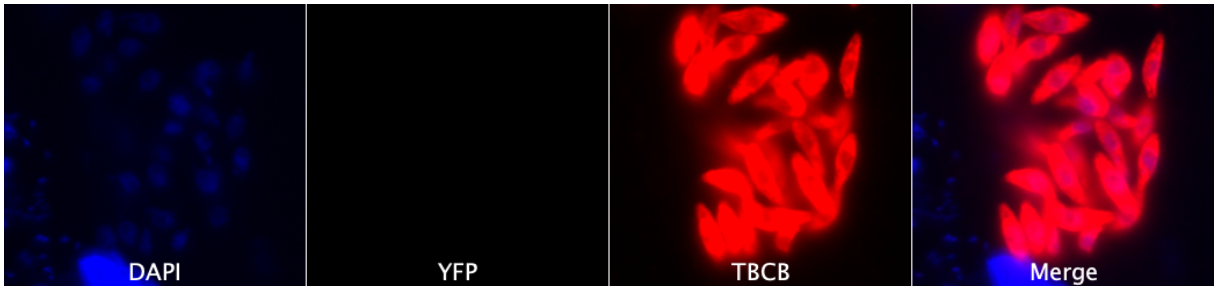

Figure 65. TgTBCB KO is not induced by rapamycin. HFF cells were invaded with *T. gondii* for 24 h in the presence of rapamycin, cells were immunostained with antibodies against TgTBCB (red). DNA was stained with DAPI (blue). In the presence of rapamycin, Myc-TBCB should be excised from *T. gondii* genome, by Cre recombinase, and YFP should be expressed. Images were acquired using the Leica DMRA2 DMR HC microscope. Scale bar 20 µm.

Considering all these negative results, we decided to confirm the expression and integrity of the Cre recombinase in our strain, specifically the two inactive Cre fragments that are induced in the presence of rapamycin. For this propose, specific primers for each Cre recombinase fragment were selected. These primers were used to amplify the two Cre recombinase fragments from cDNA, to check their presence in the genome and the respective expression.

The expression of cre recombinase inactive fragment 1 (PCR product of 500 pb) was only detected in the RNA extracted from the positive control, indicator strain. On the other hand, the expression of Cre recombinase inactive fragment 2 (PCR product of 1100pb) was detected in the clonal lines, in the original strain (RH::DiCreΔku80ΔHX strain) and in the control strain (indicator). These results showed that the original strain RH::DiCreΔku80ΔHX, and consequently all isolated clones, only express one of the two inactive Cre recombinase fragments (Figure 66 and 67). Thereby, we could not have a functional Cre recombinase enzyme to excise our gene of interest.

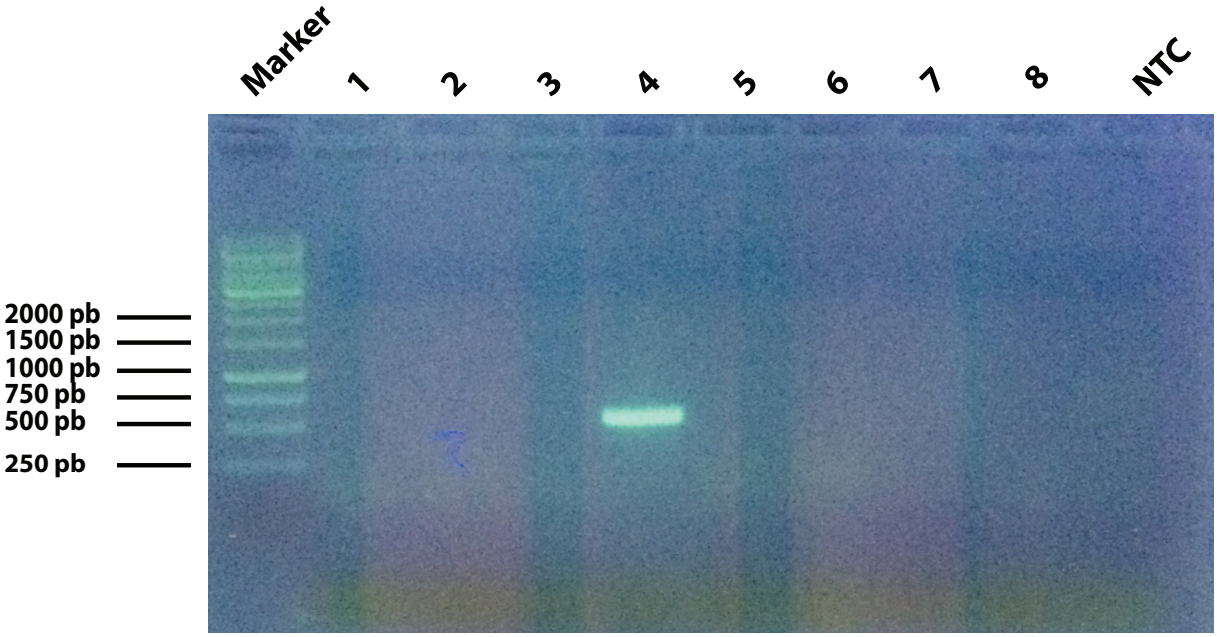

Figure 66. Cre recombinase inactive fragment 1 is not expressed in the original strain (RH::DiCreΔku80ΔHX). Electrophoretic analysis (1 % agarose gel) of the PCR to confirm the expression of Cre recombinase inactive fragment 1 (500 pb). M - GeneRuler 1 kb DNA Ladder. 1 – cDNA synthesized from total RNA extracted from the clonal line 1. 2 – cDNA synthesized from total RNA extracted from the clonal line 2. 3 – cDNA synthesized from total RNA extracted from RH::DiCreΔku80ΔHX strain. 4 – cDNA synthesized from total RNA extracted from positive control, indicator strain. 5 – Clonal line 1, total RNA treated with DNase. 6 – Clonal line 2, total RNA treated with DNase. 7 – RH::DiCreΔku80ΔHX strain, total RNA treated with DNase. 8 – Indicator strain, positive control, total RNA treated with DNase. From 5-8 DNA genomic contamination control. NTC – Non-template control.

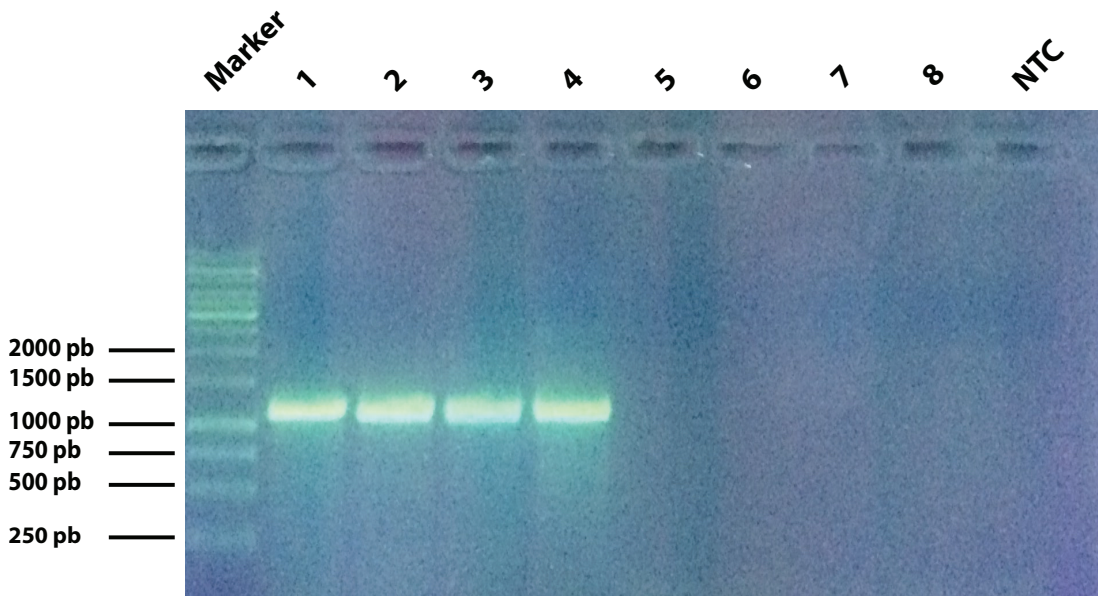

Figure 67. Cre recombinase inactive fragment 2 is expressed in all tested strains. Electrophoretic analysis (1 % agarose gel) of the PCR to confirm the expression of Cre recombinase inactive fragment 2 (1100 pb). M - GeneRuler 1 kb DNA Ladder. 1 – cDNA synthesized from total RNA extracted from the clonal line 1. 2 – cDNA synthesized from total RNA extracted from the clonal line 2. 3 – cDNA synthesized from total RNA extracted from RH::DiCreΔku80ΔHX strain. 4 – cDNA synthesized from total RNA extracted from positive control, indicator strain. 5 – Clonal line 1, total RNA treated with DNase. 6 – Clonal line 2, total RNA treated with DNase. 7 – RH::DiCreΔku80ΔHX strain, total RNA treated with DNase. 8 – Indicator strain, positive control, total RNA treated with DNase. From 5-8 DNA genomic contamination control. NTC – Non-template control.

In summary, when the correct transfection conditions were established and the TgTBCB KO clonal line positive for homologous recombination was isolated, we could not induce the excision of Myc-TgTBCB cDNA by Cre recombinase in the presence of rapamycin. To overcome this problem, we established three approaches as described below.

a) Our first approach was to do a transient transfection of our Myc-TBCB conditional clonal lines with the Cre recombinase inactive fragment 1, in order to induce the TBCB KO and proceed with the TBCB KO characterization. We successfully cloned the Cre recombinase inactive fragment 1 and transfected transiently the Myc-TBCB inducible KO clonal line. Following the addition of rapamycin, we confirmed the KO induction by the GFP presence in the immunofluorescence. In fact, we confirmed the excision of the Myc-TBCB cDNA and the YFP cDNA expression, resulting in YFP-expressing parasites (green KO parasites) (Figure 68). However, since our clonal line was already resistant to the HXGPRT, due to our previous transfection, and we did not have any other plasmid available with a different resistance marker, it was impossible to select for a stable transfection. We observed that in the induced pool, with a mix population of induced and not induced parasites, the induced ones decreased over time and did not survive for more than 1 week. This observation suggests that TgTBCB is important, if not essential, to the parasite survival.

b) We also tested our frozen stocks of "inducible" strains for the expression and the integrity of the Cre recombinase. The positive strains were selected, and we restarted the transfection protocol to obtain inducible KO clonal line. But, unfortunately, all the clonal lines were again negative for homologous recombination, by genomic PCR.

c) Another approach could be a direct KO of TgTBCB gene instead of the gene-swap strategy. However, the low efficiency of homologous recombination that we were observing together with the indication that TgTBCB can be essential for parasite propagation, led us to abandon this approach.

Taking the points above into consideration, we decided to explore a new methodology to obtain the TgTBCB KO, the CRISPR/Cas9 system.

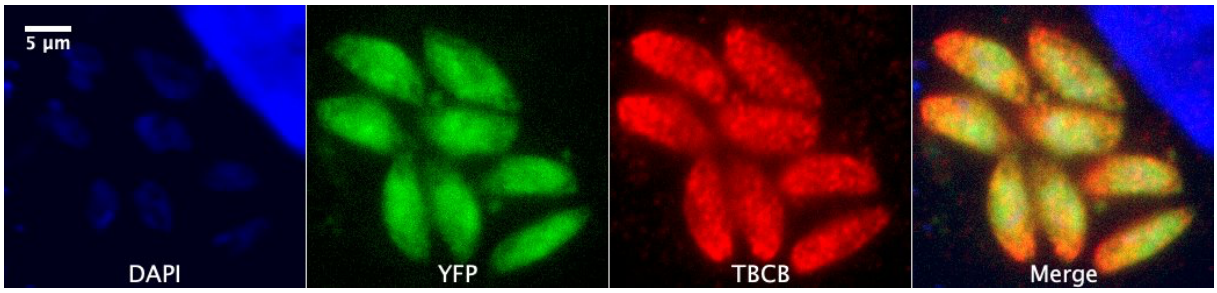

Figure 68. TgTBCB KO induction after transient transfection with Cre recombinase inactive fragment 1. TgTBCB KO clonal line was transfected with the Cre recombinase inactive fragment 1, and subsequently induced for 24 h with rapamycin. Cells were immunostained with antibodies against TgTBCB (red). DNA was stained with DAPI (blue). In the presence of rapamycin, the MycTBCB was excised from *T. gondii* genome, by Cre recombinase, and YFP was expressed. Images were acquired using the Leica DMRA2 DMR HC microscope. Scale bar 5 µm.

8.2. *T. gondii* TBCB conditional knockout using the CRISPR/Cas9 system

The second methodology used to evaluate the role of TBCB in *T. gondii* was the CRISPR/Cas9 system. Since 2014, this system has been widely used in *T. gondii* to disrupt protein-coding sequences based on transfection of a guide RNA into parasites constitutively expressing Cas9 (Shen, Brown, Lee, & Sibley, 2014; Sidik et al., 2016). Meissner lab is developing a CRISPR/Cas9 inducible system, based on DiCre system, where a SplitCas9 enzyme is expressed in two inactive fragments, each of them fused to one of the rapamycin-binding proteins FRB and FKBP. The addition of rapamycin brings FRB and FKBP together, reconstituting the functional enzyme. Using this mechanism, we have the capacity to control the exact moment when the system is triggered, a key tool for the study of essential genes.

The initial cloning and transfection process to get a TgTBCB inducible KO strain by CRISPR/Cas9 system was started in Glasgow at Meissner lab. Succinctly, we explored two different approaches to create a knockout strain for TgTBCB with the Cas9. One with gRNAs

directed to the TgTBCB gene exons and, an alternative approach, with gRNAs directed to introns to be used in combination with the TgTBCB DiCre plasmid construct in an attempt to favor the homologous recombination at the TgTBCB endogenous locus.

We transfected three different gRNAs (different sequences which targeted the first TgTBCB exon) and select 6 clones for the TgTBCB gene (2 clones for each gRNA). These clones were brought to Portugal and the studies for their characterization were done in our lab. Unfortunately, only one of the clones was in fact positive by PCR for gRNA random integration, so our studies were conducted with that positive clone.

8.2.1. WB analysis showed that *T. gondii* TBCB amount decreases after CRISPR/Cas9 KO induction

The confirmation of the TgTBCB gene inactivation was done by WB analysis after clonal line KO induction with rapamycin for 72 h. This analysis confirmed the complete depletion of the TgTBCB protein after 72 h of induction and shows that there is no alteration in the levels of acetylated and α-tubulin in soluble protein extracts (Figure 69A). On the other hand, when analyzing the insoluble extracts (where are the MTs), we found a reduction in the acetylated, glutamylated and α-tubulin protein levels. Since TgTBCB is not present in the insoluble protein extracts, it was not possible to address its depletion under this condition (Figure 69B).

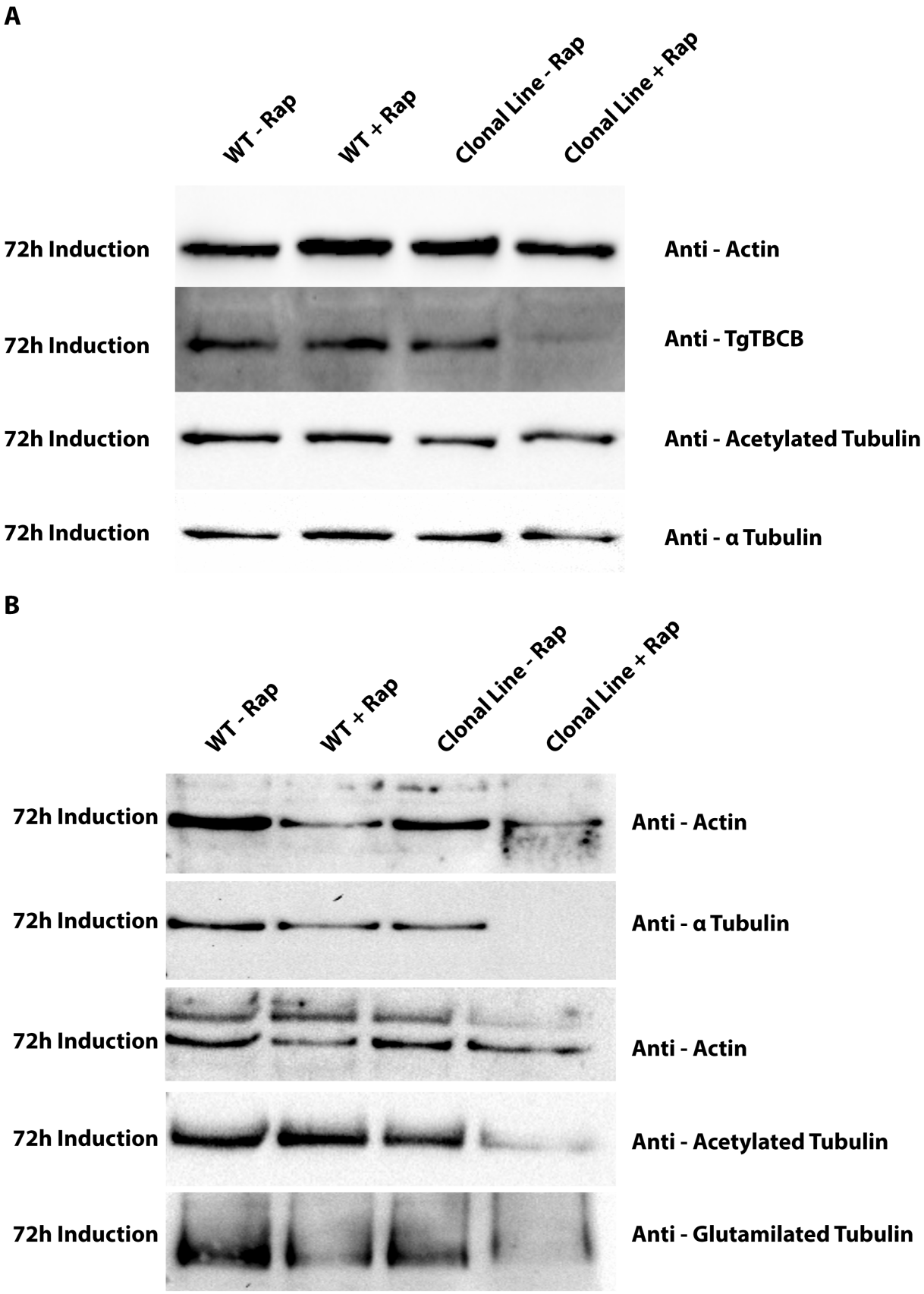

Figure 69. WB analysis of protein extracts, 72 h after TgTBCB KO induction. Soluble (A) and insoluble (B) protein extracts, from the TgTBCB inducible KO clonal line and the control (wild-type, WT - splitCas9 strain), with and without rapamycin (Rap), were analysed by 15 % SDS-PAGE followed by WB with TgTBCB specific polyclonal serum (A), anti-Acetylated tubulin antibody (A and B), anti-α-Tubulin antibody (A and B) and anti-Actin antibody (loading control, A and B).

After confirming a decrease in the amount of TgTBCB protein upon KO induction, we decided to isolate a TgTBCB KO clone to characterize the KO effect. However, all the attempts to isolate a clone by limit dilutions were unsuccessful. Many parasites died in culture and the isolated clones were negative for TgTBCB KO suggesting, once again, that this gene is essential. Under these circumstances, the TgTBCB KO had to be induced before each experiment.

8.2.2. Genomic DNA PCR: detection of the mutations in the first TgTBCB exon

In this system, after KO induction occurs a hydrolysis (DNA double strand cut) in the genomic DNA followed by a non-homologous repair. Usually this repair involves a deletion or an insertion that inactivates the target gene.

After 24 h of TgTBCB KO induction, genomic DNA was extracted from tachyzoites and the gRNA target region was amplified by PCR. The PCR product was sequenced, the sequencing was perfect until the predicted hydrolysis site and, after this site, we lost the sequencing reaction, probably due to the great diversity of sequences (each parasite undergoes a different DNA repair). This result suggests that the TgTBCB DNA mutation occurred at the expected site.

8.2.3. Phenotypic characterization of *T. gondii* TBCB conditional KO

For these studies, the parasites, control and inducible KO clonal line, were treated with rapamycin or left untreated for 48 h when free viable egressed parasites were collected, counted and used to perform the experiments.

According to the standard protocol, we should have performed a plaque assay, as a primary assay, for the characterization of the TgTBCB KO. However, considering the lifespan of these parasites after the KO induction (no more than a week) it was not possible to perform this assay.

Regarding the invasion assay, confluent monolayers of HFF cells were invaded for 1 h with the same number of transgenic or control tachyzoites. Then, extracellular parasites were removed, and cells were incubated for more 18 h before fixation. After that, the cells were processed for immunofluorescence and the number of parasitophorous vacuoles, corresponding to successful invasion, was scored. Interestingly, we observed a remarkably reduction of the TgTBCB KO ability to invade the host cells. In fact, the induced clonal line showed a decrease of 61% in its ability to invade the HFF cells in comparison to the control parasites (Figure 70).

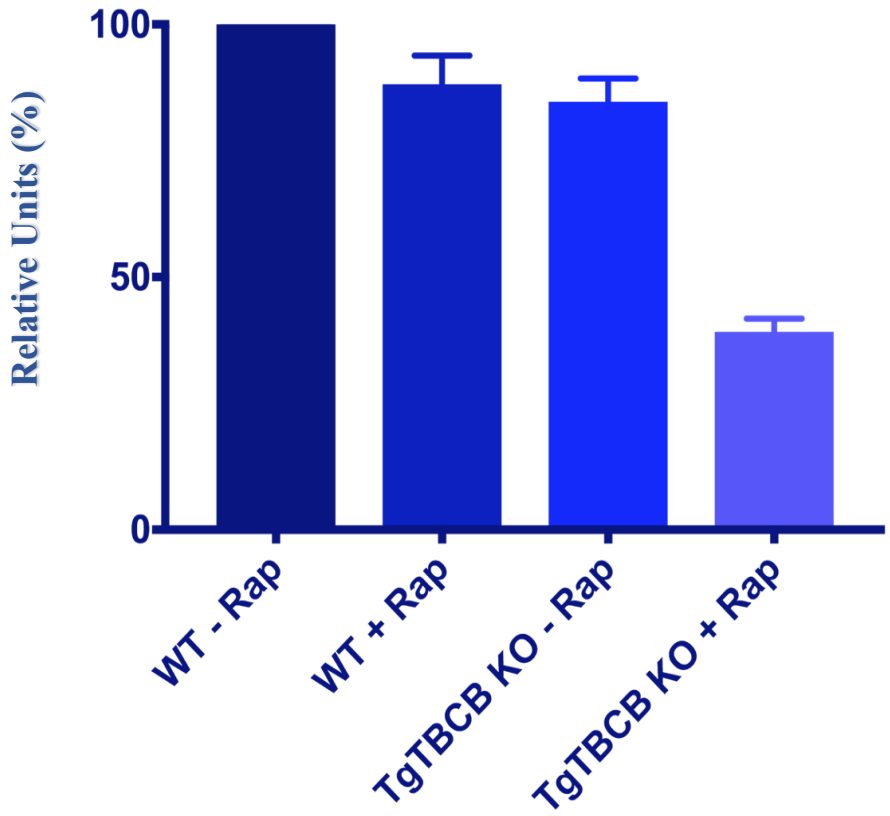

Figure 70. TgTBCB KO decreases the ability to invade host cells. In the invasion assays, the number of invaded parasites was counted in 6 fields using a 40× objective and calculated as a percentage value of control parasites (wild-type, WT - SplitCas9 strain not induced) normalized to 100 %. *$p < 0.001$. The p values were determined in comparison to the control. The graphic bars are the normalized values ± SEM (error bars) of three independent assays. Statistical significance was calculated using a student t-test. (+ Rap) means rapamycin added and (– Rap) means no rapamycin added.

Concerning the replication assay, it was performed to analyze the ability of *T. gondii* tachyzoites to undergo normal intracellular replication. In this assay we also found an enormous decrease in the replication capability of the induced TgTBCB clonal line. In fact, the KO parasite line showed a huge increase in the frequency of two parasites per vacuole and a decrease in the other categories, mostly in eight and more than eight (+8) parasites per vacuole (Figure 71).

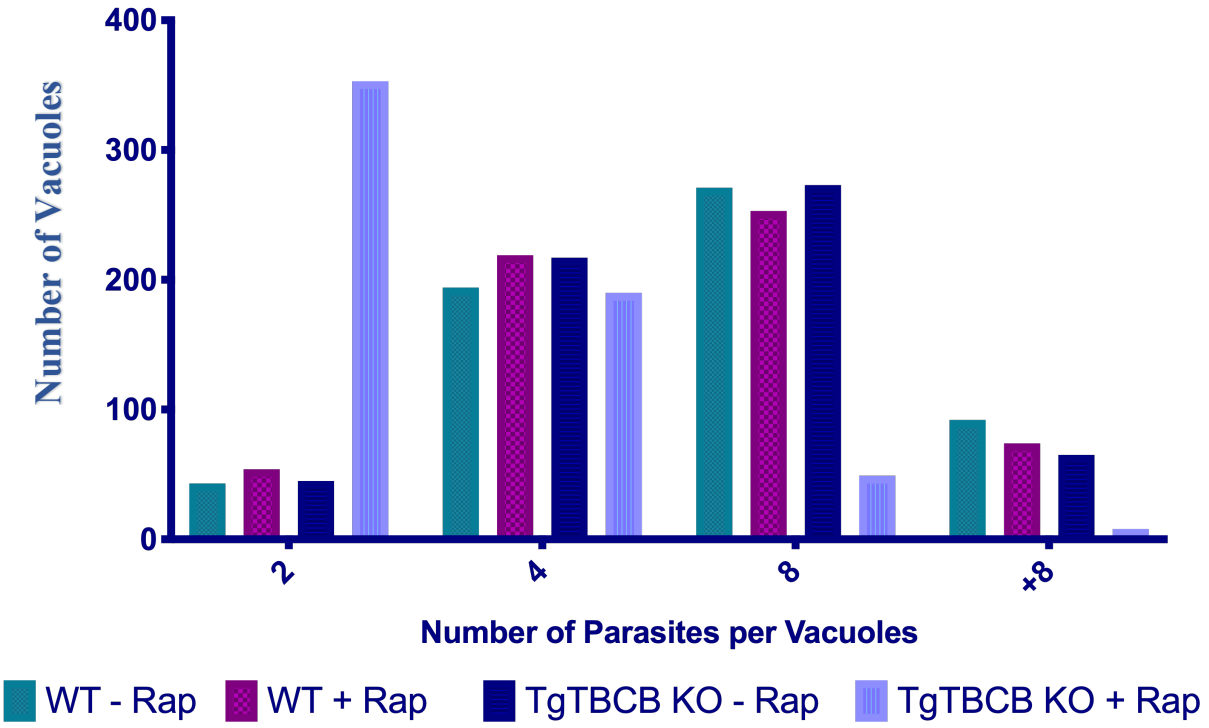

Figure 71. TgTBCB KO affects the replication rate in *T. gondii*. The replication assay shows that "TgTBCB KO + Rap" presents more vacuoles with 2 parasites and the other strains (WT-Rap, WT+Rap and TgTBCB-Rap) presented more vacuoles with 8 parasites. Total number of vacuoles counted in 3 independent experiments (200 vacuoles counted per experiment). The graphic bars are the number of the vacuoles with 2, 4, 8 or more parasites (+8). (WT) is the wild type control strain (SplitCas9 strain) (+ Rap) means rapamycin added and (– Rap) means no rapamycin added.

Like the plaque assay, the egress assay was not preformed since the time needed to perform this assay was more than the viable time of the induced KO parasites lines.

8.2.4. Cellular characterization of the *T. gondii* TBCB KO by Immunofluorescence

To further understand what was happening during the lytic cycle of the parasite we inoculated HFF cells and, at the same time, the KO was induced with rapamycin for 24 h, 48 h and 72 h. Afterwards the parasites were fixed with methanol or paraformaldehyde and processed for immunofluorescence, using antibodies against TgTBCB, acetylated tubulin (stains the subpellicular MTs), polyglutamylated tubulin (stains close to the conoid and progressively decreases towards the distal end of the subpellicular MTs) and centrin (stains the centrioles from centrosome).

Interestingly, after 24 h it is still possible to detect TgTBCB, but some parasites already show replication problems, presenting parasites dividing with four daughter cells forming inside instead of two. It seems that they lose the cell polarity and replication control (Figures

72, 73 and 74). Curiously, in these control cells, it is possible to observe the TgTBCB in the daughter cells.

The anti-centrin stains the centrioles that are part of the centrosome (MTOC). Each centrosome has two centrioles, but with this resolution, it is difficult to distinguish the two centrioles dots, being detectable only one dot per centrosome. In interphase, the parasites have one centrosome (one dot) and when replicating present two centrosomes (two dots). In our studies, it was possible to observe KO TgTBCB cells with three or four centrosomes (Figure 74).

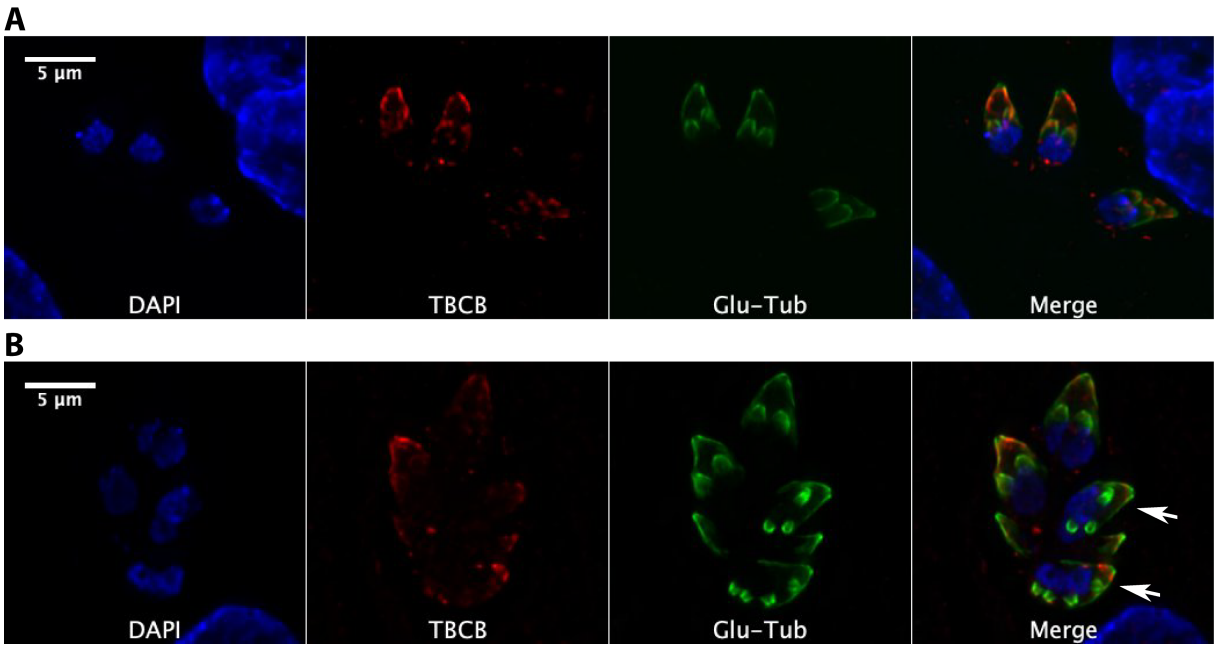

Figure 72. TgTBCB KO, polyglutamylated tubulin staining 24 h after induction. A - Control - TgTBCB KO Clonal line not induced. **B** - TgTBCB KO Clonal line induced for 24 h. HFF cells were invaded and 24 h later were fixed with paraformaldehyde and immunostained with antibodies against TgTBCB (red) and polyglutamylated tubulin (green). DNA was stained with DAPI (blue). In TgTBCB KO parasites it is possible to observe parasites with four daughter cells (white arrows). Images were acquired with Olympus AppliedPrecision DeltaVision Core system**.** Scale bars, 5 µm.

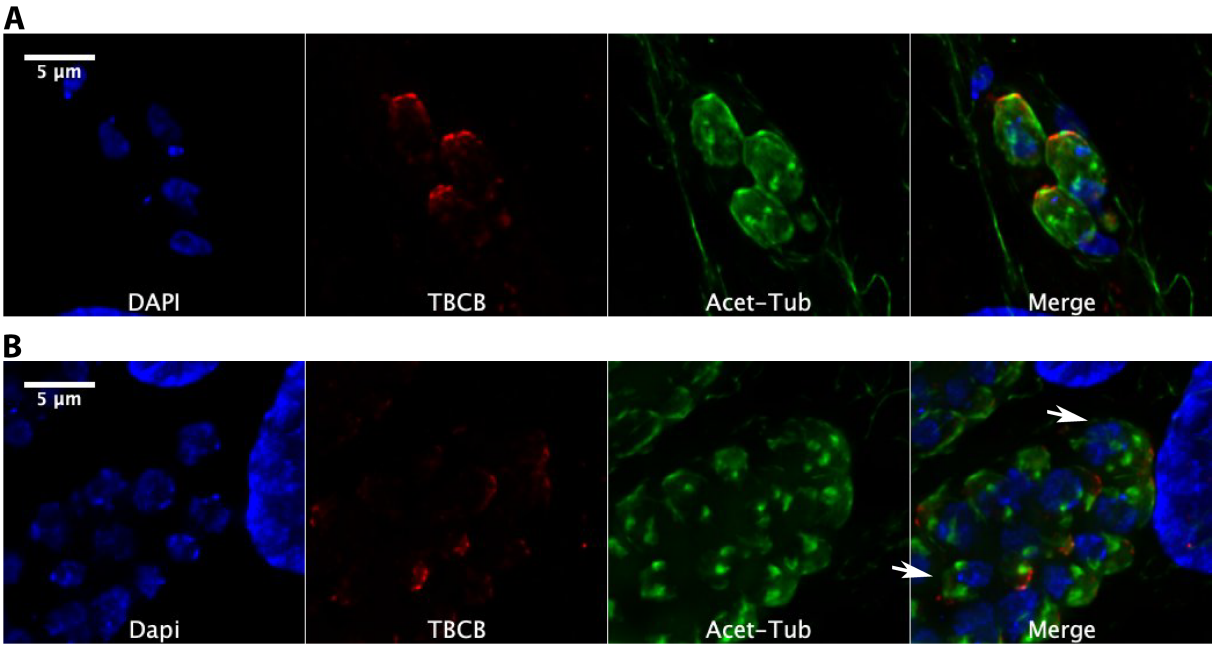

Figure 73. TgTBCB KO, acetylated tubulin staining 24 h after induction. A - Control - TgTBCB KO Clonal line not induced. **B** - TgTBCB KO Clonal line induced for 24 h. HFF cells were invaded and 24 h later were fixed with methanol and immunostained with antibodies against TgTBCB (red) and acetylated tubulin (green). DNA was stained with DAPI (blue). In TgTBCB KO parasites it is possible to observe parasites with four daughter cells (white arrows). Images were acquired with Olympus AppliedPrecision DeltaVision Core system. Scale bars, 5 µm.

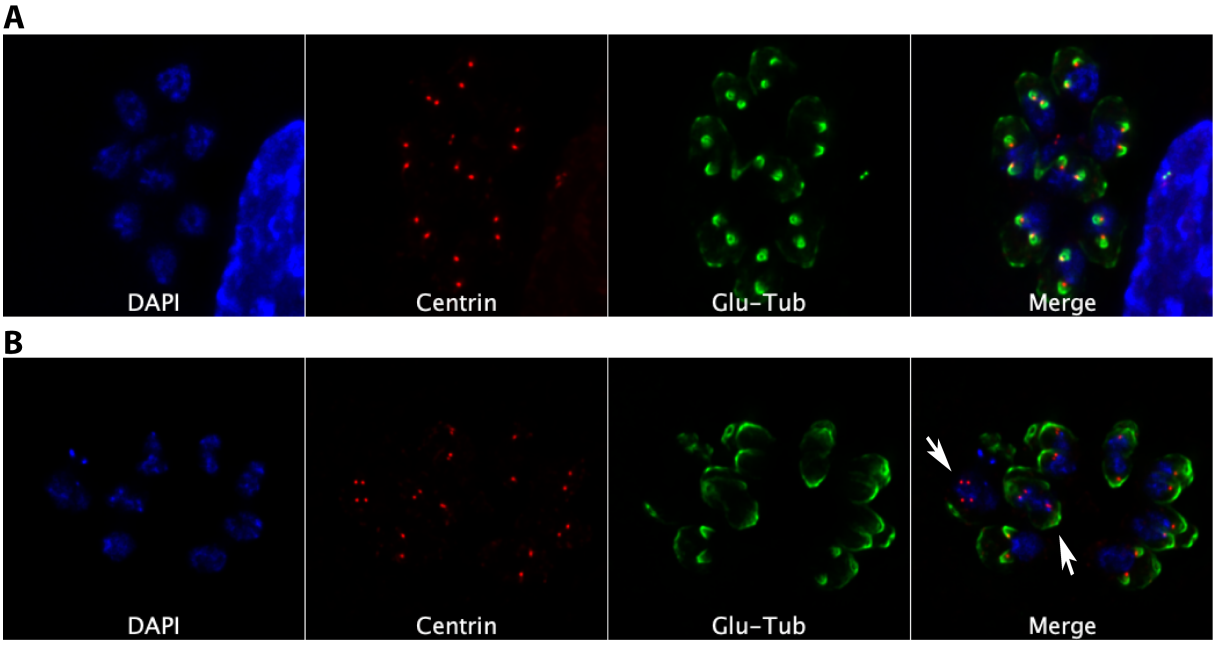

Figure 74. TgTBCB KO, centrin staining 24 h after induction. A - Control - TgTBCB KO Clonal line not induced. **B** - TgTBCB KO Clonal line induced for 24 h HFF cells were invaded and 24 h later were fixed with methanol and immunostained with antibodies against centrin (red) and polyglutamylated tubulin (green). DNA was stained with DAPI (blue). In TgTBCB KO parasites it is possible to observe that all parasites already duplicate the centrioles, it is also possible to observe replicating cells with four and three centrosomes instead of two (white arrows). Images were acquired with Olympus AppliedPrecision DeltaVision Core system. Scale bars, 5 µm.

After 48 h of invasion the replication problems were more marked, the parasitophorous vacuoles only presented a few parasites that at certain point were unable to replicate showing a vast disorganization. At this stage, the number of parasites presenting problems in replication is much higher. The polyglutamylated and acetylated tubulin already showed some alterations in its regular staining, namely the decrease in the staining intensity. The acetylated tubulin is weaker, slightly present at the anterior pole of the parasite and additionally it stained the parasitophorous vacuole. Apparently, the parasites did not complete the division, the centrosomes are able to replicate, but the parasites have very large nucleus that seem to be unable to divide. The TBCB signal is decreasing and diffusing along the parasite (Figures 75, 76 and 77).

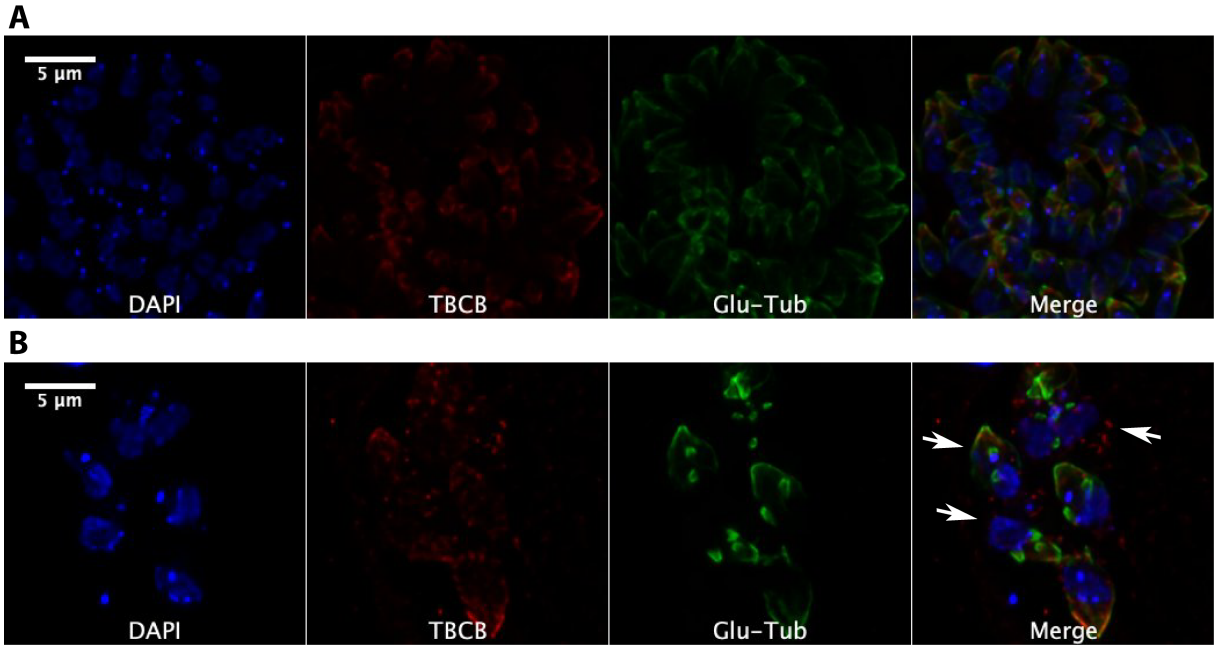

Figure 75. TgTBCB KO, polyglutamylated tubulin staining 48 h after induction. A - Control - TgTBCB KO Clonal line not induced. **B** - TgTBCB KO Clonal line induced for 48 h. HFF cells were invaded and 48 h later were fixed with paraformaldehyde and immunostained with antibodies against TgTBCB (red) and polyglutamylated tubulin (green). DNA was stained with DAPI (blue). In TgTBCB KO parasites it is possible to observe parasites that failed several rounds of cell divisions (white arrows). Images were acquired with Olympus AppliedPrecision DeltaVision Core system. Scale bars, 5 µm.

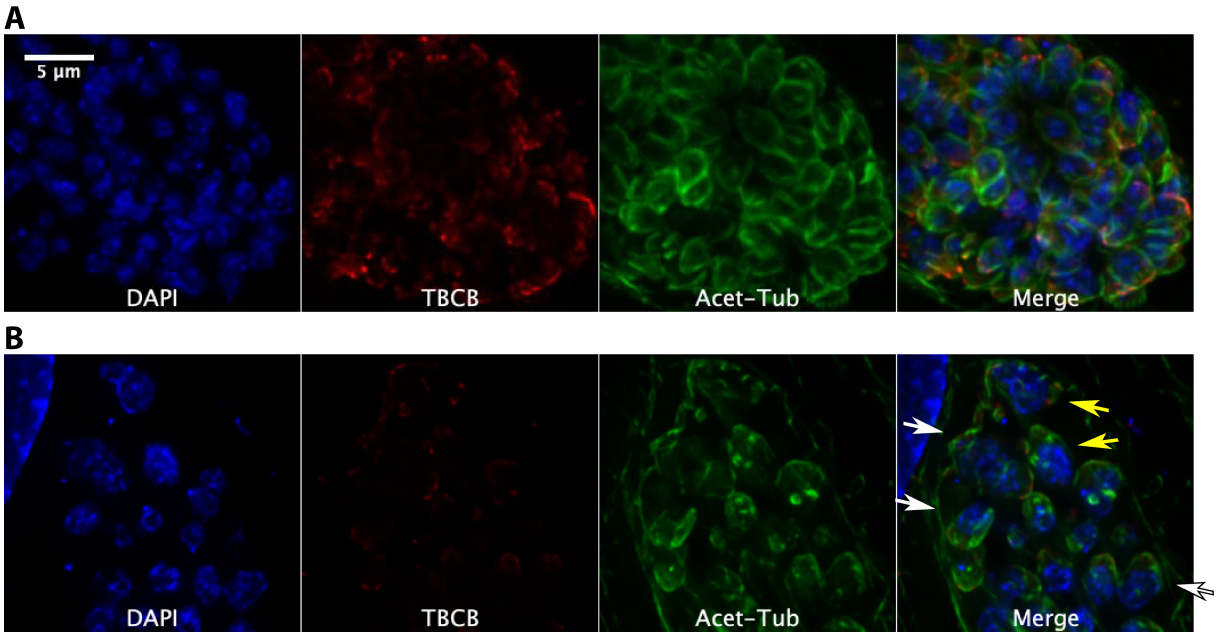

Figure 76. TgTBCB KO, acetylated tubulin staining 48 h after induction. A - Control - TgTBCB KO Clonal line not induced. **B** - TgTBCB KO Clonal line induced for 48 h. HFF cells were invaded and 48 h later were fixed with methanol and immunostained with antibodies against TgTBCB (red) and acetylated tubulin (green). DNA was stained with DAPI (blue). In TgTBCB KO parasites it is possible to observe parasites with big nucleus (yellow arrows), probably due to the failure of cell divisions, the acetylated tubulin staining is weaker, presents only at the anterior pole of the parasite and additionally it stained the parasitophorous vacuole (white arrows). Images were acquired with Olympus AppliedPrecision DeltaVision Core system. Scale bars, 5 µm.

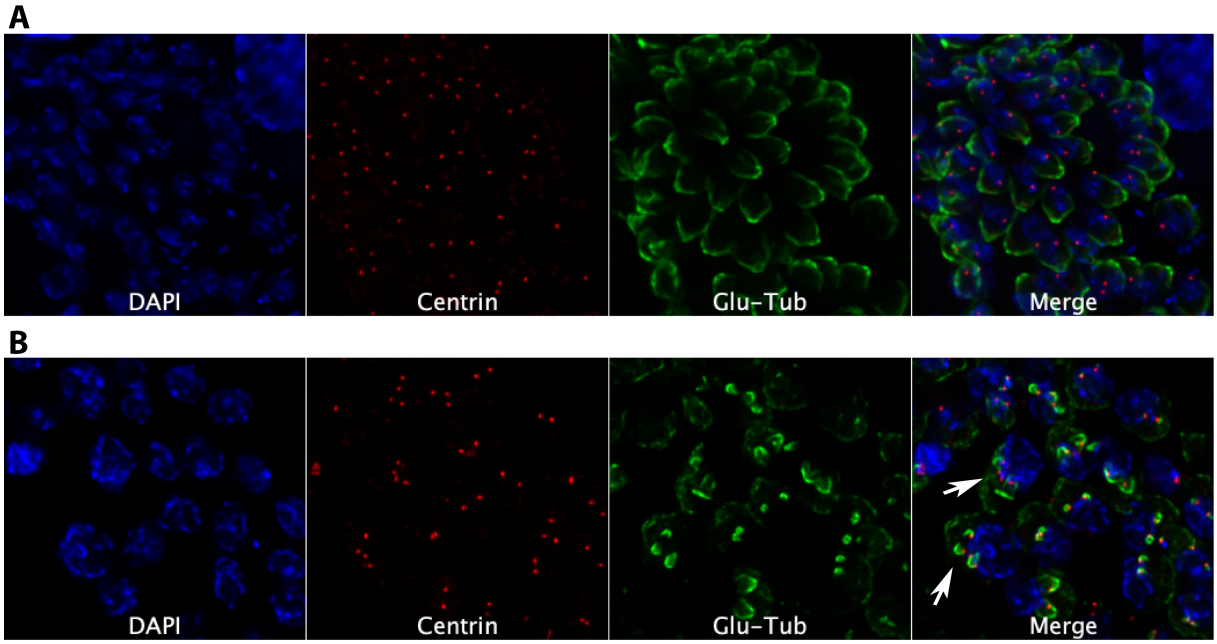

Figure 77. TgTBCB KO, centrin staining 48 h after induction. A - Control - TgTBCB KO Clonal line not induced. **B** - TgTBCB KO Clonal line induced for 48 h. HFF cells were invaded and 48h h later were fixed with methanol and immunostained with antibodies against centrin (red) and polyglutamylated tubulin (green). DNA was stained with DAPI (blue). In TgTBCB KO parasites it is possible to observe parasites with an abnormal number of centrioles, probably due to centriole duplication without an effective cell division (white arrows). Images were acquired with Olympus AppliedPrecision DeltaVision Core system. Scale bars, 5 µm.

Finally, after 72 h of invasion the parasitophorous vacuoles lost their entire organization, the parasites seemed to be dying inside the vacuoles and showed drastic alterations in the polyglutamylated tubulin normal staining, namely the decrease in the staining intensity, as the polyglutamylated tubulin signal is much weaker, with shorter and disorganized subpellicular MTs. The acetylated tubulin signal is also weaker and abnormal (seems to stain only MTs at the anterior pole of the parasite and with an aberrant MT cytoskeleton) and the TBCB staining is not detectable. Their nucleus is dramatically bigger than the control and parasites accumulate multiple centrosomes per cell but are unable to finish the replication process (Figure 78, 79 and 80).

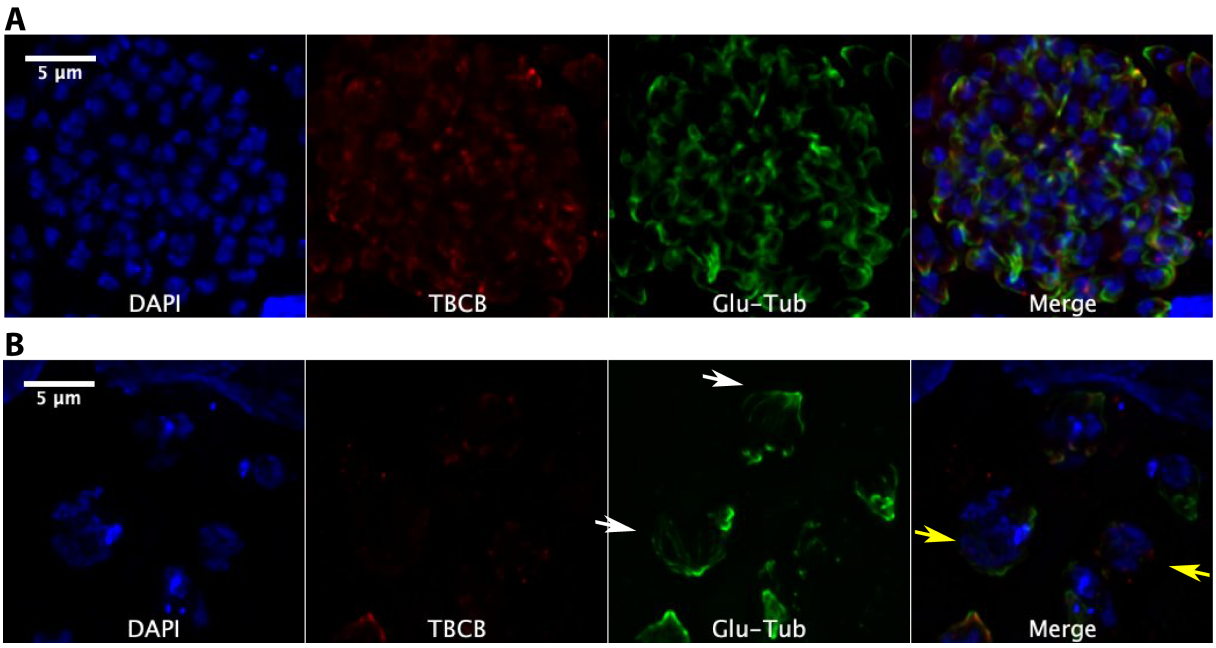

Figure 78. TgTBCB KO, polyglutamylated tubulin staining 72 h after induction. A - Control - TgTBCB KO Clonal line not induced. **B** - TgTBCB KO Clonal line induced for 72 h. HFF cells were invaded and 72 h later were fixed with paraformaldehyde and immunostained with antibodies against TgTBCB (red) and polyglutamylated tubulin (green). DNA was stained with DAPI (blue). In TgTBCB KO parasites it is possible to observe the clear decrease in the TgTBCB staining, a decrease in the glutamylated tubulin staining, the presence of a big nucleus (yellow arrows) and also the presence of shorter and disarranged subpellicular MTs (white arrows). Images were acquired with Olympus AppliedPrecision DeltaVision Core system. Scale bars, 5 µm.

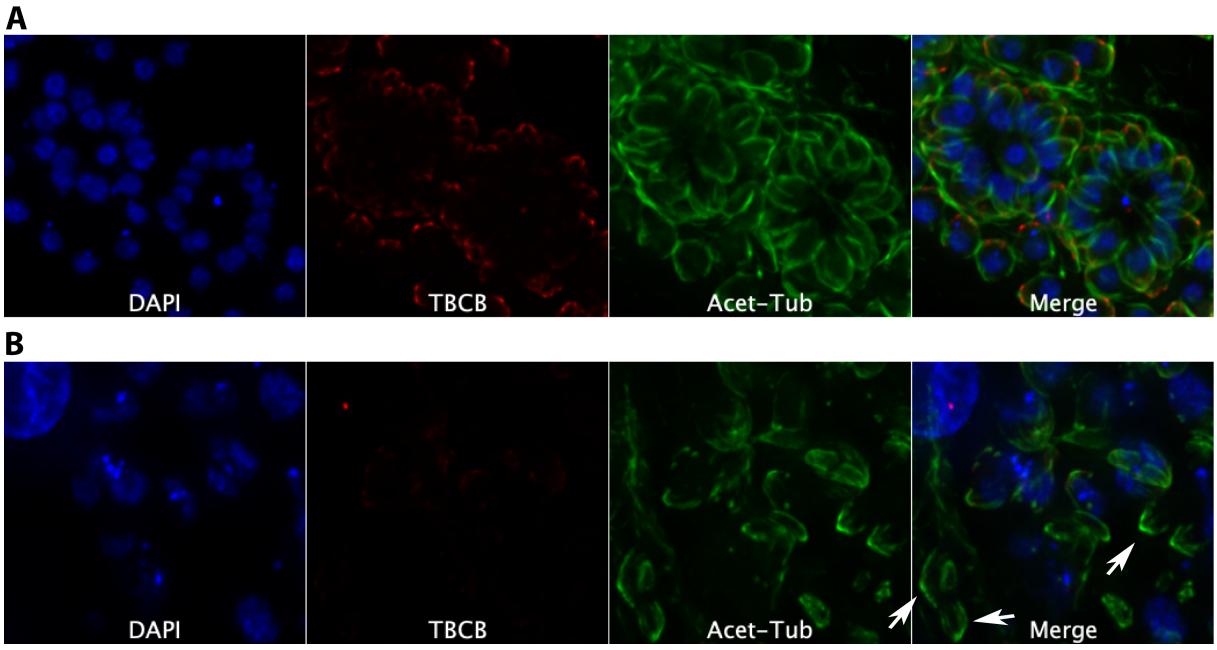

Figure 79. TgTBCB KO, acetylated tubulin staining 72 h after induction. A - Control - TgTBCB KO Clonal line not induced. **B** - TgTBCB KO Clonal line induced for 72 h. HFF cells were invaded and 72 h later were fixed with methanol and immunostained with antibodies against TgTBCB (red) and acetylated tubulin (green). DNA was stained with DAPI (blue). In TgTBCB KO parasites it is possible to observe the clear decrease in the TgTBCB staining, a decrease in the acetylated tubulin staining that seems to dye only MTs at the anterior pole of the parasite and with an aberrant MT cytoskeleton (white arrows). Images were acquired with Olympus AppliedPrecision DeltaVision Core system. Scale bars, 5 µm.

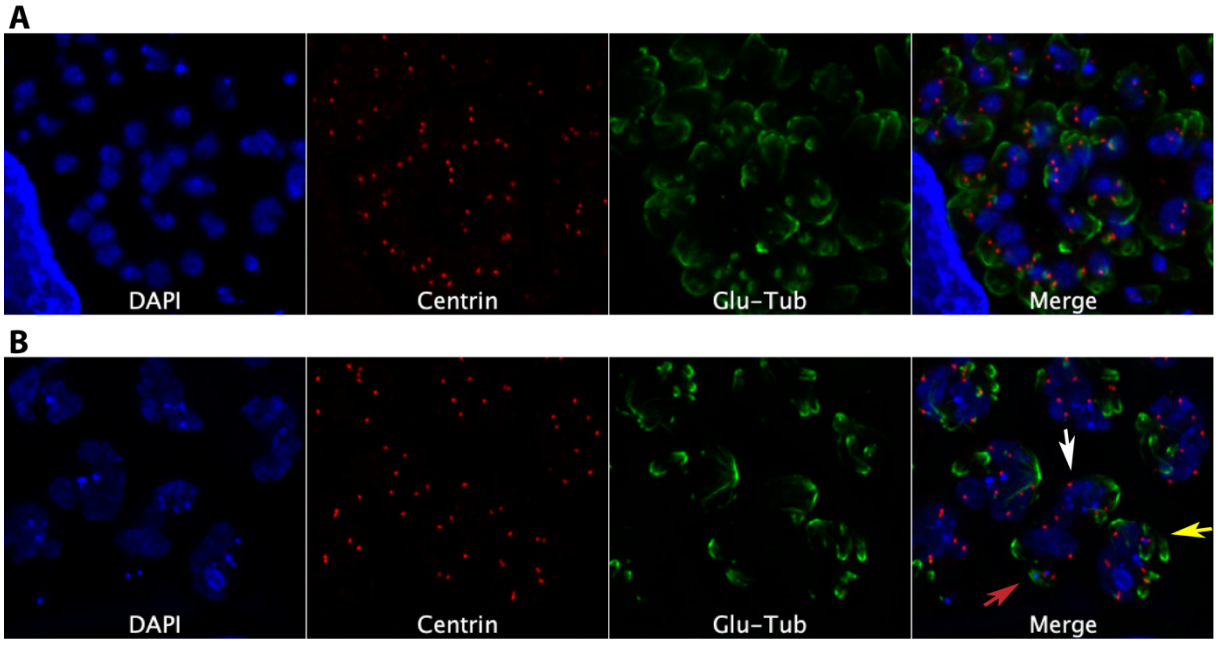

Figure 80. TgTBCB KO, centrin staining 72 h after induction. A - Control - TgTBCB KO Clonal line not induced. **B** - TgTBCB KO Clonal line induced for 72 h. HFF cells were invaded and 72 h later were fixed with methanol and immunostained with antibodies against centrin (red) and polyglutamylated tubulin (green). DNA was stained with DAPI (blue). In TgTBCB KO parasites it is possible to observe multiple centrosomes (yellow arrow), a decrease in the glutamylated tubulin staining (red arrow) and the presence of a big nucleus (white arrow). Images were acquired with Olympus AppliedPrecision DeltaVision Core system. Scale bars, 5 µm.

8.2.5. Nuclear size and cellular morphology comparative analysis of *T. gondii* TBCB conditional knockout

At a recent meeting, Markus Meissner group presented a series of observations suggesting that Cas9 is toxic to *T. gondii* (Stortz, Gow, Meissner, & Jiménez-Ruiz, 2017). This toxicity is the result of a low efficiency of this parasite for repairing the Cas9 induced DNA double strand breaks, what can lead to Cas9 mediated gene disruption within the first lytic cycle of *T. gondii* parasites. Apparently, the DNA repair machinery in *T. gondii* may be unable to repair Cas9-induced DNA double strand breaks in up to 65% of all induced parasites. Their cytotoxic effects manifested are predominantly aberrant nuclei combined with abnormal cellular morphology (Stortz et al., 2017).

These observations raised on us a huge concern and one major doubt, since the phenotype found in our assays could be due to the Cas9 toxicity and not the TgTBCB KO. In order to confirm our previous results, new IFs were made with a pre-induction step, to overcome the first lytic cycle where the Cas9 toxicity was described. The objective was to make a comparison between our previous findings and the outcome with previously induced parasites for 24 h and subsequently re-inoculated for more 24 h, making a total of 48h. We studied in particular the replication phenotypes, cellular morphology and the nuclear size, although other findings were also considered.

We started by a nuclear size assay. To access it, the nuclear size of the parasites from the previous IFs and the new IFs was compared using the Analyze particles tool from ImageJ. The same threshold was used between control and induced parasites by experiment. In the first IF assays we observed an increase in the nuclear size of the KO parasites in all time points (Figure 81, 82 and 83). That increase in the nuclear size was confirmed in the new IF assays with the re-inoculation of TgTBCB KO egressed parasites (Figures 84 and 85).

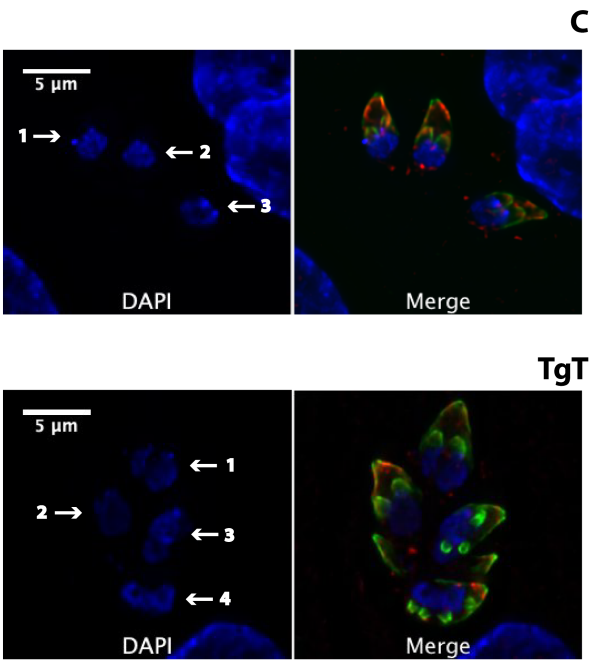

Nuclear Size

	Area	Mean	StdDev
1	3.862	673.737	357.320
2	3.545	616.504	167.030
3	4.232	529.239	290.842

Nuclear Size

	Area	Mean	StdDev
1	7.862	746.935	288.378
2	6.740	541.543	144.016
3	8.747	887.024	405.439
4	7.453	1085.707	457.478

Figure 81. TgTBCB KO increases the nuclear size, 24 h after induction. Nuclear size assay, representative results obtained by an aleatory analysis of the nuclear size. **Control** - TgTBCB KO Clonal line not induced. **TgTBCB KO** - TgTBCB KO Clonal line induced and inoculated in HFF cells during 24 h. Cells were fixed with methanol and immunostained with antibodies against TgTBCB (red) and polyglutamylated tubulin (green). DNA was stained with DAPI (blue). Scale bars, 5 µm. Area - Area of selection in square pixels. Mean – Average of the mean grey value within the selection. Standard Deviation - Standard deviation of the grey values used to generate the mean grey value.

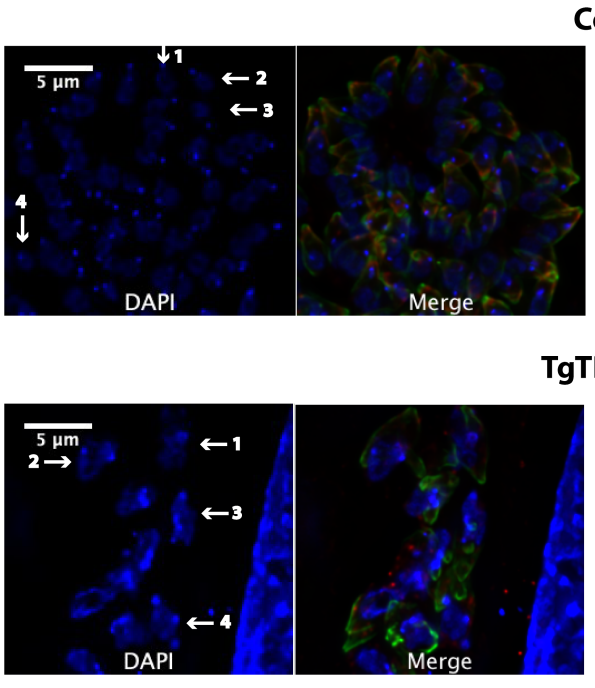

Nuclear Size

	Area	Mean	StdDev
1	1.433	319.022	153.294
2	1.426	333.696	148.149
3	1.056	346.091	85.313
4	1.274	355.417	158.540

Nuclear Size

	Area	Mean	StdDev
1	2.878	395.292	155.260
2	4.278	469.394	227.229
3	4.898	552.363	245.826
4	4.542	526.877	297.439

Figure 82. TgTBCB KO increases the nuclear size, 48 h after induction. Nuclear size assay, representative results obtained by an aleatory analysis of the nuclear size. **Control** - TgTBCB KO Clonal line not induced. **TgTBCB KO** - TgTBCB KO Clonal line induced and inoculated in HFF cells during 48 h. Cells were fixed with methanol and immunostained with antibodies against TgTBCB (red) and polyglutamylated tubulin (green). DNA was stained with DAPI (blue). Scale bars, 5 µm. Area - Area of selection in square pixels. Mean – Average of the mean grey value within the selection. Standard Deviation - Standard deviation of the grey values used to generate the mean grey value.

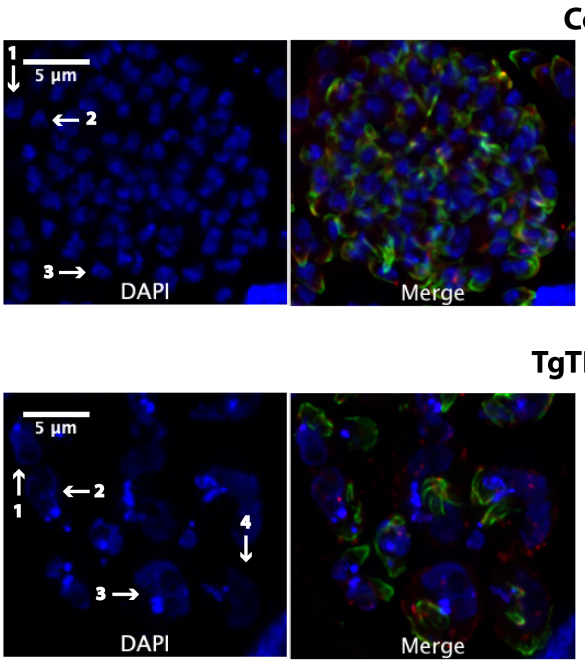

Nuclear Size

	Area	Mean	StdDev
1	2.462	1139.129	520.198
2	1.683	1028.986	529.200
3	1.822	1225.621	635.094

Nuclear Size

	Area	Mean	StdDev
1	6.021	631.008	429.776
2	7.156	668.433	832.731
3	12.477	716.037	569.816
4	6.489	420.102	273.010

Figure 83. TgTBCB KO increases the nuclear size, 72 h after induction. Nuclear size assay, representative results obtained by an aleatory analysis of the nuclear size. **Control** - TgTBCB KO Clonal line not induced. **TgTBCB KO** - TgTBCB KO Clonal line induced and inoculated in HFF cells during 72 h. Cells were fixed with methanol and immunostained with antibodies against TgTBCB (red) and polyglutamylated tubulin (green). DNA was stained with DAPI (blue). Scale bars, 5 µm. Area - Area of selection in square pixels. Mean – Average of the mean grey value within the selection. Standard Deviation - Standard deviation of the grey values used to generate the mean grey value.

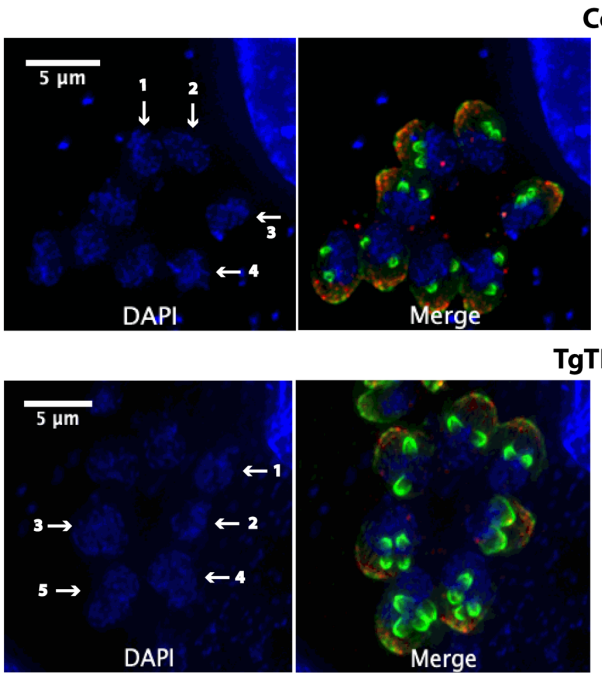

Nuclear Size

	Area	Mean	StdDev
1	5.592	254.699	8.762
2	5.922	254.431	12.034
3	5.459	255.000	0.000
4	5.334	255.000	0.000

Nuclear Size

	Area	Mean	StdDev
1	8.074	254.374	12.619
2	6.172	254.727	8.339
3	10.272	254.672	9.139
4	11.599	255.000	0.000
5	10.114	253.336	20.541

Figure 84. TgTBCB KO egressed tachyzoites increases the nuclear size, 24 h after re-inoculation. Nuclear size assay, representative results obtained by an aleatory analysis of the nuclear size. **Control** - TgTBCB KO Clonal line not induced. **TgTBCB KO** - TgTBCB KO Clonal line induced for 24 h, egressed and re-inoculated in HFF cells for 24 h. Cells were fixed with methanol and immunostained with antibodies against TgTBCB (red) and polyglutamylated tubulin (green). DNA was

stained with DAPI (blue). Scale bars, 5 µm. Area - Area of selection in square pixels. Mean – Average of the mean grey value within the selection. Standard Deviation - Standard deviation of the grey values used to generate the mean grey value.

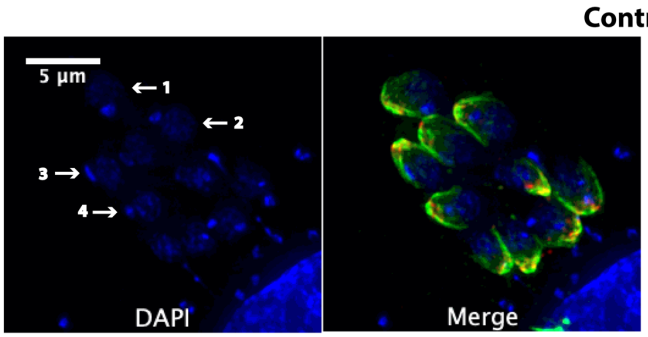

Nuclear Size

	Area	Mean	StdDev
1	4.397	251.171	31.034
2	4.766	252.881	23.165
3	4.113	240.674	58.766
4	3.690	250.894	32.123

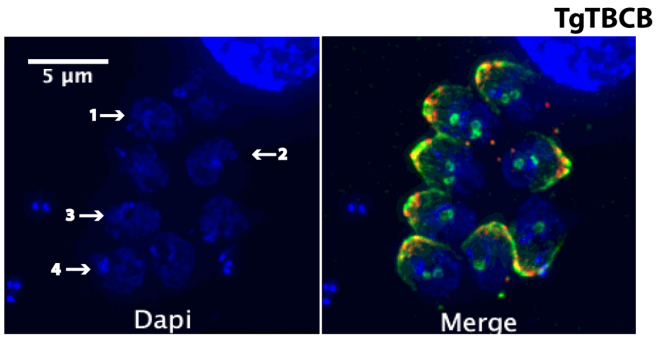

Nuclear Size

	Area	Mean	StdDev
1	7.711	255.000	0
2	7.083	255.000	0
3	7.394	253.406	20.105
4	8.318	252.774	23.731

Figure 85. TgTBCB KO egressed tachyzoites increases the nuclear size, 24 h after re-inoculation. Nuclear size assay, representative results obtained by an aleatory analysis of the nuclear size. **Control** - TgTBCB KO Clonal line not induced. **TgTBCB KO** - TgTBCB KO Clonal line induced for 24 h, egressed and re-inoculated in HFF cells for 24 h. Cells were fixed with methanol and immunostained with antibodies against TgTBCB (red) and polyglutamylated tubulin (green). DNA was stained with DAPI (blue). Scale bars, 5 µm. Area - Area of selection in square pixels. Mean – Average of the mean grey value within the selection. Standard Deviation - Standard deviation of the grey values used to generate the mean grey value.

Subsequent, the IF's were used to study and compared the cellular morphology of the parasites. As in the new assays the parasites were pre-induced for 24 h and subsequently re-inoculated for more 24 h, making a total of 48 h, that results were mainly compared with the 48 h time point of the first IF assays. The new IFs assays corroborate the same morphology findings observed previously. Beyond the huge nucleus, the parasites have obviously replication problems, in fact they cannot complete the endodyogeny, having more than two daughter cells per parasite under replication (Figure 86). They also lost their cell polarity control, the polyglutamylated tubulin staining is weaker and abnormal and the parasitophorous vacuole already exposed the vast disorganization (Figure 86 and 87). Therefore, the complete loss of TBCB signal, which was previously observed at 72 h, was not observed in this experiment.

These results indicated that this phenotype is most likely related to the TgTBCB KO and not the Cas 9 toxicity. In fact, the presence of a single and unusually enlarged nucleus was already associated with the disruption of the MT dynamics (Morrissette & Sibley, 2002b; Shaw, Compton, Roos, & Tilney, 2000; Striepen et al., 2000).

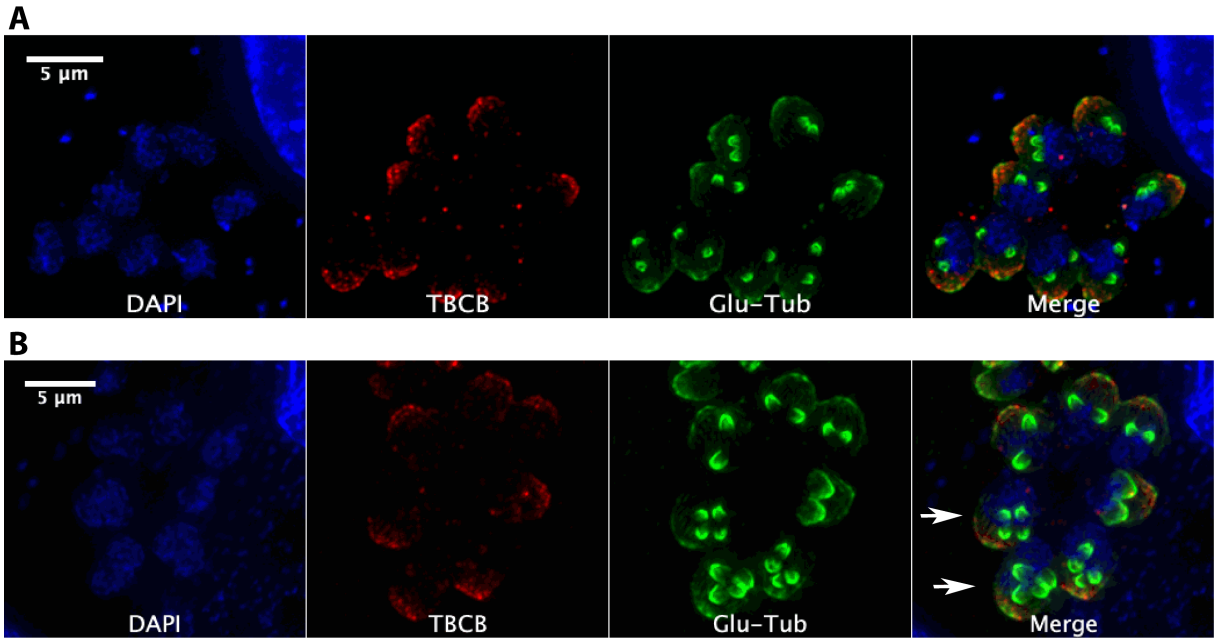

Figure 86. TgTBCB KO egressed tachyzoites, 24 h after re-incubation, also present replication alterations. **A** - TgTBCB KO Clonal line not induced. **B** - TgTBCB KO Clonal line induced for 24 h, egressed and re-inoculated in HFF cells for 24 h. Cells were fixed with methanol and immunostained with antibodies against TgTBCB (red) and polyglutamylated tubulin (green). DNA was stained with DAPI (blue). Similar to our previous results, some TgTBCB KO tachyzoites have four daughter cells instead of two (white arrows). Images were acquired with Olympus AppliedPrecision DeltaVision Core system. Scale bars, 5 µm.

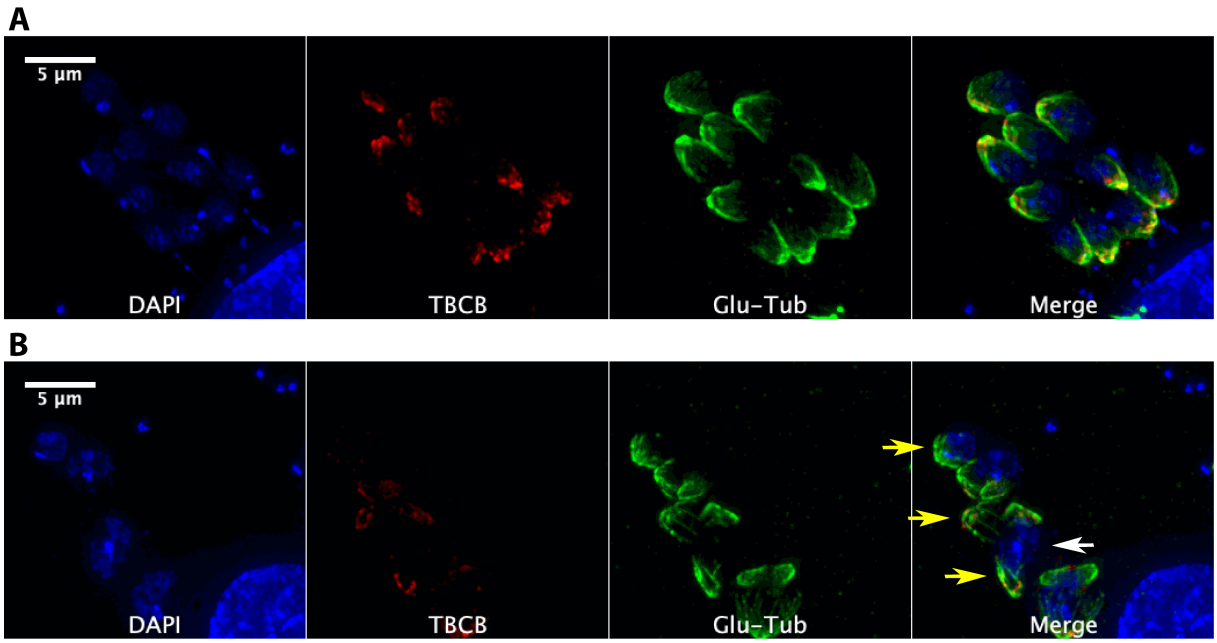

Figure 87. TgTBCB KO egressed tachyzoites, 24 h after re-incubation, also present a decrease in the tubulin glutamylated staining. A - TgTBCB KO Clonal line not induced. **B** - TgTBCB KO Clonal line induced for 24 h, egressed and re-inoculated in HFF cells for 24 h. Cells were fixed with methanol and immunostained with antibodies against TgTBCB (red) and polyglutamylated tubulin (green). DNA was stained with DAPI (blue). Similar to our previous results, some TgTBCB KO tachyzoites have with shorter and deregulated subpellicular MTs (yellow arrows), plus huge nuclei (white arrow). Images were acquired with Olympus AppliedPrecision DeltaVision Core system. Scale bars, 5 µm.

8.2.6. *T. gondii* TBCB conditional knockout analysis by Electron Microscopy

To understand in more detail the problems found in the parasite replication, concisely the findings in the nuclear size and in its division, we analyzed the induced clonal line by electronic microscopy. For that, the clonal line was induced for 48 h and then processed with the appropriated protocol.

Interestingly, the parasites without TgTBCB are able to replicate the DNA and divide the nucleus, but seem to be unable to finish replication, since we found several parasites with two nucleus and abnormal morphology, losing their shape and polarity. The parasitophorous vacuole showed some disorganization and parasites with two or one huge nucleus are extremely abundant. (Figure 88).

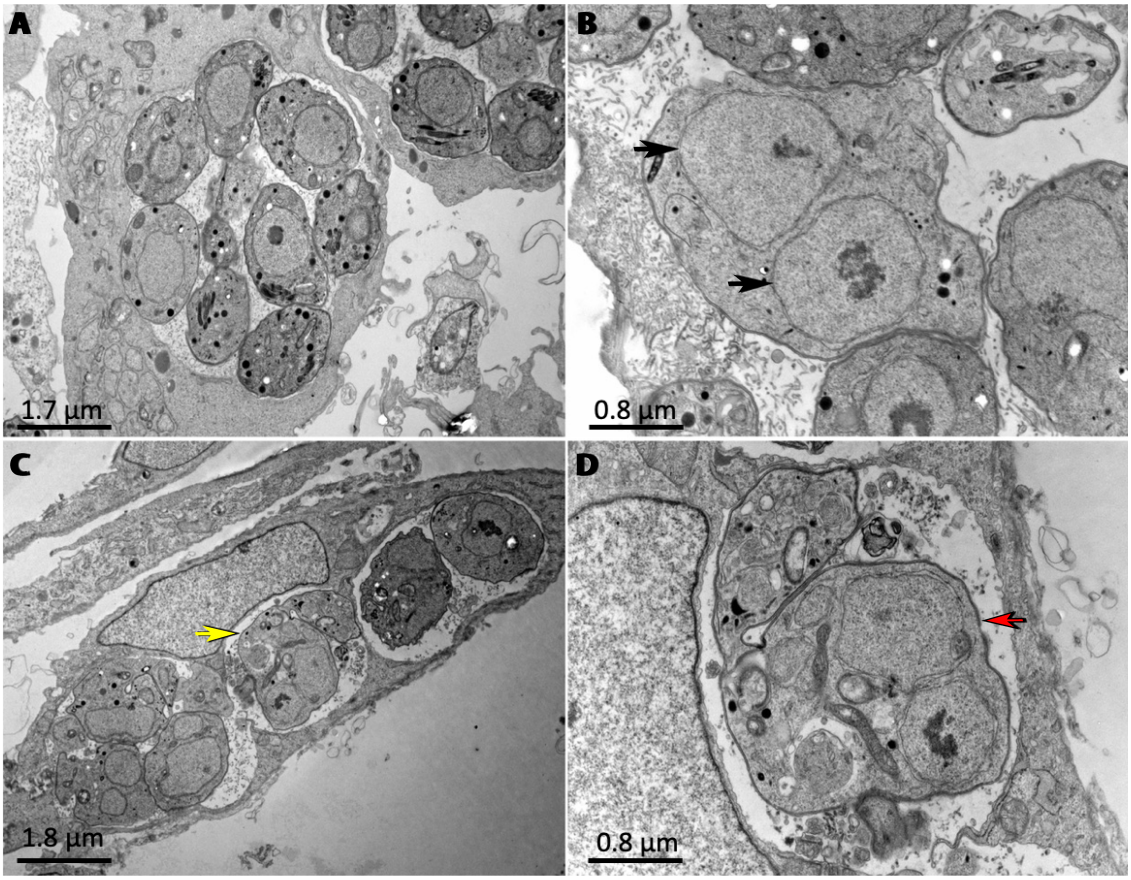

Figure 88. Electron microscopy of infected HFF cells. A - Control not induced. **B to D** - TgTBCB KO Clonal line induced with rapamycin during 48 h. In TgTBCB KO parasites it is possible to observe big and round parasites with multiple nuclei, or a single big nucleus, without daughter (red and black arrows). Tachyzoites grew as enormous intracellular inclusions, are incapable of cell division and had a non-polarized nature (yellow arrow). Scale bars, 0.8 to 1.8 µm.

Intentionally blank page

Chapter IV: Discussion

The search of molecular targets that can be involved in the *Toxoplasma gondii* MT remodelling during host cell invasion led us to investigate the role of TgTBCB during this process. TBCB is one of the TBCs that are involved in the ‘‘postchaperonin’’ tubulin folding pathway. TBCs are responsible for the acquisition of the quaternary conformation of the αβ-heterodimer after tubulin monomers have reached their tertiary structure and have also been implicated in the regulation of MT dynamics (Kortazar et al., 2007; Lewis et al., 1997; Lopez-Fanarraga et al., 2001).

The search for the TBCB gene in the *T. gondii* genome started with a simple quest in the ToxoDB to “Tubulin Cofactor”. Since we did not find any candidate for a “Tubulin Cofactor” gene, we had to use a second approach, the Blast engine from ToxoDB. We blasted the aminoacid sequence of Human TBCB (HsTBCB) isoform 1 against the *T. gondii* genome. The results obtained were encouraging, since the predicted gene for the TgTBCB was identified in all *T. gondii* strains in the database with the same high Score and E-value. Moreover, the results were similar when we used the HsTBCB isoform 2 instead the isoform 1. In fact, the TgTBCB predicted protein share an identity of 38 % with the HsTBCB isoform 1 and encodes a protein sequence of 273 amino acids, with an expected molecular mass (MM) of approximately 30 kDa and a pI of 5.14. This protein is slightly bigger than the HsTBCB isoform 1, with 244 amino acids, and share the characteristic domains, cytoskeleton-associated protein glycin-rich (CAP-Gly, at the C-terminal region) and ubiquitin-like domain (UbL, at the N-terminal region). The localization of these domains is conserved and was taken into consideration when planning the subsequent cloning strategies. We decided not to add any tag to C-terminal region of TgTBCB, to minimize possible interferences with the CAP-Gly domain which is known to be a MT association module (S. Li et al., 2002). In our cloning strategies all tags were added to the N-terminal region of TgTBCB, near the UbL domain, expecting to preserve the functionality of its main domain and consequently the interaction with the MTs (S. Li et al., 2002).

When we analysed the functional domains shared between the HsTBCB and TgTBCB, we found similarities and differences that contribute to explain some of our findings during the experimental work:

a) TgTBCB CAP-Gly domain (amino acids 181 to 257 - 76 residues). CAP-Gly domains are small protein modules with approximately 80 residues, conserved in organisms from yeast to human (Weisbrich et al., 2007). They are known to have several glycine residues, which are responsible for the name, that are highly conserved and contribute to the fold of the domain (Fleming, Morgan, Fyfe, Kelly,

& Hunter, 2013). These domains harbor an GK(N/H)DG sequence (highly conserved) that specifically recognize EE[Y/F] sequence motifs which are found at the C-terminus of α-tubulin and several MT tip-binding proteins (Fleming et al., 2013; S. Li et al., 2002; Weisbrich et al., 2007). The interaction between CAP-Gly and EE[Y/F] protein tails regulates a wide range of important MT-based processes in all eukaryotic organisms and thus is fundamental for controlling MT function (Weisbrich et al., 2007). In addition, CAP-Gly domains are also involved in coordinating complex cellular functions, such as distribution of membrane organelles and intracellular signaling (Steinmetz & Akhmanova, 2008). When we analyzed the report from the Protein Homology/analogY Recognition Engine (Annex I), it is clear that the TgTBCB predicted CAP-Gly domain has 76 amino acidic residues, is composed by six ß-sheets, one α-helix and has eight glycine residues. But the more interesting finding is the absence of the highly conserved GK(N/H)DG sequence. Instead, in *T. gondii*, we found the sequence GCTDG, preserving only the first G and the last DG amino acids. In fact, it is peculiar, since this sequence is highly conserved inside the phylum Apicomplexa. This sequence is immediately preceded by another highly conserved amino acid sequence in Apicomplexa, the GVALDEPL, which starts in the third ß-sheets of the CAP-Gly domain and ends immediately before the GCTDG sequence. There is one more conserved sequence among apicomplexan organisms, located in the last amino acids of the TBCB protein, the EVGDFPPIDP. This sequence starts in the last predicted ß-sheet of TBCB protein and ends immediately before the last disordered amino acid sequence of the TgTBCB protein which ends with the motif DEI/M, as occurs in TBCB from other species. Moreover, in the EVGDFPPIDP motif, the sequence DFPPIDP is recognized by the SH3 (Src Homology 3) domains, which are small protein modules of about 50-60 residues found in proteins involved in biological processes as diverse as signal transduction pathways, cytoskeleton organization, membrane traffic or organelle assembly (Dinkel et al., 2016), leaving open the question if they play any important role in Apicomplexa TBCBs. The last motif found in the TgTBCB is the DEI/M, is an extremely important motif (similar to the EE[Y/F] motif) required for the self-inhibition of the TBCB CAP-Gly domain and for the formation of the TBCE-TBCB heterodimer that promotes the dissociation of the tubulin dimer (Carranza et al., 2013). In fact, the importance of a preserved GKNDG motif for binding C-terminal EE[Y/F] protein tails is supported by the finding that the CAP350 CAP-Gly domain, in which the lysine

(K) and aspartate (D) residues are replaced by asparagines (N), does not interact with MTs (Weisbrich et al., 2007). However, the first CAP-Gly domain of the tumor suppressor for human familial cylindromatosis (CYLD) also contains substitutions in the GKNDG motif ((the lysine (K) and asparagine (N) residues are replaced by phenylalanine (F) and threonine (T), respectively)) even though it retains the capacity to interact with MTs. How this specific residue changes affect EE[Y/F] binding or whether this particular CAP-Gly domain interacts with MTs through another binding site remains untested (Steinmetz & Akhmanova, 2008).

b) TgTBCB UbL domain (amino acids 25 to 107). This domain is known to contain seven lysine (K) residues that are targets for covalent modification and also may provide a mean whereby protein folding and the population of complex assemblies can be regulated by protein degradation or recycling (Fleming et al., 2013). It is known that the TBCB UbL domain is processed by the ubiquitin-proteasome pathway and regulates its degradation (W. Wang et al., 2005). It was also suggested that the UbL domains could mediate the interaction of TBCB and TBCE (Kortazar et al., 2007; Lytle et al., 2004), but this interaction is apparently mediated by both CAP-Gly domains (Serna et al., 2015). The TgTBCB protein has a predicted UbL domain with 82 amino acid residues and is composed by five stranded ß-sheet, a single major α-helix (between ß-sheet 2 and 3), and a short α-helix (between ß-sheet 4 and 5), as can be seen in the report for the Protein Homology/analogY Recognition Engine (Annex I). The predicted domain in TgTBCB has several lysine (K) residues and is identical to the UbL domain described for the TBCB in *C. elegans* and for human TBCE (Lytle et al., 2004; Serna et al., 2015). When we analyzed the N-region of the TgTBCB where the UbL domain is located, it is evident that, contrary to what is observed for the CAP-Gly domain, there are not conserved sequence motifs among the Apicomplexa. In fact, in terms of amino acid sequence, the UbL domain is more variable among TBCBs (Fleming et al., 2013).

c) Coiled-Coil domain. The algorithms used in our work did not predict any Coiled-Coil domain for the TgTBCB. This coiled-coil structure is located in the center of TBCB proteins and is composed of a short helical domain (Grynberg et al., 2003). Still, if we look to the report of the Protein Homology/analogY Recognition Engine (Annex I) it is possible to identify a disordered region with two longer putative α-helix, which can be a predicted coiled-coil domain. Moreover, coiled-coil domains are often found proximal to CAP-Gly domains (Lytle et al., 2004). In fact, it is also admitted for the TBCBs that the disordered residues may serve as a flexible linker

between the N-terminal UbL domain and the C-terminal CAP-Gly domain (Lytle et al., 2004).

After the identification of TgTBCB gene at ToxoDB, we decided to study its expression profile during different phases of host cell invasion by real time PCR. We analysed the TgTBCB expression in freshly egressed parasites (control, 0 h) and in parasites within host cells after invasion (0.5 h, 1 h, 4 h and 8 h). Interestingly, in comparison with the control, the only significant difference observed is a decrease in *TgTbcb* RNA levels 4 h after the invasion (to ~ 42%). These data are consistent with the Transcriptomics data from ToxoDB where the tachyzoite transcriptome time series from ME49, VEG and GT1 *T. gondii* strains of Gregory, by RNAseq, shows exactly the same result, a decrease of *TgTbcb* RNA levels 4 h post-invasion. A tachyzoite transcriptome study during invasion (RH strain) from extracellular tachyzoites, intracellular tachyzoites (immediately after invasion) and intracellular tachyzoite 2 h post-invasion, showed that genes with high mRNA levels in extracellular tachyzoites are mainly genes from cytoskeleton and trafficking/transport. After invasion, the high mRNA levels in intracellular tachyzoites are mainly from DNA replication and metabolic genes (Gaji, Behnke, Lehmann, White, & Carruthers, 2011). The observed decrease in TgTBCB mRNA levels may be related to this general regulation, but these variations occurred 2 h post-invasion and the decrease of *TgTbcb* RNA levels only occurs later (4 h) and at 8 h is already normalized. Interestingly, although not related to the parasite cytoskeleton, the accumulation of host MTs around the vacuole is time dependent and reaches its maximum 4 h after invasion (Walker et al., 2008).

Upon confirmation that the TgTBCB gene was expressed, as there are no commercial specific antibodies against TgTBCB and the antibodies against human and mouse TBCB that we tested did not recognize the TgTBCB, we decided to produce a specific anti-TgTBCB serum; a key tool for our study. For this, we produced the recombinant TgTBCB in bacteria and immunized rabbits at Dr Zabala's lab (Departamento de Biología Molecular, Facultad de Medicina, Universidad de Cantabria, Santander, Spain). In SDS-PAGE, the TgTBCB produced in bacteria had a MM of 37 kDa and consequently the produced antibody detected a soluble protein with the same MM in *T. gondii* protein extracts. This apparent discrepancy, between the molecular mass predicted theoretically (~30 kDa) and observed in SDS-PAGE (~37 kDa), was clarified by Tian *et al*. in 1997 (Tian et al., 1997). The mammalian TBCB eluted from gel filtration with an apparent mass of ~130 kDa corresponds to a single polypeptide of ~38 kDa upon analysis by SDS-PAGE and 27.561 kDa by mass spectrometry (Tian et al., 1997). Later, it was described that mammalian TBCB eluted in gel filtration with a MM 30–40% larger than deduced from its amino acid sequence, coinciding with the MM from its mobility in SDS–

PAGE, ~38 kDa. TBCB presents an apparent MM variability when analyzed by gel filtration, SDS-PAGE and also by dynamic light scattering (DLS, ~69 kDa), but after glutaraldehyde (protein crosslinker) treatment it changes to the amino acid sequence expected mobility in SDS-PAGE (~27 kDa) suggesting a stabilization by intramolecular crosslinking (Carranza et al., 2013).

Taking advantage of our specific antibody we proceed to the subcellular characterization of TgTBCB. Surprisingly, both in intracellular and extracellular tachyzoites, TgTBCB presents a polarized distribution being located mainly at the anterior region of the parasite, close to the apical complex. Until now, the only relationship between TBCB and polarity comes from studies in drosophila where dTBCB is required for the polarized localization of the axis-determining mRNAs within the oocyte and for the apico-basal polarity of the surrounding follicle cells (Baffet et al., 2012).

Performing super resolution microscopy, we confirmed the apical staining, but we also detected some stain dots just below the apical region and at the posterior pole. Co-localization assays with ISP1, known as an apical cap marker (apical region that is delimited by TgCentrin2 peripheral annuli, ~1.5 μm from apical end) (Beck et al., 2010) showed that TgTBCB is at apical cap and progressively decreases towards the distal end. Under super resolution microscopy, we observed that at the apical end the TgTBCB staining is in a ring-like shape and, below that, the staining resembles the beginning of the subpellicular MTs that are attached to the apical polar ring. Assays between TgTBCB and glutamylated tubulin, which stain progressively decreases in subpellicular MTs from the conoid towards the distal end (Plessmann et al., 2004), show a partial co-localization suggesting that TgTBCB can be coaligned with MTs and, since MTs are attached to the apical polar ring, it is also possible to observe a ring-like shape staining (see figure 89). Note that in *T. gondii*, the highly conserved GK(N/H)DG sequence of the CAP-Gly domain (Fleming et al., 2013; S. Li et al., 2002; Weisbrich et al., 2007) is dramatically different from the TBCB proteins in mammals and yeast, raising the question of whether it can still interact with tubulin and MTs. In the future, to clarify its precise localization, we will perform TgTBCB staining in comparison with the apical polar ring staining. Since to date only four proteins have been identified as part of the apical polar ring structure (RNG1, RNG2 (Katris et al., 2014; Tran et al., 2010), kinesinA and APR1 (Leung et al., 2017)) and no antibodies were produced for these proteins, this study will be done using transgenic strains with these proteins endogenously tagged.

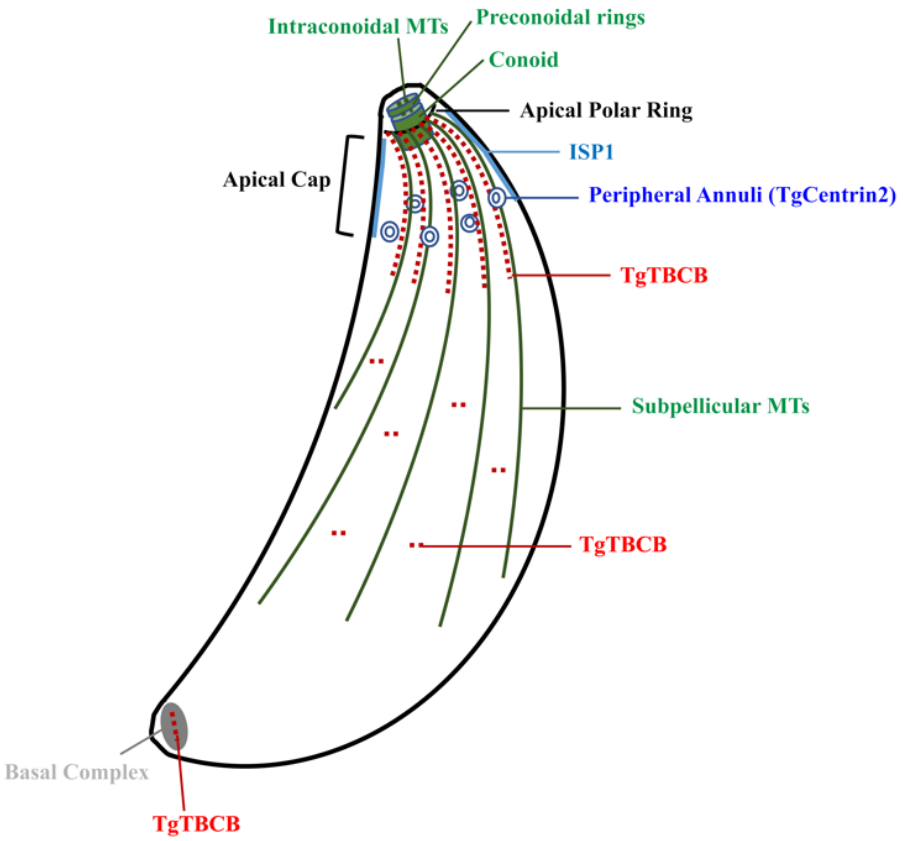

Figure 89. Schematic representation for the TBCB subcellular localization in *T. gondii*. TBCB - red dots. Subpellicular MTs - green. Basal complex - grey. Peripheral Annuli (Tg Centrin2) - dark blue. ISP 1 - light blue.

The staining of TgTBCB in replicating parasites, showed that TgTBCB seems to not be present at mitotic spindle and sometimes it is detected in the forming daughter cells, but not too early. Curiously, secretory organelles (micronemes and rhoptries), that share the same TgTBCB localization, are formed late in the parasite cell cycle and are ready for use in G1 phase parasites, the phase with the highest efficiency in egress and invasion (Nishi et al., 2008).

In human cells, TBCB is observed throughout the cell cytoplasm, at the centrosome and at the basal body of the primary cilium (Carranza et al., 2013; Kortazar et al., 2007). During mitosis, TBCB is found in the centrosomes and is located in the MTs of the spindle (near the centrosomes). At the end of mitosis, TBCB becomes more visible in the thin filaments bridging the midzone, disappearing progressively from the centrosome and concentrate in the MTs of midbody. As mitosis progresses, TBCB staining gradually increases in the MTs of the spindle midzone where MT polymerization is active (Carranza et al., 2013).

We had an anti-centrin antibody that works in *T. gondii* (kind gift from Ian Cheeseman, Whitehead Institute for Biomedical Research, MIT, US), but we could not use it for co-localization assays because it was also produced in rabbits as our antibody anti-TgTBCB. Although our TgTBCB labeling never marked any structure that resembled the centrosome, we

cannot exclude the possibility of being localized at the apical polar ring, which in *T. gondii* serves as one of the two MTOC (Morrissette & Sibley, 2002a).

The hypothesis that the polar ring is a MTOC, serving as a template for the biogenesis of the cortical MTs, comes from the 22 cortical MTs, regularly spaced, anchored to this structure (Nichols & Chiappino, 1987; Russell & Burns, 1984). However, the nucleation of cortical MTs is unknown, γ-tubulin (MT nucleator) is only detected at centrosome and not at the apical polar ring (Suvorova, Francia, Striepen, & White, 2015). The destabilization of the apical polar ring leads to problems of parasite motility and invasion, with retardation of the lytic cycle, but the parasites are still able to produce the subpellicular MTs (Leung et al., 2017).

As already mentioned, the secretory organelles are also concentrated at the apical end of the parasite (Nichols, CHIAPPINO, ultrastructure, 1983, 1983) and the discharge of these organelles is important for parasite motility and invasion. At ToxoDB, it is mentioned that TgTBCB was detected in a tachyzoite secretome (X. W. Zhou et al., 2005). In this context, we performed secreting assays where TgTBCB appears to be secreted but at a low level. We also performed co-localisation assays of TgTBCB with the secretory proteins, particularly rhoptry proteins 2 - 4 and microneme proteins 2 and 3. No co-localization was found with the rhoptry proteins 2 - 4 but for the microneme proteins 2 and 3, we observed some dots of co-localization, predominantly in intracellular tachyzoites. In *Plasmodium falciparum* there is evidence for micronemal trafficking along subpellicular MTs, suggesting that micronemes reach their final apical destination by propulsion along microtubular tracks (Schrevel et al., 2008). Curiously, not so clear as observed in our assays, MIC2-containing vesicles appear to co-align into tracks with cortical MTs at the parasite apical half (Leung et al., 2017). Defects in the apical polar ring alters the MTs organization, affecting the micronemes distribution, and leading to a reduction in MIC2 secretion (Leung et al., 2017). Being so, cortical MTs can be used to transport the microneme vesicles and the MTs disorganization could affect the transport efficiency in *T. gondii*. Considering this, TgTBCB could play a role in microneme trafficking along subpellicular MTs and its low secretion level can be explained by a contamination of the secreted fraction due its close interaction with micronemes. Our results concerning the invasion assay in the presence of TgTBCB-specific polyclonal serum, where no significant differences were observed in the invasion rate, support the idea that secreted TgTBCB has no role in the invasion process.

The first step to characterize the TBCB functions in *T. gondii* was the protein overexpression and subsequent study of its effect on the parasite. Taking in account the localization of the CAP-Gly domain in the protein amino acid sequence, all tags were cloned at the N-terminal region, near the UbL domain, to minimise possible interactions with the main

functional domain. To over-express the TgTBCB, we cloned it in three different overexpression constructs:

1) The c-myc tag is a small tag with 1.5 kDa, that was chosen to minimize the possible alterations in the TgTBCB protein function;
2) The eGFP tag (~30 kDa) is much bigger than the c-myc tag, but it is a fluorescent tag;
3) The ddFKBP, in the case of toxicity, allows us to modulate the overexpression levels in a Shield-1 dependent manner.

Subsequently, the stable transgenic parasite lines obtained for each construction were analysed by WB and by IF, in order to confirm the correct expression of the respective TgTBCB fusion protein. Using specific antibodies against the tag proteins or, alternatively, against the TgTBCB we were able to confirm by WB the expression of each recombinant protein and its expected MM. It was also possible to see that the endogenous TgTBCB is recognized with the anti-TgTBCB specific polyclonal serum in the clones with the eGFP and the ddFKBP domain and that some constructs presented truncated versions of the fusion proteins (DD-Myc-eGFP – 46.36 kDa and Myc-eGFP – 34.31 kDa) detected by the anti-Myc and anti-GFP antibodies.

The IF results support the WB outcomes, demonstrating that the three strains were overexpressing the recombinant proteins according to what was expected. The fusion proteins were localized throughout the cytoplasm of the parasite, but more concentrated at the apical end. Additionally, by IF we were able to demonstrate the responsiveness of the clonal line with the ddFKBP domain to the Shield-1 concentration.

The TgTBCB overexpression parasites showed a defect in the plating efficiency and we proceeded to the characterization of the lytic cycle steps. We observed a reduction in the invasion rate and no differences were found in the replication and egress assays, this is curious since invasion and egress have several mechanisms in common (Blader et al., 2015).

TBCB overexpression on mammalian cells leads to MT depolymerization, although less efficiently than the TBCD or TBCE overexpression. However, TBCB forms a binary complex with TBCE that greatly enhances the efficiency of this cofactor to dissociate tubulin *in vivo* and *in vitro* (Carranza et al., 2013). In drosophila cells and in fission yeast, TBCB overexpression also led to MT depolymerization (Baffet et al., 2012; Radcliffe et al., 1999). Mutants of human TBCB lacking the last three amino acids of the protein are derepressed and induce massive MTs depolymerization by sequestering the EB1 (MT plus-end binding protein) from MTs tips (Carranza et al., 2013). In *T. gondii* the TBCE protein is not characterized but, by sequence analysis, like we did for TgTBCB, we found the putative gene at ToxoDB (TgME49_285220). According to the available data at ToxoDB, this gene is expressed and it is included in

proteomic data from a "tachyzoite phosphoproteome from purified parasite or infected host cell (RH)". In this way, everything indicates that TgTBCE, the TgTBCB main partner, exists in *T. gondii*. In addition, TgEB1 has been expressed and characterized. In *T. gondii* this protein presents a nearly exclusive association with the MTs from mitotic spindle, being present at subpellicular MTs only at the growing end of daughter buds (C.-T. Chen et al., 2015b). Surprisingly, this location is not at all compatible with the location of TgTBCB suggesting that they may not be partners in *T. gondii*.

Unlike the dynamic MT cytoskeleton in mammalian cells, *T. gondii* cortical MTs are exceptionally stable. They do not display dynamic instability and are not depolymerized when the free tubulin concentration is drastically reduced by detergent extraction (Morrissette et al., 1997; Nichols & Chiappino, 1987), which leads to rapid disassembly of vertebrate MTs. The tubulin C-terminal ends, the most divergent amino acid region among tubulins, are exposed to the outer surface of the MTs (Nogales, Wolf, & Downing, 1998b), providing binding sites for several MAPs and molecular motors (Lakämper & Meyhöfer, 2005; Z. Wang & Sheetz, 2000). Also, tubulin C-terminal ends are subjected to various PTMs, most of them occurring on tubulin subunits after their polymerization into MTs: α-tubulin acetylation, detyrosinated α-tubulin, Δ5α-tubulin, Δ2α-tubulin, α- and β-tubulin polyglutamylation and α- and β-tubulin methylation (Plessmann et al., 2004; Xiao et al., 2010). These tubulin modifications alter MTs stability/dynamics by conferring them different biochemical/biophysical proprieties according to spatial and temporal cell requirements. Being so, tubulin PTMs are a powerful mechanism to generate functional tubulin diversity, forming a biochemical 'tubulin code' that can be 'read' by MTs interacting factors (Verhey & Gaertig, 2007). Cortical MTs are predominantly composed of α1- and β1-tubulin subunits, largely conserved relative to human tubulin homologues (>85 % identity and 90 % similarity), which can be modulated by PTM and consequently by parasite-specific MT-binding or -modifying proteins. Despite the fact that no relationship has yet been established with tubulin PTM, studies revealed that cortical MTs are differentially decorated with proteins along their length in a complex but defined pattern (Hu, Roos, & Murray, 2002b; Jun Liu et al., 2016; Morrissette et al., 1997), the coating proteins. TgTBCB can be partner of these MT interacting proteins and its overexpression may cause an imbalance in these interactions affecting the MT organization and consequently the host cell invasion. As we already mentioned, MT disorganization affects MIC2 vesicles distribution (the vesicles are spread throughout the cell instead of being concentrated at the apical region) compromising motility and invasion (Leung et al., 2017).

Our first approach to stablish a conditional KO of the TgTBCB was done with the DiCre system (Andenmatten et al., 2012). The main advantage of this system is the possibility to induce the KO in a specific time set, which can be very useful in case of the gene of interest (GOI) is essential for the parasite. The disadvantage of this system is the cloning process, it is often not easy to amplify the big homology arms and the cloning strategy is complex. In addition, the homologous recombination itself is not easy to achieve in *T. gondii*. For this reason, we used the *ΔKu80 ΔHXGPRT* strain expressing the DiCre to increase the hypothesis of a successful homologous recombination (Andenmatten et al., 2012). Such as many eukaryotes, *T. gondii* preferentially uses the nonhomologous-end-joining (NHEJ) pathway to repair a double-strand break (DSB) in DNA, the exogenous targeting DNA can be integrated anywhere into the genome independent of DNA sequence homology. The *KU80* is found to be an essential component of a functional NHEJ pathway, which does not rely on DNA sequence homology, instead, NHEJ involves direct ligation of the broken DNA ends. Being so, the *ΔKu80* strain exhibit a markedly higher gene replacement efficiency compared to wild-type strains, allowing the efficient targeting of gene replacements, gene KO and gene "knock-ins" in *T. gondii* (Fox, Ristuccia, Gigley, & Bzik, 2009). In our case, even using this strain, the gene replacement efficiency was very low. Only one clone from more than one hundred isolated were in fact positive for homologous recombination. In the beginning, we thought it was due to the transfection conditions but, after several adjustment and variations in the transfection settings, the replacement efficiency was still null. Another critical factor that could influence this problem is the length of the genomic targeting flanks, that should be at least 620 bp and is also important that genomic targeting flanks are generated from the same strain of *T. gondii* (Rommereim et al., 2013). In our particular case, our genomic targeting flanks were designed with 2000 bp each, but they were not generated from the same strain used for the transfection. This could explain the low success rate observed. In fact, we used as template the RHΔHX strain and not the RH:SlipCas9⊿ku80 and this could explain the problem. Additionally, we also admit that TgTBCB has an extremely low gene targeting frequency at the locus (Rommereim et al., 2013), which could turn difficult the homologous recombination events and consequently our gene replacement efficiency was very low. Another possible explanation is related with the Restriction Enzyme Mediated Insertion (REMI) which increases the insertion of DNA in *T. gondii* genome (Black et al., 1995). In almost all our transfection attempts, we handed the single cutting restriction enzyme used to linearizing the Plasmid DNA to the transfection mix and this could have enhanced the random integration instead of the homologous recombination. By doing this the genomic DNA is cut undirected and the DNA repair mechanisms are activated (Black & Boothroyd, 2000).

Finally, when we isolated clonal lines positive for homologous recombination by PCR test, only one of them was in fact phenotypically positive, but inopportunely that clone was not responding to KO induction. Intriguingly, we found that the strain had lost one of two inactive Cre fragments, which is difficult to explain. We tested our first RH::DiCreΔku80ΔHX strain and it was expressing correctly both inactive Cre fragments. To overcome this problem, the inactive Cre fragment that was lost was cloned in an overexpression vector and transiently transfected in our homologous recombination positive clone. Although we were able to induce the KO and confirm it by immunofluorescence, it was not possible to isolate one KO clone by limiting dilutions. In fact, our induced KO parasites were lost in one week giving us the preliminary indication that TgTBCB is an essential gene for this parasite. It was also impossible to transfect the lost inactive Cre fragment in a stable way in our clone, since the HXGPRT selection was already used and we did not have any plasmid with a different selection marker. Under these circumstances, in order to obtain the TgTBCB KO, we decided to explore a new methodology.

Finally, a possible justification for the loss of the inactive Cre fragment is related to the strain itself, as it is deleted for the *KU80* gene, an essential protein that tightly binds the DNA ends at the DSB, an early and essential step of NHEJ. Since *T. gondii* preferentially uses the NHEJ pathway to repair a DSB, this strain has the predisposition to accumulate mutations in its genome. Without its main mechanism to repair the DSB, DNA lesions may lead to the loss of chromosome segments, threatening cell survival (Fox et al., 2009; Smolarz, Wilczyński, & Nowakowska, 2014). The loss of these segments could have explained the loss of the inactive Cre fragment in our strain.

Concerning our background problems with the Di Cre system, the CRISPR/Cas9 worked as our backup option to accomplish the TBCB KO. At that time, there was only one paper about the CRISPR/Cas9 in *T. gondii*, using the standard Cas9 enzyme. The system under development in Meissner's lab, like the DiCre, uses a SplitCas9 enzyme that is expressed in two inactive fragments, each of them fused to one of the rapamycin-binding proteins FRB and FKBP. The addition of rapamycin brings FRB and FKBP together, reconstituting the functional enzyme. Using this mechanism, we have the ability to control the exact moment when the system is triggered, which in our case was a priority, since we suspected that TgTBCB KO was lethal to the parasite.

From the six conditions and the several clonal lines obtained, only one was in fact positive, so our studies were conducted with this positive clone. Once the gRNAs targeted the first exon, after induction, a protein could still be produced but with a different amino acid sequence and/or a premature stop codon.

After Cas9 disrupts the target gene, the protein concentration starts to decrease, in a period of time that depends on the stability of both mRNA and protein. Therefore, before the KO characterization, it was crucial to know when the concentration of endogenous TBCB is decreased. As soon as the induction tests started, the TBCB KO in *T. gondii* proved to be lethal to the parasite, confirming our previous hypothesis and explaining, at least in part, our unsuccessfulness with the DiCre system. In fact, after the KO induction the parasites survived for about one week in culture, so it was almost impossible to isolate one KO clone with the DiCre system. This result is in agreement with the ToxoDB data from "Genome-wide loss of function screen (CRISPR) that measures each gene's contribution to *T. gondii* fitness during infection of human fibroblasts" (Gajria et al., 2008).

The clonal line was induced with rapamycin for 72 h and analysed by WB, with antibodies against the acetylated tubulin, glutamylated tubulin, α-tubulin and the specific polyclonal serum against TgTBCB. An anti-actin antibody was used in these studies as a control.

At 72 h after induction, there was no detectable TBCB protein by WB. Therefore, the complete depletion of the TgTBCB protein occurs between 48 (data not shown) to 72 h. It is also important to say that the TgTBCB was never found in insoluble protein extracts, confirming its cytoplasmic localization, and that there was no alteration in the levels of acetylated-tubulin and α-tubulin in the soluble protein extracts. On the other hand, in the insoluble extracts an interesting reduction in the acetylated, glutamylated and α-tubulin protein levels was detected. In fact, we were not able to detect the α-tubulin.

Comparing our results with others, we note that in *Schizosaccharomyces pombe*, the Alp11^{B} (TBCB homologue) is essential for cell viability, and its KO results in a specific decrease of α-tubulin levels in whole cell extracts, that correlates with an affected MT network and defects in cell division (Radcliffe et al., 1999; Radcliffe & Toda, 2000). In Drosophila, dTBCB proved to be essential for MT network integrity and for the maintenance of tubulin levels (α-and β-tubulin) in various cell types and at various stages of development. These results could be explained by a reduced tubulin dimerization in dTBCB mutant cells (Baffet et al., 2012). However, in several mammalian cell types, the TBCB knockdown did not affect the cell viability and the tubulin levels nor does it destabilize the MT network (Lopez-Fanarraga et al., 2007; Vadlamudi et al., 2005). Nevertheless, it severely reduces the formation of new MTs (Vadlamudi et al., 2005) and results in longer axons and abnormal growth cones, suggesting that this cofactor is involved in the regulation of MT dynamics in these structures (Lopez-Fanarraga et al., 2007). The different phenotypes mentioned may be due to species specificities or to the efficiency of the technical approaches, with the mutational approach (KO) probably being more efficient than siRNA (knockdown). In the latter method the amount of the protein

is decreased and if the TBCB protein is as stable as in toxoplasma, the transient knockdown will only decrease, and not abolish, its level. Another interesting fact was the reduction in the amount of the α-tubulin, acetylated tubulin and glutamylated tubulin in the insoluble fractions.

Since the acetylated tubulin is a marker of stable MTs (L. Li & Yang, 2015), the reduction of its levels can be associated with the MT depolymerization. However, MT depolymerization should increase the pool of the soluble tubulin. The non-increase of the soluble tubulin levels may be due to the degradation / non-recycling of the tubulin heterodimer. Although we could not rule out a technical problem where there was depolymerization of all MTs (including from controls) and it was not possible to detect the variation of soluble tubulin, this hypothesis does not seem valid given the super stable nature of these MTs. The absence of TBCB may be affecting the recycling of the tubulin heterodimer; strengthening the hypothesis of tubulin degradation.

Since α-tubulin monomers could be unstable in the absence of TBCB, these results suggest a role for TgTBCB not only in the new α/β-tubulin heterodimer formation (by tubulin folding pathway) but mainly in the control of α/β-tubulin heterodimer pool through the recycling of native tubulin heterodimers. This may contribute to explain why this protein is essential to the parasite viability.

Taking into consideration the previous results, it was essential to understand the phenotype for the TBCB KO in toxoplasma, particularly the effects during the lytic cycle of the parasite, since previously we saw an invasion inhibition as consequence of TBCB overexpression. Concerning the time of the TBCB protein turnover and the viability of the KO clonal lines after induction, we decided to perform all the following assays with egressed tachyzoites 48 h after rapamycin induction. This induction ensures that all parasites used in these assays had very low levels of TBCB, or did not have it at all, and eliminates parasites that have suffered from the toxic effect of Cas9. The complete analysis of the different steps of the lytic cycle was not possible due the limitation of the TgTBCB KO life time. So, we only performed invasion and replication assays.

The invasion assays showed a remarkable reduction of the clonal line ability to invade the host cells in the absence of TgTBCB. This reduction was around 61 %, when compared to the control, and corroborates the overexpression findings. Therefore, we can say that the drastic variations in the levels of TgTBCB affects the parasite invasion rate. Taking into consideration this expressive reduction in the invasion rate, the decreased of α-tubulin, glutamylated tubulin and acetylated tubulin levels in the KO clonal line, which is probably correlated with an affected MT network and the absence of viability in the TgTBCB KO parasites, the MT cytoskeleton appears to play a very important role during the parasite invasion. So, if the parasite MT

cytoskeleton integrity is compromised, as it seems to be in the TgTBCB KO, the invasion process is drastically compromised.

Concerning the replication assay, we also found a massive decrease in the replication capability in the absence of TgTBCB. The parasites showed an enormous increase in the number of vacuoles with two parasites and a decrease in the number of vacuoles with eight or more than eight parasites, in comparison to the control. These results clearly show a problem during the parasite replication, as a consequence of the TgTBCB absence, attesting the importance of the TgTBCB for the parasite replication and suggesting a relationship with the MT cytoskeleton integrity.

The above findings gave us an overview of the TgTBCB role in the parasite, and why it is fundamental for its viability. However, further analyses were necessary to understand better what was happening in the parasite lytic cycle.

In agreement with the WB analysis, we observed by IF a decrease in the labeling of TgTBCB, glutamylated tubulin and acetylated tubulin throughout the KO induction time. The staining of glutamylated and acetylated tubulin showed that subpellicular MTs are greatly shortened, absent or disorganised. Although at 24 h of induction the decrease in protein levels is not obvious, it is already possible to observe cells that appear to have lost polarity and that, instead of having two, have four daughter cells. These cells also present four centrosomes instead of two. Over time, the parasites are unable to complete the endodyogeny, having multiple daughters, huge nucleus and several centrosomes per cell, indicating some problem in the replication and nuclear segregation. In fact, the parasitophorous vacuoles lose their entire organization.

The EM was used to further understand and explore the IFs findings in the parasite replication. In this specific assay, Cas9 was induced for 48 h and then the parasites were processed for EM. Interestingly, as we already saw in the IF assays, the KO parasites were able to replicate the DNA but in some cases, they were unable to divide the nucleus, showing a huge nucleus inside the parasite. In other cases they were able to divide the nucleus but seem unable to finish replication, since several parasites with apparently two nuclei were found. We also observed the total disorganization of the parasitophorous vacuoles, containing abnormal parasite masses that lost the polarity and the normal shape of the parasite, presenting a spherical shape, as reported in longer treatment with oryzalin (Striepen et al., 2000), a phenotype directly related with the loss of subpellicular MTs (Morrissette & Roos, 1998; Stokkermans et al., 1996).

The observations in the IF and EM assays show a clear effect of the TgTBCB KO in the MT network. The reduction in the polyglutamylated and acetylated tubulin levels observed in the IFs are in agreement with the decrease levels observed in the WB, and clearly corroborate that the integrity of the parasite MT cytoskeleton is affected in the TgTBCB KO. Moreover, the reduction of the polyglutamylated tubulin, which is specific of the subpellicular MTs, points to a mal function of the MT cytoskeleton of the parasite and may contribute to explain the phenotypical analysis, since the parasites lacking intact subpellicular MTs are incapable of invading host cells and parasites without spindle MTs are unable to complete the endodyogeny (Morrissette & Sibley, 2002b).

The specific problems found during the replication of the parasite, namely multiple centrosomes per cell, enlarged nucleus, loss of cell polarity and replication control, culminating in the entire disorganization of the parasitophorous vacuoles, are related with the loss of the MT cytoskeleton integrity. In fact, the disruption of the spindle and subpellicular MTs during the parasite division allow the parasites to grow in size and replicate their genome but arrests the nuclear division (Shaw et al., 2000; Morrissette & Sibley, 2002; Striepen et al., 2000). Additionally, parasites treated with oryzalin, dinitroanilines (MT depolymerizing drugs) and taxol (MT stabilization drugs) resulted in the development of large abnormal parasite masses that contained multiple centrin labelled structures, indicating that centrosome replication proceeded despite the failure of the parasite to successfully complete cell division (Shaw et al., 2000; Striepen et al., 2000). Nevertheless, some parasites are still able to divide successfully over the initial 24 h of that treatment but in the great majority the daughter cell budding was markedly reduced, the parasite nucleus increased substantially in size and became highly lobed (Shaw et al., 2000). That description substantiates our findings in IF and EM, as we saw exactly the same phenotypical problems in the KO parasites.

Furthermore, the loss of polarity in a TBCB KO background also occurs in *T. gondii*, as previously reported in Drosophila, a multicellular organism (Baffet et al., 2012). Since in *T. gondii* the cell polarity and the shape are controlled by the subpellicular MTs (Morrissette & Roos, 1998; Stokkermans et al., 1996), which in TgTBCB KO parasites are obviously compromised, the problems observed in the cell polarity and shape are most probably related with the KO.

Consequently, as in Drosophila (Baffet et al., 2012), our hypothesis is that the TgTBCB is essential to maintain a functional MT network that can sustain the invasion, replication and cell polarity.

In summary, since the loss of TgTBCB after the KO induction is gradual, the parasite MT cytoskeleton network is gradually affected, presumably due to the impossibility to form and mainly to recycle the α/β-tubulin heterodimer. Consequently, and since the intracellular parasites committed to division approximately 6-8 h post-invasion (Shaw et al., 2000), some parasites were still able to initiate daughter cell budding, in particular, parasites that still could form intranuclear MT spindles and were able to manufacture and assemble, with varying degrees of success, new daughter conoids with the accompanying IMC and associated MTs. In some cases, there were still able to undergo the correct nuclear division and fission. However, that parasite nucleus never became anchored into the developing daughters, resulting in parasites that cannot finish the daughter cell budding, as daughter cell budding requires and is driven by MT polymerization (Shaw et al., 2000). In the most severely affected parasites, the subpellicular and presumptively the spindle MTs are completely and irreversibly disturbed, resulting in the loss of cell polarity and the shape, forming enormous intracellular inclusions, that are incapable of cell division, as the nuclear division and budding ceased, but have a nucleus dramatically increased in size. The conjugation of all these effects leads to parasite death in approximately one week after TgTBCB KO induction.

Chapter V: Concluding Remarks

Toxoplasma gondii is one of the world's most prevalent and successful parasites. Its invasion process is a key step for the parasite success, otherwise the parasite would not be able to infect such a wide range of hosts. Being so, the accurate undertaking of the mechanisms and proteins involved in parasite invasion is crucial in order to develop new effective vaccination strategies and new therapeutics towards the *T. gondii* and the Apicomplexa parasites.

We started by searching, studying and comparing the TBCB protein sequence in toxoplasma and in other Apicomplexa parasites. Doing that we were able to conclude that the toxoplasma TBCB protein has a low identity with TBCB Human isoform 1 and is slightly bigger. Nevertheless, both proteins conserve the main functional domains, namely the CAP-Gly (C-terminal region) and the UbL domain (N-terminal region), in identical positions. However, we were unable to identify the coil-coil domain in the parasite protein.

The TgTBCB CAP-Gly domain does not harbor the conserved GK(N/H)DG sequence that specifically recognize the EE[Y/F] motifs, founded at the C-terminus of α-tubulin and several MTs tip-binding proteins. Instead, in *T. gondii* we identified the sequence GCTDG, which only preserved the first G and the last DG amino acids from that conserved sequence. On the other hand, we recognized the DEI/M motif, which is extremely important for the TBCBs since it is required for TBCE–TBCB heterodimer formation and it also auto inhibits its own CAP-Gly domain, apparently controlling the mechanism of MT depolymerization. Interestingly, we also found two highly conserved sequences in Apicomplexa CAP-Gly domains, the GVALDEPL and the EVGDFPPIDP, leaving open the question if they play any important role in Apicomplexa TBCBs.

Concerning the protein sub-cellular localization in the parasite, we concluded that TgTBCB localizes at the anterior region of the parasite, close to the apical complex and immediately below the conoid. However, we did not find any evidence of a possible localization at the centrosome or in the mitotic spindle MTs as it was described in mammalian cells. Using the super resolution microscopy, we could confirm the cytoplasmic localization of the protein and possible interaction with the glutamylated-tubulin, demonstrating that the TBCB in *T. gondii* is a soluble cytoplasmic protein that it may interact with the subpellicular MTs, mainly at the the apical cap, and conserves the same localization in extracellular and in intracellular tachyzoites. Additionally, we admit that TgTBCB could be in close association with the subpellicular MTs and once they taper to be attached to the apical polar ring we observed a TgTBCB ring-like shape staining in this region. Nevertheless, as the apical polar ring is one MTOC of the parasite (Morrissette & Sibley, 2002a), and in human cells the TBCB is present

in the MTOC (Kortazar et al., 2007), we cannot exclude the hypothesis that TgTBCB could be associated to the apical polar ring.

Considering the TgTBCB localization in the apical region of the parasite and the evidences of its presence in the tachyzoite secretome (X. W. Zhou et al., 2005), we postulated that it could be present in the secretory organelles of the parasite. In fact, the super resolution microscopy confirmed some dots of co-localization with some microneme proteins, what could indicate a possible presence in that secretory vesicle or a possible interaction with microneme. To address this hypothesis, we have done a secretion analysis and an invasion assay in the presence of an anti-TgTBCB specific polyclonal serum. The interpretation of both results led us to admit that the TgTBCB could be involved in some kind of micronemal trafficking by propulsion along subpellicular MTs tracks, as it has been suggested in the Plasmodium (Schrevel et al., 2008) and since in *T. gondii* defects in the apical polar ring alters the MTs organization, affecting the micronemes distribution, and leading to a reduction in MIC2 secretion (Leung et al., 2017). However, further studies are needed to confirm this hypothesis.

Regarding the over-expressing results, we can conclude that the TBCB overexpression in *T. gondii* leads to a pronounced decrease in the parasite invasion rate, but no differences were found in the replication and egress rates. No further assays were performed to prove the MT network destabilization upon TBCB overexpression in the parasite. However, we observed by IF an interaction of the TgTBCB with the subpellicular MTs, an essential structure for the host cells invasion (Morrissette & Sibley, 2002b). In addition, TBCB overexpression in drosophila, yeast and mammals has been shown to trigger MT network destabilization, yet with some differences (Baffet et al., 2012; Fanarraga, Villegas, Carranza, Castaño, & Zabala, 2009; Kortazar et al., 2007; Lopez-Fanarraga et al., 2007; Radcliffe et al., 1999; W. Wang et al., 2005). Putting these evidences together, we hypothesise that the reduction in the *T. gondii* invasion rate, observed in the TBCB overexpression backgrounds, can be explained by a depolymerizing event of the subpellicular MT cytoskeleton of the parasite, even if these MTs are relatively stable and highly resistant to depolymerizing conditions (Morrissette & Sibley, 2002a).

Characterizing the TgTBCB KO, we observed that the depletion of the TgTBCB protein is followed by the decrease of α-tubulin, acetylated and glutamylated tubulin levels. By IF was possible to show the decrease of the acetylated and polyglutamylated tubulin, which, in conjugation with the above observation, reveals an extremely affected MT network in the parasite. As a consequence, the KO parasites were less efficient at invading the host cell (reduction of approximately 61%) and had serious problems in the replication (approximately 50% less efficient to replicate), being unable to survive in culture for more than one week. As

observed by IFs and Electron microscopy, the parasites that were able to invade the host cell showed problems in the replication, such as cells with multiple centrosomes, huge or multiple nucleus per cell, loss of cell polarity, loss of cell shape and replication control, culminating in the entire disorganization of the parasitophorous vacuoles. Putting together all these evidences, we concluded that since the TgTBCB is gradually lost after the KO induction, it is clear that the parasite MTs cytoskeleton network also follows this trend, being gradually affected and degraded. This happens due to the impossibility to form new and/or to recycle the α/β-tubulin heterodimer, and as a directed consequence of that, the parasite cannot add new heterodimer on its MT cytoskeleton or polymerize new MTs. Moreover, the specific decrease in α-tubulin levels is directly related with the instability of those unfolded monomers in the absence of TBCB. Consequently, since the α-tubulin monomers could not be chaperoned by the TgTBCB, they were immediately degraded by the parasite.

Therefore, the TgTBCB KO compromises irreversibly the parasite tubulin folding pathway, the tubulin recycling and subsequently the MT cytoskeleton network, causing the total and irreversible loss of the MT cytoskeleton in the parasite. Furthermore, the TgTBCB proves to be an essential protein to the parasite, being required to generate a functional MT network, which is indispensable to sustain the invasion, replication and cell polarity of the parasite. Being so, the TgTBCB can be a new target for therapeutic approaches to control *T. gondii* replication.

Intentionally blank page

Chapter VI: Future perspectives

To study the role of a protein in a cell, we need to study its sub-cellular localization, the abundance and turnover, the post-translational modifications of the protein, its activity and interaction with other cell components, etc., being aware that these aspects are intrinsically linked and that to properly understand one of them we need to know the others. In the specific case of our work, we only covered some of those aspects and much more can and should be done.

One field that we started to explore but, unfortunately, we could not finish, was the identification of the proteins that interact with TgTBCB *in vivo*. One of our main future perspectives is to complete this part of our work using the BioID system (proximity- dependent biotin identification system); a genetic tool to detect TBCB proximal and interacting proteins in *Toxoplasma gondii*. BioID is a protein interaction detection method that requires tagging a protein of interest with a modified form of a bacterial biotin ligase, the BirA (Roux, Kim, Raida, & Burke, 2012). BirA biotinilates the binding partners and near neighbors of the fused protein in native cellular conditions. After the biotin tagging, cells can be lysed in as stringent conditions as needed without loss of the tag that is what will be detected by streptavidin-coated agarose beads in the pull-down step.

Regarding the localization of the protein we will perform co-localization assays between TgTBCB and at least one of the proteins from the apical polar ring. Of course, this new door will be opened as soon as the interaction studies are done, as all of the fields are intrinsically linked together.

In terms of post-translational modifications, there is already one report demonstrating that the TBCB function is regulated by the Pak1.This can be a very interesting study in *T. gondii*, but since Pak1 is just a predicted protein, it can be a great challenge. However, the deep understanding of how TBCB activity is regulated in the parasite will have unequivocally great value.

Concerning the activity of the protein, there are several proteins reported to interact with the TBCB and modulate its activity. The main one is the TBCE, its partner. Therefore, it will be very interesting to study this other cofactor in the parasite and its interaction with TBCB. We already tried to amplify the TgTBCE cDNA but we think that there is a problem with the TBCE annotation.

Finally, the overexpression and the KO lines should be further explored by performing:

- immunofluorescence of secreted proteins to check their localization in the presence of excess or in the absence of the TgTBCB

- immunofluorescence assays to explore the pattern of tubulin post-translation modifications in the presence of high levels of TgTBCB

- MT depolymerizing assays to test the subpellicular MT stability in the presence of excess or in the absence of TgTBCB

- native protein electrophoresis to evaluate the levels of the soluble tubulin heterodimer in the presence of excess or in the absence of TgTBCB

Ultimately, a future perspective much more distant but possible, is the development of a new drug that specifically interacts with the parasite TBCB and blocks its activity. We saw that the TgTBCB protein is very different from the Human isoform 1 and that the Apicomplexa have high conserved sequences on its TBCB's proteins, consequently it can also be a possibility to be explored, in order to develop a new treatment for those parasites.

Bibliography

Afonso, E., Thulliez, P., & Gilot-Fromont, E. (2006). Transmission of *Toxoplasma gondii* in an urban population of domestic cats (Felis catus). *International Journal for Parasitology*, *36*(13), 1373–1382. http://doi.org/10.1016/j.ijpara.2006.07.010

Agop-Nersesian, C., Egarter, S., Langsley, G., Foth, B. J., Ferguson, D. J. P., & Meissner, M. (2010). Biogenesis of the Inner Membrane Complex Is Dependent on Vesicular Transport by the Alveolate Specific GTPase Rab11B. *PLoS Pathogens*, *6*(7), e1001029–15. http://doi.org/10.1371/journal.ppat.1001029

Agop-Nersesian, C., Naissant, B., Ben Rached, F., Rauch, M., Kretzschmar, A., Thiberge, S., et al. (2009). Rab11A-Controlled Assembly of the Inner Membrane Complex Is Required for Completion of Apicomplexan Cytokinesis. *PLoS Pathogens*, *5*(1), e1000270–15. http://doi.org/10.1371/journal.ppat.1000270

Amos, L. A., & Schlieper, D. (2005). Microtubules and maps. *Advances in Protein Chemistry*, *71*, 257–298. http://doi.org/10.1016/S0065-3233(04)71007-4

An ensemble of specifically targeted proteins stabilizes cortical microtubules in the human parasite. (2016). An ensemble of specifically targeted proteins stabilizes cortical microtubules in the human parasite, 1–23. http://doi.org/10.1091/mbc.E15-11-0754)

Andenmatten, N., Egarter, S., Jackson, A. J., Jullien, N., Herman, J.-P., & Meissner, M. (2012). Conditional genome engineering in *Toxoplasma gondii* uncovers alternative invasion mechanisms. *Nature Methods*, *10*(2), 125–127. http://doi.org/10.1038/nmeth.2301

Anderson-White, B. R., Ivey, F. D., Cheng, K., Szatanek, T., Lorestani, A., Beckers, C. J., et al. (2011). A family of intermediate filament-like proteins is sequentially assembled into the cytoskeleton of *Toxoplasma gondii*. *Cellular Microbiology*, *13*(1), 18–31. http://doi.org/10.1111/j.1462-5822.2010.01514.x

Anderson-White, B., Beck, J. R., Chen, C.-T., Meissner, M., Bradley, P. J., & Gubbels, M.-J. (2012). Cytoskeleton assembly in *Toxoplasma gondii* cell division. *International Review of Cell and Molecular Biology*, *298*, 1–31. http://doi.org/10.1016/B978-0-12-394309-5.00001-8

Azimzadeh, J., & Bornens, M. (2007). Structure and duplication of the centrosome. *Journal of Cell Science*, *120*(Pt 13), 2139–2142. http://doi.org/10.1242/jcs.005231

Baffet, A. D., Benoit, B., Januschke, J., Audo, J., Gourhand, V., Roth, S., & Guichet, A. (2012). Drosophila tubulin-binding cofactor B is required for microtubule network formation and for cell polarity. *Molecular Biology of the Cell*, *23*(18), 3591–3601. http://doi.org/10.1091/mbc.E11-07-0633

Banaszynski, L. A., Chen, L.-C., Maynard-Smith, L. A., Ooi, A. G. L., & Wandless, T. J. (2006). A Rapid, Reversible, and Tunable Method to Regulate Protein Function in Living Cells Using Synthetic Small Molecules. *Cell*, *126*(5), 995–1004. http://doi.org/10.1016/j.cell.2006.07.025

Barta, J. R. (1989). Phylogenetic analysis of the class Sporozoea (phylum Apicomplexa Levine, 1970): evidence for the independent evolution of heteroxenous life cycles. *The Journal of Parasitology*, *75*(2), 195–206.

Bartolini, F., Tian, G., Piehl, M., Cassimeris, L., Lewis, S. A., & Cowan, N. J. (2005). Identification of a novel tubulin-destabilizing protein related to the chaperone cofactor E. *Journal of Cell Science*, *118*(Pt 6), 1197–1207. http://doi.org/10.1242/jcs.01719

Baum, J., Papenfuss, A. T., Baum, B., Speed, T. P., & Cowman, A. F. (2006). Regulation of apicomplexan actin-based motility. *Nature Reviews. Microbiology*, *4*(8), 621–628. http://doi.org/10.1038/nrmicro1465

Beck, J. R., Fung, C., Straub, K. W., Coppens, I., Vashisht, A. A., Wohlschlegel, J. A., & Bradley, P. J. (2013). A Toxoplasma palmitoyl acyl transferase and the palmitoylated armadillo repeat protein TgARO govern apical rhoptry tethering and reveal a critical role for the rhoptries in host cell invasion but not egress. *PLoS Pathogens*, *9*(2), e1003162. http://doi.org/10.1371/journal.ppat.1003162

Beck, J. R., Rodriguez-Fernandez, I. A., de Leon, J. C., Huynh, M.-H., Carruthers, V. B., Morrissette, N. S., & Bradley, P. J. (2010). A novel family of Toxoplasma IMC proteins displays a hierarchical organization and functions in coordinating parasite division. *PLoS Pathogens*, *6*(9), e1001094. http://doi.org/10.1371/journal.ppat.1001094

Berrueta, L., Kraeft, S. K., Tirnauer, J. S., Schuyler, S. C., Chen, L. B., Hill, D. E., et al. (1998). The adenomatous polyposis coli-binding protein EB1 is associated with cytoplasmic and spindle microtubules. *Proceedings of the National Academy of Sciences of the United States of America*, *95*(18), 10596–10601.

Besteiro, S., Dubremetz, J.-F., & Lebrun, M. (2011). The moving junction of apicomplexan parasites: a key structure for invasion. *Cellular Microbiology*, *13*(6), 797–805. http://doi.org/10.1111/j.1462-5822.2011.01597.x

Bezanilla, M., Gladfelter, A. S., Kovar, D. R., & Lee, W.-L. (2015). Cytoskeletal dynamics: a view from the membrane. *The Journal of Cell Biology*, *209*(3), 329–337. http://doi.org/10.1083/jcb.201502062

Bhamidipati, A., Lewis, S. A., & Cowan, N. J. (2000). ADP ribosylation factor-like protein 2 (Arl2) regulates the interaction of tubulin-folding cofactor D with native tubulin. *The Journal of Cell Biology*, *149*(5), 1087–1096.

Biochemistry, M. B. A., 1976. (1976). A rapid and sensitive method for the quantitation of microgram quantities of protein utilizing the principle of protein-dye binding. *Elsevier*, *72*(1-2), 248–254. http://doi.org/10.1016/0003-2697(76)90527-3

Black, M. W., & Boothroyd, J. C. (2000). Lytic cycle of *Toxoplasma gondii*. *Microbiology and Molecular Biology Reviews: MMBR*, *64*(3), 607–623.

Black, M., Seeber, F., Soldati, D., Kim, K., & Boothroyd, J. C. (1995). Restriction enzyme-mediated integration elevates transformation frequency and enables co-transfection of *Toxoplasma gondii*. *Molecular and Biochemical Parasitology*, *74*(1), 55–63.

Blader, I. J., Coleman, B. I., Chen, C.-T., & Gubbels, M.-J. (2015). Lytic Cycle of *Toxoplasma gondii*: 15 Years Later. *Annual Review of Microbiology*, *69*, 463–485. http://doi.org/10.1146/annurev-micro-091014-104100

Boothroyd, J. C., & Dubremetz, J.-F. (2008). Kiss and spit: the dual roles of Toxoplasma rhoptries. *Nature Reviews. Microbiology*, *6*(1), 79–88. http://doi.org/10.1038/nrmicro1800

Bornens, M. (2012). The centrosome in cells and organisms. *Science*, *335*(6067), 422–426. http://doi.org/10.1126/science.1209037

Braun, L., Brenier-Pinchart, M. P., & Yogavel, M. (2013). A Toxoplasma dense granule protein, GRA24, modulates the early immune response to infection by promoting a direct and sustained host p38 MAPK activation. *Journal of …*, *210*(10), 2071–2086. http://doi.org/10.1084/jem.20130103

Brossier, F., & David Sibley, L. (2005). *Toxoplasma gondii*: Microneme protein MIC2. *The International Journal of Biochemistry & Cell Biology*, *37*(11), 2266–2272. http://doi.org/10.1016/j.biocel.2005.06.006

Bu, W., & Su, L.-K. (2003). Characterization of functional domains of human EB1 family proteins. *Journal of Biological Chemistry*, *278*(50), 49721–49731. http://doi.org/10.1074/jbc.M306194200

Carranza, G., Castaño, R., Fanarraga, M. L., Villegas, J. C., Gonçalves, J., Soares, H., et al. (2013). Autoinhibition of TBCB regulates EB1-mediated microtubule dynamics. *Cellular and Molecular Life Sciences*, *70*(2), 357–371. http://doi.org/10.1007/s00018-012-1114-2

Carruthers, V. B., & Sibley, L. D. (1997). Sequential protein secretion from three distinct organelles of *Toxoplasma gondii* accompanies invasion of human fibroblasts. *European Journal of Cell Biology*.

Carruthers, V. B., & Sibley, L. D. (1999). Mobilization of intracellular calcium stimulates microneme discharge in *Toxoplasma gondii*. *Molecular Microbiology*, *31*(2), 421–428.

Carruthers, V. B., & Tomley, F. M. (2008). Microneme Proteins in Apicomplexans. In *Molecular Mechanisms of Parasite Invasion* (Vol. 47, pp. 33–45). New York, NY: Springer New York. http://doi.org/10.1007/978-0-387-78267-6_2

Carruthers, V., & Boothroyd, J. C. (2007). Pulling together: an integrated model of Toxoplasma cell invasion. *Current Opinion in Microbiology*, *10*(1), 83–89. http://doi.org/10.1016/j.mib.2006.06.017

Cassimeris, L. (2002). The oncoprotein 18/stathmin family of microtubule destabilizers. *Current Opinion in Cell Biology*, *14*(1), 18–24.

Cesbron-Delauw, M. F. (1994). Dense-granule organelles of *Toxoplasma gondii*: their role in the host-parasite relationship. *Parasitology Today*, *10*(8), 293–296. http://doi.org/10.1016/0169-4758(94)90078-7

Chandramohanadas, R., Davis, P. H., Beiting, D. P., Harbut, M. B., Darling, C., Velmourougane, G., et al. (2009). Apicomplexan parasites co-opt host calpains to facilitate their escape from infected cells. *Science*, *324*(5928), 794–797. http://doi.org/10.1126/science.1171085

Chen, A. L., Kim, E. W., Toh, J. Y., Vashisht, A. A., & Rashoff, A. Q. (2015a). Novel components of the Toxoplasma inner membrane complex revealed by BioID. *MBio*. http://doi.org/10.1128/mBio.02357-14

Chen, C.-T., Kelly, M., Leon, J. de, Nwagbara, B., Ebbert, P., Ferguson, D. J. P., et al. (2015b). Compartmentalized Toxoplasma EB1 bundles spindle microtubules to secure accurate chromosome segregation. *Molecular Biology of the Cell*, *26*(25), 4562–4576. http://doi.org/10.1091/mbc.E15-06-0437

Conde, C., & Cáceres, A. (2009). Microtubule assembly, organization and dynamics in axons and dendrites. *Nature Reviews. Neuroscience*, *10*(5), 319–332. http://doi.org/10.1038/nrn2631

Conduit, P., Wainman, A. & Raff, J. Centrosome function and assembly in animal cells. Nat Rev Mol Cell Biol 16, 611–624 (2015). https://doi.org/10.1038/nrm4062

Cunningham, L. A., & Kahn, R. A. (2008). Cofactor D functions as a centrosomal protein and is required for the recruitment of the gamma-tubulin ring complex at centrosomes and organization of the mitotic spindle. *Journal of Biological Chemistry*, *283*(11), 7155–7165. http://doi.org/10.1074/jbc.M706753200

De Forges, H., Bouissou, A., & Perez, F. (2012). Interplay between microtubule dynamics and intracellular organization. *The International Journal of Biochemistry & Cell Biology*, *44*(2), 266–274. http://doi.org/10.1016/j.biocel.2011.11.009

De Souza, W., & Attias, M. (2010). Subpellicular microtubules in apicomplexa and trypanosomatids. *Structures and Organelles in Pathogenic Protists*. http://doi.org/10.1007/978-3-642-12863-9_2

De Souza, W., Martins-Duarte, E. D. S., Lemgruber, L., Attias, M., & Vommaro, R. C. (2010). Organização estrutural do taquizoíto de *Toxoplasma gondii*. *Scientia Medica*, *20*(1), 131–143.

Delorme-Walker, V., Abrivard, M., Lagal, V., Anderson, K., Perazzi, A., Gonzalez, V., et al. (2012). Toxofilin upregulates the host cortical actin cytoskeleton dynamics, facilitating Toxoplasma invasion. *Journal of Cell Science*, *125*(Pt 18), 4333–4342. http://doi.org/10.1242/jcs.103648

Desai, A., & Mitchison, T. J. (1997). Microtubule polymerization dynamics. *Annual Review of Cell and Developmental Biology*, *13*(1), 83–117. http://doi.org/10.1146/annurev.cellbio.13.1.83

Dimitrov, A., Quesnoit, M., Moutel, S., Cantaloube, I., Poüs, C., & Perez, F. (2008). Detection of GTP-tubulin conformation in vivo reveals a role for GTP remnants in microtubule rescues. *Science*, *322*(5906), 1353–1356. http://doi.org/10.1126/science.1165401

Dinkel, H., Van Roey, K., Michael, S., Kumar, M., Uyar, B., Altenberg, B., et al. (2016). ELM 2016--data update and new functionality of the eukaryotic linear motif resource. *Nucleic Acids Research*, *44*(D1), D294–300. http://doi.org/10.1093/nar/gkv1291

Dlugonska, H. (2008). Toxoplasma rhoptries: unique secretory organelles and source of promising vaccine proteins for immunoprevention of toxoplasmosis. *Journal of Biomedicine & Biotechnology*, *2008*, 632424. http://doi.org/10.1155/2008/632424

Donald, R. G., & Roos, D. S. (1993). Stable molecular transformation of *Toxoplasma gondii*: a selectable dihydrofolate reductase-thymidylate synthase marker based on drug-resistance mutations in malaria. *Proceedings of the National Academy of Sciences of the United States of America*, *90*(24), 11703–11707.

Donald, R. G., & Roos, D. S. (1994). Homologous recombination and gene replacement at the dihydrofolate reductase-thymidylate synthase locus in *Toxoplasma gondii*. *Molecular and Biochemical Parasitology*, *63*(2), 243–253.

Donald, R. G., Carter, D., Ullman, B., & Roos, D. S. (1996). Insertional tagging, cloning, and expression of the *Toxoplasma gondii* hypoxanthine-xanthine-guanine phosphoribosyltransferase gene. Use as a selectable marker for stable transformation. *Journal of Biological Chemistry*, *271*(24), 14010–14019. http://doi.org/10.1074/jbc.271.24.14010

Doxsey, S. (2001). Re-evaluating centrosome function. *Nature Reviews. Molecular Cell Biology*, *2*(9), 688–698. http://doi.org/10.1038/35089575

Duarte, A., Castro, I., Pereira da Fonseca, I. M., Almeida, V., Madeira de Carvalho, L. M., Meireles, J., et al. (2010). Survey of infectious and parasitic diseases in stray cats at the Lisbon Metropolitan Area, Portugal. *Journal of Feline Medicine and Surgery*, *12*(6), 441–446. http://doi.org/10.1016/j.jfms.2009.11.003

Dubey, J. P. (2008). The history of *Toxoplasma gondii* - the first 100 years. *The Journal of Eukaryotic Microbiology*, *55*(6), 467–475. http://doi.org/10.1111/j.1550-7408.2008.00345.x

Dubey, J. P. (1998). Advances in the life cycle of *Toxoplasma gondii*. *International Journal for Parasitology*, *28*(7), 1019–1024.

Dubey, J. P. (2009). History of the discovery of the life cycle of *Toxoplasma gondii*. *International Journal for Parasitology*. http://doi.org/10.1016/j.ijpara.2009.01.005

Dubey, J. P., & Frenkel, J. K. (1972). Cyst-induced toxoplasmosis in cats. *The Journal of Protozoology*, *19*(1), 155–177.

Dubey, J. P., Lindsay, D. S., & Speer, C. A. (1998). Structures of *Toxoplasma gondii* tachyzoites, bradyzoites, and sporozoites and biology and development of tissue cysts. *Clinical Microbiology Reviews*, *11*(2), 267–299.

Dubey, J. P., Vianna, M. C. B., Sousa, S., Canada, N., Meireles, S., Correia da Costa, J. M., et al. (2006). Characterization of *Toxoplasma gondii* isolates in free-range chickens from Portugal. *The Journal of Parasitology*, *92*(1), 184–186. http://doi.org/10.1645/GE-652R.1

Dubremetz, J.-F. (2007). Rhoptries are major players in *Toxoplasma gondii* invasion and host cell interaction. *Cellular Microbiology*, *9*(4), 841–848. http://doi.org/10.1111/j.1462-5822.2007.00909.x

Elmore, S. A., Jones, J. L., Conrad, P. A., Patton, S., Lindsay, D. S., & Dubey, J. P. (2010). *Toxoplasma gondii*: epidemiology, feline clinical aspects, and prevention. *Trends in Parasitology*, *26*(4), 190–196. http://doi.org/10.1016/j.pt.2010.01.009

Esteves, F., Aguiar, D., Rosado, J., Costa, M. L., de Sousa, B., Antunes, F., & Matos, O. (2014). *Toxoplasma gondii* prevalence in cats from Lisbon and in pigs from centre and south of Portugal. *Veterinary Parasitology*, *200*(1-2), 8–12. http://doi.org/10.1016/j.vetpar.2013.12.017

Fanarraga, M. L., Bellido, J., Jaén, C., Villegas, J. C., & Zabala, J. C. (2010). TBCD links centriologenesis, spindle microtubule dynamics, and midbody abscission in human cells. *PLoS ONE*, *5*(1), e8846. http://doi.org/10.1371/journal.pone.0008846

Fanarraga, M. L., Párraga, M., Aloria, K., del Mazo, J., Avila, J., & Zabala, J. C. (1999). Regulated expression of p14 (cofactor A) during spermatogenesis. *Cell Motility and the Cytoskeleton*, *43*(3), 243–254. http://doi.org/10.1002/(SICI)1097-0169(1999)43:3<243::AID-CM7>3.0.CO;2-0

Fanarraga, M. L., Villegas, J. C., Carranza, G., Castaño, R., & Zabala, J. C. (2009). Tubulin cofactor B regulates microtubule densities during microglia transition to the reactive states. *Experimental Cell Research*, *315*(3), 535–541. http://doi.org/10.1016/j.yexcr.2008.10.045

Ferguson, D. J. P. (2002). *Toxoplasma gondii* and sex: essential or optional extra? *Trends in Parasitology*, *18*(8), 355–359.

Flegr, J., Prandota, J., Sovičková, M., & Israili, Z. H. (2014). Toxoplasmosis--a global threat. Correlation of latent toxoplasmosis with specific disease burden in a set of 88 countries. *PLoS ONE*, *9*(3), e90203. http://doi.org/10.1371/journal.pone.0090203

Fleming, J. R., Morgan, R. E., Fyfe, P. K., Kelly, S. M., & Hunter, W. N. (2013). The architecture of Trypanosoma bruceitubulin-binding cofactor B and implications for function. *FEBS Journal*, *280*(14), 3270–3280. http://doi.org/10.1111/febs.12308

Fletcher, D. A., & Mullins, R. D. (2010). Cell mechanics and the cytoskeleton. *Nature*, *463*(7280), 485–492. http://doi.org/10.1038/nature08908

Fontalba, A., Paciucci, R., Avila, J., & Zabala, J. C. (1993). Incorporation of tubulin subunits into dimers requires GTP hydrolysis. *Journal of Cell Science*, *106 (Pt 2)*, 627–632.

Fox, B. A., Ristuccia, J. G., Gigley, J. P., & Bzik, D. J. (2009). Efficient gene replacements in *Toxoplasma gondii* strains deficient for nonhomologous end joining. *Eukaryotic Cell*, *8*(4), 520–529. http://doi.org/10.1128/EC.00357-08

Fox, B. A., Sanders, K. L., Rommereim, L. M., Guevara, R. B., & Bzik, D. J. (2016). Secretion of Rhoptry and Dense Granule Effector Proteins by Nonreplicating *Toxoplasma gondii* Uracil Auxotrophs Controls the Development of Antitumor Immunity. *PLoS Genetics*, *12*(7), e1006189. http://doi.org/10.1371/journal.pgen.1006189

Francia, M. E., & Striepen, B. (2014). Cell division in apicomplexan parasites. *Nature Reviews. Microbiology*, *12*(2), 125–136. http://doi.org/10.1038/nrmicro3184

Frenkel, J. K., Dubey, J. P., & Miller, N. L. (1970). *Toxoplasma gondii* in cats: fecal stages identified as coccidian oocysts. *Science*, *167*(3919), 893–896.

Frénal, K., & Soldati-Favre, D. (2009). Role of the Parasite and Host Cytoskeleton in Apicomplexa Parasitism, 1–10. http://doi.org/10.1016/j.chom.2009.05.013

Frénal, K., Polonais, V., Marq, J. B., Stratmann, R., Limenitakis, J., & Soldati-Favre, D. (2010). Functional Dissection of the Apicomplexan Glideosome Molecular Architecture, 1–15. http://doi.org/10.1016/j.chom.2010.09.002

Gaji, R. Y., Behnke, M. S., Lehmann, M. M., White, M. W., & Carruthers, V. B. (2011). Cell cycle-dependent, intercellular transmission of *Toxoplasma gondii* is accompanied by marked changes in parasite gene expression. *Molecular Microbiology*, *79*(1), 192–204. http://doi.org/10.1111/j.1365-2958.2010.07441.x

Gajria, B., Bahl, A., Brestelli, J., Dommer, J., Fischer, S., Gao, X., et al. (2008). ToxoDB: an integrated *Toxoplasma gondii* database resource. *Nucleic Acids Research*, *36*(Database issue), D553–6. http://doi.org/10.1093/nar/gkm981

Galjart, N. (2005). CLIPs and CLASPs and cellular dynamics. *Nature Reviews. Molecular Cell Biology*, *6*(6), 487–498. http://doi.org/10.1038/nrm1664

Gao, Y., Vainberg, I. E., Chow, R. L., & Cowan, N. J. (1993). Two cofactors and cytoplasmic chaperonin are required for the folding of alpha- and beta-tubulin. *Molecular and Cellular Biology*, *13*(4), 2478–2485.

Garcia-Mayoral, M. F., Castaño, R., Fanarraga, M. L., Zabala, J. C., Rico, M., & Bruix, M. (2011). The solution structure of the N-terminal domain of human tubulin binding cofactor C reveals a platform for tubulin interaction. *PLoS ONE*, *6*(10), e25912. http://doi.org/10.1371/journal.pone.0025912

Gargaté, M. J., Ferreira, I., Vilares, A., Martins, S., Cardoso, C., Silva, S., et al. (2016). *Toxoplasma gondii* seroprevalence in the Portuguese population: comparison of three cross-sectional studies spanning three decades. *BMJ Open*, *6*(10), e011648. http://doi.org/10.1136/bmjopen-2016-011648

Gaskins, E., Gilk, S., DeVore, N., Mann, T., Ward, G., & Beckers, C. (2004). Identification of the membrane receptor of a class XIV myosin in Toxoplasma gondii. *The Journal of Cell Biology*, *165*(3), 383–393. http://doi.org/10.1083/jcb.200311137

Georgiev, D. (2003). Revisiting the microtubule based quantum models of mind: tubulin bound GTP cannot pump microtubule coherence or provide energy for alpha<-> beta computation ….

Gilbert, L. A., Ravindran, S., Turetzky, J. M., Boothroyd, J. C., & Bradley, P. J. (2007). *Toxoplasma gondii* targets a protein phosphatase 2C to the nuclei of infected host cells. *Eukaryotic Cell*, *6*(1), 73–83. http://doi.org/10.1128/EC.00309-06

Gonçalves, J., Tavares, A., Carvalhal, S., & Soares, H. (2010). Revisiting the tubulin folding pathway: new roles in centrosomes and cilia. *Biomolecular Concepts*, *1*(5-6), 423–434. http://doi.org/10.1515/bmc.2010.033

Goodson, H. V., & Jonasson, E. M. (2018). Microtubules and Microtubule-Associated Proteins. *Cold Spring Harbor Perspectives in Biology*, *10*(6). http://doi.org/10.1101/cshperspect.a022608

Gould, S. B., Tham, W.-H., Cowman, A. F., McFadden, G. I., & Waller, R. F. (2008). Alveolins, a new family of cortical proteins that define the protist infrakingdom Alveolata. *Molecular Biology and Evolution*, *25*(6), 1219–1230. http://doi.org/10.1093/molbev/msn070

Grynberg, M., Jaroszewski, L., & Godzik, A. (2003). Domain analysis of the tubulin cofactor system: a model for tubulin folding and dimerization. *BMC Bioinformatics*, *4*, 46. http://doi.org/10.1186/1471-2105-4-46

Gubbels, M.-J., & Duraisingh, M. T. (2012). Evolution of apicomplexan secretory organelles. *International Journal for Parasitology*, *42*(12), 1071–1081. http://doi.org/10.1016/j.ijpara.2012.09.009

Gubbels, M.-J., White, M., & Szatanek, T. (2008). The cell cycle and *Toxoplasma gondii* cell division: Tightly knit or loosely stitched? *International Journal for Parasitology*, *38*(12), 1343–1358. http://doi.org/10.1016/j.ijpara.2008.06.004

Hage-Sleiman, R., Herveau, S., Matera, E.-L., Laurier, J.-F., & Dumontet, C. (2010). Tubulin binding cofactor C (TBCC) suppresses tumor growth and enhances chemosensitivity in human breast cancer cells. *BMC Cancer*, *10*, 135. http://doi.org/10.1186/1471-2407-10-135

Hage-Sleiman, R., Herveau, S., Matera, E.-L., Laurier, J.-F., & Dumontet, C. (2011). Silencing of tubulin binding cofactor C modifies microtubule dynamics and cell cycle distribution and enhances sensitivity to gemcitabine in breast cancer cells. *Molecular Cancer Therapeutics*, *10*(2), 303–312. http://doi.org/10.1158/1535-7163.MCT-10-0568

Hager, K. M., Striepen, B., Tilney, L. G., & Roos, D. S. (1999). The nuclear envelope serves as an intermediary between the ER and Golgi complex in the intracellular parasite Toxoplasma gondii. *Journal of Cell Science*, *112 (Pt 16)*, 2631–2638.

Hall, C. I., Reese, M. L., Weerapana, E., Child, M. A., Bowyer, P. W., Albrow, V. E., et al. (2011). Chemical genetic screen identifies Toxoplasma DJ-1 as a regulator of parasite secretion, attachment, and invasion. *Proceedings of the National Academy of Sciences of the United States of America*, *108*(26), 10568–10573. http://doi.org/10.1073/pnas.1105622108

Harding, C. R., & Meissner, M. (2014). The inner membrane complex through development of *Toxoplasma gondii* and Plasmodium. *Cellular Microbiology*, *16*(5), 632–641. http://doi.org/10.1111/cmi.12285

Hartmann, J., Hu, K., He, C. Y., Pelletier, L., Roos, D. S., & Warren, G. (2006). Golgi and centrosome cycles in Toxoplasma gondii. *Molecular and Biochemical Parasitology*, *145*(1), 125–127. http://doi.org/10.1016/j.molbiopara.2005.09.015

Haugwitz, M., Nourzaie, O., Gandlur, S., & Sagawa, H. (2008). ProteoTuner: a novel system with rapid kinetics enables reversible control of protein levels in cells and organisms. *BioTechniques*, *44*(3), 432–433. http://doi.org/10.2144/000112825

Heald, R., & Nogales, E. (2002). Microtubule dynamics. *Journal of Cell Science*, *115*(1), 3–4.

Heidemann, S. R., & McIntosh, J. R. (1980). Visualization of the structural polarity of microtubules. *Nature*, *286*(5772), 517–519. http://doi.org/10.1042/EBC20180028

Herm-Götz, A., Agop-Nersesian, C., Münter, S., Grimley, J. S., Wandless, T. J., Frischknecht, F., & Meissner, M. (2007). Rapid control of protein level in the apicomplexan Toxoplasma gondii. *Nature Methods*, *4*(12), 1003–1005. http://doi.org/10.1038/nmeth1134

Hill, D. E., & Chirukandoth, S. (2005). Biology and epidemiology of *Toxoplasma gondii* in man and animals. *Animal Health Research …*. http://doi.org/10.1079/AHR2005100

Hirata, D., Masuda, H., Eddison, M., & Toda, T. (1998). Essential role of tubulin-folding cofactor D in microtubule assembly and its association with microtubules in fission yeast. *The EMBO Journal*, *17*(3), 658–666. http://doi.org/10.1093/emboj/17.3.658

Hortua Triana, M. A., Márquez-Nogueras, K. M., Vella, S. A., & Moreno, S. N. J. (2018). Calcium signaling and the lytic cycle of the Apicomplexan parasite Toxoplasma gondii. *Biochimica Et Biophysica Acta. Molecular Cell Research*, *1865*(11 Pt B), 1846–1856. http://doi.org/10.1016/j.bbamcr.2018.08.004

Howe, D. K., & Sibley, L. D. (1995). *Toxoplasma gondii* comprises three clonal lineages: correlation of parasite genotype with human disease. *The Journal of Infectious Diseases*, *172*(6), 1561–1566.

Hoyt, M. A., Macke, J. P., Roberts, B. T., & Geiser, J. R. (1997). Saccharomyces cerevisiae PAC2 functions with CIN1, 2 and 4 in a pathway leading to normal microtubule stability. *Genetics*, *146*(3), 849–857.

Hu, K. (2008). Organizational changes of the daughter basal complex during the parasite replication of Toxoplasma gondii. *PLoS Pathogens*, *4*(1), e10. http://doi.org/10.1371/journal.ppat.0040010

Hu, K., Johnson, J., Florens, L., Fraunholz, M., Suravajjala, S., DiLullo, C., et al. (2006). Cytoskeletal components of an invasion machine--the apical complex of Toxoplasma gondii. *PLoS Pathogens*, *2*(2), e13. http://doi.org/10.1371/journal.ppat.0020013

Hu, K., Mann, T., Striepen, B., Beckers, C. J. M., Roos, D. S., & Murray, J. M. (2002a). Daughter cell assembly in the protozoan parasite Toxoplasma gondii. *Molecular Biology of the Cell*, *13*(2), 593–606. http://doi.org/10.1091/mbc.01-06-0309

Hu, K., Roos, D. S., & Murray, J. M. (2002b). A novel polymer of tubulin forms the conoid of Toxoplasma gondii. *The Journal of Cell Biology*, *156*(6), 1039–1050. http://doi.org/10.1083/jcb.200112086

Hunter, C. A., & Sibley, L. D. (2012). Modulation of innate immunity by *Toxoplasma gondii* virulence effectors. *Nature Reviews. Microbiology*, *10*(11), 766–778. http://doi.org/10.1038/nrmicro2858

Hutchison, W. M., Dunachie, J. F., Siim, J. C., & Work, K. (1969). Life cycle of toxoplasma gondii. *Br Med J*.

Huynh, M.-H., & Carruthers, V. B. (2006). Toxoplasma MIC2 Is a Major Determinant of Invasion and Virulence. *PLoS Pathogens*, *2*(8), e84–10. http://doi.org/10.1371/journal.ppat.0020084

Innes, E. A. (2010). A brief history and overview of Toxoplasma gondii. *Zoonoses and Public Health*, *57*(1), 1–7. http://doi.org/10.1111/j.1863-2378.2009.01276.x

Janke, C., & Montagnac, G. (2017). Causes and Consequences of Microtubule Acetylation. *Current Biology : CB*, *27*(23), R1287–R1292. http://doi.org/10.1016/j.cub.2017.10.044

Jiménez-Ruiz, E., Wong, E. H., Pall, G. S., & Meissner, M. (2014). Advantages and disadvantages of conditional systems for characterization of essential genes in Toxoplasma gondii. *Parasitology*, *141*(11), 1390–1398. http://doi.org/10.1017/S0031182014000559

Job, D., Valiron, O., & Oakley, B. (2003). Microtubule nucleation. *Current Opinion in Cell Biology*, *15*(1), 111–117. http://doi.org/10.1016/S0955-0674(02)00003-0

Jung, C., Lee, C. Y. F., & Grigg, M. E. (2004). The SRS superfamily of Toxoplasma surface proteins. *International Journal for Parasitology*, *34*(3), 285–296. http://doi.org/10.1016/j.ijpara.2003.12.004

Juwana, J. P., Henderikx, P., Mischo, A., Wadle, A., Fadle, N., Gerlach, K., et al. (1999). EB/RP gene family encodes tubulin binding proteins. *International Journal of Cancer*, *81*(2), 275–284.

Kafsack, B. F. C., & Carruthers, V. B. (2010). Apicomplexan perforin-like proteins. *Communicative & Integrative Biology*, *3*(1), 18–23.

Kafsack, B. F. C., Pena, J. D. O., Coppens, I., Ravindran, S., Boothroyd, J. C., & Carruthers, V. B. (2009). Rapid membrane disruption by a perforin-like protein facilitates parasite exit from host cells. *Science*, *323*(5913), 530–533. http://doi.org/10.1126/science.1165740

Katris, N. J., van Dooren, G. G., McMillan, P. J., Hanssen, E., Tilley, L., & Waller, R. F. (2014). The apical complex provides a regulated gateway for secretion of invasion factors in Toxoplasma. *PLoS Pathogens*, *10*(4), e1004074. http://doi.org/10.1371/journal.ppat.1004074

Keeling, P. J., Burger, G., Durnford, D. G., Lang, B. F., Lee, R. W., Pearlman, R. E., et al. (2005). The tree of eukaryotes. *Trends in Ecology & Evolution*, *20*(12), 670–676. http://doi.org/10.1016/j.tree.2005.09.005

Keller, C. E., & Lauring, B. P. (2005). Possible regulation of microtubules through destabilization of tubulin. *Trends in Cell Biology*, *15*(11), 571–573. http://doi.org/10.1016/j.tcb.2005.09.008

Kelley, L. A., Mezulis, S., Yates, C. M., Wass, M. N., & Sternberg, M. J. E. (2015). The Phyre2 web portal for protein modeling, prediction and analysis. *Nature Protocols*, *10*(6), 845–858. http://doi.org/10.1038/nprot.2015.053

Khan, A., Dubey, J. P., Su, C., Ajioka, J. W., Rosenthal, B. M., & Sibley, L. D. (2011). Genetic analyses of atypical *Toxoplasma gondii* strains reveal a fourth clonal lineage in North America. *International Journal for Parasitology*, *41*(6), 645–655. http://doi.org/10.1016/j.ijpara.2011.01.005

Kim, K., & Weiss, L. M. (2004). Toxoplasma gondii: the model apicomplexan. *International Journal for Parasitology*, *34*(3), 423–432. http://doi.org/10.1016/j.ijpara.2003.12.009

Kimura, Y., Kurabe, N., Ikegami, K., Tsutsumi, K., Konishi, Y., Kaplan, O. I., et al. (2010). Identification of tubulin deglutamylase among Caenorhabditis elegans and mammalian cytosolic carboxypeptidases (CCPs). *The Journal of Biological Chemistry*, *285*(30), 22936–22941. http://doi.org/10.1074/jbc.C110.128280

Klaren, V., & Kijlstra, A. (2002). Toxoplasmosis, an overview with emphasis on ocular involvement. *Ocular Immunology and Inflammation*, *10*(1), 1–26. http://doi.org/10.1076/ocii.10.1.1.10330

Kollman, J. M., Merdes, A., Mourey, L., & Agard, D. A. (2011). Microtubule nucleation by γ-tubulin complexes. *Nature Reviews. Molecular Cell Biology*, *12*(11), 709–721. http://doi.org/10.1038/nrm3209

Kortazar, D., Carranza, G., Bellido, J., Villegas, J. C., Fanarraga, M. L., & Zabala, J. C. (2006). Native tubulin-folding cofactor E purified from baculovirus-infected Sf9 cells dissociates tubulin dimers. *Protein Expression and Purification*, *49*(2), 196–202. http://doi.org/10.1016/j.pep.2006.03.005

Kortazar, D., Fanarraga, M. L., Carranza, G., Bellido, J., Villegas, J. C., Avila, J., & Zabala, J. C. (2007). Role of cofactors B (TBCB) and E (TBCE) in tubulin heterodimer dissociation. *Experimental Cell Research*, *313*(3), 425–436. http://doi.org/10.1016/j.yexcr.2006.09.002

Kubo, T., Yanagisawa, H.-A., Yagi, T., Hirono, M., & Kamiya, R. (2010). Tubulin polyglutamylation regulates axonemal motility by modulating activities of inner-arm dyneins. *Current Biology: CB*, *20*(5), 441–445. http://doi.org/10.1016/j.cub.2009.12.058

L'Hernault, S. W., & Rosenbaum, J. L. (1985). Chlamydomonas alpha-tubulin is posttranslationally modified by acetylation on the epsilon-amino group of a lysine. *Biochemistry*, *24*(2), 473–478. http://doi.org/10.1021/bi00323a034

Lacroix, B., van Dijk, J., Gold, N. D., Guizetti, J., Aldrian-Herrada, G., Rogowski, K., et al. (2010). Tubulin polyglutamylation stimulates spastin-mediated microtubule severing. *The Journal of Cell Biology*, *189*(6), 945–954. http://doi.org/10.1083/jcb.201001024

Laemmli, U. K. (1970). Cleavage of structural proteins during the assembly of the head of bacteriophage T4. *Nature*, *227*(5259), 680–685.

Lakämper, S., & Meyhöfer, E. (2005). The E-hook of tubulin interacts with kinesin's head to increase processivity and speed. *Biophysical Journal*, *89*(5), 3223–3234. http://doi.org/10.1529/biophysj.104.057505

Lamarque, M. H., Papoin, J., Finizio, A.-L., Lentini, G., Pfaff, A. W., Candolfi, E., et al. (2012). Identification of a new rhoptry neck complex RON9/RON10 in the Apicomplexa parasite Toxoplasma gondii. *PLoS ONE*, *7*(3), e32457. http://doi.org/10.1371/journal.pone.0032457

Lampson, M. A., & Kapoor, T. M. (2006). Targeting protein stability with a small molecule. *Cell*, *126*(5), 827–829. http://doi.org/10.1016/j.cell.2006.08.023

Lavine, M. D., & Arrizabalaga, G. (2008). Exit from Host Cells by the Pathogenic Parasite Toxoplasma gondiiDoes Not Require Motility. *Eukaryotic Cell*, *7*(1), 131–140. http://doi.org/10.1128/EC.00301-07

LeDizet, M., & Piperno, G. (1987). Identification of an acetylation site of Chlamydomonas alpha-tubulin. *Proceedings of the National Academy of Sciences of the United States of America*, *84*(16), 5720–5724. http://doi.org/10.1073/pnas.84.16.5720

Lei, T., Wang, H., Liu, J., Nan, H., & Liu, Q. (2014). ROP18 is a key factor responsible for virulence difference between *Toxoplasma gondii* and Neospora caninum. *PLoS ONE*, *9*(6), e99744. http://doi.org/10.1371/journal.pone.0099744

Lekutis, C., Ferguson, D. J., Grigg, M. E., Camps, M., & Boothroyd, J. C. (2001). Surface antigens of Toxoplasma gondii: variations on a theme. *International Journal for Parasitology*, *31*(12), 1285–1292.

Leung, J. M., He, Y., Zhang, F., Hwang, Y.-C., Nagayasu, E., Liu, J., et al. (2017). Stability and function of a putative microtubule-organizing center in the human parasite Toxoplasma gondii. *Molecular Biology of the Cell*, *28*(10), 1361–1378. http://doi.org/10.1091/mbc.E17-01-0045

Lewis, S. A., Tian, G., biology, N. C. T. I. C., 1997. (1997). The α-and β-tubulin folding pathways. *Elsevier*, *7*(12), 479–484. http://doi.org/10.1016/S0962-8924(97)01168-9

Li, L., & Yang, X.-J. (2015). Tubulin acetylation: responsible enzymes, biological functions and human diseases. *Cellular and Molecular Life Sciences*, *72*(22), 4237–4255. http://doi.org/10.1007/s00018-015-2000-5

Li, R., & Gundersen, G. G. (2008). Beyond polymer polarity: how the cytoskeleton builds a polarized cell. *Nature Reviews. Molecular Cell Biology*, *9*(11), 860–873. http://doi.org/10.1038/nrm2522

Li, S., Finley, J., Liu, Z. J., Qiu, S. H., Chen, H., Luan, C. H., et al. (2002). Crystal Structure of the Cytoskeleton-associated Protein Glycine-rich (CAP-Gly) Domain. *Journal of Biological Chemistry*, *277*(50), 48596–48601. http://doi.org/10.1074/jbc.M208512200

Liao, G., Nagasaki, T., & Gundersen, G. G. (1995). Low concentrations of nocodazole interfere with fibroblast locomotion without significantly affecting microtubule level: implications for the role of dynamic microtubules in cell locomotion. *Journal of Cell Science*, *108 (Pt 11)*, 3473–3483.

Lindsay, D. S., Blagburn, B. L., & Braud, K. O. (1995). A review of *Toxoplasma gondii* and muscular Toxoplasmosis. *Bam*.

Liu, Jun, He, Y., Benmerzouga, I., Sullivan, W. J., Morrissette, N. S., Murray, J. M., & Hu, K. (2016). An ensemble of specifically targeted proteins stabilizes cortical microtubules in the

human parasite Toxoplasma gondii. *Molecular Biology of the Cell*, *27*(3), 549–571. http://doi.org/10.1091/mbc.E15-11-0754

Liu, Jun, Wetzel, L., Zhang, Y., Nagayasu, E., Ems-McClung, S., Florens, L., & Hu, K. (2013). Novel thioredoxin-like proteins are components of a protein complex coating the cortical microtubules of Toxoplasma gondii. *Eukaryotic Cell*, *12*(12), 1588–1599. http://doi.org/10.1128/EC.00082-13

Lopes, A. P., Cardoso, L., & Rodrigues, M. (2008). Serological survey of *Toxoplasma gondii* infection in domestic cats from northeastern Portugal. *Veterinary Parasitology*, *155*(3-4), 184–189. http://doi.org/10.1016/j.vetpar.2008.05.007

Lopes, A. P., Dubey, J. P., Darde, M. L., & CARDOSO, L. (2014). Epidemiological review of *Toxoplasma gondii* infection in humans and animals in Portugal. *Parasitology*, *141*(13), 1699–1708. http://doi.org/10.1017/S0031182014001413

Lopes, A. P., Dubey, J. P., Neto, F., Rodrigues, A., Martins, T., Rodrigues, M., & Cardoso, L. (2013). Seroprevalence of *Toxoplasma gondii* infection in cattle, sheep, goats and pigs from the North of Portugal for human consumption. *Veterinary Parasitology*, *193*(1-3), 266–269. http://doi.org/10.1016/j.vetpar.2012.12.001

Lopes, A. P., Santos, H., Neto, F., Rodrigues, M., Kwok, O. C. H., Dubey, J. P., & Cardoso, L. (2011). Prevalence of antibodies to *Toxoplasma gondii* in dogs from northeastern Portugal. *The Journal of Parasitology*, *97*(3), 418–420. http://doi.org/10.1645/GE-2691.1

Lopes, A. P., Vilares, A., Neto, F., Rodrigues, A., Martins, T., Ferreira, I., et al. (2015). Genotyping Characterization of *Toxoplasma gondii* in Cattle, Sheep, Goats and Swine from the North of Portugal. *Iranian Journal of Parasitology*, *10*(3), 465–472.

Lopez-Fanarraga, M., Avila, J., Guasch, A., Coll, M., & Zabala, J. C. (2001). Review: postchaperonin tubulin folding cofactors and their role in microtubule dynamics. *Journal of Structural Biology*, *135*(2), 219–229. http://doi.org/10.1006/jsbi.2001.4386

Lopez-Fanarraga, M., Carranza, G., Bellido, J., Kortazar, D., Villegas, J. C., & Zabala, J. C. (2007). Tubulin cofactor B plays a role in the neuronal growth cone. *Journal of Neurochemistry*, *100*(6), 1680–1687. http://doi.org/10.1111/j.1471-4159.2006.04328.x

Lourido, S., & Moreno, S. N. J. (2015). The calcium signaling toolkit of the Apicomplexan parasites *Toxoplasma gondii* and Plasmodium spp. *Cell Calcium*, *57*(3), 186–193. http://doi.org/10.1016/j.ceca.2014.12.010

Lovett, J. L., & Sibley, L. D. (2003). Intracellular calcium stores in *Toxoplasma gondii* govern invasion of host cells. *Journal of Cell Science*, *116*(Pt 14), 3009–3016. http://doi.org/10.1242/jcs.00596

Ludueña, R. F. (1993). Are tubulin isotypes functionally significant. *Molecular Biology of the Cell*, *4*(5), 445–457.

Lundin, V. F., Leroux, M. R., & Stirling, P. C. (2010). Quality control of cytoskeletal proteins and human disease. *Trends in Biochemical Sciences*, *35*(5), 288–297. http://doi.org/10.1016/j.tibs.2009.12.007

Lytle, B. L., Peterson, F. C., Qiu, S.-H., Luo, M., Zhao, Q., Markley, J. L., & Volkman, B. F. (2004). Solution structure of a ubiquitin-like domain from tubulin-binding cofactor B. *Journal of Biological Chemistry*, *279*(45), 46787–46793. http://doi.org/10.1074/jbc.M409422200

Mann, T., & Beckers, C. (2001). Characterization of the subpellicular network, a filamentous membrane skeletal component in the parasite Toxoplasma gondii. *Molecular and Biochemical Parasitology*, *115*(2), 257–268.

Marcelino, E., Martins, T. M., Morais, J. B., Nolasco, S., Cortes, H., Hemphill, A., et al. (2011). Besnoitia besnoiti protein disulfide isomerase (BbPDI): molecular characterization, expression and in silico modelling. *Experimental Parasitology*, *129*(2), 164–174. http://doi.org/10.1016/j.exppara.2011.06.012

Margolis, R. L., & Wilson, L. (1998). Microtubule treadmilling: what goes around comes around. *BioEssays: News and Reviews in Molecular, Cellular and Developmental Biology*, *20*(10), 830–836. http://doi.org/10.1002/(SICI)1521-1878(199810)20:10<830::AID-BIES8>3.0.CO;2-N

Martins-de-Souza, D., Gattaz, W. F., Schmitt, A., Rewerts, C., Maccarrone, G., Dias-Neto, E., & Turck, C. W. (2009). Prefrontal cortex shotgun proteome analysis reveals altered calcium homeostasis and immune system imbalance in schizophrenia. *European Archives of Psychiatry and Clinical Neuroscience*, *259*(3), 151–163. http://doi.org/10.1007/s00406-008-0847-2

Martín, H., Rodríguez-Pachón, J. M., Ruiz, C., Nombela, C., & Molina, M. (2000a). Regulatory mechanisms for modulation of signaling through the cell integrity Slt2-mediated pathway in Saccharomyces cerevisiae. *Journal of Biological Chemistry*, *275*(2), 1511–1519.

Martín, L., Fanarraga, M. L., Aloria, K., & Zabala, J. C. (2000b). Tubulin folding cofactor D is a microtubule destabilizing protein. *FEBS Letters*, *470*(1), 93–95.

Meek, B., Back, J. W., Klaren, V. N. A., Speijer, D., & Peek, R. (2002). Protein disulfide isomerase of *Toxoplasma gondii* is targeted by mucosal IgA antibodies in humans. *FEBS Letters*, *522*(1-3), 104–108.

Meissner, M., Breinich, M. S., Gilson, P. R., & Crabb, B. S. (2007). Molecular genetic tools in Toxoplasma and Plasmodium: achievements and future needs. *Current Opinion in Microbiology*, *10*(4), 349–356. http://doi.org/10.1016/j.mib.2007.07.006

Melki, R., Rommelaere, H., Leguy, R., Vandekerckhove, J., & Ampe, C. (1996). Cofactor A is a molecular chaperone required for beta-tubulin folding: functional and structural characterization. *Biochemistry*, *35*(32), 10422–10435. http://doi.org/10.1021/bi960788r

Mercier, C., Adjogble, K. D. Z., Däubener, W., & Delauw, M.-F.-C. (2005). Dense granules: are they key organelles to help understand the parasitophorous vacuole of all apicomplexa parasites? *International Journal for Parasitology*, *35*(8), 829–849. http://doi.org/10.1016/j.ijpara.2005.03.011

Mital, J., Meissner, M., Soldati, D., & Ward, G. E. (2005). Conditional expression of *Toxoplasma gondii* apical membrane antigen-1 (TgAMA1) demonstrates that TgAMA1 plays a critical role in host cell invasion. *Molecular Biology of the Cell*, *16*(9), 4341–4349. http://doi.org/10.1091/mbc.e05-04-0281

Mitchison, T., & Kirschner, M. (1984). Dynamic instability of microtubule growth. *Nature.com*, *312*, 237–242. http://doi.org/10.1007/s11538-018-0531-2

Montoya, J. G., & Liesenfeld, O. (2004). Toxoplasmosis. *Lancet (London, England)*, *363*(9425), 1965–1976. http://doi.org/10.1016/S0140-6736(04)16412-X

Morisaki, J. H., Heuser, J. E., & Sibley, L. D. (1995). Invasion of *Toxoplasma gondii* occurs by active penetration of the host cell. *Journal of Cell Science*, *108 (Pt 6)*, 2457–2464.

Morrissette, N. (2015). Targeting Toxoplasma tubules: tubulin, microtubules, and associated proteins in a human pathogen. *Eukaryotic Cell*, *14*(1), 2–12. http://doi.org/10.1128/EC.00225-14

Morrissette, N. S., & Roos, D. S. (1998). Toxoplasma gondii: a family of apical antigens associated with the cytoskeleton. *Experimental Parasitology*, *89*(3), 296–303. http://doi.org/10.1006/expr.1998.4277

Morrissette, N. S., & Sibley, L. D. (2002a). Cytoskeleton of apicomplexan parasites. *Microbiology and Molecular Biology Reviews: MMBR*, *66(1)*, 21–38. http://doi.org/10.1128/MMBR.66.1.21-38.2002

Morrissette, N. S., & Sibley, L. D. (2002b). Disruption of microtubules uncouples budding and nuclear division in Toxoplasma gondii. *Journal of Cell Science*, *115*(Pt 5), 1017–1025.

Morrissette, N. S., Murray, J. M., & Roos, D. S. (1997). Subpellicular microtubules associate with an intramembranous particle lattice in the protozoan parasite Toxoplasma gondii. *Journal of Cell Science*, *110 (Pt 1)*, 35–42.

Mostowy, S., & Cossart, P. (2012). Septins: the fourth component of the cytoskeleton. *Nature Reviews. Molecular Cell Biology*, *13*(3), 183–194. http://doi.org/10.1038/nrm3284

Nawrotek, A., Knossow, M., & Gigant, B. (2011). The determinants that govern microtubule assembly from the atomic structure of GTP-tubulin. *Journal of Molecular Biology*, *412*(1), 35–42. http://doi.org/10.1016/j.jmb.2011.07.029

Nichols, B. A., & Chiappino, M. L. (1987). Cytoskeleton of Toxoplasma gondii. *Wiley Online Library*. http://doi.org/10.1111/j.1550-7408.1987.tb03162.x

Nichols, B. A., CHIAPPINO, M. L., ultrastructure, G. O. J. O., 1983. (1983). Secretion from the rhoptries of *Toxoplasma gondii* during host-cell invasion. *Elsevier*, *83*(1), 85–98. http://doi.org/10.1016/S0022-5320(83)90067-9

Ning, H.-R., Huang, S.-Y., Wang, J.-L., Xu, Q.-M., & Zhu, X.-Q. (2015). Genetic Diversity of *Toxoplasma gondii* Strains from Different Hosts and Geographical Regions by Sequence Analysis of GRA20 Gene. *The Korean Journal of Parasitology*, *53*(3), 345–348. http://doi.org/10.3347/kjp.2015.53.3.345

Nishi, M., Hu, K., Murray, J. M., & Roos, D. S. (2008). Organellar dynamics during the cell cycle of Toxoplasma gondii. *Journal of Cell Science*, *121*(Pt 9), 1559–1568. http://doi.org/10.1242/jcs.021089

Nogales, E., Wolf, S. G., & Downing, K. H. (1998a). Erratum: Structure of the αβ tubulin dimer by electron crystallography. *Nature*, *393*(6681), 191–191. http://doi.org/10.1038/30288

Nogales, E., Wolf, S. G., & Downing, K. H. (1998b). Structure of the αβ tubulin dimer by electron crystallography. *Nature*, *391*(6663), 199–203.

Nolasco, S., Bellido, J., Gonçalves, J., Zabala, J. C., & Soares, H. (2005). Tubulin cofactor A gene silencing in mammalian cells induces changes in microtubule cytoskeleton, cell cycle

arrest and cell death. *FEBS Letters*, *579*(17), 3515–3524. http://doi.org/10.1016/j.febslet.2005.05.022

Panda, D., Miller, H. P., Banerjee, A., Ludueña, R. F., & Wilson, L. (1994). Microtubule dynamics in vitro are regulated by the tubulin isotype composition. *Proceedings of the National Academy of Sciences of the United States of America*, *91*(24), 11358–11362. http://doi.org/10.1073/pnas.91.24.11358

Pappas, G., Roussos, N., & Falagas, M. E. (2009). Toxoplasmosis snapshots: global status of *Toxoplasma gondii* seroprevalence and implications for pregnancy and congenital toxoplasmosis. *International Journal for Parasitology*, *39*(12), 1385–1394. http://doi.org/10.1016/j.ijpara.2009.04.003

Pelletier, L., Stern, C. A., Pypaert, M., Sheff, D., Ngô, H. M., Roper, N., et al. (2002). Golgi biogenesis in Toxoplasma gondii. *Nature*, *418*(6897), 548–552. http://doi.org/10.1038/nature00946

Pierson, G. B., Burton, P. R., & Himes, R. H. (1978). Alterations in number of protofilaments in microtubules assembled in vitro. *The Journal of Cell Biology*, *76*(1), 223–228.

Plessmann, U., Reiter-Owona, I., & Lechtreck, K.-F. (2004). Posttranslational modifications of alpha-tubulin of Toxoplasma gondii. *Parasitology Research*, *94*(5), 386–389. http://doi.org/10.1007/s00436-004-1220-7

Radcliffe, P. A., & Toda, T. (2000). Characterisation of fission yeast alp11 mutants defines three functional domains within tubulin-folding cofactor B. *Molecular & General Genetics: MGG*, *263*(5), 752–760.

Radcliffe, P. A., Hirata, D., Vardy, L., & Toda, T. (1999). Functional dissection and hierarchy of tubulin-folding cofactor homologues in fission yeast. *Molecular Biology of the Cell*, *10*(9), 2987–3001. http://doi.org/10.1091/mbc.10.9.2987

Radke, J. R., Striepen, B., Guerini, M. N., Jerome, M. E., Roos, D. S., & White, M. W. (2001). Defining the cell cycle for the tachyzoite stage of Toxoplasma gondii. *Molecular and Biochemical Parasitology*, *115*(2), 165–175.

Rayala, S. K., Martin, E., Sharina, I. G., Molli, P. R., Wang, X., Jacobson, R., et al. (2007). Dynamic interplay between nitration and phosphorylation of tubulin cofactor B in the control of microtubule dynamics. *Proceedings of the National Academy of Sciences of the United States of America*, *104*(49), 19470–19475. http://doi.org/10.1073/pnas.0705149104

Reis, Y., Cortes, H., Viseu Melo, L., Fazendeiro, I., Leitão, A., & Soares, H. (2006). Microtubule cytoskeleton behavior in the initial steps of host cell invasion by Besnoitia besnoiti. *FEBS Letters*, *580*(19), 4673–4682. http://doi.org/10.1016/j.febslet.2006.07.050

Robert-Gangneux, F., & Dardé, M.-L. (2012). Epidemiology of and diagnostic strategies for toxoplasmosis. *Clinical Microbiology Reviews*, *25*(2), 264–296. http://doi.org/10.1128/CMR.05013-11

Rogowski, K., van Dijk, J., Magiera, M. M., Bosc, C., Deloulme, J.-C., Bosson, A., et al. (2010). A family of protein-deglutamylating enzymes associated with neurodegeneration. *Cell*, *143*(4), 564–578. http://doi.org/10.1016/j.cell.2010.10.014

Roiko, M. S., & Carruthers, V. B. (2009). New roles for perforins and proteases in apicomplexan egress. *Cellular Microbiology*, *11*(10), 1444–1452. http://doi.org/10.1111/j.1462-5822.2009.01357.x

Rommereim, L. M., Hortua Triana, M. A., Falla, A., Sanders, K. L., Guevara, R. B., Bzik, D. J., & Fox, B. A. (2013). Genetic manipulation in Δku80 strains for functional genomic analysis of Toxoplasma gondii. *Journal of Visualized Experiments: JoVE*, (77), e50598. http://doi.org/10.3791/50598

Roostalu, J., & Surrey, T. (2017). Microtubule nucleation: beyond the template. *Nature Reviews. Molecular Cell Biology*, *18*(11), 702–710. http://doi.org/10.1038/nrm.2017.75

Roux, K. J., Kim, D. I., Raida, M., & Burke, B. (2012). A promiscuous biotin ligase fusion protein identifies proximal and interacting proteins in mammalian cells. *The Journal of Cell Biology*, *196*(6), 801–810. http://doi.org/10.1083/jcb.201112098

Russell, D. G., & Burns, R. G. (1984). The polar ring of coccidian sporozoites: a unique microtubule-organizing centre. *Journal of Cell Science*, *65*(1), 193–207.

Sabin, A. B. (1939). Biological and immunological identity of Toxoplasma of animal and human origin. *Experimental Biology and Medicine*, *41*(1), 75–80. http://doi.org/10.3181/00379727-41-10577

Sabin, A. B., & Olitsky, P. K. (1937). TOXOPLASMA AND OBLIGATE INTRACELLULAR PARASITISM. *Science*, *85*(2205), 336–338. http://doi.org/10.1126/science.85.2205.336

Sander, J. D., & Joung, J. K. (2014). CRISPR-Cas systems for editing, regulating and targeting genomes. *Nature Biotechnology*, *32*(4), 347–355. http://doi.org/10.1038/nbt.2842

Schaap, I. A. T., Carrasco, C., de Pablo, P. J., MacKintosh, F. C., & Schmidt, C. F. (2006). Elastic response, buckling, and instability of microtubules under radial indentation. *Biophysical Journal*, *91*(4), 1521–1531. http://doi.org/10.1529/biophysj.105.077826

Schaefer, M. K. E., Schmalbruch, H., Buhler, E., Lopez, C., Martin, N., Guénet, J.-L., & Haase, G. (2007). Progressive motor neuronopathy: a critical role of the tubulin chaperone TBCE in axonal tubulin routing from the Golgi apparatus. *The Journal of Neuroscience: the Official Journal of the Society for Neuroscience*, *27*(33), 8779–8789. http://doi.org/10.1523/JNEUROSCI.1599-07.2007

Schrevel, J., Asfaux-Foucher, G., Hopkins, J. M., ROBERT, V., BOURGOUIN, C., PRENSIER, G., & Bannister, L. H. (2008). Vesicle trafficking during sporozoite development in Plasmodium berghei: ultrastructural evidence for a novel trafficking mechanism. *Parasitology*, *135*(Pt 1), 1–12. http://doi.org/10.1017/S0031182007003629

Seeber, F. (1997). Consensus sequence of translational initiation sites from *Toxoplasma gondii* genes. *Parasitology Research*, *83*(3), 309–311.

Serna, M., Carranza, G., Martin-Benito, J., Janowski, R., Canals, A., Coll, M., et al. (2015). The structure of the complex between -tubulin, TBCE and TBCB reveals a tubulin dimer dissociation mechanism. *Journal of Cell Science*, *128*(9), 1824–1834. http://doi.org/10.1242/jcs.167387

Sharp, D. J., & Ross, J. L. (2012). Microtubule-severing enzymes at the cutting edge. *Journal of Cell Science*, *125*(Pt 11), 2561–2569. http://doi.org/10.1242/jcs.101139

Shaw, M. K., Compton, H. L., Roos, D. S., & Tilney, L. G. (2000). Microtubules, but not actin filaments, drive daughter cell budding and cell division in Toxoplasma gondii. *Journal of Cell Science*, *113 (Pt 7)*, 1241–1254.

Shen, B., Brown, K. M., Lee, T. D., & Sibley, L. D. (2014). Efficient gene disruption in diverse strains of *Toxoplasma gondii* using CRISPR/CAS9. *MBio*, *5*(3), e01114–14. http://doi.org/10.1128/mBio.01114-14

Sibley, L. D., & Boothroyd, J. C. (1992). Virulent strains of *Toxoplasma gondii* comprise a single clonal lineage. *Nature*, *359*(6390), 82–85. http://doi.org/10.1038/359082a0

Sibley, L. D., Khan, A., Ajioka, J. W., & Rosenthal, B. M. (2009). Genetic diversity of *Toxoplasma gondii* in animals and humans. *Philosophical Transactions of the Royal Society of London. Series B, Biological Sciences*, *364*(1530), 2749–2761. http://doi.org/10.1098/rstb.2009.0087

Sidik, S. M., Huet, D., Ganesan, S. M., Huynh, M.-H., Wang, T., Nasamu, A. S., et al. (2016). A Genome-wide CRISPR Screen in Toxoplasma Identifies Essential Apicomplexan Genes. *Cell*, *166*(6), 1423–1435.e12. http://doi.org/10.1016/j.cell.2016.08.019

Skariah, S., Bednarczyk, R. B., McIntyre, M. K., Taylor, G. A., & Mordue, D. G. (2012). Discovery of a novel *Toxoplasma gondii* conoid-associated protein important for parasite resistance to reactive nitrogen intermediates. *Journal of Immunology (Baltimore, Md.: 1950)*, *188*(7), 3404–3415. http://doi.org/10.4049/jimmunol.1101425

Smitt, O., & Winblad, S. (1948). A report on congenital toxoplasmosis. *Acta Pathologica Microbiologica ….* http://doi.org/10.1111/j.1699-0463.1948.tb00697.x

Smolarz, B., Wilczyński, J., & Nowakowska, D. (2014). DNA repair mechanisms and *Toxoplasma gondii* infection. *Archives of Microbiology*, *196*(1), 1–8. http://doi.org/10.1007/s00203-013-0944-0

Sousa, S. de, Ajzenberg, D., Canada, N., Freire, L., Costa, J. M. C. D., Darde, M. L., et al. (2006). Biologic and molecular characterization of *Toxoplasma gondii* isolates from pigs from Portugal. *Veterinary Parasitology*, *135*(2), 133–136. http://doi.org/10.1016/j.vetpar.2005.08.012

Sousa, S., Thompson, G., Silva, E., Freire, L., Lopes, D., Correia da Costa, J. M., et al. (2009). Determination of the more adequate modified agglutination test cut-off for serodiagnosis of *Toxoplasma gondii* infection in sheep. *Zoonoses and Public Health*, *56*(5), 252–256. http://doi.org/10.1111/j.1863-2378.2008.01187.x

Stedman, T. T., Sussmann, A. R., & Joiner, K. A. (2003). *Toxoplasma gondii* Rab6 mediates a retrograde pathway for sorting of constitutively secreted proteins to the Golgi complex. *Journal of Biological Chemistry*, *278*(7), 5433–5443. http://doi.org/10.1074/jbc.M209390200

Steinborn, K., Maulbetsch, C., Priester, B., Trautmann, S., Pacher, T., Geiges, B., et al. (2002). The Arabidopsis PILZ group genes encode tubulin-folding cofactor orthologs required for cell division but not cell growth. *Genes & Development*, *16*(8), 959–971. http://doi.org/10.1101/gad.221702

Steinmetz, M. O., & Akhmanova, A. (2008). Capturing protein tails by CAP-Gly domains. *Trends in Biochemical Sciences*, *33*(11), 535–545. http://doi.org/10.1016/j.tibs.2008.08.006

Stokkermans, T. J., Schwartzman, J. D., Keenan, K., Morrissette, N. S., Tilney, L. G., & Roos, D. S. (1996). Inhibition of *Toxoplasma gondii* replication by dinitroaniline herbicides. *Experimental Parasitology*, *84*(3), 355–370. http://doi.org/10.1006/expr.1996.0124

Stortz, J. F., Gow, M., Meissner, M., & Jiménez-Ruiz, E. (2017). *Cas9 activity compromises nuclear integrity and cellular morphology in T. gondii*. *Toxo 14 The 14th biennial conference of the Toxoplasma gondii research community* (pp. 1–234).

Striepen, B., Crawford, M. J., Shaw, M. K., Tilney, L. G., Seeber, F., & Roos, D. S. (2000). The plastid of *Toxoplasma gondii* is divided by association with the centrosomes. *The Journal of Cell Biology*, *151*(7), 1423–1434.

Su, C., Evans, D., Cole, R. H., Kissinger, J. C., Ajioka, J. W., & Sibley, L. D. (2003). Recent expansion of Toxoplasma through enhanced oral transmission. *Science*, *299*(5605), 414–416. http://doi.org/10.1126/science.1078035

Suryavanshi, S., EddE, B., Fox, L. A., Guerrero, S., Hard, R., Hennessey, T., et al. (2010). Tubulin glutamylation regulates ciliary motility by altering inner dynein arm activity. *Current Biology: CB*, *20*(5), 435–440. http://doi.org/10.1016/j.cub.2009.12.062

Suvorova, E. S., Francia, M., Striepen, B., & White, M. W. (2015). A novel bipartite centrosome coordinates the apicomplexan cell cycle. *PLoS Biology*, *13*(3), e1002093. http://doi.org/10.1371/journal.pbio.1002093

Swedlow, J. R., Hu, K., Andrews, P. D., Roos, D. S., & Murray, J. M. (2002). Measuring tubulin content in Toxoplasma gondii: a comparison of laser-scanning confocal and wide-field fluorescence microscopy. *Proceedings of the National Academy of Sciences of the United States of America*, *99*(4), 2014–2019. http://doi.org/10.1073/pnas.022554999

Sweeney, K. R., Morrissette, N. S., LaChapelle, S., & Blader, I. J. (2010). Host cell invasion by *Toxoplasma gondii* is temporally regulated by the host microtubule cytoskeleton. *Eukaryotic Cell*, *9*(11), 1680–1689. http://doi.org/10.1128/EC.00079-10

Szabo, E. K., & Finney, C. A. M. (2016). Toxoplasma gondii: One Organism, Multiple Models. *Trends in Parasitology*. http://doi.org/10.1016/j.pt.2016.11.007

Szolajska, E., & Chroboczek, J. (2011). Faithful chaperones. *Cellular and Molecular Life Sciences*, *68*(20), 3307–3322. http://doi.org/10.1007/s00018-011-0740-4

Tan, H., Liao, H., Zhao, L., Lu, Y., Jiang, S., Tao, D., et al. (2017). HILI destabilizes microtubules by suppressing phosphorylation and Gigaxonin-mediated degradation of TBCB. *Nature Publishing Group*, *7*(1), 46376. http://doi.org/10.1038/srep46376

Teixidó-Travesa, N., Roig, J., & Lüders, J. (2012). The where, when and how of microtubule nucleation - one ring to rule them all. *Journal of Cell Science*, *125*(Pt 19), 4445–4456. http://doi.org/10.1242/jcs.106971

Tenter, A. M., Heckeroth, A. R., & Weiss, L. M. (2000). Toxoplasma gondii: from animals to humans. *International Journal for Parasitology*, *30*(12-13), 1217–1258. http://doi.org/10.1016/S0020-7519(00)00124-7

Tessmer, U., & Dernick, R. (1989). Preparative separation of poliovirus structural polypeptides by sodium dodecyl sulfate-polyacrylamide gel electrophoresis, copper staining and electroelution, and induction of monospecific antisera. *Electrophoresis*, *10*(4), 277–279. http://doi.org/10.1002/elps.1150100414

Tian, G., Bhamidipati, A., Cowan, N. J., & Lewis, S. A. (1999). Tubulin folding cofactors as GTPase-activating proteins. GTP hydrolysis and the assembly of the alpha/beta-tubulin heterodimer. *Journal of Biological Chemistry*, *274*(34), 24054–24058.

Tian, G., Huang, M. C., Parvari, R., Diaz, G. A., & Cowan, N. J. (2006). Cryptic out-of-frame translational initiation of TBCE rescues tubulin formation in compound heterozygous HRD. *Proceedings of the National Academy of Sciences of the United States of America*, *103*(36), 13491–13496. http://doi.org/10.1073/pnas.0602798103

Tian, G., Huang, Y., Rommelaere, H., Vandekerckhove, J., Ampe, C., & Cowan, N. J. (1996). Pathway leading to correctly folded beta-tubulin. *Cell*, *86*(2), 287–296.

Tian, G., Jaglin, X. H., Keays, D. A., Francis, F., Chelly, J., & Cowan, N. J. (2010a). Disease-associated mutations in TUBA1A result in a spectrum of defects in the tubulin folding and heterodimer assembly pathway. *Human Molecular Genetics*, *19*(18), 3599–3613. http://doi.org/10.1093/hmg/ddq276

Tian, G., Lewis, S. A., Feierbach, B., Stearns, T., Rommelaere, H., Ampe, C., & Cowan, N. J. (1997). Tubulin subunits exist in an activated conformational state generated and maintained by protein cofactors. *The Journal of Cell Biology*, *138*(4), 821–832.

Tian, G., Thomas, S., & Cowan, N. J. (2010b). Effect of TBCD and its regulatory interactor Arl2 on tubulin and microtubule integrity. *Cytoskeleton (Hoboken, N.J.)*, *67*(11), 706–714. http://doi.org/10.1002/cm.20480

Tilney, L. G., & Tilney, M. S. (1996). The cytoskeleton of protozoan parasites. *Current Opinion in Cell Biology*, *8*(1), 43–48. http://doi.org/10.1016/S0955-0674(96)80047-0

Tovey, C. A., & Conduit, P. T. (2018). Microtubule nucleation by γ-tubulin complexes and beyond. *Essays in Biochemistry*, *62*(6), 765–780. http://doi.org/10.1042/EBC20180028

Tran, J. Q., de Leon, J. C., Li, C., Huynh, M.-H., Beatty, W., & Morrissette, N. S. (2010). RNG1 is a late marker of the apical polar ring in Toxoplasma gondii. *Cytoskeleton (Hoboken, N.J.)*, *67*(9), 586–598. http://doi.org/10.1002/cm.20469

Tran, J. Q., Li, C., Chyan, A., Chung, L., & Morrissette, N. S. (2012). SPM1 Stabilizes Subpellicular Microtubules in Toxoplasma gondii. *Eukaryotic Cell*, *11*(2), 206–216. http://doi.org/10.1128/EC.05161-11

Tyler, J. S., Treeck, M., & Boothroyd, J. C. (2011). Focus on the ringleader: the role of AMA1 in apicomplexan invasion and replication. *Trends in Parasitology*, *27*(9), 410–420. http://doi.org/10.1016/j.pt.2011.04.002

Vadlamudi, R. K., Barnes, C. J., Rayala, S., Li, F., Balasenthil, S., Marcus, S., et al. (2005). p21-activated kinase 1 regulates microtubule dynamics by phosphorylating tubulin cofactor B. *Molecular and Cellular Biology*, *25*(9), 3726–3736. http://doi.org/10.1128/MCB.25.9.3726-3736.2005

Vainberg, I. E., Lewis, S. A., Rommelaere, H., Ampe, C., Vandekerckhove, J., Klein, H. L., & Cowan, N. J. (1998). Prefoldin, a chaperone that delivers unfolded proteins to cytosolic chaperonin. *Cell*, *93*(5), 863–873.

van Dijk, J., Rogowski, K., Miro, J., Lacroix, B., EddE, B., & Janke, C. (2007). A targeted multienzyme mechanism for selective microtubule polyglutamylation. *Molecular Cell*, *26*(3), 437–448. http://doi.org/10.1016/j.molcel.2007.04.012

Verhey, K. J., & Gaertig, J. (2007). The tubulin code. *Cell Cycle (Georgetown, Tex.)*, *6*(17), 2152–2160. http://doi.org/10.4161/cc.6.17.4633

Vinayak, S., Brooks, C. F., Naumov, A., & Suvorova, E. S. (2014). Genetic manipulation of the *Toxoplasma gondii* genome by fosmid recombineering. *MBio*. http://doi.org/10.1128/mBio.02021-14

Vitre, B., Coquelle, F. M., Heichette, C., Garnier, C., Chrétien, D., & Arnal, I. (2008). EB1 regulates microtubule dynamics and tubulin sheet closure in vitro. *Nature Cell Biology*, *10*(4), 415–421. http://doi.org/10.1038/ncb1703

Voloshin, O., Gocheva, Y., Gutnick, M., Movshovich, N., Bakhrat, A., Baranes-Bachar, K., et al. (2010). Tubulin chaperone E binds microtubules and proteasomes and protects against

misfolded protein stress. *Cellular and Molecular Life Sciences*, *67*(12), 2025–2038. http://doi.org/10.1007/s00018-010-0308-8

Waap, H., Cardoso, R., Leitão, A., Nunes, T., Vilares, A., Gargaté, M. J., et al. (2012). In vitro isolation and seroprevalence of *Toxoplasma gondii* in stray cats and pigeons in Lisbon, Portugal. *Veterinary Parasitology*, *187*(3-4), 542–547. http://doi.org/10.1016/j.vetpar.2012.01.022

Waap, H., Nunes, T., Vaz, Y., & Leitão, A. (2016). Serological survey of *Toxoplasma gondii* and Besnoitia besnoiti in a wildlife conservation area in southern Portugal. *Veterinary Parasitology, Regional Studies and Reports*, *3-4*, 7–12. http://doi.org/10.1016/j.vprsr.2016.05.003

Waap, H., Vilares, A., Rebelo, E., Gomes, S., & Ângelo, H. (2008). Epidemiological and genetic characterization of *Toxoplasma gondii* in urban pigeons from the area of Lisbon (Portugal). *Veterinary Parasitology*, *157*(3-4), 306–309. http://doi.org/10.1016/j.vetpar.2008.07.017

Walker, M. E., Hjort, E. E., Smith, S. S., Tripathi, A., Hornick, J. E., Hinchcliffe, E. H., et al. (2008). *Toxoplasma gondii* actively remodels the microtubule network in host cells. *Microbes and Infection / Institut Pasteur*, *10*(14-15), 1440–1449. http://doi.org/10.1016/j.micinf.2008.08.014

Wang, J.-L., Huang, S.-Y., Behnke, M. S., Chen, K., Shen, B., & Zhu, X.-Q. (2016). The Past, Present, and Future of Genetic Manipulation in Toxoplasma gondii. *Trends in Parasitology*, *32*(7), 542–553. http://doi.org/10.1016/j.pt.2016.04.013

Wang, W., Ding, J., Allen, E., Zhu, P., Zhang, L., Vogel, H., & Yang, Y. (2005). Gigaxonin interacts with tubulin folding cofactor B and controls its degradation through the ubiquitin-proteasome pathway. *Current Biology: CB*, *15*(22), 2050–2055. http://doi.org/10.1016/j.cub.2005.10.052

Wang, Y., & Yin, H. (2015). Research advances in microneme protein 3 of Toxoplasma gondii. *Parasites & Vectors*, *8*(1), 384. http://doi.org/10.1186/s13071-015-1001-4

Wang, Z., & Sheetz, M. P. (2000). The C-terminus of tubulin increases cytoplasmic dynein and kinesin processivity. *Biophysical Journal*, *78*(4), 1955–1964. http://doi.org/10.1016/S0006-3495(00)76743-9

Webster, J. P., Kaushik, M., Bristow, G. C., & McConkey, G. A. (2013). *Toxoplasma gondii* infection, from predation to schizophrenia: can animal behaviour help us understand human

behaviour? *The Journal of Experimental Biology*, *216*(Pt 1), 99–112. http://doi.org/10.1242/jeb.074716

Weisbrich, A., Honnappa, S., Jaussi, R., Okhrimenko, O., Frey, D., Jelesarov, I., et al. (2007). Structure-function relationship of CAP-Gly domains. *Nature Structural & Molecular Biology*, *14*(10), 959–967. http://doi.org/10.1038/nsmb1291

Welch, M. D., & Mullins, R. D. (2002). Cellular control of actin nucleation. *Annual Review of Cell and Developmental Biology*, *18*, 247–288. http://doi.org/10.1146/annurev.cellbio.18.040202.112133

White, M. W., Jerome, M. E., Vaishnava, S., Guerini, M., Behnke, M., & Striepen, B. (2004). Genetic rescue of a *Toxoplasma gondii* conditional cell cycle mutant. *Molecular Microbiology*, *55*(4), 1060–1071. http://doi.org/10.1111/j.1365-2958.2004.04471.x

Wilking, H., Thamm, M., Stark, K., & Aebischer, T. (2016). Prevalence, incidence estimations, and risk factors of *Toxoplasma gondii* infection in Germany: a representative, cross-sectional, serological study. *Scientific …*. http://doi.org/10.1038/srep22551

World Health Organization. (2016). Global Tuberculosis Report 2015. Geneva, Switzerland: World Health Organization. http://doi.org/10.1016/j.jstrokecerebrovasdis.2016.11.115

Xiao, H., Bissati, El, K., Verdier-Pinard, P., Burd, B., Zhang, H., Kim, K., et al. (2010). Post-translational modifications to *Toxoplasma gondii* alpha- and beta-tubulins include novel C-terminal methylation. *Journal of Proteome Research*, *9*(1), 359–372. http://doi.org/10.1021/pr900699a

Zabala, J. C., & Cowan, N. J. (1992). Tubulin dimer formation via the release of alpha- and beta-tubulin monomers from multimolecular complexes. *Cell Motility and the Cytoskeleton*, *23*(3), 222–230. http://doi.org/10.1002/cm.970230306

Zetsche, B., Volz, S. E., & Zhang, F. (2015). A split-Cas9 architecture for inducible genome editing and transcription modulation. *Nature Biotechnology*, *33*(2), 139–142. http://doi.org/10.1038/nbt.3149

Zhou, X. W., Kafsack, B. F. C., Cole, R. N., Beckett, P., Shen, R. F., & Carruthers, V. B. (2005). The Opportunistic Pathogen *Toxoplasma gondii* Deploys a Diverse Legion of Invasion and Survival Proteins. *Journal of Biological Chemistry*, *280*(40), 34233–34244. http://doi.org/10.1074/jbc.M504160200

Zhou, Y., Zhang, H., Cao, J., Gong, H., & Zhou, J. (2016). Epidemiology of toxoplasmosis: role of the tick Haemaphysalis longicornis. *Infectious Diseases of Poverty*, *5*(1), 14. http://doi.org/10.1186/s40249-016-0106-0

Intentionally blank page

Annexes

Annex I

Annex I. Protein Homology/analogY Recognition Engine Report for the *T. gondii* TBCB.

Intentionally blank page